Non-toxic concentrations of α-synuclein exacerbate Parkinson's disease-like cell death by inducing mitochondrial dysfunction.

by

Sally JM Williamson

A thesis submitted for the degree of Doctor of Philosophy

The University of Edinburgh

2008

Declaration

I declare that the work presented in this thesis is my own work and has not been submitted for any other degree or professional qualification. During the course of this study, work was carried out as part of a research group, where outside collaborations are stated within the body of the thesis.

Acknowledgement

I would like to convey my sincerest appreciation to my supervisors (Dr Paul Jones and Dr John Sharkey) and to Prof. James McCulloch, for their help and guidance throughout the course of this study. In particular I would like to thank Dr Paul Jones for his support and patience with me throughout this thesis.

I would also like to extend my gratitude to Prof Vladimir Buchman who kindly gifted the synuclein plasmids for the use in the study and his continued guidance, Dr Duncan Short for his expertise in protein prurification and entertaining office and lab antics, and Dr John White (EPIC) for the generation of large scale cultures. Without their contribution this work would not have been possible. It was also a pleasure to work with all the members of A.C.E. and Edinburgh University staff that I was inflicted upon to work with or through my search for equipment. I would especially like to thank the research assistants in A.C.E whose invaluable experience and knowledge was essential. Most of all I want to thank Paul Jones, Louise Dickson, Ian Heron and Joe Hodgkiss for keeping me more or less sane through the long days and really becoming my second family during my time at Edinburgh, I have missed the lunch time walks and late coffee chats.

I would like to thank my Mother, Father, Grandma, my brother Paul and Marta for their continued support through all my studies, which without their help I would not have attempted this endevour.

Finally I would like to dedicate this thesis to my dearest husband Dr Simon Clark and my best friend Karen Bellis, who have kept me going when there did not seem to be an end and I needed someone to put me back together.

Thank you.

Abstract

α-Synuclein (α-syn), is a self-aggregating protein that has been identified as a pathologically important component in a number of diseases, such as Parkinson's disease (PD). PD, a progressive neurological disorder affecting 1 in 500 people, results in motor dysfunction following the loss of dopaminergic neurones of the nigrastriatal pathway. A pathological hallmark of PD is the presence of α-syn containing Lewy bodies and Lewy neurites. Although α-syn has been linked to PD by both histology and genetic studies on familial PD, neither the physiological function nor the pathophysiological role of α-syn in PD has been fully elucidated. This thesis examines the cellular responses to exogenously applied recombinant α-syn under normal and disease-like conditions. Within this thesis large-scale expression and purification of α-syn was successfully established, reproducibly producing large quantities of pure recombinant α-syn that was utilised within *in vitro* experiments. In SHSY-5Y neuroblastoma cells, α-syn (10 and 30 μM) significantly decreased NAD(P)H levels after 48 h incubation, indicative of either cell death or disruption to energy metabolism of the cells. However, α-syn (0.1 - 30 μM) did not induce cell death, as determined by the LDH assay, even when the cells were exposed for 48 h. Therefore our studies show that under normal, physiological conditions, α-syn is not inherently toxic, but does result in a decrease of total cellular energy levels.

The mitochondrial toxin, 1-methyl-4-phenylpyridinium ion (MPP^+), induced cell death in SHSY-5Y cells that was both concentration- and time-dependent. α-Syn (30 μM) significantly exacerbated MPP^+-induced cell death in this model of PD. This suggests that while α-syn is normally non-toxic, under PD-like conditions it can exacerbate the cell death process. We identified that α-syn (30 μM) significantly increased cytosolic Ca^{2+} levels in a time-dependent manner as well as increasing the levels of the apoptotic mediator, cytochrome c (cyt c). The release of cyt c from the mitochondria into the cytosol is indicative of mitochondrial dysfunction and pore formation within mitochondrial membranes. However, α-syn-induced increase in cytosolic Ca^{2+} was not blocked by the mitochondrial pore inhibitor, cyclosporine A. This suggests that α-syn effects were not mediated through the mitochondrial pore

usually associated with dysfunction and cyt c release. α-Syn therefore releases cyt c and Ca^{2+} by a separate mechanism, such as the formation of α-syn protofibril pores. This was further compounded by data that showed that α-syn (30 μM) significantly decreased mitochondrial membrane potential after 48 h incubation. The loss of the mitochondrial membrane potential coincided with a decrease in NAD(P)H. These data would therefore suggest that physiologically α-syn induces a low, non-toxic effect on the mitochondrial membrane. Under pathological conditions similar to PD however, this mitochondrial stress mediated by α-syn acts to exacerbate cell death.

Contents

List of figures and tables

Tables

Abbreviations

α-Syn	-	α-synuclein
β-Syn	-	β-synuclein
γ-Syn	-	γ-synuclein
A	-	alanine
ACh	-	acetylcholine
AD	-	Alzheimer's disease
Amp	-	ampicillin
AR-JP	-	autosomal recessive juvenile parkinsonism
ATP	-	adenosine triphosphate
BCSG1	-	breast cancer-specific gene 1
cAMP	-	adenyl cyclase 5'-adenosine
chlora	-	chloramphenicol
Chr	-	chromosome
CK	-	casein kinases
CNS	-	central nervous system
COMT	-	catechol-omethyl transferase
CsA	-	cyclosporine A
cyt c	-	cytochrome c
D1	-	dopamine D1 receptor
D2	-	dopamine D2 receptor
D3	-	dopamine D3 receptor
D4	-	dopamine D4 receptor
D5	-	dopamine D5 receptor
DA	-	dopamine
DAG	-	diacylglycerol
DAGK	-	diacylglycerol kinase
DAT	-	dopamine transporter
DBS	-	deep brain stimulation
DLB	-	dementia with Lewy bodies
DMEM	-	Dulbecco's modified Eagle's medium
E2	-	substrate specific ubiquitin-conjugated enzyme
E3	-	ubiquitin-protein ligase
ERK:	-	extracellular signal-regulated kinase
ETC	-	electron transport chain
E	-	glutamic acid
EPIC	-	Edinburgh Protein Interaction Centre
EtBr	-	ethidium bromide
FA	-	fatty acids
FABP	-	fatty acid binding protein
(B)-FABP	-	brain specific fatty acid binding protein
FCS	-	foetal calf serum
FPLC	-	fast protein liquid chromatography
G	-	glycine
GABA	-	γ-amino-butyric acid
GRK	-	G protein-coupled receptor kinase
GRK5	-	G protein-coupled receptor kinase 5
GP	-	globus pallidus
I	-	isolucine
IPTG	-	isopropyl β-D-1-thiogalactopyranoside
K	-	lysine

L-DOPA	-	3,4-dihydroxyphenylalanine
LB	-	Lewy bodies
LC	-	locus coeruleus
LD_{50}	-	lethal dose of 50 %
LDH	-	lactate dehydrogenase
LDH assay	-	CytoTox96® Non-Radioactive Cytotoxicity assay
LMP	-	low melting point
LN	-	Lewy neurites
LRRK2	-	leucine-rich repeat kinase 2
MAO-B	-	monoamine oxidase-B
mitochondrial pore	-	mitochondrial permeability transition pore
$MPDP^+$	-	1-methy-4-phenyl-2,3-dihydropyridine
MPP^+	-	1-methyl-4-phenylpyridine
MPPP	-	1-methyl 4-phenyl 4-propionoxypiperidine
MPTP	-	1-methyl 4-phenyl 1,2,3,6-tetrahydropyridine
MSA	-	multisystem atrophy
MTS assay	-	CellTiter 96® AQueous One Solution Reagent assay
NaAc	-	sodium acetate
NAC	-	non-amyloid component
OD	-	optical density
P	-	proline
PA	-	phosphatidic acid
Parkin	-	ubiqitin protein ligase
PAP	-	phosphatidic acid phosphohydrolase
PCR	-	polymerase chain reaction
PD	-	Parkinson's disease
PINK1	-	PTEN-induced kinase 1
PKC	-	protein kinase C
PKA	-	protein kinase A
PLD	-	phospholipase D
PNP 14	-	phosphoneuroprotein 14
PNS	-	peripheral nervous system
ROS	-	reactive oxygen species
Ser	-	serine
SDS	-	sodium dodecyl sulphate
SHSY-5Y	-	SHSY-5Y human neuroblastoma cells
SN	-	substantia nigra
SNpc	-	substantia nigra pars compacta
SNpr	-	substantia nigra pars reticularis
STN	-	subthalamic nucleus
STS	-	staurosporine
T	-	threonine
TH	-	tyrosine hydroxlase
UCH-L1	-	ubiquitin carboxyl-terminal hydrolase-L1
UPS	-	ubiquitin-proteasome system
VMAT2	-	vesicular monoamine transporter
wt	-	wild type

Chapter 1: Introduction

1.1 Synuclein Proteins

1.1.1 Synucleins and the synuclein family.

Synucleins are a small family of soluble proteins that potentially have a role in a number of disorders such as Parkinson's disease (PD). Ranging in size from 127 to 140 amino acids, the family consists of 4 members; α-, β-, γ-synuclein and synoretin. The family of proteins have a high level of sequence conservation and are also conserved across a number of animal species (Maroteaux and Scheller 1991; Buchman, 1998; Lavedan, 1998). α-Synuclein (α-syn) was first identified by Maroteaux *et al*. (1988) in the electric ray (*torpedo californica*). β-Synuclein (β-syn) was subsequently identified by Nakajo *et al*. (1990) and originally termed phosphoneuroprotein 14 (PNP 14), (Nakajo *et al*., 1990; Nakajo *et al*., 1993). However, PNP 14 was observed to share a high percentage of sequence homology and localisation with α-syn leading to its renaming to β-syn (Jakes *et al*., 1994; Shibayama-Imazu *et al*., 1998). A short while later γ-syn was discovered by Ji *et al*. in 1997, who isolated the *γ-syn* gene within breast cancer and originally named *breast cancer-specific gene 1* (*BCSG1*) (Ji *et al*., 1997). The gene was quickly re-classified after its homology to *α-syn* was characterised (Lavaden *et al*., 1998; Buchman *et al*., 1998). Synoretin was identified in the brain and retinal cells by Surguchov *et al*. (1999). Interestingly the synoretin protein shows more homology to γ-syn than α-syn (Surguchov *et al*., 1999). Since the identification of the synuclein family, the chromosomal loci for each of the synuclein genes has been identified; *α-syn* is located at 4q21.3 (Spillantini *et al*., 1995; Shibasaki *et al*., 1995); *β-syn* at 5q35 (Spillantini *et al*., 1995); *γ-syn* at 10q23 (Lavedan *et al*., 1998). However, the

chromosomal location for *synoretin* has not at present been identified (Murray *et al.*, 2001).

Synuclein proteins are expressed throughout the body with highest expression levels in the central and peripheral nervous systems (CNS and PNS), especially in the brain (Jakes *et al*., 1994; Buchman *et al*., 1998; Lavedan, 1998). Immunohistochemical studies of α-, β- and γ-syn expression in the brain indicated that the synuclein proteins were expressed within similar regions of the brain, predominantly in the thalamus, substantia nigra (SN), hippocampus, caudate nucleus and amygdala (Lavedan, 1998), although β-syn was shown to have lower expression levels compared to α-syn and γ-syn (Shibayama-Imazu *et al*., 1993; Lavedan, 1998).

Outwith the CNS further immunohistochemical studies have shown hetrogeneous expression of α-, β- and γ-syn in a diverse range of tissues and cells (Jakes *et al*., 1994). γ-Syn has been shown to have considerable expression in the PNS (Buchman *et al*., 1998; Ninkina *et al*., 1999) as well as within skin and retinal cells (Ninkina *et al*., 1999). γ-Syn was, as mentioned previously, identified within breast cancer cells and has also been suggested to be over-expressed in ovarian tumours (Ji *et al*., 1997; Lavedan *et al*., 1998). α-Syn expression has been shown in platelets, haematopoietic cells, neuromuscular or junctions and cardiac tissue (Uéda *et al*., 1994; Li *et al*., 2002; Michell *et al*., 2005). β-Syn has been shown to have localised expression in sertoli cells of the testis (Shibayama-Imazu *et al*., 1998). However, synoretin has only been shown to be expressed in the brain and retinal cells (Surguchov *et al*., 1999)

1.1.2 Structure of α-syn.

At the molecular level, all members of the synuclein family contain a phospholipid binding N-terminal and a negatively charged acidic C-terminal (Uversky *et al*., 2002). They exhibit 55 – 62 % sequence conservation with similar domain organisation (Lavedan, 1998; Uversky *et al*., 2002), containing several repeats of an 11 residue motif (containing variations of a "KTKEGV" residue sequence; see figure 1.1) (Buchman *et al.*, 1998; Ninkina *et al.*, 1998; Murray *et al.*, 2001). α-Syn and β-syn have identical carboxyl termini (Lavedan, 1998) and very similar structures (Tsigelny *et al*., 2007). The C-terminal sequence of α-syn is highly conserved across species; human α-syn has been shown to be 95.3 % identical to the rodent sequence (Polymeropoulos *et al.,* 1997). There are only 6 amino acid differences, one of these being the amino acid at position 53. This is normally an alanine (A) in humans and a threonine (T) in rodents. However, the substitution, A53T in humans, has been shown to be one of the mutations which is linked to a familial form of PD (Lavedan, 1998).

The organisation of synuclein sequences causes the formation of a random coil structure when in solution (Wienreb *et al*., 1996). The coils contain a hydrophobic region that interacts with membranes and allows penetration of synuclein proteins into the bilayer interior of the membranes and helps stabilise the lipid-protein interaction (Davidson *et al*., 1998). Within the α-syn sequence, amino acids 61 – 96 are identical to the non-amyloid component (NAC) of amyloid plaques found in Alzheimer's disease (AD) (Iwai *et al*., 1995; Weinreb *et al*., 1996). These residues are also thought to be important in phospholipid binding and

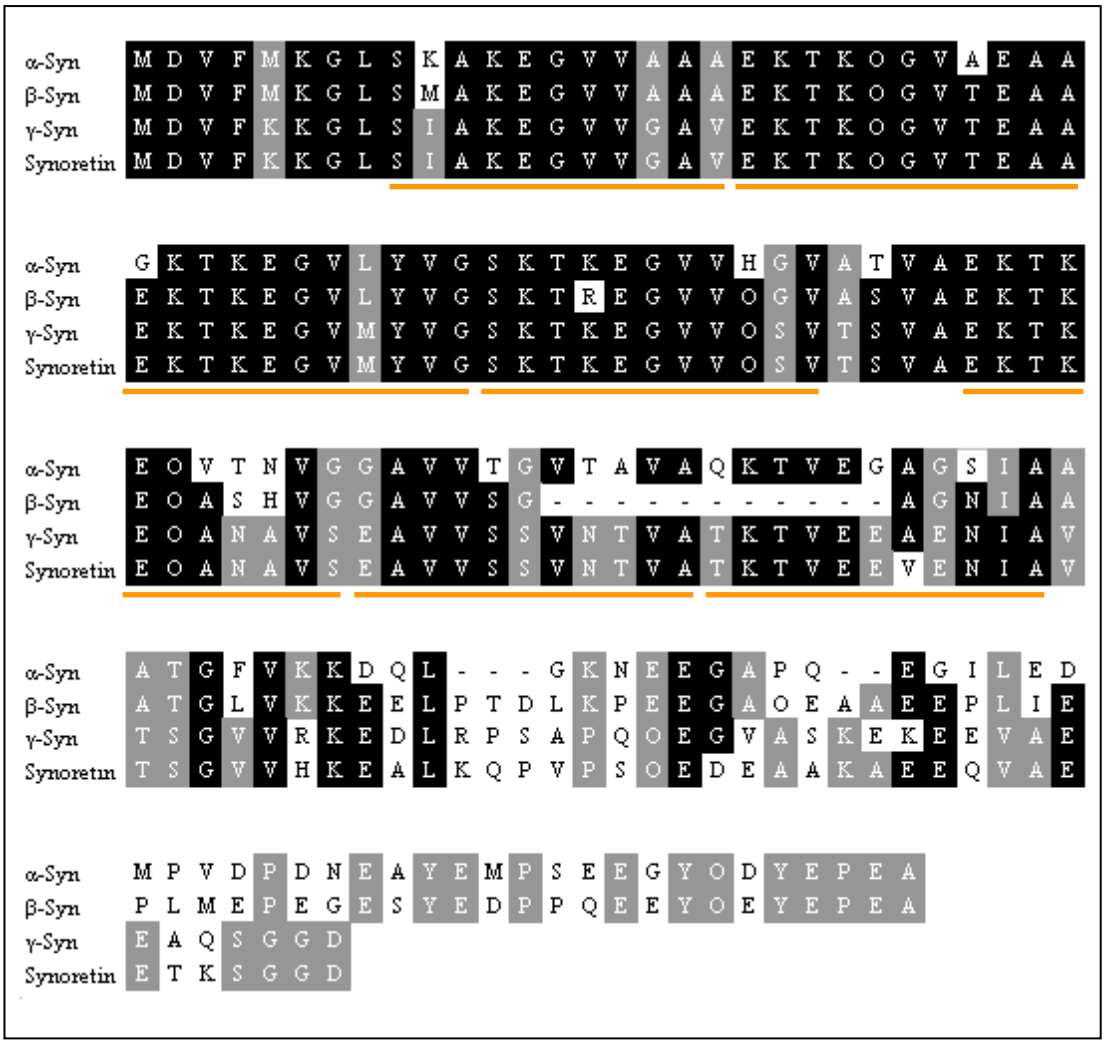

Figure 1.1: The comparison of synuclein family amino acid sequences.

The total number of residues in α-, β-, γ-synuclein and synoretin proteins are 140, 134, 127 and 127 respectively. The amino acid sequence alignments of human synucleins are compared above. The identification of the 11 residue repeats are indicated by orange lines. Residues that are shared by 2 synuclein family members are highlighted in grey and 3 or more are highlighted in black. Gaps within the sequences are indicated with dashes (adapted from Davidson *et al.*, 1998 and Chandra *et al.*, 2003).

chaperone properties of α-syn. With the isolation of NAC in amyloid plaques the NAC region of α-syn has been implicated in the capacity of α-syn to aggregate and form fibrils in diseases such as PD and dementia with Lewy bodies (DLB) (Weinreb *et al*., 1996). This has been further supported through the inability of β-syn to aggregate under physiological conditions; β-syn is almost identical to α-syn but does not contain the NAC region (Weinreb *et al*., 1996). This theory is however complicated by γ-syn, which contains the NAC region and forms dimers, but does not aggregate (Uversky *et al*., 2002). Studies have shown that although β-syn and γ-syn do not aggregate they are able to reduce α-syn aggregation, possibly through binding to the dimerised and protofibril forms of α-syn, preventing completion of the aggregation process (Uversky *et al*., 2002; Tsigelny *et al*., 2007).

α-Syn has been show to have a primarily random structure within the cytosol of cells, (Ischiropoulos, 2003). However, upon binding to phospholipid membranes, α-syn undergoes a conformational change converting to a predominantly α-helical structure (figure 1.2 and figure 1.3) (Davidson *et al.,* 1998). The C-terminal (residues 96 - 140) of α-syn appeared to remain unstructured upon α-syn binding to phospholipid membranes (Bussell and Eliezer 2003; Chandra *et al*., 2003; Ulmer *et al*., 2005). As α-syn is randomly structured in solution, the secondary structure only occurs after α-syn has bound to a phospholipid membrane. This secondary structure forms overtime through the penetration of α-syn into the lipid matrix (Narayanan and Scarlata, 2001).

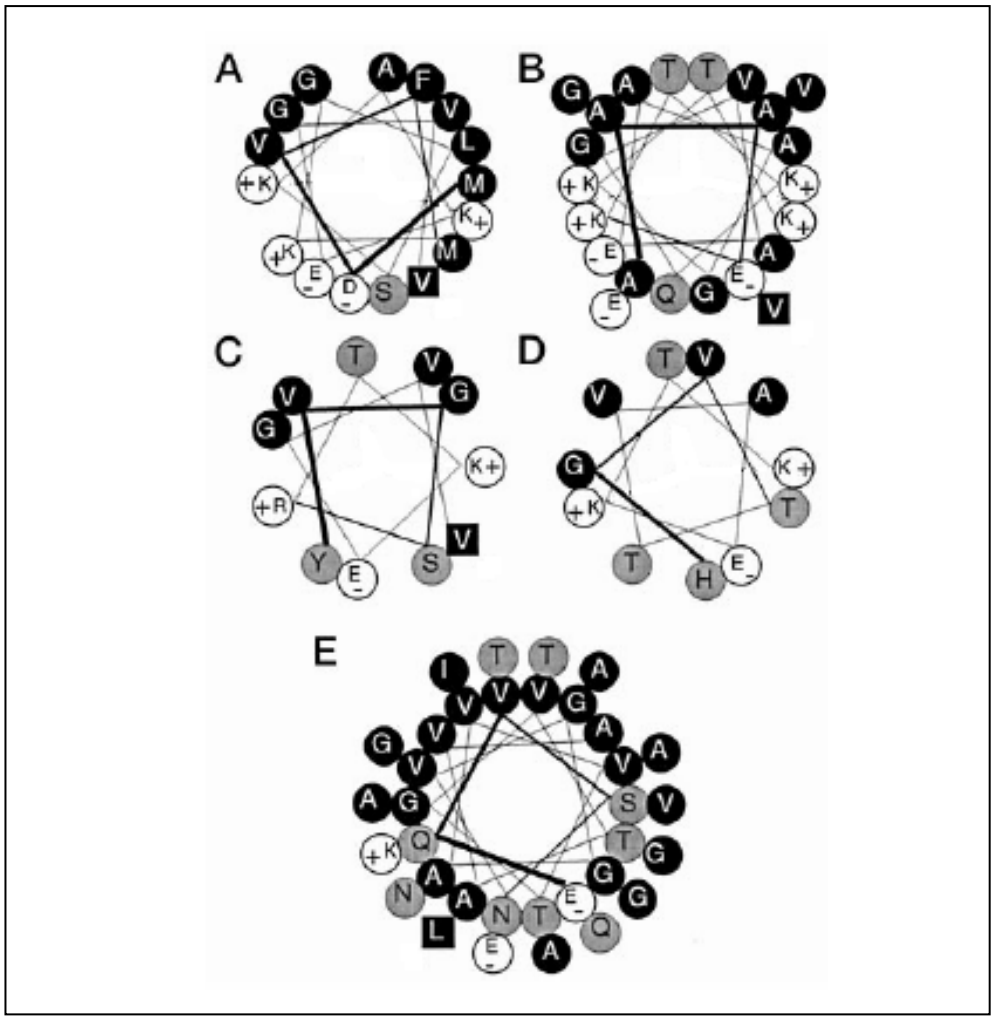

Figure 1.2: Helical wheel predication of α-syn secondary structure.

An idealised α-helix wheel analysis of residues 1 to 96 containing 11 residue repeats producing a 5 α-helical secondary structure within the N-terminal of α-syn. Non-polar residues are shaded black, polar residues are shaded grey, and charged residues are unshaded (adapted from Davidson *et al.*, 1998) Each of the five a-helices are shown: **A**) helix 1 composed of 1 – 15; **B**) helix 2 composed of 17 – 37; **C**) helix 3 composed of 39 – 48; D) helix 4 composed of 50 – 60; **E**) helix 5 composed of 61 – 93

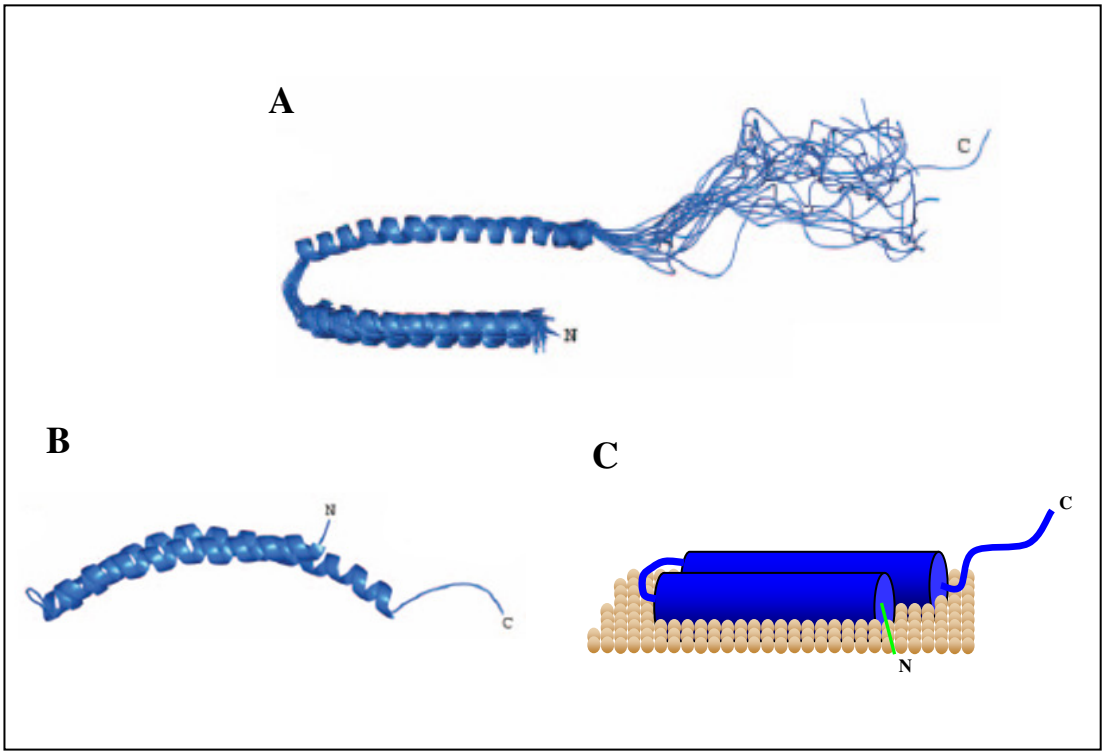

Figure 1.3: Computer schematic of the structure of phospholipid bound α-syn.

Using NMR the membrane bound structure of α-syn has been interpreted by Ulmer *et al* (2005), where **A)** shows the ensembly of twenty structures superimposed on top of each other. The N-terminal forms two α-helices with a short linking region between the helices and the unstructured C-terminal (analysis by NMR by Ulmer *et* al., 2005). **B)** A side view of the average α-syn structure showing the curve α-helices when membrane bound (analysis by NMR by Ulmer *et* al., 2005). **C)** Shows the structure within a phospholipid membrane with the N-terminal partially inserted into the membrane and the C-terminal unstructured which does not interact with the membrane.

α-Syn preferentially binds to highly curved and acidic membranes (Davidson *et al.*, 1998) as opposed to neutral or positively charged flatter membranes, giving evidence towards α-syn being involved in vesicle transport and regulations in cells (Davidson *et al.*, 1998; Narayanan and Scarlata, 2001). The curvature of the bound phospholipid membrane appears to alter the position of the α-helices of α-syn such that the helices fold in on themselves becoming parallel (as opposed to relatively flat membranes where helices remain linear) (Bussell and Eliezer 2003; Chandra *et al*., 2003; Ulmer *et al*., 2005). This implies that the linking region acts like a hinge between the two helices separating them depending on the curvature of the membrane to which α-syn is bound (Ulmer *et al*., 2005).

1.1.2.1 α-Syn oligomer formation.

Though primarily a soluble protein, α-syn has been shown to under go abnormal assembly that results in its oligermisation and the formation of fibrils. α-Syn fibrils have been identified with the formation of Lewy bodies (LB) and Lewy neurites (LN) within synucleinopathies such as PD.

While α-syn has the potential to self-aggregate, the aggregation rate can be augmented by a number of cellular and environmental factors such as; metals (Al^{3+}, Cu^{2+} and Fe^{2+}) (Paik *et al.,* 1999; Uversky *et al.,* 2001; Golts *et al.,* 2002), neurotoxins (1-methyl-4-phenylpyridine (MPP^{+}) and rotenone) (Kalivendi *et al.,* 2004), cytochrome c (cyt c), calcium (Ca^{2+}) and dopamine (DA) (Hashimoto *et al.,*1999; Lowe *et al.,* 2004; Cappai *et al.,* 2005). The aggregation of α-syn arises through α-syn undergoing a conformational change from a random α-helical

structure to β-sheet formation, leading to the formation of fibrils (El-Agnaf *et al.,* 1998). During the aggregation process α-syn forms homodimers, which could adopt non-propagating and propagating conformations (Tsigelny *et al.,* 2007). The propagating dimers can consist of pentamers and hexamers that can form ring structures (Tsigelny *et al.,* 2007). Further to this α-syn has been shown through atomic force microscopy and other methods, to form a number of intermediates including spheres, chains of spheres and rings, all of which are referred to as protofibrils (Conway *et al.,* 2000a; Ding *et al.,* 2002; Hoyer *et al.,* 2004). The α-syn protofibril rings have been shown to bind to synthetic membranes and permeablise vesicles (Volles *et al.,* 2001; Ding *et al.,* 2002; Volles and Lansbury 2002; Tsigelny *et al.,* 2007). This ability is similar to that observed by some bacterial toxins or a detergent-like mechanism, which perforate membranes through the insertion of pore-like structures. This would indicate that the formation α-syn aggregates could induce a toxic effect upon cells through the possible formation of pores (Ding *et al.,* 2002; Lashuel *et al.,* 2002; Volles *et al.,* 2002). Aggregation of α-syn could also lead to the loss of function of soluble α-syn (by virtue of its decreased levels) in cellular processes that include the regulation of synaptic plasticity (George *et al*., 1995), DA biosynthesis and regulation (Perez *et al*., 2002; Baptista *et al*., 2003; Wersinger and Sidhu, 2003a; Yavich *et al*., 2004) and regulation of vesicle transport (Yavich *et al*., 2004; Wersinger and Sidhu, 2005; Roy *et al*., 2007).

1.1.3 Functional role of α-syn.

The cellular role of α-syn has not yet been fully defined. α-Syn has however, been implicated in a number of different cellular processes within neurones which include the regulation of synaptic plasticity (George *et al*., 1995) and neuronal differentiation (Hashimoto *et al*., 1997; Satoh and Kuroda, 2001). Recently however, it seems to be emerging that primary roles of α-syn may lie in the regulation of synaptic vesicles, such as vesicle trafficking and recycling (see section 1.1.3.1.3) (Yavich *et al*., 2004; Wersinger and Sidhu, 2005; Roy *et al*., 2007). α-Syn has also been implicated in the regulation of DA, including DA biosynthesis, and regulation of DA transporters (DAT) (sections 1.1.3.2 and 1.1.3.3) (Perez *et al*., 2002; Baptista *et al*., 2003; Wersinger and Sidhu, 2003a; Yavich *et al*., 2004).

1.1.3.1 Indication of α-syn functions through sequence homology.

1.1.3.1.1 α-Syn as a chaperone protein.

Homology studies on the sequence of α-syn have identified similarities to the chaperone proteins termed 14-3-3 proteins (Ostrervoa *et al*., 1999) (figure 1.4) and fatty acid binding proteins (FABP) (Sharon *et al*., 2001). Further support for a role as a chaperone protein is provided by structural studies that show α-syn interaction with phospholipid membranes (Davidson *et al*., 1998; Bussell and Eliezer 2003; Chandra *et al*., 2003; Ulmer *et al*., 2005) and other proteins such as 14-3-3 proteins, protein kinase C, phospholipase D2 and DAT (Ostrervoa *et al*., 1999; Wersinger and Sidhu, 2003a; Roy *et al*., 2007).

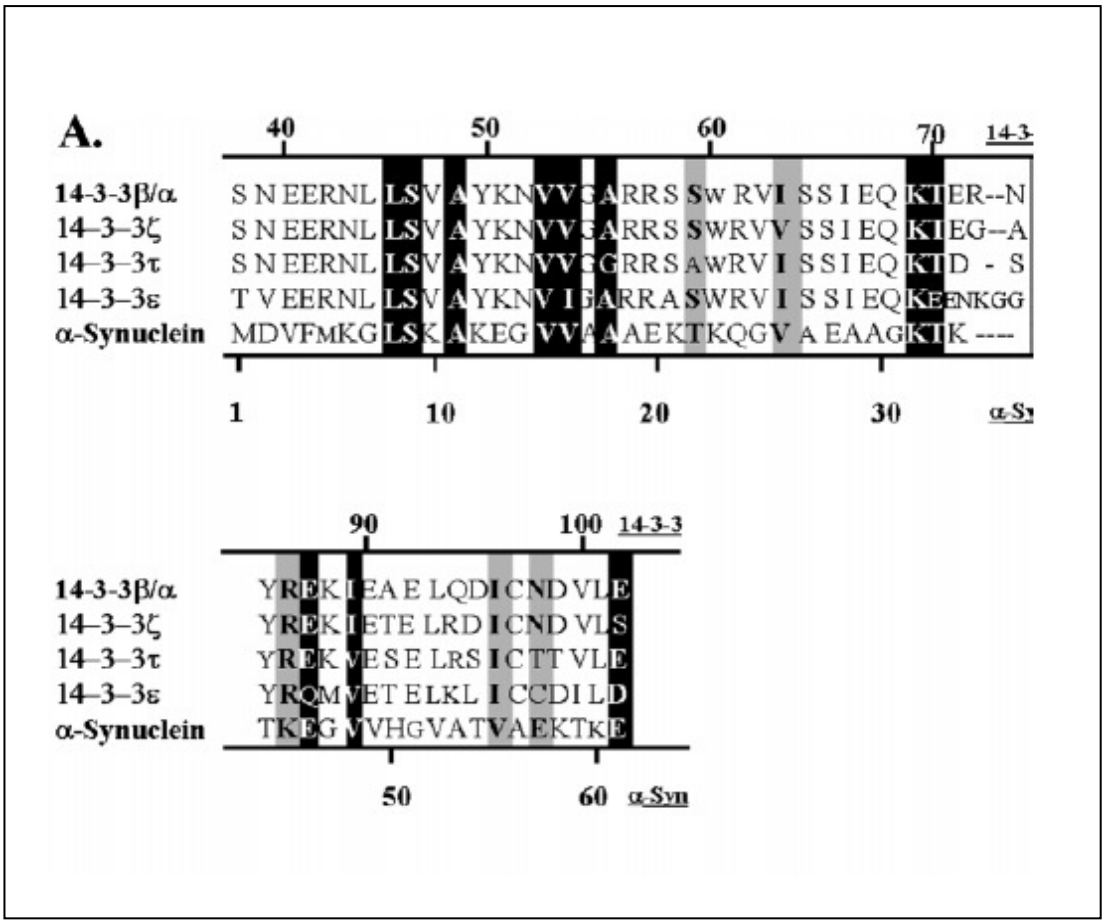

Figure 1.4: Sequence homology of α-syn and 14-3-3 proteins.

The homology between α-syn N-terminal (amino acid 1 to 60) and amino acids 38 – 102 of 14-3-3 proteins are compared. Regions in white letters on black background identify exact matches between the sequences; black letters on grey indicates amino acids with similar properties. (Taken from Ostrervoa *et al*., 1999)

While the homology between α-syn N-terminal and 14-3-3 proteins (Ostrerova *et al*., 1999) coincides with the highly conserved region of the N-terminus that is present in all the synuclein proteins (see figure 1.1) there is no report of similar 14-3-3 ligand binding for β- and γ-syn.

1.1.3.1.2 α-Syn as a fatty acid-binding protein.

Homology studies have highlighted sequence similarities between α-syn and FABP (Sharon *et al*., 2001). Sharon *et al*. (2001), demonstrated that two 18 residue regions in the α-syn sequence at the N- and C-termini share homology with a signature motif characteristic of FABP (55 % and 67 % respectively). As FABP are a diverse family of ~ 15 kDa cytosolic lipid transport proteins, α-syn may be involved in the transportation of fatty acids (FA) between aqueous and membrane phospholipid compartments. FABP expression has been shown to be tissue specific (Kurtz *et al*., 1994; Sharon *et al*., 2001). For example in the brain, brain specific FABP ((B)-FABP) was identified as a 14.5 kDa protein localised to glial cells (Kurtz *et al*., 1994). α-Syn does not co-express with (B)-FABP in glial cells (Sharon *et al*., 2001), but is however, present in almost all other cell types within the brain (Uéda *et al*., 1993; Jake *et al*., 1994). This has led to the suggestion that α-syn may be a novel brain specific FABP and associates with fatty acids such as oleic acid through the regions of homology (Sharon *et al*., 2001).

It is important to note, that α-syn may not be a novel brain FABP, but rather a chaperone for vesicles including, but not limited to fatty acid-transport (Lücke *et al*., 2006). This theory was borne out by Lücke *et al.* (2006), who showed that α-syn

bound to the negatively charged surface of oleic acid bilayers, but did not appear to bind other FA (Golovko *et al*., 2005, Lücke *et al*., 2006). Lücke *et al.* (2006) concluded that α-syn did not act as an intracellular FA carrier, but that the binding of α-syn to oleic acids was simply an intrinsic property to interact with negatively charged membranes (Lücke *et al*., 2006). The N-terminal sequence of β-syn is almost identical to α-syn (as shown in figure 1.5) (Sharon *et al*., 2001) and therefore would also share homology to the same FABP motif. While the N-terminal region of α-syn may or may not be involved in phospholipid binding, it may be the case, however, that the C-terminus of α-syn may also bind fatty acids and interact with proteins such as microtubulin and DAT (Wersinger and Sidhu, 2003a; Wersinger and Sidhu, 2005; Roy *et al*., 2007).

Figure 1.5: Identification of fatty acid-binding motif within α-, β- and γ-syn sequences.

The total number of residues in each protein is 140, 134, and 127 respectively. Residues which are shared between 2 or all the synuclein sequences are highlighted in black. The green boxes indicate the regions of the synuclein sequences which show homology with the fatty acid-binding protein signature motif. Gaps in the β and γ sequences relative to α-syn are indicated with dashes (adapted using Sharon *et al*., 2001 and Chandra *et al*., 2003).

1.1.3.1.3 α-Syn involvement in vesicle trafficking.

α-Syn has been shown to be a potent inhibitor of Phospholipase D (PLD) enzymes through *in vitro* studies by Jenco *et al.* (1998). PLD enzymes are a family of enzymes which are involved in lipid mediated signalling cascades and vesicle trafficking (Payton *et al*., 2004). The PLD family consist of two isoforms, PLD1 and PLD2 (Colley *et al*., 1997). PLD1 and PLD2 are a phosphatidycholine-specific hydrolases that metabolise phosphatidylcholine to generate choline (used in the production of the neurotransmitter acetylcholine, and phoshatidic acid; PA (Colley *et al*., 1997). PA and its metabolites exhibit second messenger properties that are involved in the mediation of vesicular transport, mitogeneis, receptor-mediated endocytosis and cytoskeleton rearrangement (Colley *et al*., 1997). PA has also been associated with the recruitment of adaptor molecules that trigger the building of vesicles from donor membranes (Jenco *et al*., 1998). Furthermore, PA is metabolised by diacylglycerol kinase to produce diacylglycerol (DAG), which is involved in the activation of protein kinase C (PKC) and other diacylglycerol-dependent enzymes (Jenco *et al*., 1998; Nishizuka, 1995). Activated PKC isoforms are involved in the activation of protein by phosphorylation, such as DAT (Chang *et al*., 2001). In summary, it would appear that PLDs are involved in the regulation of neurotransmitter generation through the production of choline and the regulation of DAT and the vesicle cycle (figure 1.6). PLD inhibition therefore suggests a role of α-syn in all these downstream events.

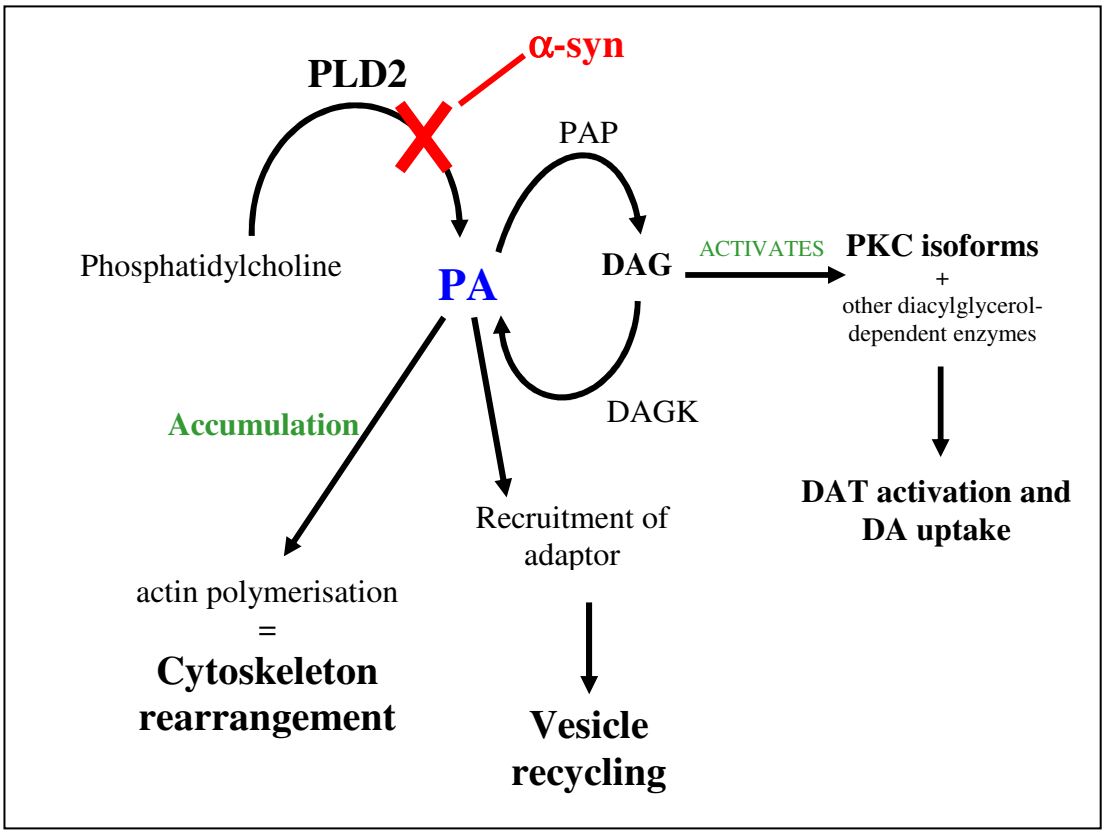

Figure 1.6: A basic schematic of the PLD2 pathway and it's inhibition by α-syn.

The schematic shows the production of Phosphatidic acid (PA) from phosphatidylcholine by Phospholipase D2 (PLD2) and how PA and PA metabolites effect different cellular pathways; cytoskeleton rearrangement, vesicle recycling, dopamine (DA) uptake by dopamine transporter (DAT) activation. α-Syn inhibits PA metabolism and blocks the subsequent pathways. Key: DAG (Diacylglycerol), DAGK (Diacylglycerol kinase), PA (Phosphatidic acid), PAP (Phosphatidic acid phosphohydrolase), PKC (Protien kinase C) and PLD2 (Phospholipase D2).

α-Syn inhibition of PLD2 was shown to be modulated by the phosphorylation of α-syn at serine 129 (ser129), as well at tyrosine 125 or tyrosine 136 (Payton *et al*., 2004). Within the cell, such phosphorylation of α-syn can be achieved by various seryl/threonyl proteins such as calmodulin kinase II (calcium-dependent manner), casein kinases (CK1 and CK2) and G protein-coupled receptor kinases (GRK) (Pronin *et al*., 2000). Activated G protein-coupled receptor kinase 5 (GRK5) showed the highest efficiency of phosphorylating α-syn specifically in the presence of phospholipids (Pronin *et al*., 2000; Martinez *et al*., 2003).

The binding of α-syn to phospholipid membranes may enhance its phosphorylation due to a conformational change increasing the accessibility of ser129 residue (Pronin *et al*., 2000; Payton *et al*., 2004). Furthermore, the expression level of α-syn within neurones also appears to influence the phosphorylation of α-syn by the activation of GRK5 via the Ca^{2+}-calmodulin complex (Chuang *et* al., 1996; Pronin *et al*., 2000; Martinez *et al*., 2003). In the absence of α-syn, the Ca^{2+}-calmodulin complex inhibits GRK5 by preventing autophosphorylation, activation and the phosphorylation of other substrates. However, in the presence of α-syn, the complex stimulates GRK5 autophoshorylation and increases the phosphorylation of α-syn (Martinez *et al*., 2003). This would suggest that α-syn may act as a switch to convert the Ca^{2+}-calmodulin complex from inhibitor to an activator of GRK5 (Martinez *et al*., 2003).

α-Syn has been further implicated in the regulation of vesicle trafficking by a study that showed α-syn increased vesicle-mediated α-granule secretion from platelets (Park *et al*., 2002). This suggests a role for α-syn that is not just limited to neuronal

synapses but, potentially many cell types (Uéda *et al*., 1994; Li *et al*., 2002; Michell *et al*., 2005).

1.1.3.2 α-Syn regulation of DA biosynthesis.

α-Syn has been implicated in a number of mechanisms, such as an interaction with DAT, inhibition of tyrosine hydroxylase (TH), PKC and extracellular signal-regulated kinase (ERK), which directly regulate/modulate the biosynthesis of DA (Ostrerova *et al*., 1999; Perez *et al*., 2002).

DA is a member of the catecholamine family of neurotransmitters belonging to the larger monoamines family (Kingsley, 2000; Longstaff, 2000). Catecholamines are found throughout both the CNS and PNS (Kingsley, 2000; Longstaff, 2000). In the CNS, the cell bodies of dopaminergic neurones are concentrated in the basal ganglia; primarily the substantia nigra pars compacta (SNpc) and dopaminergic neuronal terminals in stratum (York, 1970; Kingsley, 2000). DA is synthesised by the hydroxylation of tyrosine by TH to produce the 3,4-dihydroxyphenylalanine (L-DOPA) intermediate, which is then decarboxylated to produce DA (figure 1.7) (Longstaff, 2000). The production of DA is regulated by the availability of TH, which acts as a rate-limiting step. In order for TH to convert tyrosine to L-DOPA, TH is phosphorylated at two serine residues, ser 19 and 40 (Haycock, 1990; Kumer and Vrana, 1996; Kleppe *et al*., 2001). 14-3-3 protein and Ca^{2+}/calmodulin-dependent protein kinase II have been shown to be the main enzymes that phosphorylate TH at theses serine residues (Haycock, 1990; Kumer and Vrana, 1996; Kleppe *et al*., 2001).

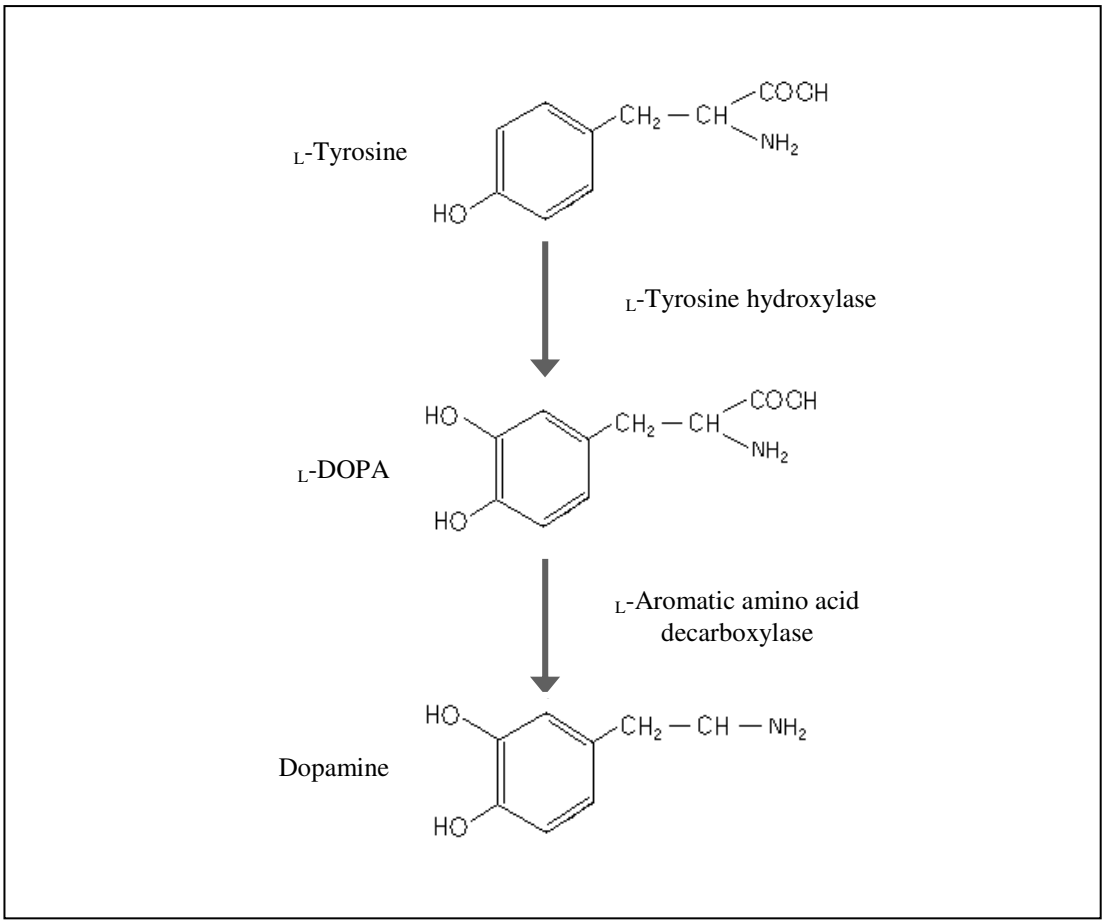

Figure 1.7: DA synthesis from L-Tyrosine (adapted from Longstaff, 2000).

14-3-3 proteins interact and increases the active half life of a number of ligands including TH (Itagaki *et al*., 1999; Perez *et al*., 2002). α-Syn, by binding dephosphorylated TH, decreases DA synthesis and maintains TH deactivation (Perez *et al*., 2002). α-Syn also binds MAP kinase (inhibiting ERK activation) and inhibiting both Ca^{2+}/calmodulin-dependent protein kinases (Ostrerova *et al*., 1999) and further decreasing TH activity (Perez *et al*., 2002).

1.1.3.3 α-Syn regulation of DAT.

A number of studies have implicated α-syn in the regulation of DA re-uptake from the presynaptic cleft through the ability of α-syn to associate with DAT and reduce DAT activity (Ostrervoa *et al*., 1999; Wersinger and Sidhu, 2003a; Sidhu *et al*., 2004).

DAT is a member of a large family of Na^+- and Cl^--dependent transporters that share a common topology of 12 putative transmembrane domains containing numerous consensus sequences for N-linked glycosylation. These transmembrane domains also contain recognised phosphorylation sites for PKA, PKC and calmodulin kinase II, which when phosphorylated, activate DAT and the uptake of DA from the synaptic cleft (Wersinger *et al.*, 2004). It is speculated that the regulation of DAT is a crucial component in the maintenance of dopaminergic neurotransmission and the levels of intracellular DA (Lee *et al*., 2001; Wersinger *et al*., 2004). The rapid shuttling of DAT to and from the plasma membrane is thought to be one of the main mechanisms involved in the regulation of DAT activity and of DA cytosolic concentration (Sidhu *et al*., 2004 ; Wersinger and Sidhu, 2005). Within the presynaptic terminal, α-syn has

been implicated as one of the proteins involved in the transportation of DAT to and from the plasma membrane (Wersinger and Sidhu, 2005).

α-Syn forms a heteromeric complex with DAT, with the last 22 residues of DAT associating with residues 58 – 107 of α-syn, a region that is in the NAC region (Lee *et al*., 2001; Wersinger and Sidhu, 2003a). Cells co-expressing α-syn and DAT, showed a 35 % reduction in DAT activity compared to cells transfected with DAT alone. α-Syn previously been shown to associate with a number of cytoskeletal protein such as tubulin, microtubulin, tau (Jensen *et al*., 1999; Zhou *et al*., 2004; Alim *et al*., 2004), and can also associate with α- and β-tubulin when in complex with DAT (Wersinger and Sidhu 2005). α-Syn has also been shown to increase DAT mobility and targeting to the plasma membrane, leading to the suggestion that it acts as an anchor tethering DAT to the microtubular network prior to its transportation across the cytoplasmic membrane (Wersinger and Sidhu, 2003a; Wersinger and Sidhu, 2005). This hypothesis was further strengthened by the suggestion of α-syn as a possible slow component-b protein of axonal transport (Roy *et al*., 2007), shuttling DAT to and from the cellular membrane.

A consequence of α-syn regulating vesicle trafficking, DA biosynthesis and reuptake, is the increased exposure of the cell to the cytotoxic properties of DA (Wersinger and Sidhu, 2003b). This interaction between α-syn and DA may be important in the link between α-syn and neurodegenerative disorders such as PD (Rochet *et al*., 2004; Follmer *et al*., 2007).

1.2 Parkinson's disease.

While a physiological role of α-syn is only just beginning to emerge, an involvement in the pathophysiology of diseases such as PD has been recognised for decades. PD is a progressive neurological disorder first described in 1817 by Dr James Parkinson in the essay entitled "An Essay on the Shaking Palsy'' (Parkinson J, 2002 (reprint)). While the majority of PD patients present with idiopathic PD, 5 - 10 % of PD patients have a pre-disposing genetic mutation for PD (Cordato and Chan, 2004; Gandhi and Wood, 2005). These genetic abnormalities all link directly or indirectly to α-syn.

1.2.1 Symptoms and neuropathology of PD.

PD is clinically a movement disorder with patients initially presenting with resting tremor, rigidity, loss of balance and bradykinesia (slowness of movement). With the development of the disease the symptoms increase in severity and the patient develops secondary symptoms including loss of dexterity, difficulties in co-ordination, visual symptoms such as hallucinations or loss of vision, depression, pain and sensory discomfort, sexual difficulty, blood pressure changes, dermatological changes, gastrointestinal, and urinary difficulty (Duvoisin, 1978; Lieberman and Williams, 1993; Marsden and Fahn, 1995; Valls-sole and Valldeoriola, 2002). Many PD patients develop a characteristic walk of a fast-shuffling gait, finding it hard to start walking and once in motion finding it equally as difficult to change direction or stop quickly (Longstaff, 2000). The progression of symptoms are mirrored by degeneration of the dopaminergic cell bodies within the basal ganglia, specifically the SNpc, loss of the nigrostriatal projections from the SNpc and a substabtial

reduction in DA in the striatum. The terminal decline of these dopaminergic neurones and the loss of DA in the striatum results in abnormal regulation of the motor pathways within the cortex. This is speculated to be the mechanism responsible for the development of symptoms such as bradykinesia and rigidity within the PD sufferer (figure 1.8) (Hallett and Khoshbin, 1980; Dewaide *et al.,* 2000; Valls-Solé and Valldeoriola, 2002).

Dopamine receptors are found on both the pre- and post-synaptic ends of neurones and are involved in regulating the activation and release of neurotransmitters. Different receptors modulate different reactions. D1 receptors are coupled with the adenyl cyclase 5'-adenosine (cAMP) second messenger system, enhancing the excitatory input and resulting in an increase cAMP synthesis. D2 receptors are coupled with G-proteins that inhibit adenyl cyclase, thus reducing cAMP synthesis and reducing the excitatory affect. D2 receptors are also auto-receptors on dopaminergic neurones in the SNpc and ventral tegmentum controlling DA synthesis (Herman *et al.,* 1994; Jaber *et al.*, 1996; Blandini *et al.,* 2000; Longstaff, 2000; Onn *et al.,* 2000) by reducing cAMP levels and inhibiting PKA-mediated TH synthesis (Jaber *et al.*, 1996; Longstaff, 2000). When D3 auto-receptors are activated by DA binding, they signal the closure of pre-synaptic Ca^{+2} channels that in turn reduce the release of DA into the synaptic cleft (Jaber *et al.*, 1996; Longstaff, 2000). Therefore, DA mainly acts in three mechanistic pathways. The first is the aforementioned SNpc pathway that is important in motor control (Jaber *et al.*, 1996; Rang *et al.*, 1999; Longstaff, 2000). Secondly, there are the mesolimbic/mesocortical pathways whereby dopaminergic cells based in the midbrain run axons through to the limbic

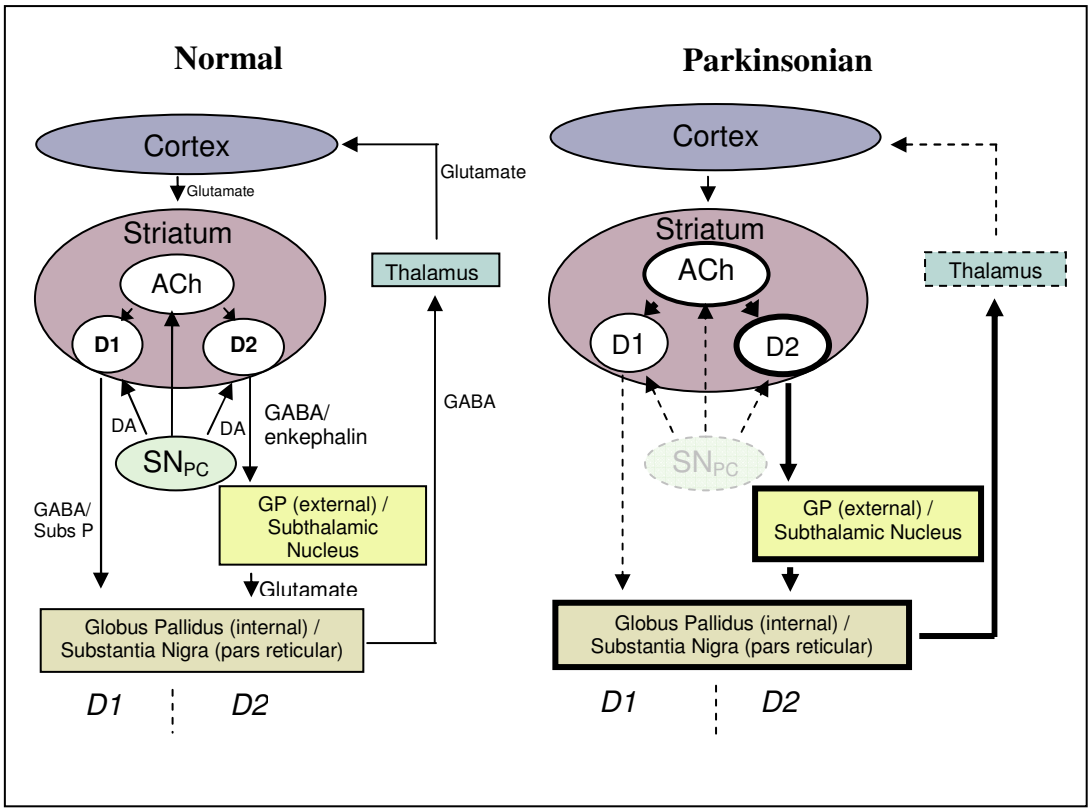

Figure 1.8: Schematic of the brain regions and pathways effected by PD.

A schematic diagram showing the normal pathways and neurotransmitters linking between the brain regions and how PD affects the pathways and reduces the neurotransmitters within these brain regions. ACh = acetylcholine (neurotransmitter), DA = dopamine (neurotransmitter), GP = Globus Pallidus and GABA = γ-amino-butyric acid (neurotransmitter) (adapted from Blandini *et al.*, 2000).

system (i.e. the cortex) and are involved in the control of emotions and drug-induced reward systems (Herman *et al.,* 1994; Jaber *et al.*, 1996). Finally, there are the tuberohypophyseal neurones located in the hypothalamus that are involved in the regulation of pituitary-gland secretions (Jaber *et al.*, 1996; Rang *et al.*, 1999). At present it is believed that, with PD-induced dopaminergic cell loss, the remaining neurones overproduce DA. The number of DA receptors and other neurones are also increased giving rise to a hypersensitive state (Herman and Abrous, 1994). These attempts by neuronal cells to preserve the integrity of DA transmission critically determine the effectiveness of drug treatments such as levodopa, which are designed to compensate for the lack of endogenously produced DA (Jaber *et al.*, 1996).

PD symptoms only present themselves when over 50 % of the dopaminergic neurones projecting into the striatum have been lost (Cornford *et al.,* 1995; Zhang *et al.,* 2000; Braak *et al.,* 2003). A definitive diagnosis of PD can only be determined upon examination of the brain at post-mortem, as a number of other degenerative diseases of CNS present with parkinsonism (PD symptoms) such as Multisystem atrophy (MSA) (Cornford *et al.,* 1995; Valls-Solé and Valldeoriola, 2002). A diagnosis of PD is confirmed by the observation of selective neuronal loss in the SN, along with the identification of characteristic α-syn containing LBs and LNs (Cornford *et al.,* 1995; Forno, 1996; Mezey *et al.,* 1998; Zhang *et al.,* 2000; Wood-Kaczmar *et al.,* 2006). However neuronal loss is also observed in the dorsal motor nucleus of the vagus, the hypothalamus, cholingeric nucleus basalis Meynert, locus coeruleus (LC), midbrain, raphe nuclei, cerebral cortex and olfactory bulb (Cornford *et al.,* 1995; Forno *et al.,* 1996). The progression of PD has been suggested to start in

the brainstem (dorsal motor neucleus of the vagal nerve) progressing into the midbrain and forebrain, and finally into the cerebral cortex (Braak *et al.,* 2003; Braak *et al.,* 2004). This is accompanied with gradual development of LBs (protein aggregates in the somata of cells) and LN (similar deposits in the axons and dendrites) of selective neurones in SN, LC, cerebral cortex, anterior thalamus, hypothalamus, amyygdala and basal forebrain (Cornford *et al.,*1995; Takahashi and Wakabayasgi*.,* 2001; Wood-Kaczmar *et al.,* 2006). Long axoned, partially or none myelinated neurones and melanin-containing dopaminergic neurones are predominately affected by the progression of PD, with short axoned cells appearing to be resistant to the pathology (Foley and Riederer, 2000; Braak *et al.,* 2003; Braak and Del Tredici 2004; Braak *et al.,* 2006).

Mitochondrial dysfunction, specifically a decrease in the activity of complex I in the electron transport chain (ETC), has been identified as a main characteristic of PD (Schapira *et al.,* 1989; Reichmann and Janetzky, 2000; Zhang *et al.,* 2000) along with increase oxidative stress (Foley and Riederer, 2000). The decrease in complex I activity has been shown to be limited to the SNpc and neurones containing high levels of melanin (Janetzky *et al.,* 1994; Reichmann and Janetzky, 2000). Interestingly, no mitochondrial dysfunction was identified within any other brain region, not even in the SNpr (Janetzky *et al.,* 1994; Reichmann and Janetzky, 2000). Analysis of mitochondrial enzymes (eg. citrate synthetase and hydroxyacyl-CoA dehydrogenase) and cyoplasmic enzymes (eg. pyruvate kinase and lactate dehydrognease) from PD brains, revealed no change in the level or activity of other mitochondrial proteins within PD brains (Schapira *et al.,* 1989; Mizuno *et al.,* 1990;

Reichmann and Janetzky, 2000). The cause of the mitochondrial dysfunction by reduced complex I activity is still not fully understood however, it is thought increased oxidative stress, free radicals (Olanow, 1993; Foley and Riederer, 2000; Martin *et al.,* 2003) and increased iron levels observed in PD patients brains, mainly in the SN (Dexter *et al.,* 1987; Sofic *et al.,* 1988; Sofic *et al.,* 1991), may be linked.

The underlying mechanisms involved in the causation of sporadic forms of PD remain obscure but a number of environmental causes have been implicated. These include, arteriosclerotic parkinsonism induced by multiple small strokes (Inzelberg *et al.,* 1994, Rang *et al.*, 1999), heavy metals (e.g. manganese or iron) (Graham, 1984; Sengstock *et al.,* 1992; Nakano, 1993; Montgomery, 1995), carbon monoxide (Klawans *et al.,* 1982) and neurotoxins such as MPP^+, rotenone (Lee *et al.* 2002; Shimohama *et al*. 2003; Fernagut and Chesselet, 2004), paraquat (Fukushima *et al.,* 1993; Liou *et al.,* 1996; Dinis-Oliveira *et al.,* 2006) and 6-hydroxydopamine (6-OHDA) (Ungerstedt, 1968; Sachs and Jonsson, 1975; Soto-Otero *et al.,* 2000) and certain drugs such as the psychiatric treatments chlorpromazine and haloperidol (Marsden and Fahn, 1995; Rang *et al.*, 1999).

Due to the progressive nature of the disease it has been suggested there is a predetermined sequence of disease progression which moves up from the brain stem and systematically progressing upwards into the cortex (figure 1.9) (Braak *et al.,* 2004). It has been suggested that a pathogen such as a neurotropic virus or a pathogen possessing unconventional, prion-like, properties could be involved in the pathogenesis of PD (Braak *et al.,* 2004). It has been implied that such a pathogen

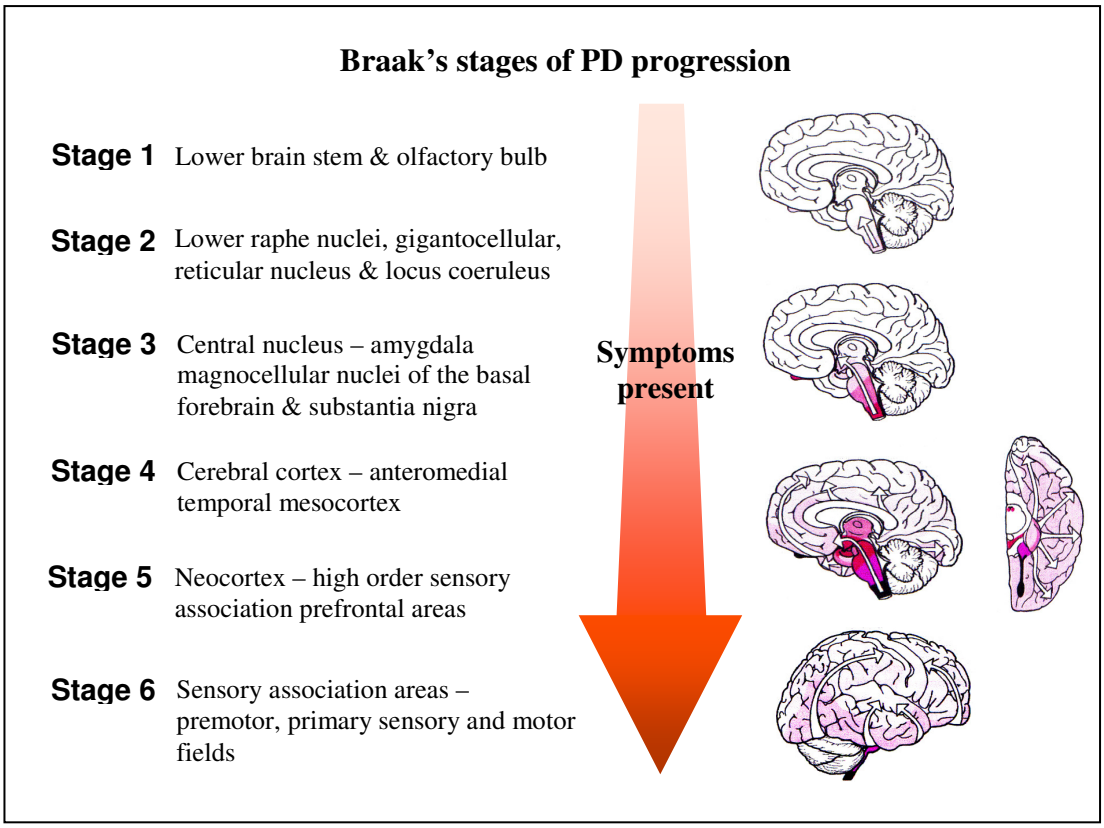

Figure 1.9: **Schematic of the Braak's stages of the progression of PD.**

Schematic representation of Braak's stages of PD showing the progression of PD through the different regions of the brain from the brain stem up through the cortex. Symptoms only present once the neurodegeneration has reached the central nucleus or stage 3. The red graduated arrows and the white arrows located in the brain diagrams, indicates the progression of the increasing neurodegeneration through the brain (adapted from Braak *et al.,* 2003).

could enter the body through the mucosa membrane of the stomach and pass into the PNS (Braak *et al.,* 2003). A possible pathogen could then be transferred directly from neurone to neurone by species-specific, selective types of synapses or by receptor mediated endocytosis, up through the PNS into the brain stem (Braak *et al.,* 2003; Braak *et al.,* 2004; Braak *et al.,* 2006). The pathogen then causes specific neuronal cell death (Braak *et al.,* 2003). This has been speculated through the observation of a large number of LBs within the PNS of the stomach (Wakabayashi *et al.,* 1993; Braak *et al.,* 2003).

1.2.1.1 Lewy bodies and Lewy neurites.

LBs and LNs were first identified and described by Fredrick Lewy (1912) (Lewy, 1912). LBs are circular intracellular inclusions of approximately 5 – 25 μm in diameter and are composed of a dense granular core with filaments radiating out giving the impression of a halo (figure 1.10A and B) (Goedert *et al.,* 1998; Mezey *et al.,* 1998; Flint Beal, 2001). The primary components of LBs are α-syn and ubiquitin (Lowe *et al.,* 1988; Cornford *et al.,* 1995; Spillantini *et al.,* 1997; Mezey *et al.,* 1998). LNs are very similar to LBs containing abnormal filaments, also primarily composed of α-syn and ubiquitin (Spillantini *et al.,* 1997; Mezy *et al.,* 1998; Goedert *et al.,* 1998) within the axons and dendrites of neurones (figure 1.10C) (Spillantini *et al.,* 1997; Spillantini *et al.,* 1998a; Spillantini *et al.,* 1998b).

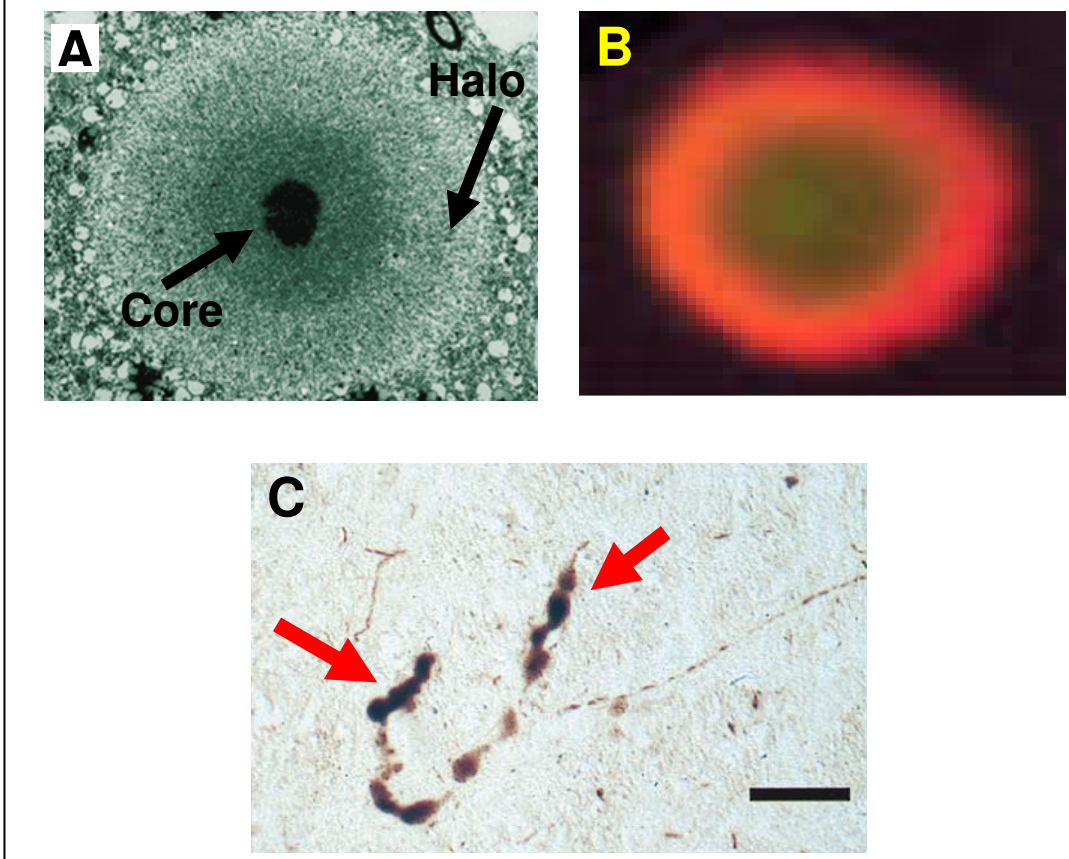

Figure 1.10: Illustrations of LBs and LNs within neurones of the substantia nigra of PD patients.

A) Transmission electron mircograph of a LB at 6,000 x magnification with arrows highlighting the core and halo of the LB (adapted from Forno, 1996). **B)** LB located in compact zone of the SN. Two colour image of the LB stained for ubiquitin (green) and α-syn (red), which identifies the core as being primarily ubiquitin, with some α-syn (overlaying as orange) and the α-syn radiating out to form the periphery of the LB (red) (adapted from Mezey *et al.,* 1998). **C)** LN double-stained for α-syn and ubiquitin in neurones located in the SN. The Bar = 90 mm and the red arrows indicate the LN (adapted from Spillantini *et al.,* 1998b).

1.2.2 Synucleinopathies.

Through the identification of α-syn as the major protein involved in the formation of LBs (Spillantini *et al.,* 1997), α-syn has been linked to a number of neurodegenerative disorders classified as synucleinopathies (see table 1.1) (Duda *et al.,* 2000; Murray *et al.,* 2001). Within this group of neurodegenerative disorders, disease progression sees the neurodegeneration of brain regions that contain selectively vulnerable populations of neurones (Murray *et al.,* 2001) and the development of pathologic lesions composed of aggregated α-syn (Duda *et al.,* 2000). Diseases such as; PD, DBL, MSA (Spillantini *et al.,* 1998a), LB variant of AD (Takeda *et al.,* 1998; Wirths *et al.,* 2000), and neurodegeneration with brain iron accumulation type I (Arawaka *et al.,* 1998) have been classed as synucleinopathies (Duda *et al.,* 2000; Galvin *et al.,* 2001; Murray *et al.,* 2001). With these disorders the patient develops either parkinson-like symptoms, dementia or a combination of both (Galvin *et al.,* 2001). For example, in both LB variant of AD and DLB, progressive dementia is seen in the sufferer, with the presence of LB staining positive for α-syn in the cortex, senile plaques and neurofibrillary tangles also develop within both disorders (McKeith *et al.,* 1996; Takeda *et al.,* 1998; Spillantini *et al.,* 1998a; Spillantini *et al.,* 1998b; Wirths *et al.,* 2000). In the case of LB variant AD the patients develop mild parkinsonism symptoms (increase in essential tremor, bradykinesia, mild neck rigidity, and slowing of rapid alternating movements) with progressive dementia indistinguishable from AD (Hansen *et al.,* 1990). With DBL the patients develop similar parkinsonism symptoms to PD including bradykinesia and rigidity (but not resting tremors) and visual hallucinations (McKeith *et al.,* 1996; Geser *et al.,* 2005). However DLB patients also develop progressive late-onset

Table 1.1: Synucleinopathies.

Parkinson's Disease
- Sporadic
- Familial with α-syn mutations
- Familial with mutations other than α-syn

Dementia with Lewy bodies
- "Pure" Lewy body dementia
- Lewy body variant of Alzheimer disease
- Family Alzheimer disease with amyloid precursor protein mutations
- Family Alzheimer disease with presenilin-1 mutations
- Family Alzheimer disease with presenilin-2 mutations
- Down syndrome

Multiple system atrophy
- Shy-Drager syndrome
- Striatonigral degeneration
- Olivopontocerebellar atrophy

Neurodegeneration with brain iron accumulation, type I
- Hallervoden-Spatz syndrome
- Neuroaxonal dystrophy

Picks disease

Other diseases that may have synuclein-immunoreactive lesions
- Traumatic brain injury
- Amyotrophic lateral sclerosis

Examples of neurological disorders which are classed as synucleinopathies (adapted from Galvin *et al.,* 2001)

AD-like dementia which is associated with the formation of cortical LBs (McKeith *et al.,* 1996) as the number of cortical LBs correlates with the severity of dementia (Sameul *et al.,* 1996). Through the investigation of one synucleinopathy it is hoped that this would help to understand the other neurodegenerative disorders and lead to the development of possible therapeutic treatments (Duda *et al.,* 2000; Galvin *et al.,* 2001; Murray *et al.,* 2001).

1.2.3 Therapeutic interventions for PD.

There are many treatments available to PD patients, from drug treatment through to surgical interventions. However, none of the available treatments at present are a cure and they do not stop the progression of the disease (Carlsson *et al.,* 2007; Singh *et al.,* 2007). The therapies for PD are symptomatic against the consequences of PD pathophysiology (Bittar, 2006; NCC-CC, 2006; Carlsson *et al.,* 2007; Singh *et al.,* 2007). The main drugs initially used are the oral administration of either levodopa (a DA precursor), a DA agonist or a combination. (figure 1.11) (Carlsson *et al.,* 2007; Singh *et al.,* 2007). To reduce peripheral metabolism of levodopa, it is often combined with a peripheral dopa decarboxylase inhibitor, such as carbidopa or benserazide, increasing the amount of levodopa that crosses the blood-brain barrier (NCC-CC, 2006). The progression of the disease leads to increasing concentrations of levodopa required to maintain the levels of control over the motor symptoms which leads the development of motor complications caused by the levodopa, such as; involuntary movement or dyskinesias, dystonia, response fluctuations (‘wearing off’).

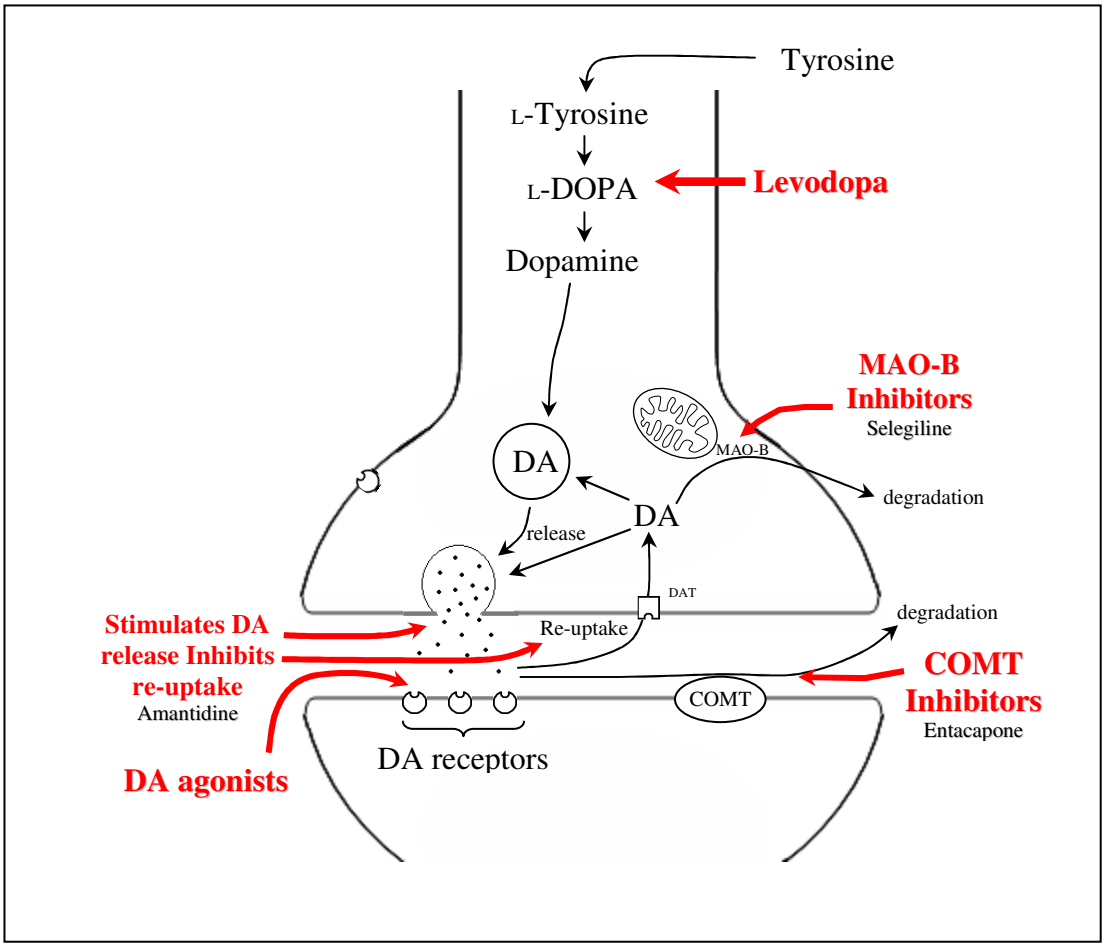

Figure 1.11: Schematic of dopaminergic synapse and examples of PD drugs that influence DA synthesis, degradation, uptake or mimic DA.

The diagram shows examples drugs that are used to treat PD such as inhibitors of DA degradation by inhibiting Monoamine oxidase B (MAO-B) by selegiline and inhibition of catechol-Omethyl transferase (COMT) by entacapone, leading to increased levels of DA reuptake. Amantidine is speculated to inhibit DA uptake and increase DA release increasing activation of DA receptors. Levodopa increases DA synthesis and finally there are DA agonists that mimicking DA binding and activating DA receptors and finally (Adapted from Singh *et al.,* 2007).

DA agonists mimic the effects of DA by binding directly to the posts-synaptic DA receptors (figure 1.11). DA agonists are divided in to two categories; ergot-derivatives such as bromocriptine, pergolide, lisuride and cabergoline, and non-ergot derivatives including ropinirole, pramipexole, apomorphine and piribedil (Singh *et al.,* 2007).

Other therapies include monoamine Oxidase-B (MAO-B) inhibitors, such as selegiline and rasagiline (primarily used in later PD stages to decrease DA metabolism). Amantadine (possibly works by increasing DA release and reducing uptake), catechol-Omethyl transferase (COMT) inhibitors (e.g. entacapone and tolcapone that work similar to the MAO-B inhibitors by reducing the metabolism of DA increasing the half-life of levodopa by 30 - 50 %) (figure 1.11) (NCC-CC, 2006; Singh *et al.,* 2007).

There are also a number of different neurosurgical procedures that can be employed to alleviate individual symptoms of PD ranging from subthalamotomy to deep brain stimulation (NCC-CC, 2006). Such treatments for individual symptoms are extremely varied and tend to be viewed as a last resort for patients who respond to drugs, but have severe side-effects or severe fluctuations in response to medication (NCC-CC, 2006). The preferred surgeries tend to be deep brain stimulation (DBS) where a quadripolar electrode is inserted in to the subthalamic nucleus (STN), globus pallidus interna or the thalamus (Lozano, 2001; Hashimoto *et al.*, 2002; Lopiano *et al.*, 2002; NCC-CC, 2006; Singh *et al.,* 2007). The more invasive surgery,

subthalamotomy, involves the destruction of the thalamus, globus pallidus or the STN (Weekly, 1995; NCC-CC, 2006).

Stem cell transplantation is another approach to repair damaged areas of the brain, with the potential of long-term relief from symptoms and eventually the possibility of a cure (Storch and Schwarz, 2002; Lindvall and Kokaia, 2006). In principle, the experimental technique involves the implantation of dopaminergic neurones, derived from stem cells, into an adult living brain in order to replace and regenerate the damaged neuronal systems (e.g. by releasing growth factors) (Hynes and Rosenthal, 2000; Storch and Schwarz, 2002; Lindvall and Kokaia, 2006). The stem cells used are primarily embryonic stem cells, but researchers are also looking into using stems cells isolated from; foetuses, the adult brain, bone marrow stoma, liver, skin and muscle (Hynes and Rosenthal, 2000; Lindvall and Kokaia, 2006; Singh *et al.,* 2007). At present the approaches are still in the early stages of development with low cell survival and potentially fatal side effects in a few patients (Clarkson and Freed, 1999; Kompoliti *et al.,* 2007; Singh *et al.,* 2007).

1.2.4 Familial Parkinson's Disease.

Familial PD is attributed to rare mutations that cause autosomal recessive and dominant parkinsonism. Six gene loci have been fully characterised which contain PD inducing mutations; α-syn, Ubiquitin carboxyl-terminal hydrolase-L1 (UCH-L1), ubiqitin protein ligase (Parkin), PTEN-induced kinase 1 (PINK1), DJ-1 and Leucine-rich repeat kinase 2 (LRRK2) (Polymeropoulos *et al.,* 1997; Leroy *et al.,* 1998; Alvarez *et al.,* 2001; Abou-Sleiman *et al.,* 2004; Paisán-Ruíz *et al.,* 2004; Valente *et*

al., 2004; Sellbach *et al.,* 2006). Further loci have been associated with familial PD, but the specific genes have not been isolated (table 1.2) (Le and Appel, 2004, and Sellbach *et al.,* 2006).

Table 1.2: Loci and genes which cause familial forms of PD.

Locus	Chromosome	Gene	Inheritance	Onset
PARK1	4q21 - q23	*α-synuclein*	AD	Middle - late
PARK2	6q25 - q27	*parkin*	AR	Early - juvenile
PARK3	2p13	-	AD	Late
PARK4	4p15	-	AD	Late
PARK5	4p14	*UCH-L1*	AD	Late
PARK6	1p35 - p36	*PINK1*	AR	Early
PARK7	1p36	*DJ-1*	AR	Early
PARK8	12p11.2 - q13.1	*LRRK2*	AD	Late
PARK9	1p36	-	AR	Juvenile
PARK10	1p32	-	-	Late
NR4A2	2q	-	AD	Late

List of suspected genes and loci of familial forms of PD. AD and AR indicated whether the locus contains a mutation that causes autosomal dominant (AD) or autosomal recessive (AR) PD. (Adapted from Le and Appel, 2004, and Sellbach *et al.,* 2006)

1.2.4.1 Structural mutations of α-syn.

The involvement of α-syn in the pathophysiology of PD has been speculated since the identification of aggregated α-syn as the main LB protein (Spillantini *et al.,* 1997). Currently there are a number of possible theories as to this involvement of the α-syn protein in disease progression. Although the wild-type (wt), monomeric form of α-syn does not appear to be detrimental to the cell (and may have a physiological function) it has the potential to form aggregates as previously mentioned (Section 1.1.2.1). Increases in α-syn concentration, oxidative stress and the presence of DA may all cause an increase in α-syn aggregation (Hashimoto *et al.,*1999; Lowe *et al.,* 2004; Cappai *et al.,* 2005). The presence of the NAC region in α-syn is believed to increase the proteins ability to aggregate and form fibrils (via protofibril intermediates) (Uversky *et al*., 2002).

The identification of α-syn ability to self-aggregate and α-syn presence in LB has lead to the hypothesis implicating aggregated α-syn as being toxic and involved in the progression of PD (El-Agnaf *et al.,* 1998). However a number of alternative theories have since been suggested, such that the fibril formation of α-syn maybe a protective mechanism sequestering the potentially toxic intermediate (protofibril) form of α-syn (Conway *et al.,* 2000a). This theory implies, therefore, that either the protofibril or monomeric form of α-syn is the pathogenic form. The discovery of three missense point mutations in α-syn has shed some light as to the mechanisms involved in PD progression in relation to the α-syn protein. The mutant forms of α-syn, which have been linked to early onset PD, have been shown to have varying rates of aggregation that appears to affect their toxicity in cells compared to wt

α-syn. The A30P mutation was shown to form protofibrils quicker than wt α-syn, although full aggregation appears to be at the same rate (Narhi *et al.,* 1999; Greenbaum *et al.,* 2005). Therefore the A30P mutation promoted the formation of protofibrils but not fibrils. The A53T mutation promotes the formation of full fibrils removing α-syn from the cellular system and promoting an increase in α-syn expression, further aggregation and the presence of protofibrils. Triplication of the *α-syn* gene increases α-syn protein expression and is linked to late onset PD, identifying the accumulation of α-syn promotes aggregation of α-syn and the formation of protofibrils (Section 1.1.2.1) (Singleton *et al.,* 2003; Farrer *et al.,* 2004; Miller *et al.,* 2004; Singleton *et al.,* 2004). However, this does not discount the soluble or the fibril form as being the pathogenic agent in PD, but highlights its involvement through its aggregation pathways.

1.2.4.1.1 α-Syn A53T mutation.

The A53T mutation in α-syn was first characterised in a cohorts of PD patients from the same Italian/Greek family by Polymeropoulos *et al*. (1997). This mutated form of the α-syn protein is indistinguishable from the wt protein in both its cytosolic and membrane bound conformations (Conway *et al*. 1998; Jo *et al*. 2002). However, the A53T mutation was seen to have an increased rate of aggregation compared to the wt (Conway *et al*. 1998). *In vitro*, the over expression of in A53T α-syn in cells increased both the number of protein inclusions and toxicity (Zach *et al.,* 2007).

1.2.4.1.2 α-Syn E46K mutation.

The E46K mutation, first described by Zarranz *et al*. (2004), was isolated from a Spanish family. It was found that the mutation at residue 46 changed the polarity of the surrounding residues, resulting in an alteration of the function of this region of α-syn (i.e. an increase in the proteins ability to bind negatively charged liposomes) (Choi *et al*. 2004). In a similar respect to the A53T mutation, the E46K mutation also has an increased rate of fibril formation (Choi *et al*. 2004; Greenbaum *et al*. 2005), where the formed filaments tend to be more tightly twisted than seen in the A53T mutation (Choi *et al*. 2004).

1.2.4.1.3 α-Syn A30P mutation.

The third α-syn mutation, in a German family, was first described by Krüger *et al*. (1998). Again, like the A53T mutation, the A30P mutation does not appear to affect the overall cytosolic structure of the protein (Conway *et al*. 1998). The mutated protein does, however, appear to have a reduced capacity for binding cellular vesicles via electrostatic interactions (Jensen *et al*. 1998). This has been suggested to lead to a build up of protein in neural cell bodies resulting in aggregation (Kahle *et al*. 2000). Interestingly, the A30P mutation has an increased rate of aggregation (albeit the slowest of the three mutations), but expresses the slowest rate of fibril formation (Narhi *et al*. 1999). This would suggest that the A30P mutant α-syn favours the formation of the protofibril intermediates rather than the full aggregated fibril form of α-syn. Furthermore, the A30P α-syn mutant is not able to undergo the conformational change required for the binding of the protein to lipid membranes

(i.e. the random coil to α-helix). This loss of function increases the cytosolic fraction of α-syn, further promoting fibril formation (Jo *et al*. 2002).

Interestingly, Jo *et al*. 2002 expressed both the A53T and A30P mutant proteins *in vitro*. The A30P mutant was found to be dominant over the A53T mutant in terms of impairing membrane binding properties of α-syn. There was an overall increased rate in aggregation (Narhi *et al*. 1999).

1.2.4.2 Familial PD through increased α-syn expression.

Multiple copies of the α-syn gene were identified within a family, termed the Iowa kindred, which caused early onset of PD and increased the speculation that α-syn played a role in the pathogenesis of disease progression (Singleton *et al.,* 2003; Farrer *et al.,* 2004; Miller *et al.,* 2004; Singleton *et al.,* 2004). Within the Iowa kindred a triplication of the α-syn gene gave rise to four fully functional copies of the α-syn gene within the chromosome (Chr 4q) (Miller *et al.,* 2004). The triplication of the gene does not appear to cause any alteration in the functional role of α-syn. However, as all four genes are fully functional this leads to an increased expression of α-syn protein and a doubling of the concentration of the protein and mRNA within the brain (Miller *et al.,* 2004). The increased concentration of α-syn appears to increase the rate of α-syn aggregation and induces the early-onset of PD with an average age of approximately 34 years, and an increased likelihood of developing dementia (Farrer *et al.,* 2004; Singleton *et al.,* 2004). A duplication of the α-syn gene has also been identified in a separate family, but unlike the triplication of α-syn, this

induces late onset PD, which appears indistinguishable from idiopathic PD (Ibáñez, *et al.,* 2004; Chartier-Harlin *et al.,* 2004; Fuchs *et al.,* 2007).

1.2.4.3 Familial PD induced by UPS dysfunction.

Mutations in two important enzymes involved in the Ubiquitin-proteasome system (UPS) have been identified (UCH-L1 and parkin, see below). These mutations can result in their loss of function and ultimately result in the development of autosomal PD. The UPS plays an essential role in the rapid degradation of abnormal proteins within cells, targeting mislocated, misfolded, mutant and damaged proteins for degradation (McNaught *et al.,* 2001; Dev *et al.,* 2003). The system consists of a series of enzyme-mediated reactions which identify and covalently bind multiple ubiquitin molecules to abnormal proteins marking the protein for degradation by 20/26S proteasomes (figure 1.12). Initially, monomeric ubiquitin molecules are activated by ubiquitin-activation enzymes E1 through an adenosine triphosphate (ATP) mediated system (McNaught *et al.,* 2001; Dev *et al.,* 2003). The activated ubiquitin molecules are transferred to a substrate specific ubiquitin–conjugated enzyme (E2), and ubiquitin-protein ligase (E3) catalyses the ligation of the activated ubiquitin molecules on to lysine residues of the abnormal protein, marking it for degradation (McNaught *et al.,* 2001; Dev *et al.,* 2003). 20/26S proteasomes recognise the polyubiquitin tagged protein and break up the abnormal protein to produce short peptides chains and amino acids, which are subsequently recycled to produce new proteins (McNaught *et al.,* 2001; Dev *et al.,* 2003). The polyubiqitin chains are released by the 26S proteasome and dissembled by ubiquitin carboxyl-

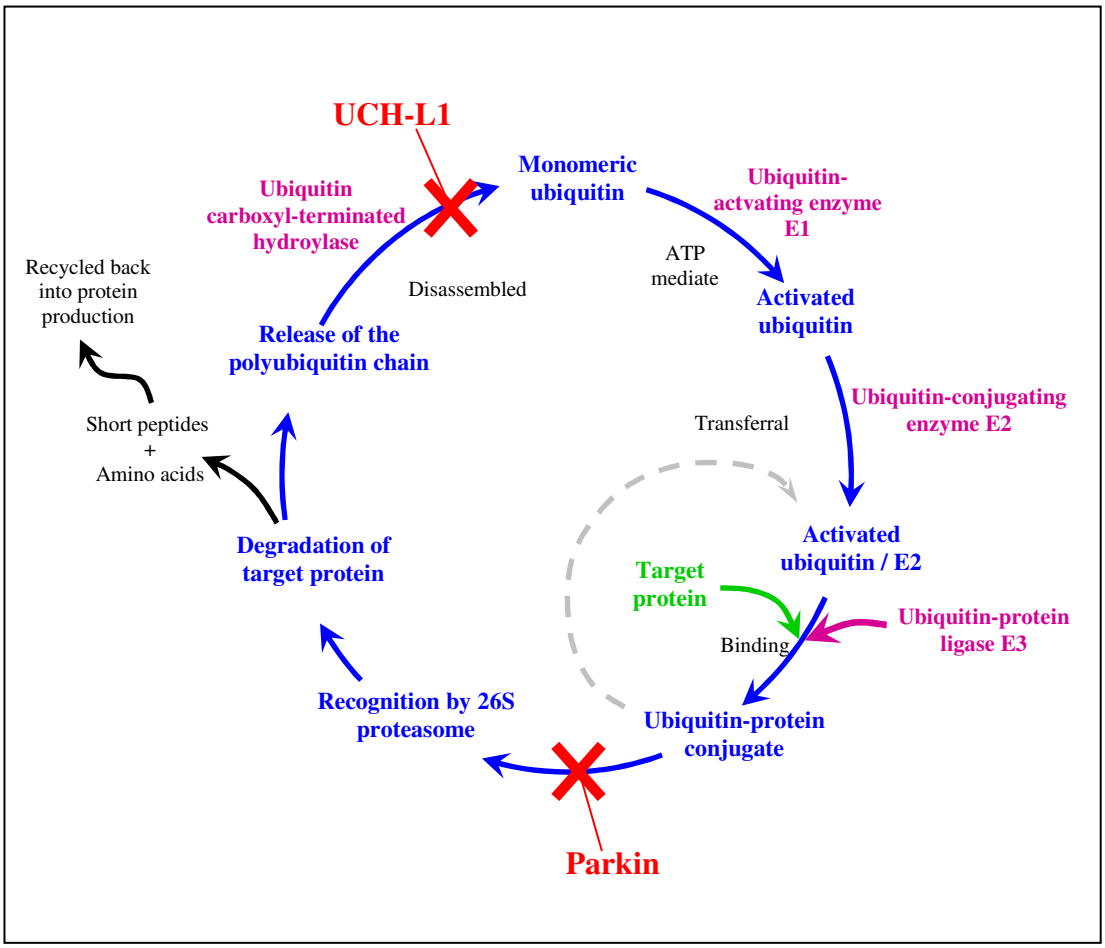

Figure 1.12: Flow diagram showing the ubiquitin-proteasome system and PD associated mutations.

The ubiquitin-proteasome system (UPS) degrades proteins targeted with polyubiquitin chains. Monomeric ubiquitin molecules are activated by the ubiquitin-activation enzyme E1 and are then transferred to ubiquitin–conjugated enzyme E2 (McNaught *et al.*,2001; Dev *et al.*, 2003). E2 enzymes and ubiquitin-protein ligase E3 bind the activated ubiquitin molecules via lysine residues on the protein targeted for degradation. This can be repeated numerous times (grey arrow) until the target protein is recognised by the 26S proteasome and degraded. Degradation produces short peptide chains and amino acids, which are recycled back into the formation of new proteins. The polyubiqitin chains are released by the 26S proteasome and disassembled by ubiquitin carboxyl-terminated hydrolases. The monomeric ubiquitin molecules are recycled in the UPS. Mutations in Parkin and UCHL-1 disrupt the pathways (marked by red crosses) and prevent the degradation of targeted proteins.

terminated hydrolases and re-enter the UPS (McNaught *et al.,* 2001; Dev *et al.,* 2003).

Ubiquitin carboxy-terminal hydrolase-L1 (UCH-L1) is a neuronal de-ubiquitination enzyme (Satoh and Kuroda, 2001) and is an essential part of the UPS (Leroy *et al.*, 1998; Satoh and Kuroda, 2001). The main role of this enzyme family is to disassemble polymeric ubiquitin to monomers by the hydrolysis of the bonds between ubiquitin molecules and small adducts (e.g. glutathione and cellular amines (McNaught *et al.,* 2001)). The substitution of a methionine (M) for isoleucine (I) at amino acid position 93 (Leroy *et al.*, 1998; Harhangi *et al.*, 1999; MacDonald, 1999; Mellick and Silburn, 2000; Satoh and Kuroda, 2001) results in a truncated protein and dysfunction of the UPS. Ultimately, the pathway affected by the mutation results in the progressive accumulation of neuronal and glial inclusions composed of ubiquitinated protein aggregates including α-syn, which are implicated in neurodegeneration (figure 1.12) (Leroy *et al.*, 1998; Harhangi *et al.*, 1999; Satoh and Kuroda, 2001).

Deletions within the 4^{th}-exon of the *parkin* gene (which codes for the ubiquitin protein ligase (E3) parkin) have been linked to autosomal recessive juvenile parkinsonism (AR-JP) (Mizuno *et al.*, 1999). Mutations in the parkin gene are the most common form of familial PD with ~ 50 % of familial cases of PD showing a parkin mutation and have been shown to range from single nucleotide deletions to hundreds of nucleotide deletions or missense mutations. The mutations in the parkin gene have been suggested to either affect the E2 enzyme binding region of parkin,

impairing the parkin protein interactions with the substrate protein, or reduce E3 ligase activity, causing improper targeting of substrates for proteasomal degradation. The consequence of either mechanism is the accumulation of potentially neurotoxic proteins such as α-syn and aggregated α-syn (figure 1.12).

1.2.4.4 Mitochondrial protein associated mutations.

The PINK1 gene, located on chromosome 1p35-p36, encodes a putative protein kinase that shows a high level of sequence homology to serine-threonine kinases of the Ca^{2+}/calmodulin family (Valente *et al.,* 2004). The PINK1 protein is primarily located within mitochondria, more specifically the mitochondrial membrane. However, beyond helping in the protection of cells from oxidative stress (Tang *et al*. 2006), its function is unknown.

Similarly, the protein encoded by the DJ-1 gene is believed to have a primary role as an antioxidant (Abou-Sleiman *et al.,* 2004), as it contains many readily oxidised residues (Kinumi *et al.,* 2004). Furthermore, the DJ-1 protein is believed to act as a redox dependent chaperone, which sequesters free radicals from the mitochondria helping to protect it from oxidative stress (it is found in both, the mitochondrial matrix and inter-membrane space as well as the cytoplasm) (Gandhi and Wood 2005). However, the exact role of this protein is still unclear and not well reported in the literature.

1.2.4.5 Leucine-rich repeat kinase 2 (LRRK2) mutations.

The Leucine-rich repeat kinase 2 (Lrrk2) protein is also known as dardarin. First termed by Paisán-Ruiz *et al* (2004), dardarin is a 286 kDa protein belonging to the family of protein kinases that has a similar sequence to the tyrosine and serine-threonine kinases, a characteristic shared with the PINK1 protein. Lrrk2 is believed to be a predominately cytoplasmic protein and may co-express with parkin to increase cytoplasmic protein aggregates and enhance their ubiquitination (Smith *et al*. 2005).

At least nine pathogenic mutations are known to exist in Lrrk2, where the mutation of the Lrrk2 protein is the most common known cause of late-onset, idiopathic and familial PD (Giasson *et al*. 2006). Two of the most common mutations in this protein, G2019S and I2020T, have been mapped to the protein kinase catalytic domain, where their presence seems to incur an increase in kinase activity (40 % in the case of the I2020T mutation) (Wood-Kaczmar *et al*. 2006). Considering the previous linking of Lrrk2 to an increase in cytoplasmic protein aggregates and their enhanced ubiquitination, it may be suggested that a mutation that leads to an increase in its kinase activity may result in an over accumulation of protein aggregates for degradation. This, with a lack of an increase in the UPS rate, may result in a backlog of protein aggregates, such as α-syn and ubiquitin leading to neurotoxicity.

1.3 Models of Parkinson disease.

To gain an understanding of the pathophysiology of PD, *in vivo* and *in vitro* models have been established using compounds such as 1-methyl 4-phenyl 1,2,3,6-

tetrahydropyridine (MPTP) and rotenone, which induce PD-like symptoms (Lee *et al.* 2002; Shimohama *et al*. 2003; Fernagut and Chesselet, 2004). *In vitro* rotenone and the metabolite of MPTP (MPP^+) inhibit complex I of the ETC resulting in mitochondrial dysfunction resulting in the loss of dopaminergic neurones in the substantial nigra *in vivo*, similar to that observed in PD patients (Lee *et al*. 2002; Shimohama *et al*. 2003). Mutant mice (null and over-expressing α-, β- and γ-syn (Fernagut and Chesselet, 2004)) and cells lines (such as human SHSY-5Y, rat PC12 and BE-(2)-M17 human neuroblastoma dopaminergic cells) which can be genetically modified to over-express syn proteins, have enabled investigation into the interaction of the synucleins in PD (Shimohama *et al.* 2003).

1.3.1 MPTP and MPP^+.

1.3.1.1 MPTP-induced PD.

MPTP was identified in 1976 through the incorrect synthesis of a synthetic heroin, 1-methyl 4-phenyl 4-propionoxypiperidine (MPPP) from meperidine (also known as Demerol) which resulted in a mixture of MPPP and MPTP (Davis *et. al.,* 1979). The injection of MPTP contaminated MPPP caused the onset of PD-like symptoms which included; rigidity, tremors, state of muteness, flat facial expressions, hallucinations, slowness of and difficulty in moving, jerking limbs and a fixed stare (Davis *et. al.*, 1979; Langston *et. al.,* 1983). The symptoms were speculated to be due to the loss and/or damage to dopaminergic neurones and alterations in the noradrenergic and serotoninergic systems. This was confirmed upon post-mortem analysis of one of the MPTP patients who died (Davis *et. al.*, 1979). The analysis of the brain showed irregular patches of discolouration in ventricular lining, destruction of the SN and the

identification of a round eosinphilic intracytoplasmic inclusion characteristic of a LB found in PD patients (Davis *et. al.*, 1979). For all the MPTP patients, symptoms were shown to be markedly improved and controlled with the use of PD treatments such as levodopa/carbidopa and DA agonists (benztropin and diazepam) (Davis *et. al.*, 1979). Reducing or the withdrawal of treatment lead to the reappearance of symptoms (Davis *et. al.*, 1979; Langston *et. al.,* 1983).

The parkinsonism-like symptoms were suspected to be caused by the synthesised MPPP being contaminated with MPTP rather than the MPPP itself (Davis *et al*., 1979; Langston *et al*., 1983). The method of MPPP synthesis documented by one of the MPTP patients was replicated and found to produce a mixture of MPPP and MPTP that was subsequently tested on rats, resulting in catatonia and rigidity (Davis *et al*., 1979). The discovery of MPTP as a chemical inducer of PD with identical symptoms and cellular damage sparked off the development of a wide variety of *in vivo* and *in vitro* models using MPTP (Frei and Richter, 1986).

Primarily, MPTP was used in primates, but has since been demonstrated to exert similar effect on several rodent models (Burns *et al.*, 1983; Langston *et al.*, 1984; Heikkila *et al.*, 1984a; Heikkila *et al.*, 1984b; Mitchell *et al.*, 1985; Fuller and Steranka, 1985; Chiba *et al.*, 1985a; Forno *et al.*, 1986; Cassarino *et al.*, 1998). Initial studies used a variety of primates to investigate the specific effects of MPTP upon the brain. Burns *et al.* (1983) showed that rhesus monkeys intravenous treated with MPTP developed parkinsonism-like symptoms such as tremors rigidity, akinenia and postural instability (Burns *et al.,* 1983). This was repeated with other studies in a

number of primate species (Langston *et al.,* 1984; Eidelberg *et al.,* 1986; Filion *et al.,* 1988). Burns *et al.* (1983) went on to show that the symptoms induced by MPTP could be reversed by treatment with $_{L}$-DOPA, similar to PD patients. Histological and immunocytochemical analysis of MPTP-treated primate brains identified loss of pigmented neurones within the par compacta of the SN, neuronal loss in LC and raphe, reduced activity of the both pallidal segments and subthalamic nucleus and depletion of DA within the striatum and SN, although there were minimal effects on DA neurones in the ventral tegmental (Burns *et al.,* 1983; Porrino *et al.,* 1987; Filion *et al.,* 1988). A further study identified the presence of inclusion bodies in the brains of MPTP-treated squirrel monkeys in the SN and LC similar to PD patients (Forno *et al.,* 1986). The similarities of MPTP-induced symptoms and neurological damage to that of PD patients means MPTP models are useful for the investigation of PD, potentially elucidating pathways and mechanisms involved in the progression of the disease as well as for the identification of possible therapeutic methods and drug treatments.

Rodent MPTP models initially showed varying effects with dose, route of administration, number and timing of injections, gender, age, strain, even variations in animals from suppliers (Speciale, 2002). The effects of MPTP were eventually clarified within the rodents once strain appropriate dosing and metabolic distributions of MPTP were characterised (Speciale, 2002). The rodent models showed varying susceptible to MPTP toxicity between rats and mice. Rats needed significantly higher doses of MPTP to induce any striatal DA reduction, SN neuronal loss and/or behavioural impairments compared to that needed for mice (Speciale,

2002). The rats' resistance to systemic MPTP toxicity is thought to be due to unique enrichment of enzymes in the blood-brain barrier that efficiently metabolise MPTP to non-toxic metabolites and swiftly removes MPTP from the brain compared to mice and humans (Riachi *et al.,* 1988; Riachi *et al.,* 1990; Speciale, 2002). Compared to the rat, the mouse has a reduced ability to remove MPTP from their system, or convert to non-toxic metabolites (Riachi *et al.,* 1988; Riachi *et al.,* 1990). Variations between mice species to MPTP toxicity has also been shown, as C57 black mice have been shown to be more susceptible to MPTP than CF1 white mice, susceptibility correlated with an ability to convert MPTP to non-toxic metabolites (Riachi *et al.,* 1988). However all strains are markedly more sensitive to MPTP compared to rats.

There are however inconsistencies between the animal model and human idiopathic PD. Firstly the majority of studies noted that the toxic effects observed within the non-human primate and rodent models dissipates overtime unlike in humans where the effects are irreversible (Drolet *et al.,* 2004). Secondly, inclusion formation is not normally observed following MPTP administration (Burns *et al*., 1983; Langston *et al*., 1984; Mitchell *et al*., 1985; Shimoji *et al*., 2005). However in the first case of human MPTP poisoning a rounded eosinophilic intracytoplasmic "Lewy body" was noted (Davis *et al.,* 1979), and some other studies in primates and rodents have subsequently identified a few LB-like inclusion (Forno *et al.,* 1986; Kowall *et al.,* 2000; Meredith *et al.,* 2002).

It has been established that MPP^+, a metabolite of MPTP is 100 times more toxic than the parent, is the toxic component (Harik *et al.,* 1987). MPTP is a fat soluble compound that can freely penetrate cellular membranes, including the blood-brain barrier (Markey *et al* 1984), and is accumulated in intracellular lysosomes in astrocytes (figure 1.13) (Riachi *et al.*, 1988; Marini *et al.*, 1992; Wong *et al.*, 1999). MPTP is metabolised into 1-methyl-4-phenyl-2,3-dihydropyridine ($MPDP^+$) by MAO-B which is predominantly located in astrocytes and serotonergic neurones (Castagnoli *et al*., 1985; Chiba *et al*., 1985a). $MPDP^+$ is an unstable ion that spontaneously oxidises to form the toxic compound MPP^+ (figure 1.14) (Javitch *et al.*, 1985; Castagnoli *et al.*, 1985; Chiba *et al.*, 1985a; Brooks *et al.*, 1989). In contrast MPP^+ only poorly crosses the blood-brain barrier (Riachi *et al.*, 1988) and as such is considerably less toxic than MPTP *in vivo*. In the brain, astrocyte metabolised MPP^+ is released into the extracellular space where it is taken up into dopaminergic neurones, located in the striatum and specifically the SN, via the DAT system (Javitch *et al.*, 1985; Chiba *et al.,* 1985b; Brooks *et al.*, 1988; Wong *et al.*, 2004; Smeyne and Jackson-Lewis, 2005). This was shown with the use of mazindol, a DA uptake inhibitor, where DA and MPP^+ uptake was blocked in mice mescenphalic neuronal primary culture (Schinelli *et al.,* 1988). This was confirmed with further inhibition studies of the DA uptake system which showed the inhibition of DAT prevented MPP^+-induced cell death (Javitch *et al.,* 1985). The selective mechanism of MPP^+ uptake via DAT explains the selective cell death observed in the MPTP users and animal models (Javitch *et al.,* 1985).

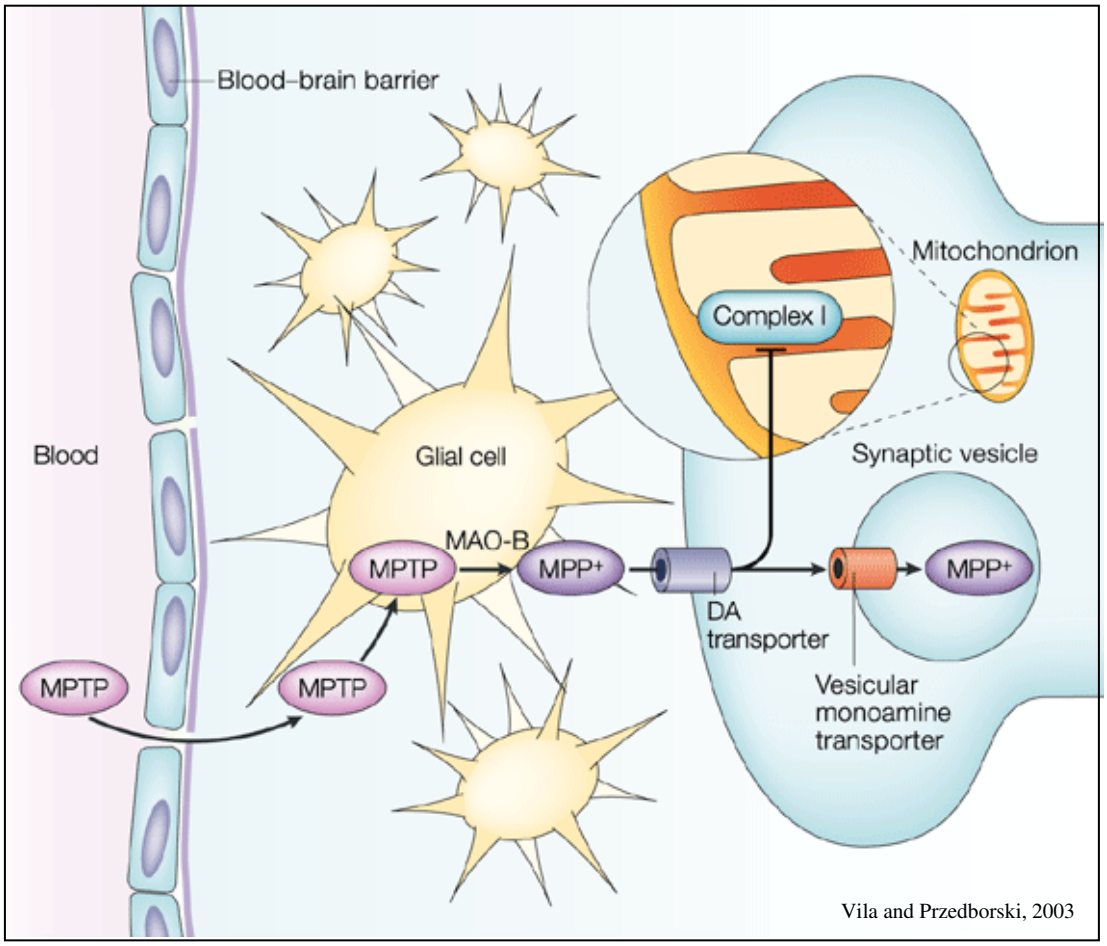

Figure 1.13: Schematic of MPTP uptake and metabolism within the brain.

Schematic of MPTP rapidly crossing the blood–brain barrier and metabolized to MPP^+ (the active toxic compound). MPP^+ is taken up by DA transporters, for which it has high affinity. Once inside DA neurones, MPP^+ is concentrated by an active process within the mitochondria, where it impairs mitochondrial respiration by inhibiting complex I of the electron transport chain (From Vila and Przedborski, 2003).

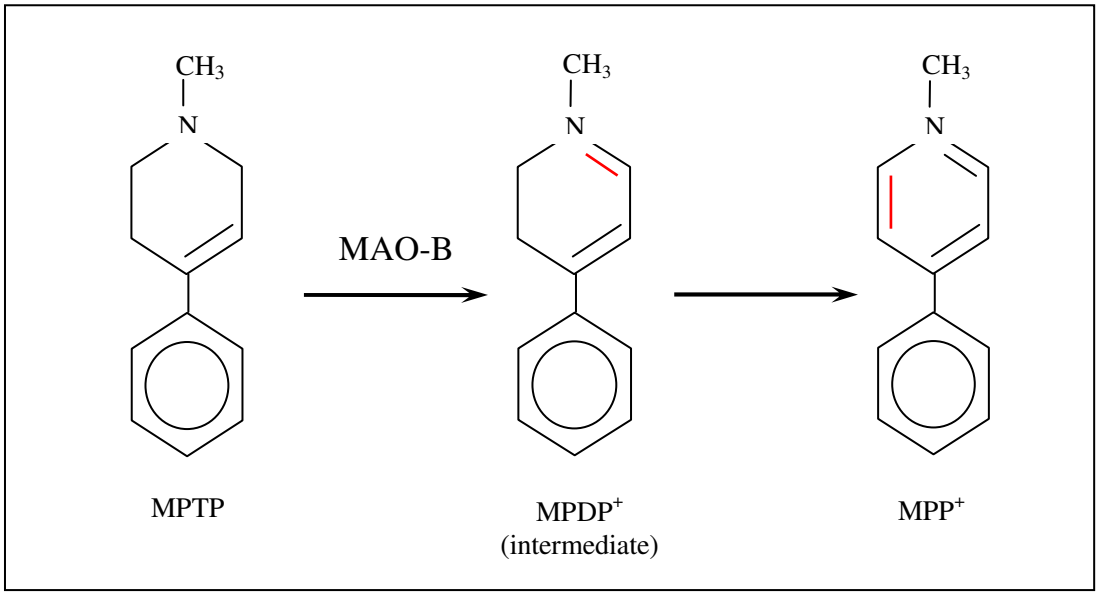

Figure 1.14: Schematic of the formation of MPP^+ from MPTP.

Metabolism of MPTP to MPP^+ by oxidation, catalysed by monoamine oxidase-B (MAO-B) and the intermediate step producing $MPDP^+$.

Neuroprotection studies have also suggest a role for the catecholamine vesicular monoamine transporter (VMAT2) in regulating MPP^+-induced toxicity (Reinhard, Jr. *et al.*, 1988; Gainetdinov *et al.*, 1998; Staal *et al.*, 2000). In dopaminergic neurones VMAT2 is extensively localised to tubulovesicles that resemble saccules of the smooth endoplasmic reticulum, and to a much lesser extent to small synaptic vesicles or large dense-core vesicles (Nirenberg *et al.,* 1996). VMAT2 normally sequesters DA to vesicles ready for release in response to stimuli (Nirenberg *et al.,* 1996). It has been shown that VMAT2 also sequesters MPP^+ into intracellular vesicles removing the MPP^+ from the cytosol and reducing toxicity (Reinhard *et al.*, 1988; Gainetdinov *et al.*, 1998; Staal *et al.*, 2000). The protective effects of VMAT2 against MPP^+ toxicity has been shown to vary between different species in relation to VMAT2 levels in the brain (Reinhard *et al.,* 1988). A study by Staal *et. al.* (2000) showed rats had a higher level of striatal VMAT2 compared to mice and as mentioned before rats have reduced susceptibility to MPP^+ toxicity (Staal *et al.,* 2000). The lower levels of VMAT2 in mice leads to less compartmentalisation of MPP^+ and therefore increased cytosolic MPP^+ and increased toxicity (Staal *et al.,* 2000). This was confirmed with the use of heterozygous knockout VMAT2 mice that showed a significant increase in susceptibility to MPTP toxicity compared to normal homozygous VMAT2 mice (Gainetdinov *et al.,* 1998).

Through the multiple variations of MPTP administration in rodents and primates models have been established that closely resemble aspects of the pathophysiology of PD. These models are now being used to identify mechanisms involved in PD and future therapeutic strategies.

1.3.1.2 Mechanics of MPTP toxicity.

MPP^+ has many toxic effects in cells including mitochondrial dysfunction, increase in ROS and oxidative stress, which lead to cell death via apoptosis or necrosis depending on the severity of the insult (Nicotra and Parvez, 2002). MPP^+ primarily acts by blocking mitochondrial respiration through inhibition NADH dehydrogenase, also known as complex I of the ETC (Ramsay *et al*., 1991; Vila and Przedborski, 2003). The ETC generating the majority of ATP along with glycolysis and the Kreb cycle, which also produce NADH that feeds in to the ETC to drive ATP production in cells (figure 1.15) (Hames and Hooper, 2000). MPP^+ enters the mitochondrial matrix by ionic diffusion actively driven by electrochemical gradient of the inner membrane (Ramsay and Singer, 1986; Smeyne and Jackson-Lewis, 2005). MPP^+ inhibition of the ETC results in a decrease in ATP generation, (figure 1.15), subsequently causing a loss of ATP-driven mitochondrial membrane potential and the generation of ROS, hydrogen peroxide and hydroxyl radicals (Wong *et al.*, 1999; Smeyne and Jackson-Lewis, 2005). Similar mitochondrial dysfunction is also observed in the post-mortem brain of PD patients (section 1.2). MPP^+ also causes a breakdown in Ca^{2+} homeostasis (Frei and Richter, 1986) and an increase in nitric oxide synthase which increases nitric oxide levels (Przedborski *et al.,* 1996). MPTP has also been shown to trigger pro-apoptotic signal, increasing phosphorylation of JNK leading to increased JNK activity; both are components of the stress-activated protein kinase system which inactivate the anti-apoptotic protein Bcl-2 (Srivastava *et al.,* 1999). This was shown through the use a JNK blocker (CEP-1347/KT-7515) which reduced nigrostriatal DA cell death in an MPTP model *in vivo* (Saporito *et al.,* 1999).

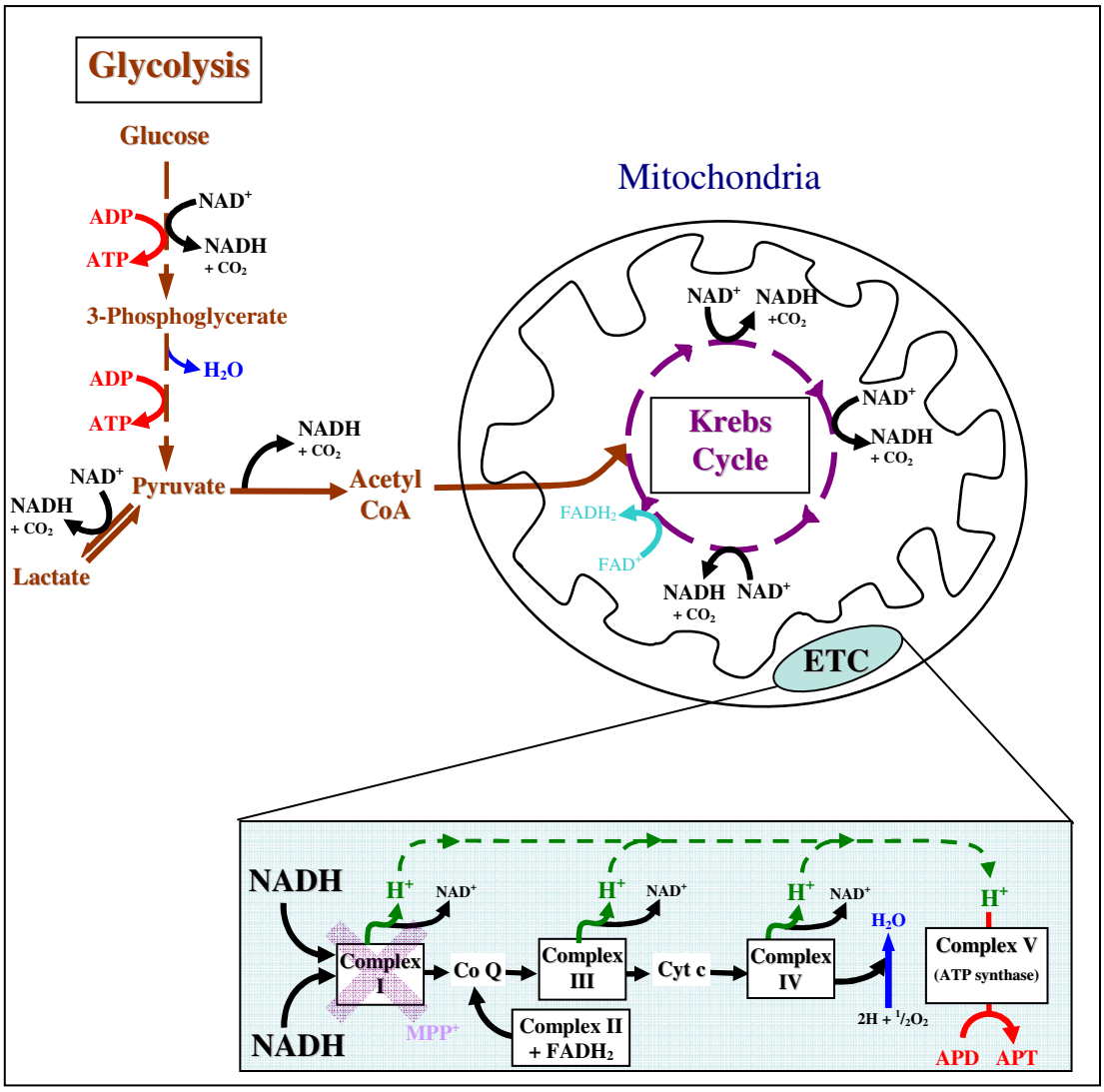

Figure 1.15: Schematic of the energy pathways that generate NADH and ATP.

Schematic of the glycolytic and Kreb cycles and the electron transport chain (ETC). The diagram shows the metabolism of glucose by glycolysis (dark red pathway) to acetyl CoA, generating NADH and ATP. Acetyl CoA feeds into the Krebs cycle within the mitochondria (purple pathway) generating NADH and FADH. NADH generated by glycolysis and the Kreb cycle is metabolised to NAD^+ through the ETC (indicated in pale blue box) ultimately generating ATP from ADP. MPP^+ inhibition is marked by a purple cross. Other Abbreviations: Flavin adenine dinucleotide (FAD), Cytochrome c (Cyto c), co-enzyme Q (Co Q).

1.4 Aims and objectives.

The aims of this project are to investigate the physiological role of α-syn in normal and PD-like conditions. Initially protein-expression in a prokaryotic system will be established to express α-syn, A53T mutant α-syn and β-syn. This will allow for a constant and renewable source of protein throughout the project. The study will then characterise α-syn-mediated physiological effects *in vitro* (in both the soluble and aggregated form) using human SHSY-5Y neuroblastoma cells. Subseqently the α-syn pathophysiological effects will be investigated in an *in vitro* MPP^+ model of PD. Through these studies we aim to elucidate α-syn involvement in the pathophysiology of PD at a molecular level. Such studies will have important implications in α-syn involvement in the progression of neurodegenerative disorders.

Chapter 2: Materials and Methods.

2.1 General Materials.

All chemicals were obtained from Sigma Chemical Co. (Pool, UK) unless otherwise stated.

2.2 Molecular Biology.

2.2.1.1 Preparation of agar culture plates.

To produce 7 % stock volume of agar, 3.5 g Lennox L agar was added to 500 ml of deionised water and sterilised by autoclaving. The agar was cooled to ~ 50 ^{o}C and antibiotics were added to the 7 % agar solution; ampicillin (amp) plates contained 50 μg/ml amp and amp and chloramphenicol (chlora) plates contained 50 μg/ml amp and 34 μg/ml chlora. The agar was poured into Petri dishes, filling each dish by approximately 2/3 and allowed to cool in a sterile hood. The set agar plates were stored at 4 ^{o}C for a maximum of 3 weeks.

2.2.1.2 Preparation of LB and peptone broths.

LB broth was produced similarly, where 25 g of LB broth powder was dissolved in 1 L of deionised water and sterilised by autoclaving. Once cooled the LB broth was stored at 25 ^{o}C. On the addition of antibiotics, LB Broth containing antibiotics was stored at 4 ^{o}C for a maximum of 3 weeks.

Peptone growth media consisted of 16 g of peptone and 5 g of sodium chloride (NaCl) dissolved in 1 L of deionised water and sterilised by autoclaving. Peptone

media was stored at 25 ^{o}C indefinitely, or on addition of antibiotics at 4 ^{o}C for a maximum of 3 weeks.

2.2.2 Transformation of plasmids into library efficiency DH5α or JM109 competent *E.coli* cells.

Transformation protocol for DH5α and JM109 competent cells was the same for all types of DNA plasmid transformed into the cells. Plasmid was added to 250 µl of cells; each set of transformations contained two vials of cells transformed with either the supplied control plasmid DNA or sterile water (no addition DNA plasmid) as transformation controls.

Vials of DH5α competent cells (Invitrogen, catalogue #18263-012) or JM109 competent cells (Promega, catalogue #L2001), were stored at -70 ^{o}C, were thawed on ice for ~ 5 min. Once defrosted 2 µl of isolated syn-containing plasmid DNA was gently mixed with the cells by trituration. Two controls vials were set-up for the transformation; control plasmid DNA (2 µl) was added to one vial of cells and a further vial was left with no addition of DNA as control of the transformation protocol. All the cells were kept on ice for 30 min with gentle agitation to prevent the cells settling. The cells were then placed in a water bath for 45 sec at 42 ^{o}C and back on to ice for 2 min to shock the cells into taking up the plasmid DNA. To the heat-shocked cells, 400 µl of pre-warmed LB broth was added and the cells incubated for 1 h at 37 ^{o}C in a shaking incubator set to 225 rpm. Cell were centrifuged at 2,700 x g for 5 min and 200 µl of supernatant removed. The cells were gently re-suspended in the remaining supernatant. The cells were spread on to pre-warmed LB agar plates

containing ampicillin (50 μg/ml) using either 150 μl or 50 μl volume of cells. Control plates were also prepared which consisted of a blank plate, cells transformed with control plasmid DNA and non-transformed cells. All the plates were incubated overnight at 37 ^{o}C.

2.2.3 Transformation of plasmids into BL21 (DE3) or BL21 (DE3)pLysS competent *E.coli* cells.

The transformation protocol for BL21 (DE3) and BL21 (DE3)pLysS competent cells is the same for all the different DNA plasmids. Only one syn-containing plasmid was added to each 250 μl volume of cells. Each transformation contained two controls; control plasmid DNA supplied added to another vial of cells and a further vial with added sterile water, no addition of DNA.

BL21 (DE3) competent cells (Invitrogen, catalogue #C6565-03) or BL21 (DE3)pLysS competent cells (Invitrogen) in 250 μl volume were defrosted on ice for ~ 5 min. 2 μl of isolated plasmid DNA (specified within results) was gently mixed with the cells by trituration. Two control vials were used for controls; one vial the cells were transformed with control plasmid DNA supplied with the cells and another vial had no DNA added to the cells. The cells were incubated on ice for 30 min and agitated every 5 min. The cells were heat-shocked by placing the tubes in to a water bath at 42 ^{o}C for 30 sec and then back onto ice for 2 min. 250 μl of pre-warmed LB broth was added to the cells and incubated for 1 h at 37 ^{o}C in a shaking incubator set to 225 rpm. At the end of the incubation, either 100 μl or 150 μl of the cells were spread on two pre-warmed LB agar plates containing ampicillin (50 μg/ml) and

chloramphenicol (34 μg/ml). Control plates were also prepared which consisted of a blank plate, cells transformed with control plasmid DNA and non-transformed cells. All the plates were incubated at 37 ^{o}C overnight.

2.2.4 Miniprep of *E.coli* cultures.

Plasmid DNA was isolated from transformed *E.coli* cells using a wizard® Plus SV Miniprep DNA purification system (Promega) following the manufactures instructions. Colonies were selected from transformation or stock plates and used to inoculate 6 – 10 ml pre-warmed LB broth (containing specific antibiotics for cell type) per colony within a 15 – 20 ml sterile tube and incubated at 37 ^{o}C in a shaking incubator overnight. Using a 2 ml micro centrifuge tube 2 ml of culture was transferred to the 2 ml tube and centrifuged at 7,400 x g for 2 min. The supernatant was gently removed and a further 2 ml of culture added prior to further centrifugation at 7,400 x g for 2 min. The supernatant was removed and a final 2 ml of culture transferred to the tube and centrifuged at 7,400 x g for 5 min. Excess media was removed. The cell pellets were re-suspended in 250 μl cell resuspension solution. 250 μl of cell lysis solution was added and the tube was inverted 4 – 6 times. The cell suspension was incubated for a maximum of 5 min at room temperature, until partial clearing of the lysate was observed. Neutralising Solution (350 μl) was mixed by inverting the tube 4 – 6 times and then the tube was centrifuged at 14,500 x g for 10 min at room temperature (figure 2.1).

Spin columns were inserted into a 2 ml collection tube and the clear lysate (supernatant) was transferred to the spin column, avoiding disturbing or transferring

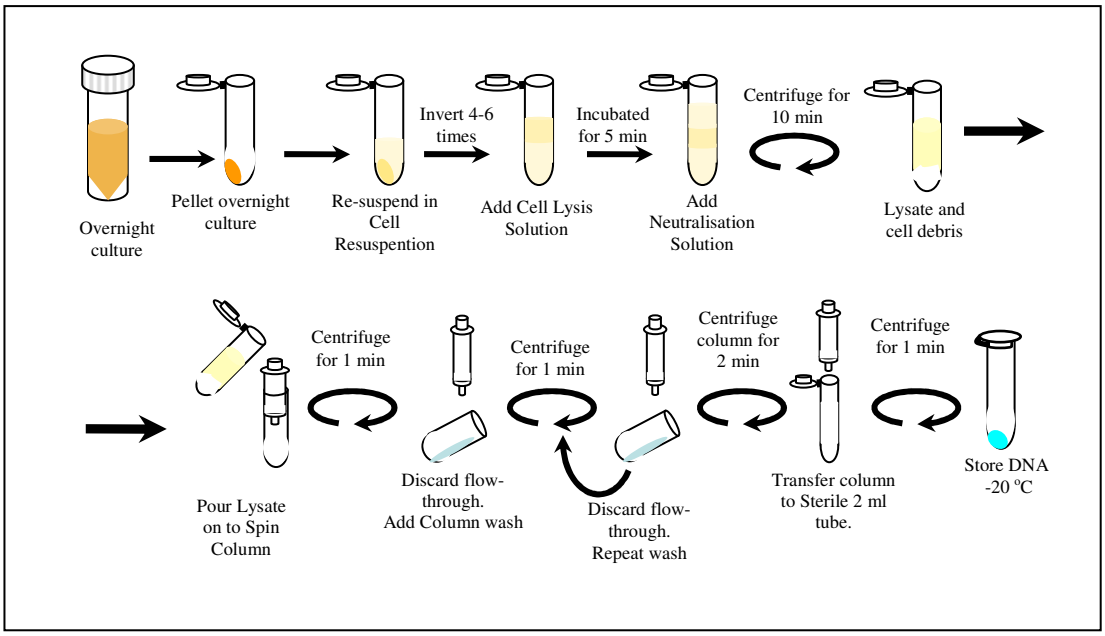

Figure 2.1: Schematic of DNA mini prep from overnight culture.

any of the white precipitate. The spin column with lysate was centrifuged at 14,500 x g for 1 min at room temperature. The spin column was removed from the collection tube and the flow through was discarded and the spin column re-inserted into the collection tube. The spin column was washed with 750 µl column wash solution and centrifuged at 14,500 x g for 1 min at room temperature. The collected wash through was discarded as before and the wash was repeated using 250 µl column wash solution. The wash through was discarded. The spin column was reinserted into the collection tube and centrifuged at 14,500 x g for 2 min at room temperature to remove any wash still present. The spin column was transferred to a sterile 2 ml micro centrifuge tube. Plasmid DNA was eluted from the spin column by adding 100 µl of sterile Nuclease-free water to the spin column and centrifuging at 14,500 x g for 1 min at room temperature (figure 2.1). The eluted DNA was capped and stored at -20 ^{o}C or used immediately for DNA restriction digest.

2.2.5 DNA restriction digests.

To identify the presence of the synuclein gene inserts within the expression vectors the plasmids were cut using restriction enzymes that cut at specific nucleotide sequences. The restriction enzymes Nde I (Promega) and Hind III (Promega) were selected as both only cut once within the plasmid. Nde I cut the plasmid within a few nucleotides prior to the start codon of the gene insert and Hind III cut within a few nucleotides of the stop codon of gene inserts. Full digestion would therefore produce two DNA fragments, the vector and gene insert.

2.2.5.1 Combined restriction digest reactions.

Initially, restriction digests used Nde I and Hind III in one restriction digest reaction to reduce DNA loss. For identification of the gene within a plasmid only small volumes of isolated plasmid were used in the digest. 2 µl of isolated plasmid DNA was mixed with 1 µl Multi-core buffer (Promega). 0.5 µl of both Nde I and Hind III was added and finally 6 µl of sterile milli-Q water was added. A control reaction was also prepared at the same time where the plasmid DNA was replaced with sterile milli-Q water. All the reactions were vortexed and incubated at 37 ^{o}C for 2 h within a water bath. To all the reactions 2 µl of loading buffer was added, vortexed, and loaded on to ethidium bromide (EtBr) 1 % agarose gel (section 2.2.6) along with a specific DNA ladder specified for each gel. The agarose gel was run at 100 V for 30 – 40 min (section 2.2.6). The gel was then visualised and photographed using a Multimager light cabinet (Alpha Innotech Corporation).

This same DNA digest protocol was also used when digesting the *α-syn* gene produced by PCR, before ligation. For the removal of the insert from the expression vector, the volume of the restriction digest reactions were increased; DNA volume was increased to 25 µl, Multi-core buffer to 5 µl, each restriction enzymes to 2.5 µl and sterile milli-Q water to 20 µl. The in increase volume digest reactions were incubated for 12 – 14 h. Water controls were always run in parallel.

2.2.5.2 Individual restriction digest reactions.

To increase the efficiency of the restriction enzyme reactions two separate reactions were performed using the specific reaction buffer for the enzymes.

The gene insert isolated by PCR and the expression vector was initially cut using the resection enzyme Nde I and buffer D (Promega). The first reaction was setup using 30 µl of DNA with 5.0 µl of Buffer D, 2.0 µl of Nde I and 13 µl of sterile milli-Q water to make the reaction volume up to 50 µl. The reaction was vortexed and incubated in a water bath at 37 ^{o}C for 3 h. Reactions heated using a PCR machine were run overnight with the PCR machine programmed incubate at 37 ^{o}C for 2 h before dropping the temperature to 4 ^{o}C and holding the temperature. A sample (5 µl) of each reaction was run on a EtBr 2 % agarose gel at 100 V for 40 min along with uncut DNA to confirm if the restriction digest was successful (section 2.2.6).

The remaining 45 µl of the digest were either run on EtBr 1 % low melting point (LMP) agarose gel and digested DNA extracted from the gel using QIAquick gel extraction kit (Qiagene) (section 2.2.7), or the Nde I cut DNA was collected via ethanol precipitation as described in section 2.2.8. For both extractions processes a 2 µl sample of isolated DNA was run on a EtBr 1 % agarose gel (section 2.2.6).

The isolated DNA was further digested by Hind III restriction enzyme to remove the gene insert from the now open expression vector. The seconded restriction enzyme reaction was setup using 30 µl of DNA (specified in results) with 5.0 µl of buffer E (Promega), 2.0 µl of Hind III and 13 µl of sterile milli-Q water to make the reaction

volume up to 50 µl. The reaction was vortexed and incubated in a water bath at 37 ^{o}C for 3 h. Again the restriction digests heated by PCR machine, the PCR machine was programmed to incubate the digest at 37 ^{o}C for 3 h, drop the temperature to 4 ^{o}C and hold.

The restriction digests were collected by either gel extraction using QIAquick gel extraction kit, isolating the gene insert by band size from a EtBr 1 % LMP agarose gel, or by ethanol precipitation of the DNA. A sample of isolated DNA was run on a EtBr 1 % agarose gel (Section 2.2.6). The above restriction digest protocol opens the restriction sites of the gene insert and the expression vector ready for the use within a ligation reaction (Section 2.2.10).

2.2.6 DNA ethidium bromide agarose gels.

EtBr agarose gels and EtBr LMP agarose gels were prepared in the same way. The agarose was dissolved in TAE buffer (40 mM Tris acetate and 2 mM EDTA (pH 8.3)) by heating agarose and TAE buffer to ~ 95 ^{o}C for 1 – 2 min without boiling. Once the agarose was dissolved it was cooled to 55 – 60 ^{o}C and 0.5 µg/ml EtBr solution was added to either agarose or LMP. The EtBr agarose or EtBr LMP was poured into a gel frame and the gel comb was inserted. Any bubbles within the gel were removed using the tip of a 200 µl pipette tip before the gel set. The ends of the gel frame and comb were removed before using the EtBr gel or EtBr LMP gel.

All the agarose gels, independent of agarose percentage or type of agarose, were loaded into an electrophoresis agarose gel tank and completely covered with TAE

buffer. DNA samples (5 – 10 µl for EtBr 1 – 2 % gels and 40 – 50 µl for LMP EtBr gels) were loaded into the wells, the order for each run noted and stated with the gel results. The agarose gels were run at 100 – 150 V for 40 – 60 min at room temperature. The agarose gels were photographed using Multimager light cabinet (Alpha Innotech Corporation) containing a UV lamp to visualise the bands.

2.2.7 DNA agarose gel extractions.

DNA fragments produced by restriction digest (Section 2.2.5) were isolated and purified using a QIAquick gel extraction kit (Qiagen) and following manufacturer's instructions. Restriction digests were run on EtBr 1 % LMP agarose gel (Section 2.2.6) and the appropriated band was identified by comparing band size to a DNA molecular weight ladder marker. Once identified, the DNA fragment was cut out of the agarose gel and added to 3 times the volumes of buffer QG (weight/volume). The gel slice was solubilised in the buffer by incubation at 50 ^{o}C for 10 min in a water bath with occasional vortexing. Once dissolved, 1 volume of isopropanol was added to the sample and vortexed. A QIAquick spin column was inserted into a 2 ml collection tube and the sample loaded into the spin column. The spin column was centrifuged at 14,500 x g for 1 min. The flow through was discarded and the spin column inserted back in to the collection tube. The spin column was subsequently washed with 0.75 ml of buffer PE by centrifuging at 14,500 x g for 1 min. The flow through was discarded and the spin column was centrifuged for 1 min at 14,500 x g. The spin column was transferred to a sterile 2 ml micro centrifuge tube and the DNA fragment eluted from the spin column by the addition of 50 µl of sterile water prior to

centrifugation for 1 min at 14,500 x g. The eluted DNA fragment was either used immediately for ligation reaction or was stored at -20 ^{o}C.

2.2.8 Ethanol precipitation of DNA.

For DNA samples retrieved by ethanol precipitation, 2 volumes of 100 % ethanol and 1/10 volume of 3 M sodium acetate (NaAc) pH 5.2 was added to the finished restriction digest.

The mixture was mixed by vortexing and incubated at -80 ^{o}C for 1 – 2 h. The reaction was centrifuged at 12,500 x g at 4 ^{o}C for 30 min. The supernatant was removed and the pellet was washed by gently adding 50 µl of 70 % ethanol without disturbing the pellet, centrifuging at 14,500 x g for 1 min and discarding the supernatant. The wash step was repeated and the pellet allowed to dry at room temperature for 5 – 10 min to allow the ethanol to evaporate. The DNA pellet was re-suspended in sterile milli-Q water and either used immediately in further reactions or stored at -20 ^{o}C.

2.2.9 Polymerase chain reaction (PCR) protocols.

For all PCR reactions using *α-syn*pRK172, forward primer sequences were designed to incorporate an Nde I restriction site into the *α-syn* start codon and a Hind III restriction site within the reverse primer directly after the *α-syn* stop codon. The primers were produced initially by MWG, but subsequently produced by Invitrogen, the sequences were as follows:

Alpha-forward Primer:

5'- CCA TAT GGA TGT ATT CAT GAA AGG ACT T- 3'

Blue highlights the sequence for Nde I cutting site

Alpha-reverse Primer:

5' – CAA GCT TTT AGG CTT CAG GTT CGT AGT C – 3'

Purple highlights the sequence for Hind III cutting site.

These *α-syn* primers were also used in PCR reactions using *α-syn*pET-22b(+) plasmid DNA to confirm the presence of the *α-syn* gene in the constructed plasmid. PCR was also used to confirm gene orientation within the *α-syn*pET-22b(+), using a T7 forward primer and a reverse *α-syn* primer (Invitrogen). The PCR cycle program was unaltered by the change in primers.

DNA isolated by mini prep was thawed on ice, pulse centrifuged and gently mixed by pipetting. PCR buffers and primers were warmed to room temperature, while 5 µl of target DNA was heated to 100 ^{o}C for 5 min. Immediately after heating the DNA the PCR reagents were added. A 50 µl PCR reaction included; 5.0 µl of 10 x PCR buffer, 0.4 µl of dNTPs each at 25 mM (Roche), 0.5 µl of the forward primer (1 pmol/µl) produced by either MWG or Invitrogen, 0.5 µl of reverse primer (1 pmol/µl) produced by either MWG or Invitrogen, 5.0 µl DNA (either *α-syn*pKR172 or *α-syn*pET-22b(+)), 38.0 µl sterile deionised water and 0.75µl high affinity Taq (Roche). Concomitant controls used sterile water in place of DNA. Once reagents were added the reaction was briefly vortexed and pulsed centrifuged and the

tubes loaded onto a PCR machine (PCR express Thermo hybrid) and PCR cycles initiated as shown in figure 2.2. PCR products from the PCR reaction were identified by running 10 µl sample of each PCR reaction and control with 2 µl of loading buffer on a 1 % EtBr agarose gel (Section 2.2.6).

2.2.9.1 PCR protocols for direct PCR from *E.coli* colonies.

JM109 cells transformed with newly ligated *α-syn*pET-22b(+) plasmid were constructed using PCR amplified *α-syn* using MWG primers (section 2.2.9).

Individual colonies produced from JM109 cell transformated with *α-syn*pET-22b(+) were selected and dipped into 50 µl of lysis buffer. The loop was then streaked across a 1 cm^2 squares on an agar plate (amp 50 µg/ml). Remaining cells on the loop were removed by resuspending the cells in the 50 µl of lysis buffer. The lysis buffer containing colony cells was vortexed before incubating at 95 ^oC for 10 min. From the lysed sample 1 – 2 µl was taken and mixed with the following PCR reagents; 10 µl of Red Taq, 1 µl of *α-syn* forward primer (MWG), 1 µl of *α-syn* reverse primer (MWG) and 6 – 7 µl of sterile deionised water. The tubes were loaded onto a PCR machine (PCR express Thermo hybrid) and the PCR cycles initiated as described in figure 2.2. PCR products from the PCR reaction were identified by running a 10 µl sample of each PCR reaction (and control) with 2 µl of loading buffer on a EtBr 1 % agarose gel (section 2.2.6).

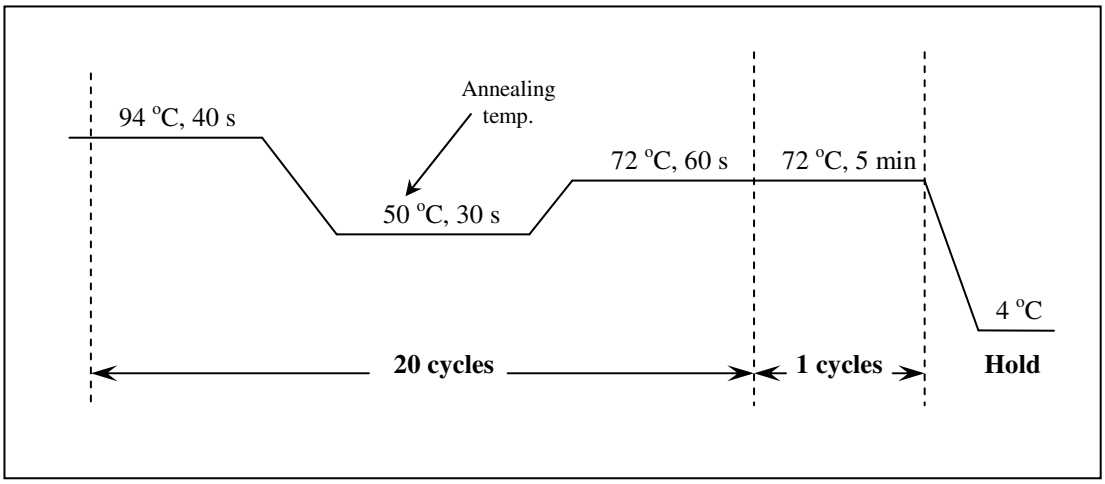

Figure 2.2: Schematic of the PCR temperature cycles.

2.2.10 Ligation of gene insert into expression vector.

The *α-syn*pET-22b(+) plasmid was constructed by inserting the *α-syn* gene generated by PCR from the *α-syn*pRK172 plasmid (section 2.2.9) into the commercially available pET-22b(+) vector (Invitrogen). Prior to the ligation reaction, the expression vector was opened by restriction digest using Nde I and Hind III (section 2.2.5.2) and purified by either gel extraction (section 2.2.7) or ethanol precipitation (section 2.2.8). The ends of *α-syn* PCR products were also cut using Nde I and Hind III (section 2.2.5.2), priming the α-syn ends for insertion into the pET-22b(+) vector. For the ligation reaction; 1 µl of ligation T4 buffer (10 x), 1 µl of open pET-22b(+) vector, 3 µl of primed *α-syn* PCR product, 1 µl of Ligase T4 (enzyme) and 5 µl sterile milli-Q water were vortexed together and incubated overnight (12 – 16 h). The reaction was initially incubated at 16 ^{o}C with the temperature gradually reduced to 4 ^{o}C. Once the reaction was finished the mix was used in a transformations of either DH5α or JM109 competent cells (section 2.2.2). The new constructed plasmid was confirmed by PCR (section 2.2.9) or restriction digest (section 2.2.5.1) of isolated plasmid DNA from colonies cultured from the transformation (section 2.2.4).

2.3 Protein expression and purification.

2.3.1 Protein expression.

2.3.1.1 LB broth expression.

BL21(DE3) competent colonies transformed with either *α-syn*pRK172 or *α-syn*pET-22b(+) plasmids, were randomly selected and used to inoculate 6 – 10 ml LB broth containing both amp (50 µg/ml) and chlora (34 µg/ml) and incubated overnight at 37 ^{o}C. Each overnight culture was then used to inoculate 100 ml pre-warmed LB

broth containing amp (50 μg/ml) and chlora (34 μg/ml) to an optical density of ~ 0.1 (read at 560 – 600 nm (OD_{600})). The culture was incubated at 37 ^{o}C, shaking until the OD_{600} reached 0.4 – 0.6 which took approximately 2 – 3 h. Once OD_{600} was reached, a 2 ml sample of the culture was collected and 0.001 M (final concentration) of isopropyl β-D-1-thiogalactopyranoside (IPTG) was added to the culture to induce protein expression within the cells. After induction, 2 ml culture samples were taken at set times specified on expression gel in the results. All samples were centrifuged at 14,500 x g for 2 min and the pellet re-suspended in 50 μl of milli-Q water and 50 μl of loading buffer (Section 2.3.2.1). The samples were stored at -20 ^{o}C prior to being run on an expression gel.

The same protocol was used for protein expression in JM109 competent cells, however samples pellets were heat-treated rather than re-suspended in milli-Q water and loading buffer (Section 2.3.7).

2.3.1.2 Peptone broth expression.

BL21(DE3) competent colonies transformed with *α-syn*pRK172 plasmid used in expression experiments using peptone media were performed in the same way as above (section 2.3.1.1), except instead of using LB broth, peptone media containing amp (50 μg/ml) and chlora (34 μg/ml) was used.

2.3.1.3 LB broth single colony inoculation.

Colonies of *α-syn*pET-22b(+) transformed BL21(DE3)pLysS cells were selected from plates and used to directly inoculate 4 x 500 ml of pre-warmed LB broth

containing amp (50 μg/ml) and chlora (34 μg/ml). The cultures were incubated at 37 ^{o}C, shaking until an OD_{600} of 0.4 – 0.6 was reached (at which point a 2 ml sample of the culture was collected and the remaining cultures were induced by the addition of 0.001 M IPTG). Then either time-course samples were then taken or all of the culture was collected 4 h after induction by IPTG. In both cases cultures were heat-treated as described in section 2.3.7.1.

2.3.1.4 10 L Fermentation - Scale-up of expression cultures.

Plasmids were taken to the Edinburgh Protein Interaction Centre (EPIC) and Brunswick BioFlo4500s 5 – 15 L fermentors were used for culture growth. Pellets were collected from the EPIC and heat-treated as in section 2.3.7.2.

2.3.2 Preparation of 16 % acrylamide SDS electrophoreses gels.

Initial experiments used 16 % acrylamide, sodium dodecyl sulphate (SDS) gels prepared in-house. To produce two gels the following mix was prepared for the 16 % SDS gel: 2 ml milli-Q water, 5.3 ml 30 % acrylamide/bis-acrylamide, 2.5 ml 1.5 M Tris (8.8 pH) and 0.1 ml 10 % SDS, 0.1 ml ammonium persulphate and 10 μl TEMED. The stacking gel prepared contained: 3.3 ml milli-Q water, 1 ml 30 % acrylamide/bis-acrylamide, 0.62 ml 1.25 M Tris (6.8 pH), 0.05 ml 10 % SDS, 0.05 ml ammonium persulphate and 10 μl TEMED.

The gel was constructed by pipetting 3 ml of the 16 % SDS gel between two glass plates. 1ml of milli-Q water was gently pipetted on top of the 16 % gel to ensure a level top of the gel. Once set the water was removed and the stacking gel was

pipetted on top of the 16 % gel to the top of the glass plates, a well comb was inserted into the stacking gel and allowed to set. When set the comb was removed and the gels were ready use.

2.3.2.1 Loading buffer for 16 % SDS gels.

For the 16 % SDS gels, 2 x laemmli loading buffer was prepared in-house for sample loading. To produce 10 ml; 1 ml 125 M Tris (6.8 pH), 4 ml 10 % SDS, 71 µl 0.1 M β-mercaphothanol, 2 ml of glycerol and 2.93 ml of milli-Q water were mixed together.

2.3.3 Electrophoresis of expression cell pellets using 16 % SDS gels.

Cell pellets collected from the expression cultures were re-suspended in 50 µl of milli-Q water and 50 µl 2 x laemmli loading buffer. All the samples were heated to 95 ^{o}C on a heat block for 5 min and allowed to cool.

The electrophoresis box was prepared, containing 2 x 16 % SDS gels making a inner chamber which was filled with 1 x SDS running buffer and allowed to overflow to half fill the outer chamber. The wells were loaded with 20 µl of the samples and 10 µl of specified marker with the order of loading noted for each individual run. The gels were run for 45 min at 200 V and 400 amps (figure 2.3).

The 16 % SDS gels were removed from the electrophoresis box and removed from between the glass plates. The stacking gel containing the wells was removed and the remaining 16 % SDS gel was stained for 1 – 2 h with coomassie blue dye. The

excess staining was removed by washing the gel in 10 % acetic acid and 20 % methanol overnight on a rocking table. The gels were photographed using a Multimager light cabinet (Alpha Innotech Corporation) and analysed using FC 8000 v3.04A FluroChem software.

2.3.4 Electrophoresis of fraction samples using NuPAGE 4 – 12 % Bis –Tis gels.

To all samples (normally ~ 37 µl) run on th NuPAGE 4 -12 % Bis –Tis 1.0 mm gels (Invitrogen), 12.5 µl of 10 x NuPAGE Sample buffer and 1.0 µl 0.1 mM DTT was added and the samples vortexed. All the samples were heated to 95 ^{o}C on a heat block for 5 min and allowed to cool.

The electrophoresis box was prepared, containing NuPAGE 4 -12 % Bis –Tis 1.0 mm gels (Invitrogen) making a inner chamber which was filled with 1 x NuPAGE® Mes SDS running buffer (Invitrogen) with 10 µl of NuPAGE antioxidant (Invitrogen) added once the chamber was full. NuPAGE® Mes SDS running buffer (Invitrogen) was also used to fill the outer chamber about 3/4 full. Samples were loaded in to the NuPAGE gels with 15 – 20 µl per well. The gels were run for 45 min at 200 V and 400 amps (figure 2.3).

The NuPAGE gels were removed from the electrophoresis box and washed three times with distilled water for 15 min. SimpleBlue SafeStain (Invitrogen) was used to stain the gels. Enough stain was added to each gel to completely cover the gel (approx. 20 ml), and incubated at room temperature on a rocking plate for 1 – 8 h. The staining reagent was removed and the gels washed twice with distilled water for

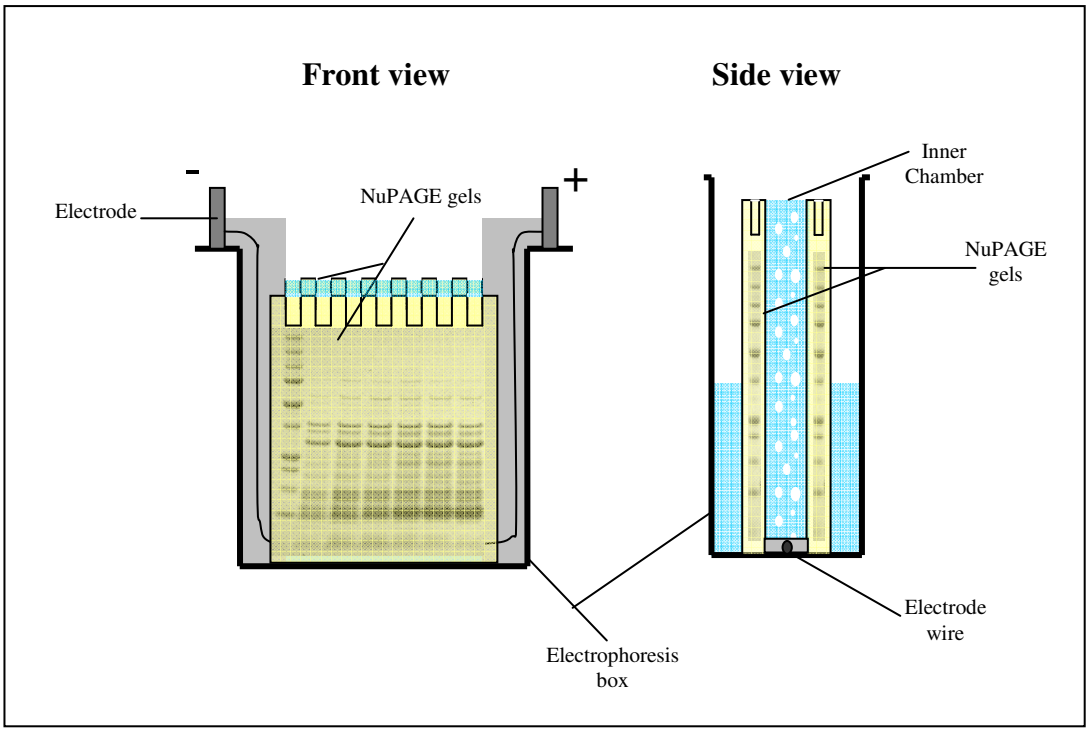

Figure 2.3: Schematic of NuPAGE gel electrophoresis setup.

15 min. On the third wash the distilled water was left for a 1 h to remove any excess stain from the gel. The gels were photographed using a Multimager light cabinet (Alpha Innotech Corporation) and analysed using FC 8000 v3.04A FluroChem software.

IMPORTANT NOTE

Changing the gels from 'homemade' SDS-PAGE gels to pre-made NuPAGE gels (Invitrogen) showed that the α-syn protein ran differently between the two types of gel; on SDS-PAGE gels α-syn appears as a band at 17 - 19 kDa whereas on NuPAGE gels α-syn appears as a band at ~ 14 kDa. This was difference has been previously identified by (Moussa *et al.* 2004).

2.3.5 Western blot positive control.

Rat cerebrum was used as the positive control for the presence of syn proteins. Frozen rat cerebrums was thawed on ice while lysis buffer was prepared (10 mM Tris (pH 7.4), 1 % SDS, PMSF (1 µl per 100 µl), proteinase inhibitors (1 µl per 1000 µl). A section of rat cerebrum weighing ~ 0.5 g was cut and homogenised using a loose fit (x 10) followed by a tight fit (x 20) homogeniser in 10 x the volume of lysis buffer (1 ml of lysis buffer to 0.1 g). The brain tissue was heated to 95 ^{o}C for 10 min and cooled on ice before centrifugation at 12,500 x g for 4 min at 4 ^{o}C. The supernatant was collected and total protein concentration was determined by BCA assay (Section 2.3.10).

A portion of the rat cerebrum supernatant was diluted to 5 mg/ml using NuPAGE loading buffer as follows; 200 µl of cerebrum sample, 2.8 ml of 10 x NuPAGE Sample buffer and 6 – 10 µl of DTT (10 mM). The cerebrum sample in loading buffer was aliquoted in to 50 µl volumes and stored at -70 ^{o}C. The remaining undiluted cerebrum supernatant was aliquoted into 0.5 ml volumes, stored at -70 ^{o}C.

2.3.6 Western blotting.

Proteins separated on either SDS-PAGE or NuPAGE gels can be detected using protein-specific antibodies by western blots. The protocol for each western blot is principally the same, with the only change being the specific primary antibodies used depending on the protein being identified on the blot. As all the primary antibodies I used were raised in mice the secondary antibody was anti mouse Ig for all western blot studies. Human α-syn (host: mouse) antibody (BD Biosciences) was used for the detection of α-syn and human β-syn (host: mouse) antibody (BD Biosciences) was used for the detection of β-syn. The dilution ratios all stayed the same irrespective of the antibody used.

Initially protein samples were loaded on to either SDS-PAGE or NuPAGE gels, and run as described in sections 2.3.3 and 2.3.4 respectively. Magic marker standards (Invitrogen) and a control samples (section 2.3.5) were also run for each experiment. During the electrophoresis of the expression gels, 4 pieces of filter paper (Amersham Biosciences) and Hybond C membrane (Amersham Biosciences) were soaked in 1 x transfer buffer (25 mM Tris, 0.15 M glycine, 200 ml methanol 800 ml distilled water) along with 6 sponges. On conclusion of electrophoresis run, the gels were

removed from the electrophoresis tanks. The gels were layered as per figure 2.4. The produced sandwich was transferred into a transfer box and the box inserted into the electrophoresis tank and locked in place. Transfer buffer was poured into the top of the transfer box until the buffer level was just above the top of the gel and membrane sandwich. The gel transfer was run for 1 h at 30 V and 400 amps.

At the end of the run the membrane was removed and washed in TBS/T (1 x Tris buffered saline (pH 8.0) containing 0.1 % Tween 20) for 5 min, three times. The membrane was then blocked with 4 % milk in TBS/T at room temperature on a rocking table for 1 h or at 4 ^{o}C overnight. The blocking solution was removed and the membrane incubated with primary antibody (1 : 5,000) in 4 % milk in TBS/T, at 4 ^{o}C overnight on a rocking table. The antibody was removed and the membrane was washed in TBS/T for 5 min. The wash procedure was repeated a further 2 times. After the washes the membrane was incubated with the secondary antibody, (anti-mouse Ig horseradish peroxidase-linked whole antibody; Amersham Biosciences, 1 : 20,000) in 4 % milk in TBS/T for 1 h at room temperature and rocking. The secondary antibody was removed and the membrane washed in TBS/T for 10 min, three times. The membrane was developed using ECL Plus Western Blotting Detection reagents (Amersham Biosciences) by following manufacturer's guidelines. In brief, detection reagents were mixed in 40 : 1 ration of reagent A and reagent B and protected from light. The excess buffer from the wash steps was drained from the membrane and the membrane was placed protein side up on to a piece of SaranWrap. The mixed detection reagents were pipetted directly on to the membrane ensure the whole membrane was covered. The membrane was incubated for 5 min at room

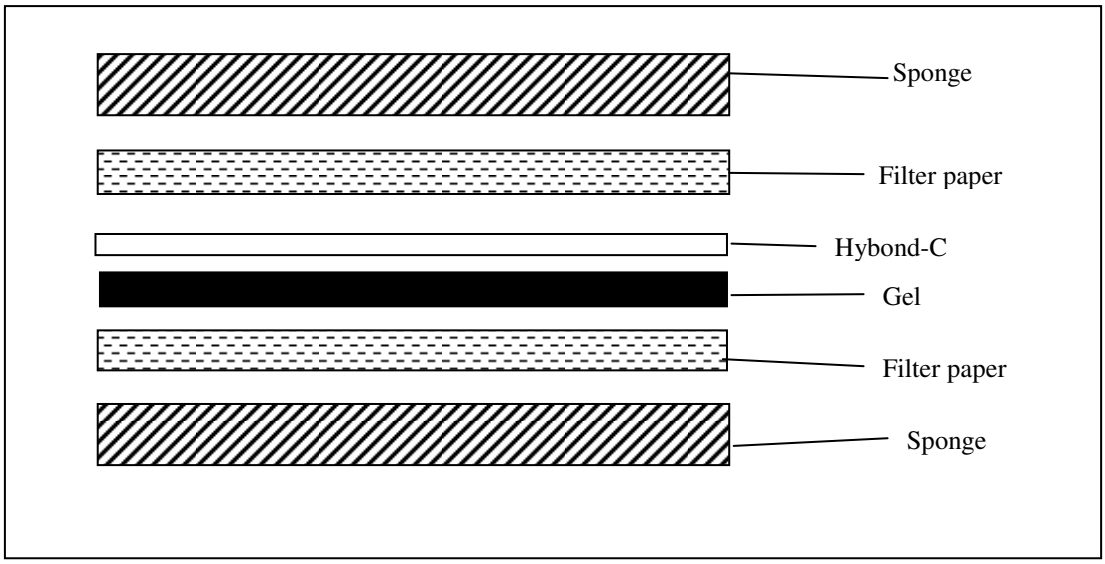

Figure 2.4: Schematic of the layers in a Western blot.

Schematic of the order of layers in a western blot; sponge, filter paper, electrophoresis gel, Hybond-C extra membrane (marked on the side facing the gel), filter paper and sponge.

temperature. Excess detection reagents were drained off. The membrane wrapped again in SaranWrap and was exposed using Chemi display of the Multimager light cabinet (Alpha Innotech Corporation) for 1 min and the exposed membrane viewed using FC 8000 v3.04A FluroChem software. Exposure time was varied depending on initially intensity of protein blots viewed.

2.3.7 Heat treatment of cell lysate.

2.3.7.1 Heat treatment of expression time course samples.

A 2 ml culture sample (from sections 2.3.1.1 to 2.3.1.3) was centrifuged at 14,500 x g for 2 min, the supernatant discarded and cell pellet washed with 0.5 ml of cold 1 x PBS by centrifuging at 14,500 x g for 2 min or 2,700 x g for 5 min. PBS was discarded and the cell pellet re-suspended in 50 – 100 µl of cold lysis buffer (0.75 M NaCl, 0.1 M Tris pH 7.0, 1 mM EDTA and 1 protease inhibitor cocktail tablets (Roche) per 10 ml and milli-Q water) by vortexing. The lysed cells were heated for 10 min at 100 ^{o}C in a water bath before cooling on ice and centrifuging at 12,500 x g for 30 min at 4 ^{o}C. The cell lysate was stored at -20 ^{o}C.

2.3.7.2 Heat treatment of expression cultures.

For 2 L expression culture, the culture was split into 4 x 500 ml centrifuge bottles and centrifuged at 4,000 x g for 15 min at 4 ^{o}C. The supernatant was discarded and each cell pellet was washed with 500 ml of cold 1 x PBS and centrifuge at 4,000 x g for 15 min at 4 ^{o}C. The 1 x PBS was discarded. Each pellet was re-suspended in the equivalent volume (approx. 5 – 10 ml) of cold lysis buffer (0.75 M NaCl, 0.1 M Tris pH 7.0, 1 mM EDTA and 1 Protease inhibitor cocktail tablets (Roche) per 10 ml and

milli-Q water) by trituration and vortexing. Once fully re-suspended, the lyised cells were heated for 10 min at 100 ^{o}C in a water bath and cooled on ice before centrifuging at 12,000 x g for 30 min at 4 ^{o}C. The cell lysate was removed to a sterile tube without disturbing the pellet. The pellet was discarded and the cell lysate was kept on ice ready for dialysis.

2.3.8 Dialysis of protein samples.

The cell lysate produced by heat treatment (section 2.3.7) was dialysed into 20 mM Tris (pH 8.2) using Slide-A-Lyzer® Dialysis cassettes with 3,500 MWCO (Pierce). The same dialysis protocol was also used for the dialysis of α-syn containing column fraction samples, although deionised water was used instead of 20 mM Tris (pH 8.2) (see sections 2.3.11).

The cassettes were hydrated according to manufactures protocol immediately before use and used for one dialysis only. In brief, the cassette was immersed in dialysis buffer for 30 s to hydrate the dialysis membrane. The cell lysate was injected into the dialysis chamber and dialysed overnight with gentle stirring at 4 ^{o}C. The dialysed sample was removed and stored at either 4 ^{o}C for same day use or at -80 ^{o}C.

2.3.9 Lyophilisation of α-syn protein.

α-Syn fractions were pooled and dialysed overnight into deionised water (section 2.3.8). After dialysis, the sample was sterilised by filtration (0.22 μm). A portion of the filtered sample was taken to determine protein concentration by BCA assay (section 2.3.10). Once the protein concentration was determined, the filtered α-syn

sample was aliquoted into ~ 1 mg quantities and frozen at -70 ^{o}C for 4 – 6 h before the tubes were freeze dried. The α-syn aliquots were kept under pressure overnight. Before being collected and stored at -70 ^{o}C. Two of the lyophilised α-syn samples were re-hydrated in 1 ml of deionised water each and the protein concentration was confirmed by BCA assay (section 2.3.10) with the BCA standards diluted in deionised water.

2.3.10 BCA assay.

All BCA assays (Pierce) were setup in a 96 well plate (Nunc) according to manufactures protocol. Test samples were analysed at appropriate dilutions and were run in triplicate. Concentration standards (Albumin, Pierce) were run concurrently (in duplicate), diluted in the same buffer as test samples. 10 µl of test sample or 20 µl of standards were loaded per well.

The BCA reagents were then prepared by adding 11 ml of reagent A to 220 µl of reagent B and vortexed. 200 µl of the mixed reagents were added to each well used (standards and samples). The plate was wrapped in tin foil, incubated at 30 ^{o}C for 1 h and was then read using an optical density 96 well plate reader (Dynex revelation 3.04) which read the plate at a wavelength of 560 nm. The protein concentration for each sample was calculated from the concentration curve produced by the standard using Reval MFC application v1.0.0.1 software.

2.3.11 Fast Protein Liquid Chromatography (FPLC).

Recombinant syn proteins were purified by ion-exchange chromatography using either a Mono-Q column, a HiTrap Q HP column or a self-poured column using Q Sepharose High Performance matrix (all from Amersham Biosciences). All columns were equilibrated in 0.02 M Tris pH8.2 (buffer A). Protein samples were dialysed into buffer A, as described in section 2.3.8, and cell debris removed by centrifugation (12,500 x g for 5 min) using a micro centrifuge before being injected onto the column. Unbound material was eluted by washing with buffer A. The 1 ml Mono-Q column was run at a flow-rate of 1 ml/min with 1 M NaCl, 0.02 M Tris pH8.2 used as the elution buffer (buffer B). The elution of bound proteins from the column was achieved by increasing the buffer B gradient from 0 – 40 % over 10 min, before raising the gradient to 100 % for 5 min to wash the column. For the HiTrap Q HP column (1 ml and 5 ml), an extra 5 min of 20 % buffer B step prior to the start of the gradient was added to remove contaminants from the column prior to elution of the syn proteins. Bound protein was eluted by increasing the gradient 20 – 40 % over 10 min. Buffer B gradient was then raised to 100 % for 4 min to wash the column. For the 1 ml HiTrap Q HP column, a 1 ml/min flow rate was used, whereas for the 5 ml HiTrap Q HP column, a 5 ml/min flow rate was used.

Self-poured columns (using Q Sepharose High Performance matrix) were run at 5 ml/min, with the increase of buffer B to 20 % gradient over 10 min. 4 ml volumes were collected over the 20 – 40 % gradient. For all the column runs the purified fractions collected were analysed by SDS-PAGE or NuPAGE gels as described in sections 2.3.3 and 2.3.4.

2.3.12 Mass Spectrometry of NuPAGE gel bands.

Collected fractions from some of the FPLC purification runs (see section 2.3.11) were analysed by NuPAGE gels. Bands from these gels were extracted and analysed by Dr Duncan Short of A.C.E. (University of Edinburgh) using mass spectrometry to identify the band corresponding to α-syn. Briefly, the bands of interest were excised from the gel and incubated with 300 µl of 200 mM ammonium bicarbonate in 50 % acetonitrile at 30 ^{o}C for 30 min to remove SDS. Supernatant was removed and the protein reduced in the presence of 20 mM dithiothreitol in 300 µl, 200 mM ammonium bicarbonate, 50 % acetonitrile and left at 30 ^{o}C for 1 h. Separate gel pieces were washed with 300 µl of 200 mM ammonium bicarbonate, 50% acetonitrile three times before the protein band was alkylated by the addition of 100 µl 50 mM iodoacetamide, 200 mM ammonium bicarbonate and 50% acetonitrile at room temperature in the dark for 20 min. Gel pieces were allowed to air dry before being reconstituted in acetonitrile. Reduced and alkylated protein gel pieces were digested with 20 µl of 12.5 µg/ml trypsin in 20 mM ammonium bicarbonate overnight at 30 ^{o}C (after a short period of gel swelling at 4 ^{o}C). Samples were spotted directly onto the MALDI sample plate utilising the dry drop method (0.5 µl each, 1:1 mix with matrix solution consisting of saturated alpha-cyano-4-hydroxy cinamic acid in 0.1 – 0.3 % TFA, 50 % MeCN,) and allowed to air dry.

2.4 Tissue Culture.

The SHSY-5Y human neuroblastoma cells (cell line No. 94030304) were obtained from the ECACC (European Collection of Cell Cultures, Salisbury, Wiltshire, UK). SHSY-5Y cells were cultured in Dulbecco's modified Eagle's medium (DMEM)

with 10 % foetal calf serum (FCS) (Gibco), 2 mM L-glutamine and 1 % penicillin and streptomycin. The cells were not cultured beyond 6 weeks or passage 18.

2.4.1 Passage of SHSY-5Y cells into 250 cm^2 flasks.

Once the cells were 80 % confluent on the bottom of the 250 cm^2 flask, they were split into new flasks. The growth media was removed and the cells washed with pre-warmed Hank's balanced salt solution (Hanks). The Hanks was removed and 5 ml of 0.25 % Trypsin-EDTA solution was added to the cells and incubated at 37 ^oC and 5 % CO_2 for maximum of 10 min. This causes the cells to rise off the bottom of the flask to be enabling collection. Trypsin was neutralised by the addition of 5 ml of pre-warmed DMEM containing 2 mM L-glutamine and 1 % penicillin, streptomycin and 10 % FCS (growth media). The cells were then centrifuged for 5 min at 200 x g at 37 ^oC. The supernatant was removed and 2 ml of fresh media was added. The cell pellet was re-suspended by gently pipetting the cells in growth media. A further 18 ml of growth media was added to the cells. 10 µl of the re-suspended cells were counted using a haemocytometer.

The re-suspended cells were transferred to new sterile 250 cm^2 flasks to a density of approximately 1 x 10^6 cells per flask. Growth media was added to each flask to give a final volume of 25 ml. The flasks were incubated at 37 ^oC, 5 % CO_2, the media was changes after 3 – 4 days growth.

2.4.2 Media change of SHSY-5Y culture flasks.

The media change was similar to the passage described above but the cells were not removed from the flasks. The growth media was removed from the cells and the cells washed with pre-warmed Hanks. To each flask, 25 ml of pre-warmed growth media was added and the cells returned to incubator until the confluence reached ~ 80 % (typically achieved after a further 3 days).

2.4.3 Seeding of SHSY-5Y on to 96 well plates.

For *in vitro* studies, cells were passaged as previously described in Section 2.4.1 and, after counting, were plated on to poly-$_D$-lysine treated 96-well plates (NUNC) at a density of 1 x 10^5 cells per well. Cells were incubated at 37 ^oC with 5 % CO_2 overnight to allow cells to adhere to the wells. Growth media was removed and the cells were washed twice with DMEM containing 2 mM L-glutamine. After the final wash, cells were available for experimental use.

2.4.4 Aggregating of α-syn protein.

α-Syn WT and A53T proteins produced commercially (rPeptide) or in-house were aggregated by re-suspending 1 mg of lyophilized α-syn (either WT or A53T) in 1 ml sterile filtered milli-Q water to give a final concentration of 69.1 μM based on molecular weight. The resuspended α-syn was aliquoted in to 55 μl volumes and incubated at 37 ^oC for 7 days. After the 7 day incubation the aggregated WT or A53T α-syn was used immediately. Thioflavin T is a dye which fluoresces at the excitation and emission of 450 and 482 nm, respectively, in the presence of α-syn fibrils (but not in the presence of soluble α-syn) (Conway *et al.,* 2000; Hoyer *et al,.* 2002).

Thioflavin T was used to monitor and confirm α-syn aggregation by a method adapted from Yoshiike *et al.,* 2003.

2.4.5 Preparation of MPP^+ stocks.

MPP^+ was dissolved in a sterile filtered milli-Q water to give a stock solution of 1 M, and used immediately used. All tips and containers with had come in to contact with MPP^+ and any unused MPP^+ solutions were disposed of in separate labelled waste containers, and incinerated.

2.4.6 MTS assay.

CellTiter 96® AQueous One Solution Reagent (Promega) (MTS assay) contains a novel tetrazolium compound that is reduced by NAD(P)H (released from metabolically active cells) to produce a coloured formazan product. The colour change induced by the reduction of MTS is monitored by reading the light absorption at 490 nm. A decrease in MTS signal is indicative of cytotoxicity and cell death.

The assay was used according to the manufactures protocol (Promega Technical bulletin TB245 – General Protocol). The cells were plated as described in section 2.4.3. Cell treatments and controls were set up in triplicate to a final volume of 100 µl. Background controls of all treatments were plated in wells not containing cells. The plates were incubated for the specified time for experiment (stated in results section 4.1).

At the end of the treatment incubation, 20 µl of pre-warmed CellTiter 96® AQueous One Solution Reagent (Promega) was added directly to all the wells giving a 1 in 6 dilution. The plates were incubated for a further 1 h at 37 °C and 5 % CO_2. After incubation, the plates were read using an optical density 96 well plate reader (Dynex revelation 3.04) at 490 nm wavelength. The plate reader was setup to automatically subtract the appropriate background from the treatment wells according to the experimental template. The data was analysed using SigmaPlot and SigmaStat and errors bars on all subsequent graphs show standard error of mean (SEM).

2.4.7 LDH assay.

CytoTox96® Non-Radioactive Cytotoxicity assay (Promega) (LDH assay) quantified cell death by measuring the release of the enzyme lactate dehydrogenase (LDH) from lysed cells. Released LDH metabolises tretrazolium salt to produce a red formazan produce. The amount of colour change is proportional to the number of lysed cells and the colour change can be detected using a visible wavelength plate reader.

The LDH assay was used according to the manufactures protocol (Promega Technical bulletin TB163 – LDH measurement). The cells were plated as described in section 2.4.3. Cell treatments (or vehicle) were performed in triplicate at a final volume of 100 µl. Triplicate wells of all treatments (each 100 µl) were also prepared in wells devoid of cells to be used as background control. Plates were incubated for the time specified for each experiment (stated in results chapter 4). Irrespective of incubation times, 90 min prior to the end of incubation, 15 µl of 10 x lysis solution (supplied with LDH assay) was added to the positive control cells (to generate

measurable cell death signal). At the end of the incubation, 50 µl of the supernatant (media) of each well was transferred to a fresh 96-well plate.

12 ml of assay buffer (supplied within the LDH assay, Promega) was added to one bottle of substrate mix (supplied within the LDH assay, Promega). Once resuspended the substrate was protected from the light and used immediately. The reconstituted substrate mix was added at 50 µl per well to all the wells of the treatment plate. The treatment plate was covered with tin foil (to protect the plate from light), incubated for 30 min at room temperature before the addition of 50 µl of stop solution (supplied within the LDH assay) to each well. The plate was run using optical density 96 well plate reader (Dynex revelation 3.04) at 490nm and analysed using Revel software within 1 h of the addition of the stop solution. The Revel software was programmed, to subtract the appropriate background from each treatment reading.

The average of the treatment, controls and lysed cells was determined and used to calculate the percentage of cytotoxicity. The percentage of cell death was calculated by the below equation (figure 2.5). The resultant data was analysed using SigmaPlot and SigmaStats, with errors bars on all subsequent graphs showing SEM.

$$\% \text{ Cell Death} = \frac{\text{Treatment} - \text{Vehicle Control}}{\text{Lysied Cells} - \text{Vehicle Control}} \times 100$$

Figure 2.5: Percentage of cell death calculated from LDH assay.

2.4.8 Cytochrome c ELISA.

2.4.8.1 Cytochrome c sample preparation.

The cells were plated as described in section 2.4.3. Cells were treated according to the concentration and incubation time stated in the results (section 4.2) in sets of triplicate wells with final volume of 100 µl per well.

At the end of the treatment incubation, the treatments were removed and the cells were washed with 100 µl of Hanks solution. The wash was removed and the cells incubated for 1 h at room temperature with 70 µl of either digitinon extraction buffer (removes cellular membrane but not vesicle or organelle membranes) or 3-[(3-Cholamidopropyl)dimethylammonio]-1-propanesulfonate (CHAPS) extraction buffer (removes all membranes). Thirty min into the incubation the cells were triturated and then incubated for a further 30 min at room temperature. Lysed cells from each triplicate were combined and centrifuged at 2,500 x g for 5 min. The supernatant was collected and stored at either -20 ^{o}C overnight or -70 ^{o}C if longer.

2.4.8.2 Solution for cytochrome c cell sample preparation.

10 x stock of 1.5 M NaCl + 100 mM HEPES-(Na/K)OH, pH 7.6: Dissolved 8.8 g NaCl (1.5 M) and 2.4 g HEPES into 80 ml of water, corrected pH to 7.6 with NaOH or KOH and then adjusted volume to 100 ml.

Digitonin Extraction Buffer:

150 mM NaCl + 10 mM HEPES – (Na/K)OH pH 7.6 (use a 10x stock)

1 % PMSF

1 % protease inhibitor cocktail

3.1 µM digitonin

CHAPS Extraction Buffer:

150 mM NaCl + 10 mM HEPES-(Na/K)OH, pH 7.6 (in a 10 x stock)

1 % PMSF

1 % protease inhibitor cocktail

1 % CHAPS detergent

2.4.8.3 Cytochrome c ELISA – Protocol.

The ELISA kit used as described within the manufactures manual (Bender MedSystems working protocol for the human Cytochrome c Module set BMS263MST). Initially, plates were coated with 100 µl/well of coating solution (1 µg/ml; 1 in 100 dilution in PBS of supplied stock solution). The plates were incubated at 2 - 8 ^{o}C overnight. The coating solution was removed and the plates were washed with 250 – 300 µl of 1 x PBS with 0.1 % tween 20 (repeated twice). On the last wash the plates were tapped dry. The coated plates were blocked with 250 µl 1 x Assay buffer per well (supplied with kit as 5 x stock and diluted with milli-Q water) and incubated for either 2 h at room temperature or overnight at 2 – 8 ^{o}C.

The samples prepared in section 2.4.8.1 were diluted in 1 x Assay buffer (1/10, 1/20, 1/50 or 1/100) and cyctochrome c standard (100 ng/ml, supplied with kit) was prepared at 0.16 ng/ml, 0.32 ng/ml, 0.63 ng/ml, 1.25 ng/ml, 2.5 ng/ml, 5.0 ng/ml and 10 ng/ml.

The blocked plates were washed twice with 1 x PBS with 0.1 % tween 20 before 100 µl of the diluted sample and standard were added to the plate. Biotin-conjugate was diluted by a ratio of 1 : 2,000 in assay buffer and 50 µl of the diluted biotin-conjugate was added to each wells, the plate was covered and incubated for 2 h at room temperature. The plate was washed three times with 1 x PBS with 0.1 % tween 20. On the final wash the plate was tapped dry.

To each well 100 µl of Streptavidin-HRP (supplied in kit and diluted to a ratio of 1 : 10,000 in 1 x assay buffer prior to use) was added. The plate was covered and incubated for a 1 h at room temperature. The plate was washed three times with 1 x PBS with 0.1 % tween 20 and tapped dry. Substrate solution was prepared (tetramethylbenzidine in milli-Q water, 2 : 1 v/v) and 100 µl added to all the wells. The plate was incubated in the dark at room temperature for 15 min. The reaction was stopped by the addition of 100 µl 4 N Sulphuric acid and the plate was read using the optical density 96 well plate reader (Dynex revelation 3.04) at 450 nm. The plate was analysed using the Revel software according to experimental template. The results were analysed using SigmaPlot and SigmaStat, with errors bars on all subsequent graphs showing SEM.

2.4.9 FLIPR Plus Ca^{2+} assay.

The FLIPR Plus calcium assay kit (Molecular Devices Corporation) is a fluorescence-based assay which utilises a cytoplasmic dye to detect changes in intracellular calcium.

The cells were plated as described in section 2.4.3. Cells were treated with specified treatments or controls in triplicate, with a final volume of 75 µl. An hour prior to the termination of the incubation time, the original cell treatments at 5 x the concentration of the original treatment and the cytoplasmic dye were prepared.

Cytoplasmic dye was prepared by warming one vial of component A (supplied with kit) to room temperature and dissolving in 10 ml of 1 x calcium buffer (diluted from x 10 Hanks buffer with Ca^{2+}/Mg^{2+} and 200 mM HEPES). To the reconstituted dye, 200 µl of 25 mM (±) sulfinpyranzone in 1 M NaOH was added. To each well, 25 µl of the treatment (to give appoperiate concentration in final volume) and 100 µl of the cytoplasmic dye was added. The cell plate was covered in tin foil and incubated for an hour at 37 ^{o}C in 5 % CO_2 before reading. Digitonin treated cells were used as a positive control. Wells allocated as positive controls were incubated initially with 75 µl serum-free media and an hour prior to termination, of digitonin (10 µM final concentration; prepared in serum-free media) and 100 µl of the dye was added to the wells.

After incubation the plate was transferred directly a Flexstation (Molecular devices) set to read at an excitation wavelength of 485 nm and emission wavelength of

527 nm (with emission cut-off at 515 nm). The generated results were analysed using SigmaPlot and SigmaStat software, with subsequent errors bars on all graphs showing SEM.

2.4.10 MitoPT™ Mitochondrial permeability transition detection kit.

The MitoPT™ Mitochondrial permeability transition detection kit (B-Bridge international, Inc.) was used to detect changes in mitochondrial membrane potential within SHSY-5Y cells treated with α-syn, using the manufacturers protocol (MitoPT™ Mitochondrial permeability transition detection kit user manual UM-MPT01, B-Bridge international, Inc.). Changes in the mitochondrial membrane potential were detected by using the fluorescent cationic dye, 5,5',6,6'-tetrachloro-1,1',3,3'-tetraethyl-benzamidazolocarbocyanin iodide, (JC-1).

For the MitoPT™ assay, SHSY-5Y cells were cultured and plated as described in section 2.4.3, to a density of 1 x 10^5 cell per well (100 µl), using black 96-well plates with clear bottom and lid (Corning Incorporated). The plated cells were treated in triplicate well sets with α-syn (30 µM) in serum-free media or appropriate controls and incubated for 0 – 48 h. STS (1 µM) was used as a positive control and serum-free media was used a negative control.

At the end of the incubations, the treatments were removed. The cells were washed with 100 µl Hanks salt solution, pre-warmed to 37 ^{o}C. The Hanks was gently removed and 50 µl of the prepared 1 x MitoPT™ solution (section 2.4.10.1) was added to each well. The plate was gently rocked to ensure the cells were completely

covered. The cells were incubated for 15 min at 37 °C, 5 % CO_2 before the 1 x MitoPT™ solution was removed. The cells were washed with 200 µl of prepared 1 x assay buffer warmed to 37 °C (section 2.4.10.1). The wash was discarded and 100 µl of fresh 1 x assay buffer was added to each well. The plate was read using a Flexstation (Molecular devices) in combination with softmax Pro computer software set to read at an excitation wavelength of 485 nm and the emission wavelength of 527 nm to detect green fluorescence followed by a second read with emission wavelength of 595 nm for the identification of red fluorescence. The results generated with analysed using SigmaPlot and SigmaStats software, with subsequent errors bars on all graphs showing SEM.

2.4.10.1 Preparation of MitoPT™ reagents.

Reconstitution of MitoPT™: all the MitoPT™ powder was dissolved in DMSO according to manufactures protocol to form 100 x stock, which was frozen immediately and protected from light at all times.

Working solution of MitoPT™: The 100 x Stock MitoPT™ was diluted 1 : 100 with 1 x assay buffer pre-warmed to 37 °C to give 1 x MitoPT™ solution.

1 x Assay buffer: pre-warmed 10 x assay buffer was diluted in a ratio of 1 : 10 in deionised water.

E.g. 60 ml 10 x Assay buffer + 540 ml Deionised water.

Chapter 3: Expression, generation and purification of synuclein proteins.

3.1 Creation of recombinant synuclein proteins.

3.1.1 Determination of synuclein gene expression in pRK172 plasmid.

The expression plasmids pRK172 containing *α-syn, β-syn* or *A53T α-syn* were kindly gifted to the group through our collaboration with Professor Vladimir Buchman. Initially, the quantity of each plasmid had to be increased to establish usable amounts. This was achieved by transforming each plasmid into DH5α *E.coli* cells cultured on LB amp agar plates as described in section 2.2.2. From each plate, colonies were picked and grown overnight on LB broth with amp. The plasmids were isolated from the overnight cultures as described in section 2.2.4. Initially, s*yn* genes were inserted into the pRK172 expression vector using Nde I and Hind III restriction enzymes. Using these restriction enzymes the isolated plasmids were digested and run on 1 % agarose EthBr gels (section 2.2.5.1 and 2.2.6) to determine the presence and orientation of the *syn* gene (figure 3.1).

Three bands were produced by DNA digest for each plasmid (figure 3.1). All digests observed a band of approximately 4 Kb and another of approximately 3 Kb. The 3 Kb band was the correct size for pKR172 vector minus *syn* insert, whereas the 4 Kb bands were the correct size for partially digested plasmid where only one restriction enzyme successfully cut the plasmid. The plasmid digests of 500 bp in lanes 2 and 4 is consistent for either *α-syn* or *A53T α-syn* (figure 3.1; lanes 2 and 4 respectively).

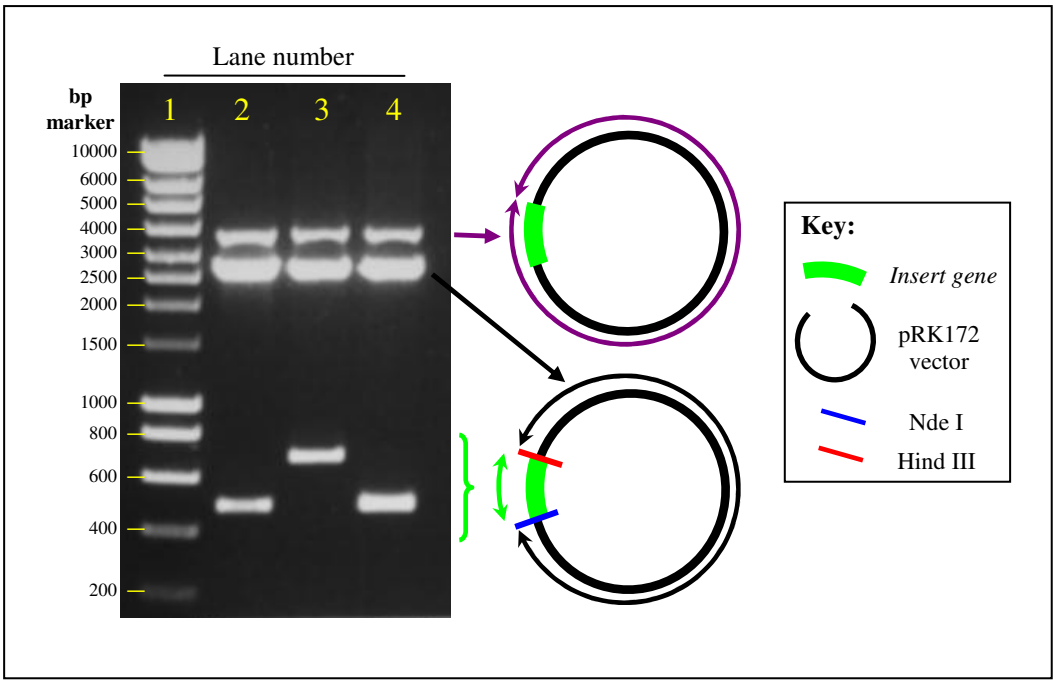

Figure 3.1: Restriction digest of *syn* containing pRK172 plasmids.

Plasmids were digested using Nde I and Hind III restriction enzymes and run on 1 % agarose EthBr gel. The figure identifies the presence of *syn* genes within the pRK172 vectors, with schematic of plasmid indicting band orientation and cutting sites (red line Hind III and blue lines Nde I cutting sites). EthBr gel Lane order was as followed; 1) HyperLadder I marker, 2) *α-syn* pRK172, 3) *β-syn* pRK172, 4) *A53T* pRK172. The 3 digest show three bands. As shown in the diagram, the band at ~ 4000bp is full plasmid as indicated by the purple arrows, showing only partial enzyme digestion. The ~ 3000 bp band is pRK172 vector minus insert, as indicated by the black arrows, and the bands at 500 – 700 bp are the *syn* inserts.

The β-syn plasmid gave a band that corresponds with the expected weight of the *β-syn* gene (approximately 700 bp) (figure 3.1; lane 3). From the DNA digest the presence of *syn* genes were identified with the correct orientation within the pRK172 vector.

3.1.2 Small scale production of protein expression of β-syn but not α-syn or A53T α-syn.

After identifying the correct inserts and increasing quantities of each *syn* plasmid, small scale expressions were carried out to discover the optimum condition and induction times for each protein expression. Initially, each plasmid was transformed into the competent cell line BL21 (DE3) and streaked on to amp and chlora containing agar plates (section 2.2.3). Colonies were picked for each plasmid and grown overnight in 10 ml LB with amp and chlora. The overnight cultures were used to inoculate 100 ml volumes of LB with amp and chlora which were grown to an OD_{600} of between 0.4 – 0.6 (growth medium used as a blank) (section 2.3.1). The OD_{600} reading of the culture was used as an indication of the cells entering the stationary phase of growth, the optimum growth phase for protein expression. Protein expression was then induced by the addition of IPTG to the culture (section 2.3.1). Full cell samples from each expression cultures were taken at 0, 0.5 h, 1 h, 2 h, 4 h and overnight for α-syn and β-syn expression cultures and at 0, 1 h, 2 h and overnight for A53T α-syn expression cultures. The cell samples were centrifuged and the pellets re-suspended in milli-Q water and laemmli loading buffer (1:1 v/v) (section 2.3.2.1) and run on SDS-PAGE gels to determine protein expression levels (section 2.3.2 and 2.3.3).

No expression was identified for either α-syn or A53T α-syn at any time of the points investigated (figure 3.2 A and B). β-Syn, however, was expressed with the intensity of the gel band increasing up to 4 h after induction of the expression culture. However, when the culture was left overnight the intensity of the β-syn band was severely reduced compared to earlier time points (figure 3.2 C). From this expression study we showed that α-syn and A53T α-syn expression was not induced under the conditions used. β-syn expression was successfully induced, with optimum expression at 4 h after induction (figure 3.2). The lack of α-syn and A53T α-syn expression could either suggest that the growth conditions were not optimum or indicative of a problem within α-syn and A53T expression vector, preventing the induction of protein expression.

3.1.3 Lack of expression of α-syn and A53T α-syn with increased stationary phase.

Although expression of β-syn was successful, similar conditions did not lead to expression of either α-syn or A53T α-syn. This could be due to the growth conditions used. The LB broth used for the culturing of the *E.coli* could be promoting a rapid increase in cell growth, reducing the length of time the cells are in stationary phase before entering the death phase of the growth cycle and therefore producing little or no protein. This would show as minimal levels of protein expression, if any at all. To determine if this was the case, we used peptone with the addition of sodium chloride as the growth media with the intention of reducing available glucose, thereby

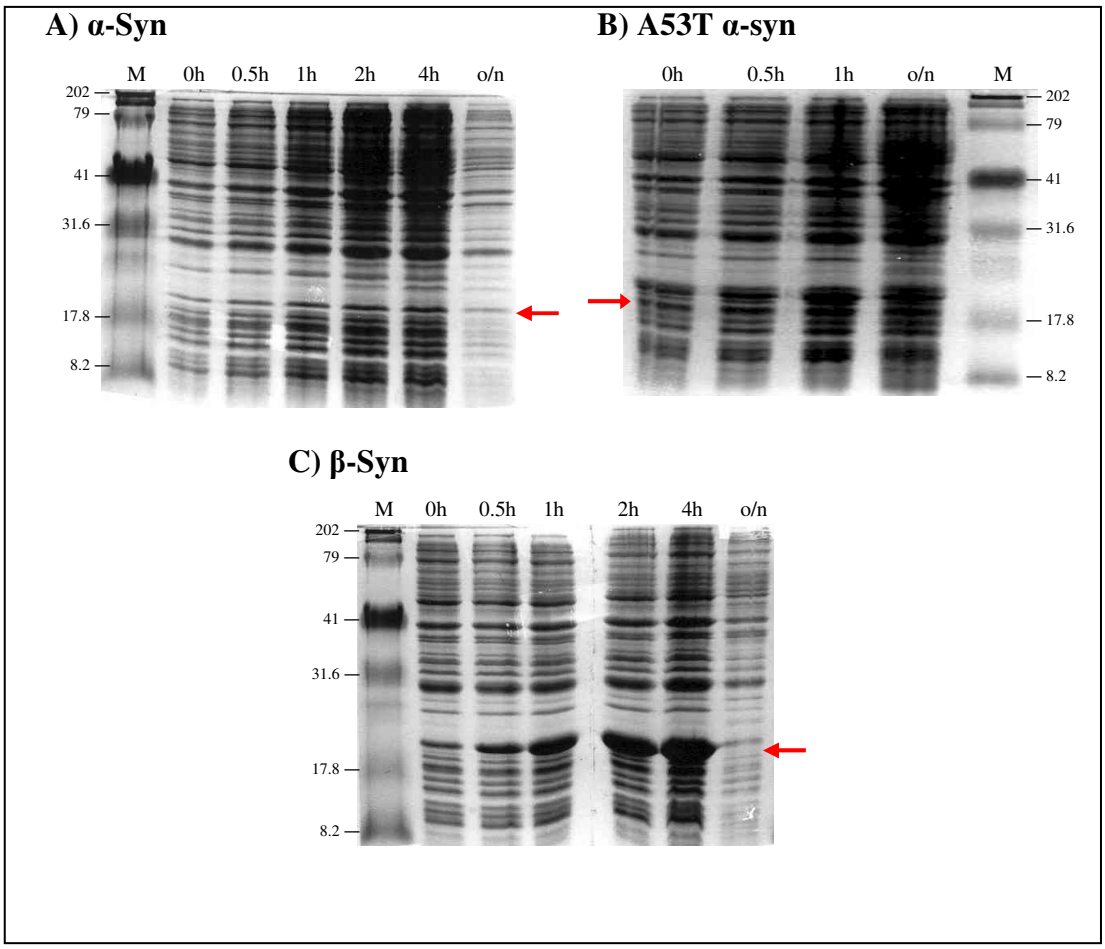

Figure 3.2: Expression trails for α-syn, β-syn and A53T α-syn proteins overtime.

SDS-PAGE expression gels were used to analyse protein levels of α-syn, β-syn and A53T from BL21 cells to determine optimum incubation time. Kaleidoscope pre-stained standards were used as marker, with red arrows marking the location of the correct band size for the syn proteins (17 - 19 kDa) on each gel. No expression was induced for either **α-syn (A)** or **A53T α-syn (B)** cultures at any time point. **β-syn (C)** expression was induced with increasing band intensity overtime up to 4 h. β-Syn expression was reduced with overnight incubation

reducing cell growth and increasing the stationary phase of the cell (the phase in where and increasing protein expression occurs) (section 2.3.1).

α-Syn and A53T α-syn BL21 glycerol stocks were used to establish colonies on amp and chlora containing agar plates. As described previously (section 3.1.2), colonies were picked and cultured overnight in either LB broth or peptone with amp and chlora. The appropriate overnight culture was used to inoculate either 100 ml volumes of LB broth or peptone, containing amp and chlora. As before, cultures were grown to an OD_{600} of 0.4 – 0.6 before inducing with IPTG. Samples of each expression culture were taken at 0, 0.5 h, 1 h, 2 h and overnight after induction, with an extra sample taken at 4 h from the α-syn culture in LB both. All samples were prepared as described previously by harvesting the cells and re-suspending the cells 1 : 1 ratio of water and laemmli loading buffer (section 2.3.4 and 3.1.2). All samples were run on NuPAGE gels as described in section 2.3.4.

The use of the peptone media reduced the total amount of cellular protein for both α-syn and A53T α-syn at all time points when compared to the amount of cellular protein from cultures grown in LB broth (figure 3.3). However, no obvious induction of expression for α-syn was observed with either growth media (figure 3.3 A and B). In slight contrast, low levels of expression were seen 30 min after induction for A53T α-syn in both the LB and peptone cultures (figure 3.3C and D).

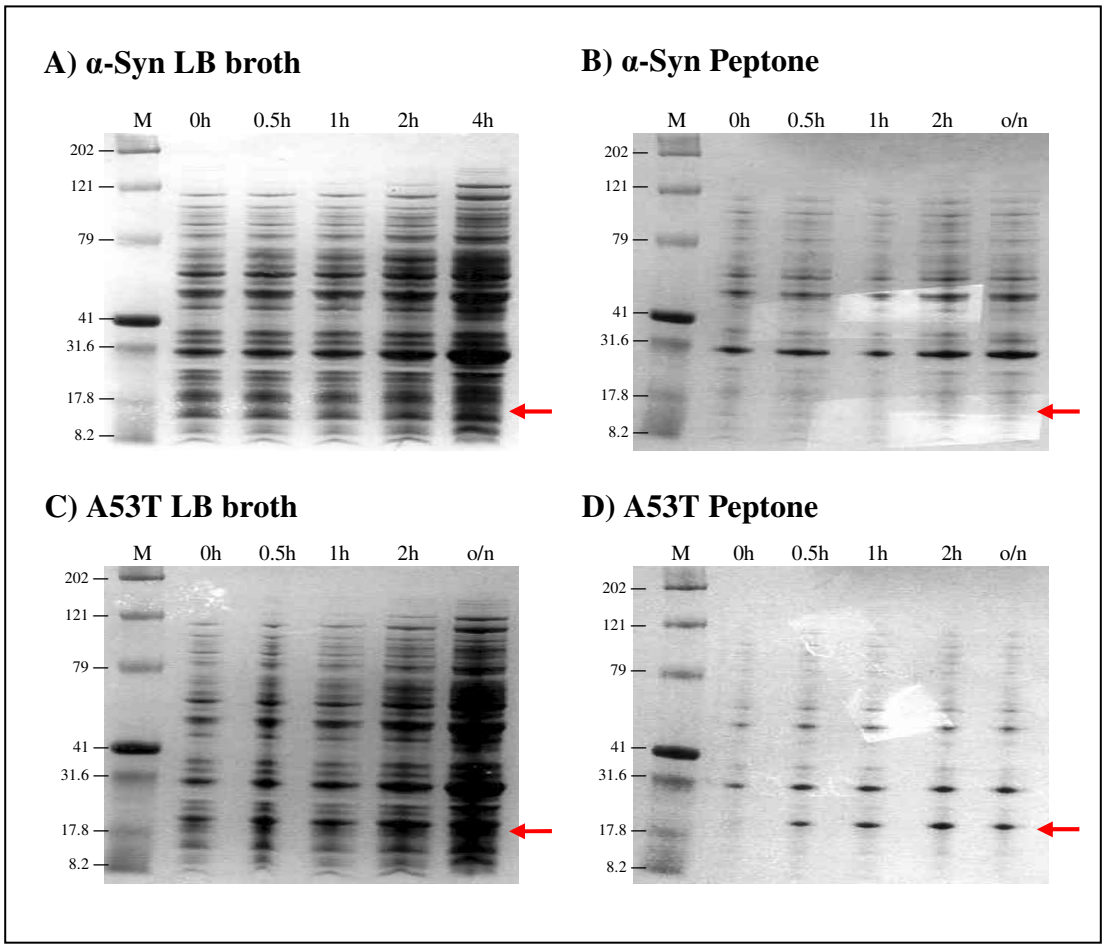

Figure 3.3: Comparison of expression of α-syn and A53T α-syn in LB broth or peptone.

NuPAGE expression gels were used to analyse expression levels of α-syn and A53T α-syn in BL21 cells over time. Kaleidoscope pre-stained standards was used as a marker, red arrows indicating the approximate band size for either α-syn or A53T α-syn on each gel. No expression was observed for α-syn cultured in either **LB broth (A)** or **peptone (B)** at any time point post-induction. Low levels of expression were observed with A53T α-syn cultured in **LB broth (C)** and **peptone (D),** where low level expression was observed after 0.5h induction.

From this study we showed that low level expression of A53T α-syn could be induced under normal conditions (in LB broth) or with an increased stationary phase (in peptone media). The low or lack of expression for both proteins could suggest that the issue may not be related to the media conditions, but due to a problem with the expression vector itself, restricting the induction of expression. However, levels of expression were still very low and α-syn did not show any expression at all.

3.1.4 Validation of low syn expression levels using immunochemical identification.

To determine the expression of α-syn, A53T α-syn and β-syn accurately and to analyse α-syn expression with greater sensitivity we used western blotting to identify if there was any α-syn expression present within the samples.

For all western blots, rat cerebrum was used as a positive control for syn proteins (section 2.3.5). Using an antibody targeted against α-syn, A53T α-syn was identified in all the A53T α-syn samples (figure 3.4 A). However, similar expression was not observed for α-syn (figure 3.4 A). Expression of β-syn was shown to increase over time (0 – 4 h) (figure 3.4 B). A53T α-syn samples, run on the β-syn western blot as negative controls, showed no expression.

Using this more sensitive method, specific expression was confirmed for both β-Syn and A53T α-syn by western blot, but not for α-syn. As for the previous study, this would imply that there is a problem with either the efficiency of *α-syn* plasmid

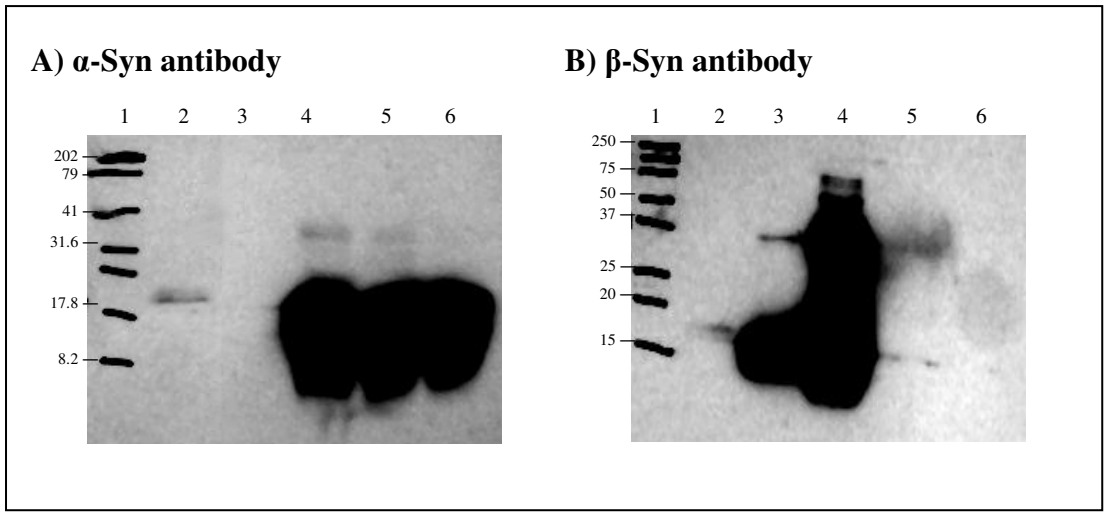

Figure 3.4: Western blots of α-syn, A53T α-syn and β-syn expression.

The western blots were run using either α-syn or β-syn antibodies with protein expression samples. **A) α-syn antibody:** lane order; 1) kaleidoscope pre-stained standards, 2) positive control of rat cerebrum. 3) α-syn 4 h after induction in LB broth. 4) A53T α-syn overnight after induction in peptone, 5) A53T α-syn expression overnight in peptone and 6) A53T α-syn 4 h after induction in LB. No expression was observed for α-syn, A53T α-syn samples suggest high levels of expression with all samples this is due to exposure time used on the film. **B) β-syn antibody:** lane order; 1) Precision plus Protein dual colour standards, 2) positive control of rat cerebrum, 3) β-Syn expression at 0 h after induction in LB, 4) β-Syn 4 h after induction in LB, 5) A53T α-syn overnight after induction in peptone and 6) A53T α-syn 4 h after induction in LB. β-Syn was seen to be expressed within both β-syn samples and no expression of A53T α-syn was detected.

transformation into the cells lines used or with the expression vector itself (figure 3.4).

3.2 Induction of α-syn expression.

Initial studies showed the presence of the *α-syn* gene in the *α-syn* plasmid (section 3.1.1); however, expression of α-syn could not be induced (section 3.1). This could suggest a problem either through poor transformation of the *α-syn* plasmid into the cell lines used or a problem in the pRK172 expression vector. To investigate these two possibilities, two studies were run in parallel. Firstly the originally gifted *α-syn* plasmid was transformed directly into competent BL21 (DE3) expression cells, where the expression was monitored. Secondly, the *α-syn* gene was removed from the pRK172 vector and inserted into a pRK172 vector isolated from the *β-syn* plasmid (section 3.2.4).

3.2.1 Transformation of *α-syn* plasmid into BL21 cells.

To investigate whether the lack of expression with α-syn was due to a problem with the transformation of the *α-syn* plasmid into BL21 (DE3) cells, the original sample of *α-syn* plasmid gifted to us was transformed directly into expression BL21 (DE3) cells (section 2.2.3 and 3.1.1). The BL21 (DE3) cells containing *α-syn* plasmid from the previous study (section 3.1.2), where the plasmid was transformed into DH5α cells before transforming into BL21 (DE3) expression cells, were also plated and grown as a control. Colonies were picked at random from each plate and cultured overnight in 6 ml LB with amp and chlora. Plasmid DNA was isolated from the overnight cultures

and digested using Nde I and Hind III DNA restriction enzymes. The digested samples were run on 1 % agarose EthBr gel.

From the EthBr gel (figure 3.5) three bands were seen for each sample. In each case a band with the apparent base pair size of ~ 500 bp, the correct size for the *α-syn* gene, was observed. However, this was seen to be markedly reduced within the *α-syn* plasmid isolated from the BL21 (DE3) cells taken from the previous study (figure 3.5). This, taken with the fact that a strong *α-syn* gene band was seen in the freshly transformed cells, would imply that the lack of α-syn expression seen previously was due to possible low levels of *α-syn* plasmid transformation.

3.2.2 Expression trials for the newly transformed *α-syn* plasmids.

The lack of α-syn expression, previously observed in sections 3.1.2 and 3.1.3, was suggested to be through low levels of *α-syn* plasmid transformation. It was observed that newly transformed BL21 (DE3) cells with *α-syn* plasmid showed relatively higher levels of *α-syn* plasmid present in the cells. The present study was preformed to observe if the increased presence of *α-syn* plasmid would lead to subsequent protein expression.

The BL21 (DE3) cells transformed with *α-syn* plasmid, from the previous study (section 3.2.1), were streaked on to amp and chlora agar plates. Colonies were randomly picked and cultured overnight in either peptone or LB broth containing amp and chlora (section 2.3.1). The overnight cultures (grown in the appropriate

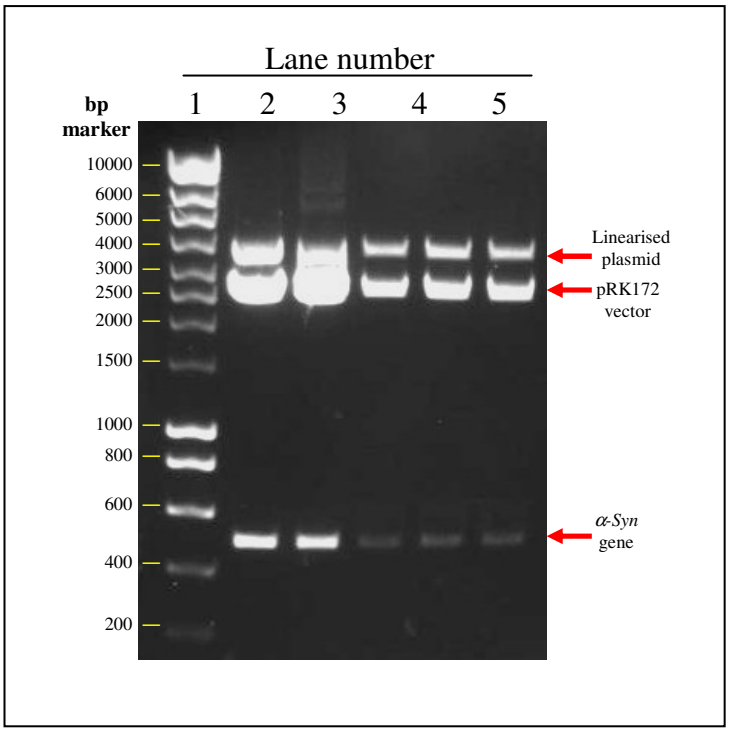

Figure 3.5: *α-Syn* plasmid DNA digest.

The digested plasmids (using Nde I and Hind III restriction enzymes) were run on a 1 % agarose gel. The gels identified the presence of the *α-syn* gene within the pRK172 vectors for all samples. Lane; 1) HyperLadder I marker, 2 – 3) *α-syn* plasmid isolated from newly transformed BL21 cells, 4 – 6) *α-syn* plasmid isolated from previous α-syn BL21 stocks. Three bands were identified in digest with no variation in band size across samples. The band at ~ 4 Kb is the correct size for full plasmid where only one enzyme digest has occurred. The band at ~ 3 Kb is consistent for pRK172 vector minus insert and the final band at 500 bp is consistent for isolated *α-syn* gene insert.

media) were used to inoculate 100 ml of either LB broth or peptone containing amp and chlora. As described previously (section 3.1.2) the expression cultures were grown to an OD_{600} between 0.4 – 0.6 before inducing with IPTG. Two samples were collected at each time point (0 h, 2 h, 4 h and overnight) for all the expressions. The samples were either re-suspended (1:1 ratio) in water and laemmli loading buffer or the samples were lysed and heat-treated as described in section 2.3.7. The supernatants were collected and mixed with laemmli loading buffer in a ratio of 1 : 1. All the samples were run on 16 % SDS-PAGE gels.

The use of LB broth expression cultures was shown to increase the expression level of α-syn compared to expression levels cultured in peptone (figure 3.6). The lysed and heat treated expression samples showed significant α-syn expression within LB and peptone samples after induction as well as a reduction in the majority of cellular proteins compared to the untreated samples (figure 3.6). Within both LB and peptone cultures, α-syn expression does not appear to increase beyond 2 h (figure 3.6 B). This could imply that the rate of α-syn production is the same as degradation rate of the α-syn.

α-Syn expression was successfully induced with the best expression levels observed using LB broth compared to peptone media. It was also established that lysing and heat treating the samples removed the majority of other cellular proteins without affecting the quantity of α-syn collected.

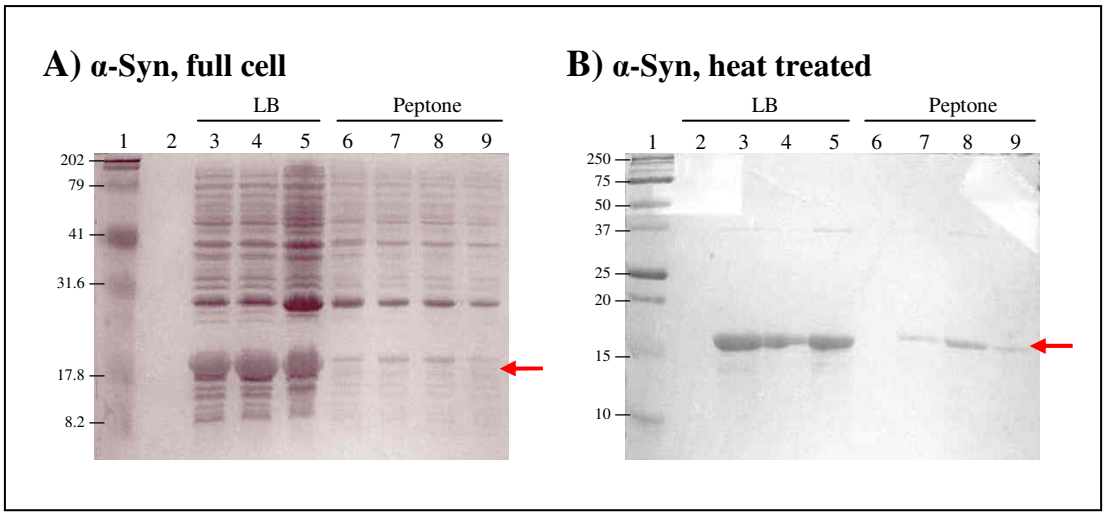

Figure 3.6: Comparison of expression of α-syn expression in LB broth or peptone.

SDS-PAGE expression gels were used to analyse the expression levels of α-syn protein within BL21 cells over time and comparing expression within LB broth and peptone growth medium. The red arrows indicate α-syn band size (~19 kDa). **A) α-Syn, full cells:** lane: 1) Kaleidoscope pre-stained standards, 2) was empty, 3) α-syn at 2 h after induction in LB, 4) α-syn at 4 h after induction in LB, and 5) α-syn overnight after induction in LB, 6) α-syn overnight after induction in peptone, 7) α-syn at 4 h after induction in peptone, 8) α-syn at 2 h after induction in peptone 9) α-syn at 0 h after induction in peptone. **B) α-Syn, heat treated:** lane; 1) Precision plus Protein dual colour standards, 2) α-syn at 0 h after induction in LB, 3) α-syn at 2 h after induction in LB, 4) α-syn at 4 h after induction in LB, 5) α-syn overnight after induction in LB, Lanes 6 – 9 were α-syn expression in peptone: 6) α-syn at 0 h after induction in peptone, 7) α-syn at 2 h after induction in peptone, 8) α-syn at 4 h after induction in peptone 9) α-syn overnight after induction in peptone. Both gels show α-syn expression in cultures grown in either LB or peptone media.

3.2.3 α-Syn expression confirmed by western blot.

To confirm the identity of the potential α-syn band observed in the previous expression (section 3.2.2), western blot was used to identify α-syn protein (section 3.1.4). The α-syn BL21 cells were plated and colonies grown overnight. The overnight cultures were used to inoculate 500 ml volumes of LB with amp and chlora and cultures grown to an OD_{600} of between 0.4 – 0.6 before inducing with IPTG. Expression samples were then collected from each culture at 0 h, 2 h, 4 h and overnight after induction. All the samples were lysed and heat treated as described in section 2.3.7 and run on a 16 % SDS-PAGE gel. The SDS-PAGE gel was then used within a western blot using a α-syn antibody (section 2.3.6).

From the western blot (figure 3.7), expression of α-syn and A53T α-syn can clearly be seen at all time points, appearing to increase from 2 h to 4 h after induction, and subsequently diminishing with longer incubation (figure 3.7). This profile of expression was mirrored with the A53T α-syn study (figure 3.7).

From these expression studies it has been shown that re-transforming the original α-syn plasmid directly into BL21 (DE3) cells resulted in successful induction of protein expression. This would suggest that the problem in expression observed in earlier expressions was due to the original *α-syn* plasmid transformation into DH5α cells subsequently effecting expression in BL21 (DE3) cells.

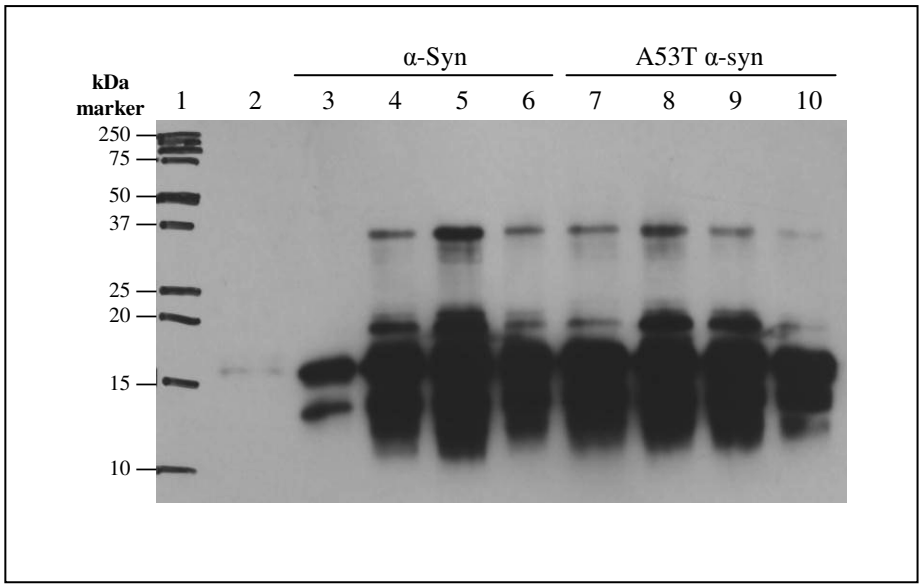

Figure 3.7: Western blots of α-syn and A53T α-syn expression.

The western blot, from SDS-PAGE gel and using a α-syn antibody, shows expression of α-syn and A53T overtime after induction. Lanes; 1) kaleidoscope pre-stained standards, 2) rat cerebrum positive control, 3) α-syn at 0 h after induction, 4) α-syn at 2 h after induction, 5) α-syn at 4 h after induction, 6) α-syn overnight after induction, 7) A53T α-syn at 0 h after induction, 8) A53T α-syn at 2 h after induction, 9) A53T α-syn at 4 h after induction, 10) A53T α-syn overnight after induction. α-Syn expression can been in all α-syn samples with increasing expression up to 4h, however expression is seen to diminish overnight. Expression was also seen for A53T α-syn in all A53T α-syn samples.

3.2.4 Concomitant study expressing α-syn using *β-syn* vector.

The *β-syn* plasmid has been shown to successfully express β-syn when transformed into BL21 (DE3) *E.coli* cells. To further investigate if the *α-syn* vector is responsible for the level of protein expression, the pRK172 vector from the *β-syn* plasmid would be extracted and used to construct a new plasmid with *α-syn*. The newly constructed plasmid would then be transformed into DH5α and BL21 (DE3) cells.

β-syn plasmid was cut using Nde I and Hind III and run on 1 % LMP agarose gel. From the gel the pRK172 vector band was identified and was cut out of the agarose gel. The pRK172 vector was purified using the QIAquick Gel extraction kit and a sample of the extracted vector was run on an agarose gel to confirm the successful isolation of the pRK172 vector band (figure 3.8A). The procedure was repeated with the *α-syn* plasmid to extract the *α-syn* gene from the plasmid (figure 3.8B). The purified pRK172 vector and *α-syn* were ligated together overnight. The newly formed α-syn plasmid was transformed into DH5α cells. Colonies were selected at random and cultured overnight. The overnight culture was used to isolated plasmid DNA. The isolated DNA was checked by DNA digest using Nde I and Hind III and run on 1 % agarose EthBr gel (figure 3.8C).

The agarose gel identified that all the samples tested contained plasmid containing *α-syn*. These studies along with those in the preceding sections (section 3.2.2 and 3.2.3) suggested the previous lack of expression was due to a fault of the *α-syn* pRK172 vector.

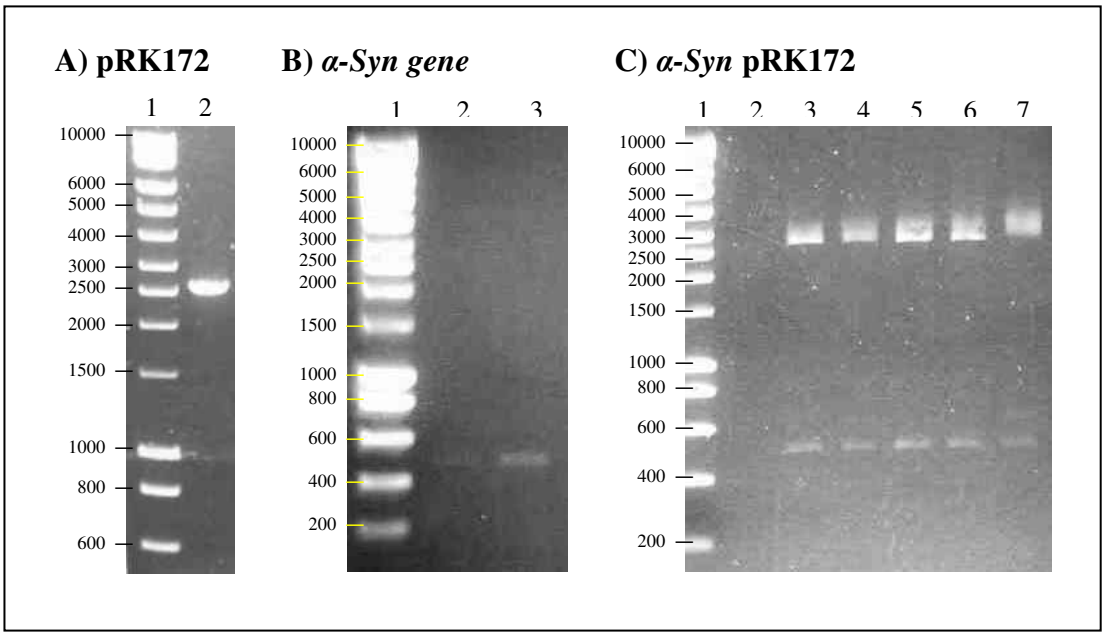

Figure 3.8: Agarose gels of the reconstruction of the *α-syn* plasmid.

All DNA samples were run on 1 % agarose EthBr gel. **A)** Shows only one band at ~3000 bp correct for the size of purified pRK172 vector cut using Nde I and Hind III from the *β-syn* plasmid, lane 1 contains 1 Kb marker, lane 2 Sample. **B)** Shows two samples both of which only show one band at ~ 500 bp are correct for purified *α-syn* gene cut using Nde I and Hind III from *α-syn* plasmid; lane 1 contains HyperLadder I. **C)** Shows restriction digest using Nde I and Hind III of the newly constructed α-syn plasmids, all contain 2 bands one of ~ 3000 bp and one ~ 500 bp; lane 1 containing HyperLadder I

3.3 Purification of synuclein proteins by FPLC.

From the previous studies, expression was induced for α-syn, A53T α-syn and β-syn (section 3.1 and 3.2). Denaturing the generated proteins with heat treatment appeared to remove the majority of the contaminating cellular proteins from the expression samples (section 2.3.7 and 3.2). However, a number of contaminating proteins were still present within the collected syn protein. To further purify the isolated syn proteins, fast protein liquid chromatography (FPLC) was utilised, using an anion exchange column to isolate syn protein from the remaining contaminates. The anion exchange column separates the proteins based on their surface charge and was selected due to the negative charge of synucleins.

3.3.1 Insufficient purification with FPLC using Mono-Q column.

β-syn expression achieved using the protocols established in section 3.1.2, using *β-syn* BL21 cells from glycerol stocks. The culture was induced and grown for 6 h. The cells were lysed and heat treated, as previous, for initial isolation of β-syn within the supernatant (section 2.3.7). β-syn supernatant was dialysed into 0.02 M Tris pH8.2 overnight using Cellu.Sep regenerated cellulose tubular membrane dialysis tubing (MWCO 4,000 – 6,000) (section 2.3.8). While the Mono-Q, 1 ml anion exchange column was hydrated and equilibrated with 0.02 M Tris pH 8.2, the dialysed β-syn protein was centrifuged and sample of the dialysed protein was used to determine protein concentration (~ 9.8 mg of β-syn as determined by BCA assay). By using 0.02 M Tris pH 8.2 with 1 M NaCl an ion gradient was produced with the mobile phase where the gradient was initiated 12 min into the column run. The gradient started at 0 % and was raised to 40 % NaCl over 10 min. To elute the

remaining proteins the NaCl gradient was increased to 100 % for 5 min before dropping to 0 % NaCl (section 2.3.11 and figure 3.9 A). The mobile phase from the column was analysed by UV at 280 nm, to indicate at which time proteins were eluted from the column, and indicating which fraction(s) may contain β-syn. A representative of each fraction was mixed with NuPAGE loading buffer and run on NuPAGE gel to analyse the fractions (figure 3.9 B).

From analysis of the gel, the majority of β-syn was eluted from the column into fractions 14 and 15. The two β-syn containing fractions were combined and the amount of protein contained was shown to be 2.5 mg, using the BCA assay (section 2.3.10). However, as other protein bands were observed in the β-syn fractions, this protocol did not generate a purity suitable for use in further experiments (figure 3.9 A).

3.3.2 High synuclein purification with FPLC using HiTrap Q HP column.

This study investigated if the replacement of the previous Mono-Q column to a HiTrap HP anion exchange column would generate purer syn product. The HiTrap Q HP column contains sepharose beads which are stronger anion exchangers than the beads in the Mono-Q anion exchange column. The FPLC protocol was also adapted from the previous study (section 3.3.1).

β-Syn produced and dialysed from the previous study (section 3.3.1) was used within the FPLC. The dialysed β-syn sample (~ 4.9 mg of protein) was centrifuged and loaded on to a 1 ml HiTrap Q HP anion exchange column. A 20 % NaCl step was

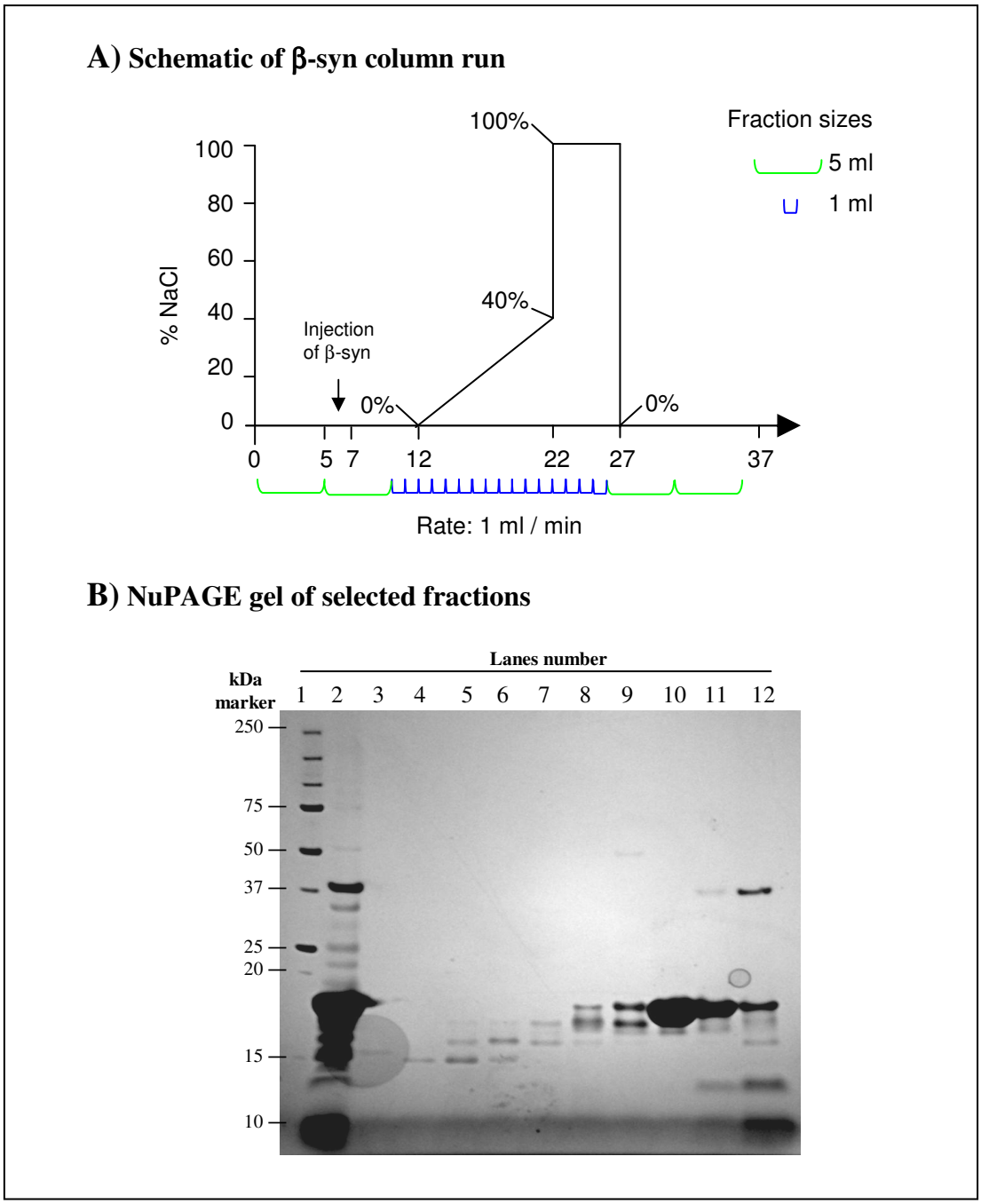

Figure 3.9: Analysis of β-syn fractions produced from column run.

A) Schematic of β-syn column run: Shows a schematic of purification of β-syn by FPLC using a mono-Q 1 ml column. The number and volume of factions are indicated within the diagram. **B) NuPAGE gel of selected fractions:** lane order; 1) Precision plus Protein unstained standards, 2) pre-column β-syn sample, 3) fraction 2, 4) fraction 8, 5) fraction 9, 6) fraction 10, 7) fraction 11, 8) fraction 12, 9) fraction 13, 10) fraction 14, 11) fraction 15, 12) fraction 16. β-syn was identified to be eluted primarily in to fraction 14 and 15, with a reduction in contaminant proteins.

added prior to the start of the gradient, such that the gradient started at 20 % NaCl and increased to 40 % NaCl over 10 min (figure 3.10A). The elution of the mobile phase from the column was monitored by UV at 280 nm throughout the run. Due to the UV monitoring specific stages of the column run were held longer than programmed (figure 3.10A). All the mobile phase was collected in fractions as shown in figure 3.10A. A sample of each fraction was analysed by gels fractionation (figure 3.10B).

Analysis of the fractions indicated β-syn protein was eluted mainly into fractions 18 and 19 with no other protein bands present (figure 3.10B). Fractions 18 and 19 were combined and the quantity of β-syn was shown to be 0.6 mg, determined by BCA assay.

Here we have shown that the eluted β-syn from the column contained no contaminating protein bands. By changing the column and adapting the protocol we have not only successfully increased the purity of our β-syn sample but have also achieved a higher concentration than was possible in the previous study (section 3.3.1)

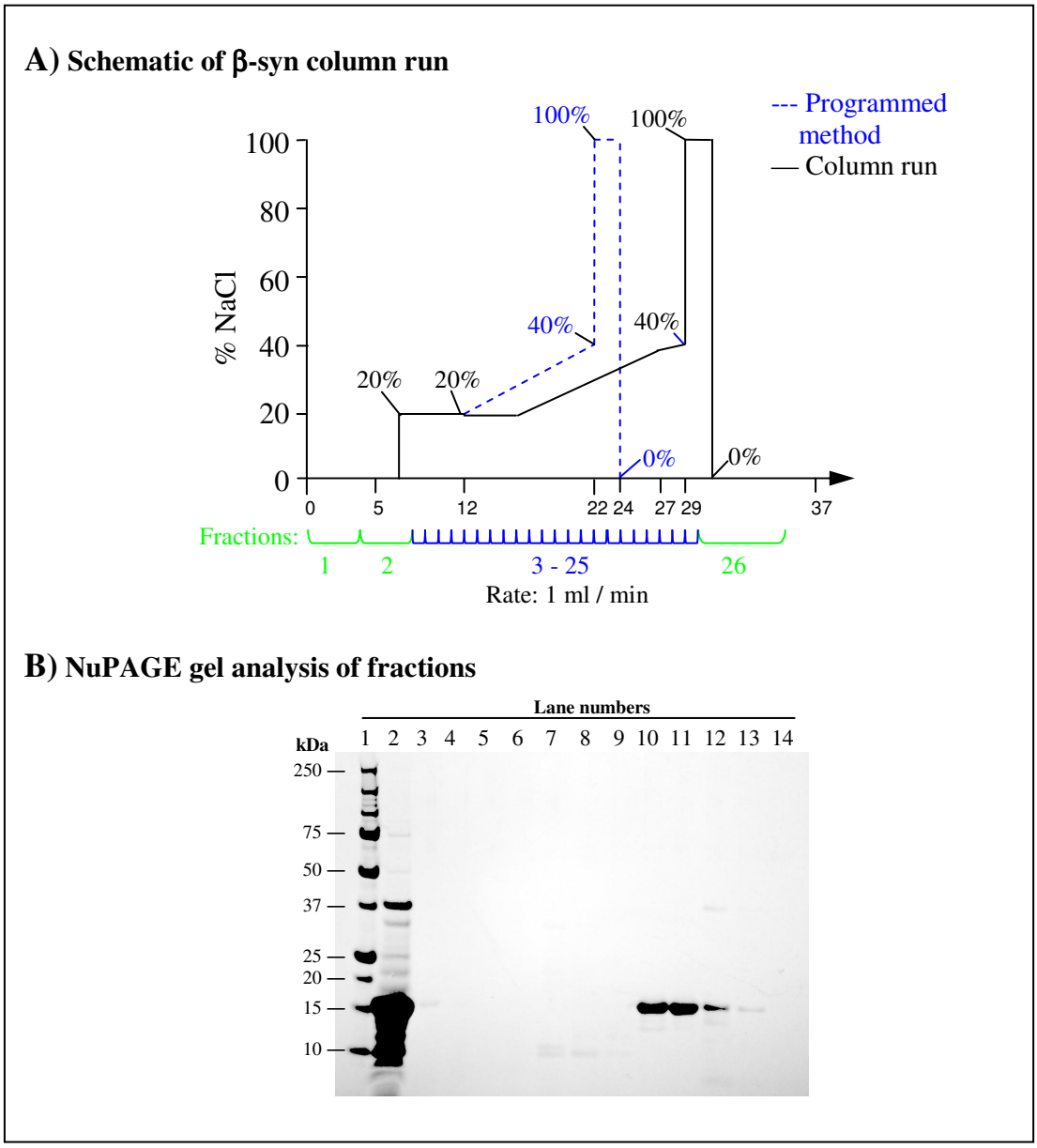

Figure 3.10: Analysis of β-syn fractions produced using a HiTrap Q HP column.

A) Schematic of the β-syn column run: shows the protocols used for the purification of β-syn by FPLC using a HiTrap Q HP 1 ml column, the alteration to the column run are overlaid on to the programmed run and the actual number of fraction and volumes collected are stated below. **B) NUPAGE gel analysis of fractions:** representative number of the fractions collected, lane order; 1) Precision plus Protein unstained standards, 2) Pre-column β-syn sample, 3) Fraction 2, 4) Fraction 3, 5) Fraction 4, 6) Fraction 6, 7) Fraction 7, 8) Fraction 8, 9) Fraction 9, 10) Fraction 18, 11) Fraction 19, 12) Fraction 22, 13) Fraction 23, 14) Fraction 24. The majority of β-syn was eluted into fractions 18 and 19.

3.3.3 Purification of α-syn using optimised FPLC protocol.

We investigated whether using a similar protocol to above (section 3.3.2) would similarly purify α-syn.

α-Syn expression was established using BL21 cells transformed with *α-syn* plasmid produced in section 3.3.2. The α-syn BL21 cells were plated on to amp and chlora containing agar plates. Colonies randomly selected were cultured overnight and used to inoculate 1 L volume of LB with amp and chlora. The expression culture was grown to an OD_{600} of 0.4 – 0.6 and induced with IPTG. The cells were harvested 4 h after induction and heat treated as described in section 2.3.7. The supernatant which contained the isolated α-syn was dialysed overnight into 0.02 M Tris pH 8.2. Dialysed α-syn was analysed by BCA assay to establish the total protein concentration (0.97 mg/ml) and 1 ml of the α-syn sample was centrifuged and loaded on to 1 ml HiTrap Q HP anion exchange column, hydrated and equilibrated with 0.02 M Tris pH 8.2. The column run was executed as previously described in section 3.3.2 (figure 3.11A). The elution of the fractions was monitored by UV at 280 nm reading throughout the run. Representatives of the fractions were run on a NuPAGE gel to analyse the protein content of the fractions (figure 3.11B).

Analysis of the gel showed that α-syn was highly purified, with no other contaminating bands (figure 3.11B). Combining α-syn-containing fractions and analysing by BCS assay, showed a protein concentration of 0.13 – 0.15 mg/ml. This was between 13 - 16 % of the original concentration of total protein loaded on to the column.

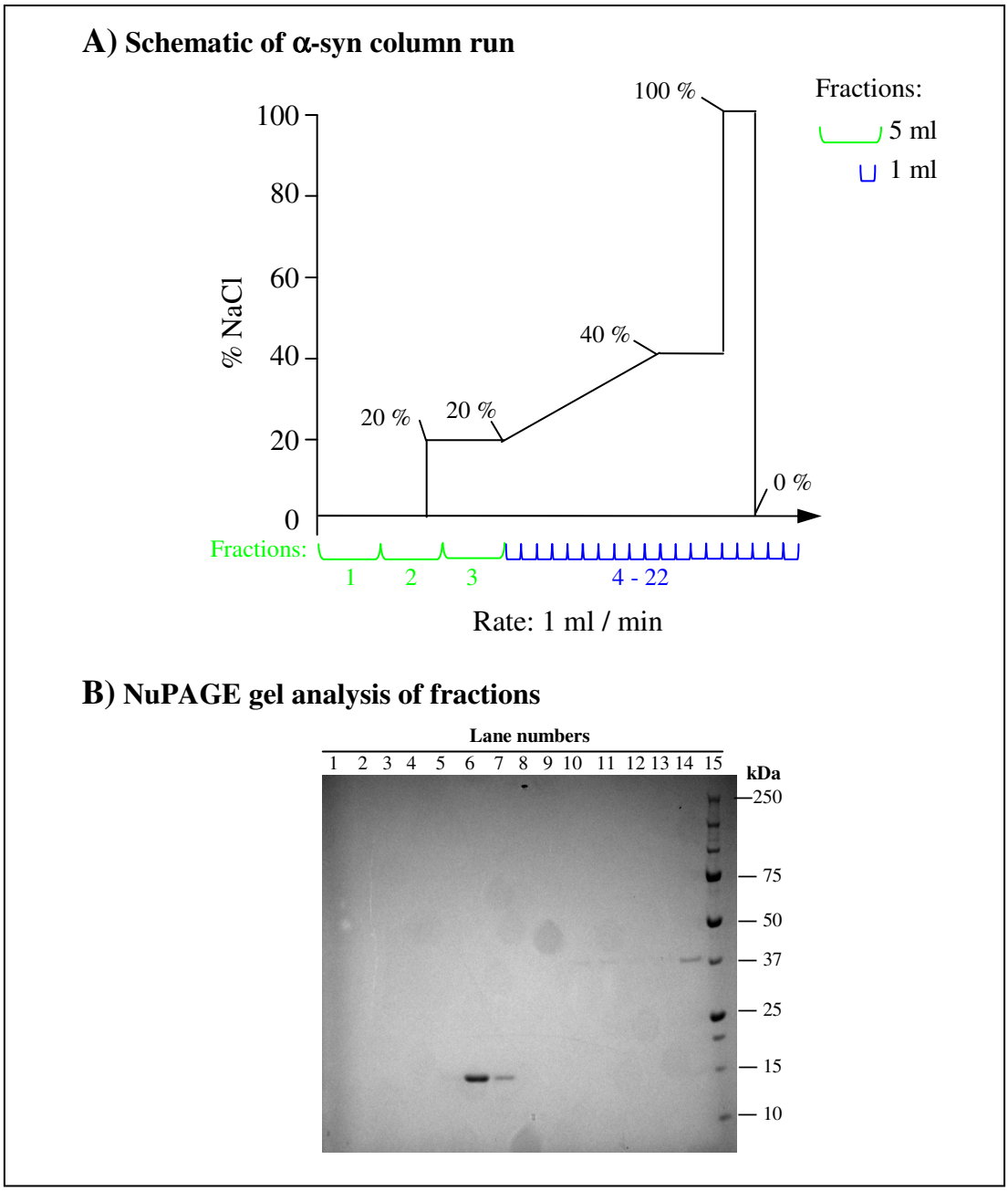

Figure 3.11: Analysis of α-syn fractions produced using a HiTrap Q HP column.

A) Schematic of the α-syn column run: illustration of the method used to purification α-syn by FPLC using a HiTrap Q HP column with the number of fractions and volumes of each showed along the bottom of the diagram. **B) NuPAGE gel analysis of fractions:** representative of the fractions collected from the column run, order of lanes; 1) Fraction 3, 2) Fraction 4, 3) Fraction 5, 4) Fraction 6, 5) Fraction 11, 6) Fraction 12, 7) Fraction 13, 8) Fraction 14, 9) Fraction 15, 10) Fraction 16, 11) Fraction 17, 12) Fraction 18, 13) Fraction 19, 14) Fraction 20, 15) Precision plus Protein unstained standards. α-Syn was eluted within to fraction 12 and 13. No contaminating protein appears to be present in any α-syn fractions.

3.4 Analysis of α-syn expression yield.

With each expression it appeared that the total concentration of pre-column protein was decreasing with each expression run, which resulted in a decrease in the yield of purified α-syn protein. To establish whether there was a decrease in protein expression and if so was it affecting the percentage of α-syn yield, the concentration of protein loaded on to the column (as measured by BSA assay) and the percentage of purified α-syn produced per expression was compared across expression runs.

Analysis of the expression runs suggested that the concentration of the pre-column protein decreased. This was confirmed for two separate 1 L culture runs (table 3.1) where the concentration decreased from 0.972 to 0.842. Increasing the culture size did not significantly increase total protein concentration (table 3.1), but did result in a decrease in the percentage of purified α-syn protein (table 3.1). This decrease in percentage yield of α-syn is indicative of a decrease in the expression of α-syn. The greater loss of yield with each subsequent experiment could suggest that the expression plasmid was rejected overtime during storage.

Table 3.1: Analysis of α-syn yield from individual α-syn expression.

Expression date	Culture volume (L)	Pre-column Concentration (mg/ml)	Total protein loaded onto column (mg)	Total of isolated α-syn (mg)	α-Syn % of total protein
19/04/2004	1.0	0.972	0.972	0.134	13.80 %
21/05/2004	1.0	0.842	5.05	0.975	19.30 %
30/06/2004	2.5	0.890	12.02	1.04	8.65 %

3.4.1 Analysis of expression levels from stock cells.

To determine if the decrease in the yield of α-syn was (section 3.4) due to issues surrounding storage, the expression levels of all the BL21 cells in glycerol stocks were analysed.

Glycerol stocks of *α-syn* BL21 cells were spread onto amp and chlora agar plates and colonies were randomly picked and cultured overnight in LB broth containing amp and chlora. The overnight cultures were used to inoculate 100 ml volumes of LB and were grown to an OD_{600} of between 0.4 – 0.5. The cultures were induced with IPTG and samples taken at 0, 1, 2, 3, 4 and 5 h after induction. All the samples were centrifuged and re-suspended in water and loading buffer (1:1 v/v). A second 5h sample was heat-treated and the supernatant prepared with loading buffer. All the samples were run on NuPAGE gels for analysis.

Analysis of the NuPAGE gels showed that there was no expression of α-syn within any of the cultures (figure 3.12). This would indicate that the *α-syn* plasmid is being rejected by the BL21 (DE3) cells with time.

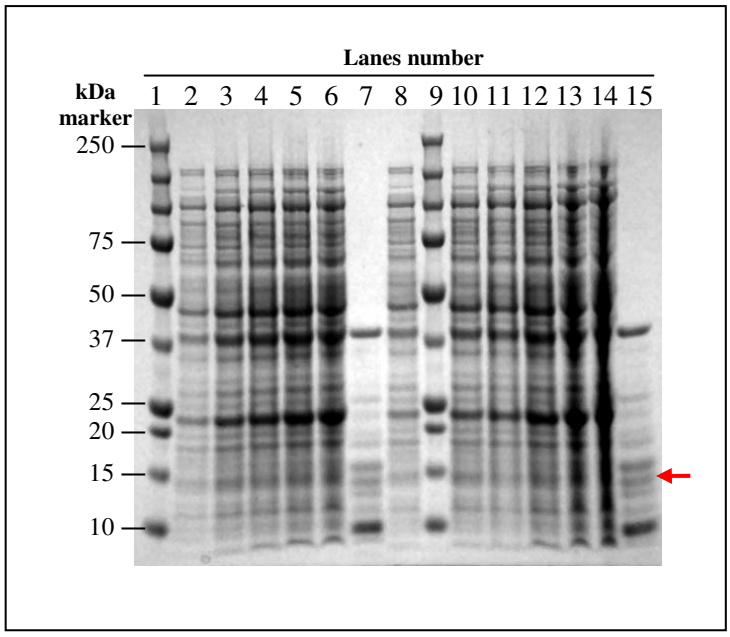

Figure 3.12: Analysis of α-syn expression overtime by NuPAGE gel.

The NuPAGE gel is representative of all the α-syn plasmid-containing stock cells. The red arrow indicates where α-syn expression should be present on the gels. Lane order: 1) Precision plus Protein unstained standards, 2) 0 h after induction, 3) 1 h after induction, 4) 2 h after induction, 5) 3 h after induction, 6) 4 h after induction, 7) 4 h after induction with sample heat treated, 8) 0 h after induction, 9) Precision plus Protein unstained standards, 10) 1 h after induction, 11) 2 h after induction, 12) 3 h after induction, 13) 4 h after induction, 14) 5 h after induction, 15) 5 h after induction with sample heat treated. No α-syn expression can be seen in any of the samples.

3.4.2 Analysis of plasmid levels in glycerol stocks.

The previous study (section 3.4.1) showed that there was no expression of α-syn from any of the glycerol stocks of BL21 cells containing *α-syn* plasmid. This suggests that the BL21 cells are a mixed population containing cells which have plasmid without the *α-syn* gene. These cells may out grow the BL21 cells still containing the plasmid with *α-syn* gene. To establish whether this is the case, the presence of the *α-syn* plasmid was investigated.

Overnight cultures of *α-syn* BL21 cells, *A53T α-syn* BL21 cells or *β-syn* BL21 cells were used to isolate *α-syn, A53T α-syn* or *β-syn* plasmid DNA as described in section 2.2.4. The isolated plasmid DNA was digested using Nde I and Hind III at 37 ^{o}C for an hour and then loaded on to EthBr 1 % agarose gel.

Analysis of the agarose gel showed a reduction in the amount of *α-syn* plasmid present within the BL21 cells. Specifically there was a reduction in the level of *α-syn* gene, rather than pRK172 vector. In comparison to the faint *α-syn* gene band, *A53T α-syn* and *β-syn* showed large bands. This implies that α-syn stocks cells contain a mixture of *α-syn* plasmid and pRK172 vector without the *α-syn* gene. The intensity of the pRK172 band at ~ 3 Kb within the *α-syn* plasmid samples does not appear to be reduced compared to the pRK172 band within the *A53T α-syn* or *β-syn* samples. The reduction in presence of the *α-syn* gene would explain the loss of *α-syn* expression observed in section 3.4.1, and would suggest the BL21 (DE3) cells are rejecting the *α-syn* plasmid (figure 3.13). However the *A53T α-syn* and *β-syn* plasmid containing BL21 cells do not appear to be affected to the same extent (figure 3.13).

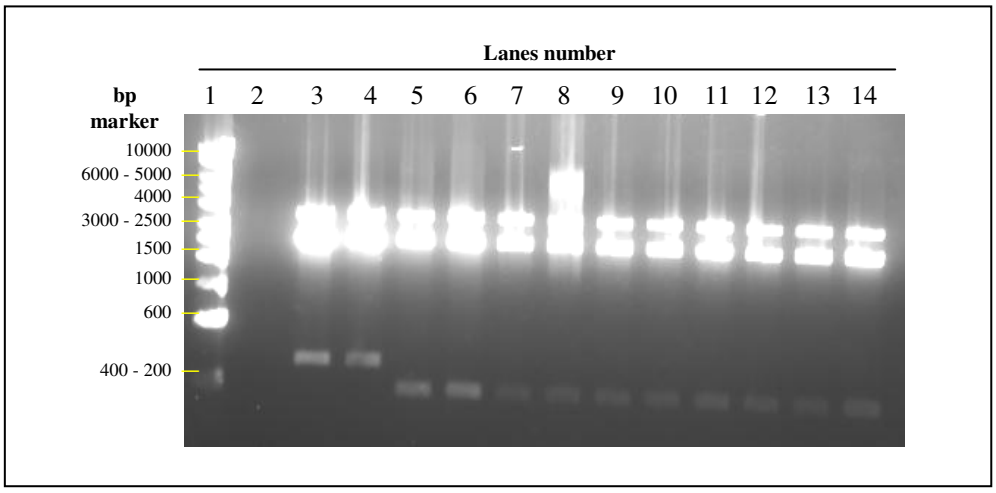

Figure 3.13: Analysis of *syn* plasmids by DNA restriction digest.

α-Syn, β-syn and A53T plasmids digested using Nde I and Hind III restriction enzymes and run on a 1 % agarose gel. The lane order was as followed; 1) Marker; HyperLadder I, 2) Water control, 3) *β-syn* plasmid, 4) *β-syn* plasmid, 5) *A53T* plasmid 6) *A53T* plasmid, Lanes 7 – 14) *α-Syn* plasmid. Three bands were identified in digest with one exception in lane 8 of *α-syn* plasmid which contained an extra band ~ 5 Kb which is likely to be undigested plasmid. All the samples show bands at ~ 4 Kb which full plasmid with insert, band at ~ 3 Kb which is correct size for pRK172 minus gene insert. The *β-syn* samples show band at ~ 550 bp correct for size for *β-syn* gene and the *A53T* samples show a band at ~ 400 bp correct for A53T *α-syn* gene. All the *α-syn* samples show only a very faint band at ~ 400 bp, correct for *α-syn* gene.

3.5 Construction of a new *α-syn* expression plasmid.

Our earlier studies showed expression of α-syn was being lost due to the BL21 (DE3) cells rejecting the *α-syn* plasmid (section 3.4). The most efficient way of restoring and increasing the expression levels of α-syn would be to reconstruct a new *α-syn* plasmid. Re-constructing the *α-syn* plasmid using a more up-to-date expression vector, such as pET-22b(+) (figure 3.14), has a number of advantages over using the pRK172, some of which are listed in table 3.2. Importantly, by using the commercial pET-22b(+) vector, we would have a fully sequenced vector map and therefore would be less likely to contain abnormalities that may lead to reduced expression or rejection from the cells, thus increasing levels of α-syn expression.

Table 3.2: Comparison of pET-22b(+) and pRK172 vectors.

pET-22b(+)	**pRK172**
Expression vector	Combination of two vectors
Fully published vector map	Full vector map not published
Option of tagging protein	--
Contains T promoters	Contains T promoters
Contains *Lac z* gene to reduce leakage of gene expression	--
Renewable and reliable source	Gifted from labs. Multiple replication and restriction digests caused alteration in sequence and cutting sites.

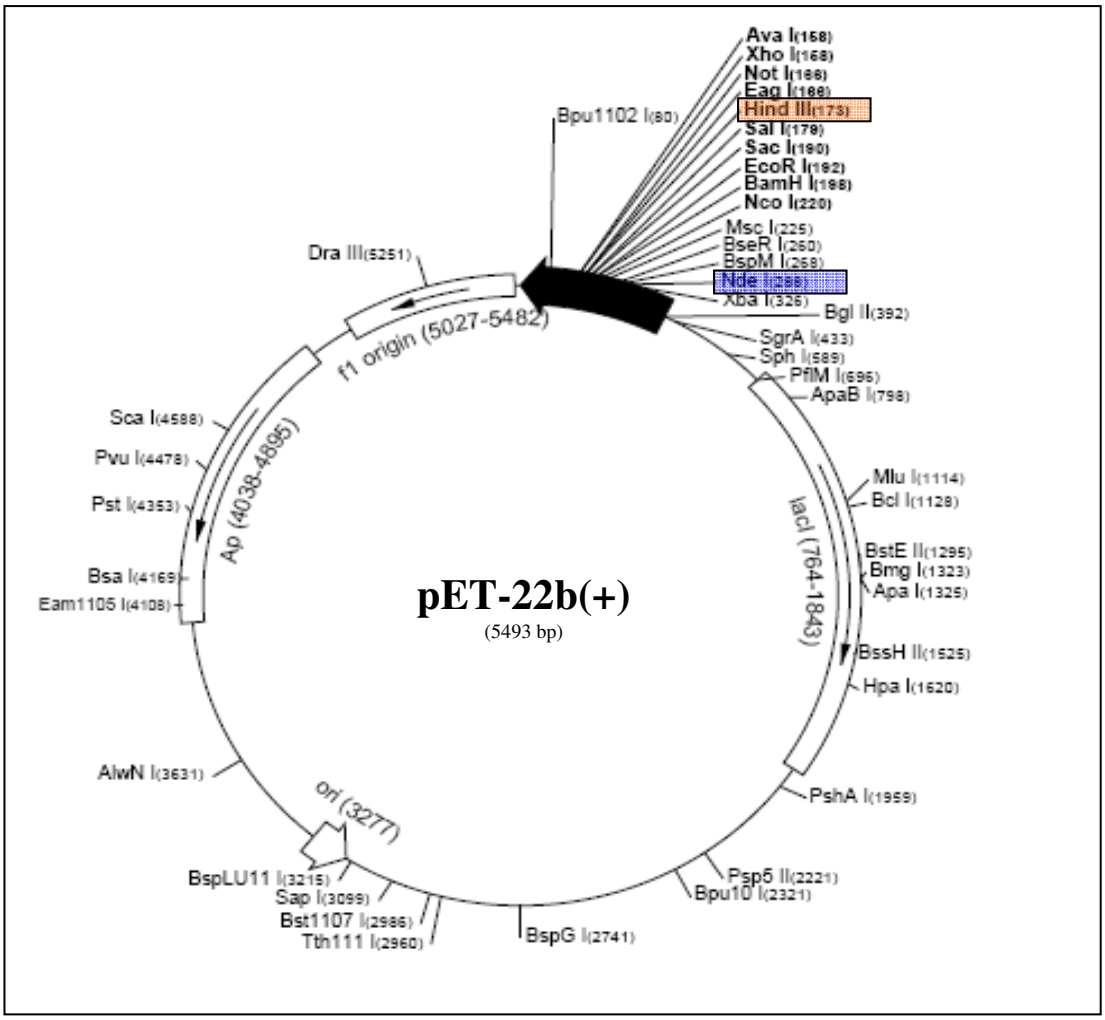

Figure 3.14: Schematic of pET-22b(+) vector showing restriction enzyme sites.

Diagram adapted from the Novagen pET-22b(+) vector manual (version TB038 12/98).

3.5.1 Isolation of *α-syn* from pRK172 plasmid by DNA digest.

To construct a new *α-syn* plasmid the *α-syn* gene had to be isolated from the original *α-syn* plasmid. The *α-syn* gene was isolated by restriction digest using Nde I and Hind III restriction enzymes. The *α-syn* DNA was extracted and purified from EthBr gel, and *A53T α-syn* and *β-syn* plasmids were used as controls.

The original *α-syn* plasmid was transformed into DH5α cells and grown on amp agar plates. Colonies were randomly selected from the plates and cultured overnight and the plasmid DNA isolated. Plasmid DNA was digested using Nde I and Hind III restriction enzymes (section 2.2.5.1) and analysed on 1 % agarose EthBr gel. One of the *α-syn*, *A53T α-syn* and *β-syn* plasmid DNA digests were run on a 1 % LMP agarose gel as described in section 2.2.6. The bands that corresponded with the *syn* gene were extracted from the gel as described in section 2.2.7 and the isolated *syn* genes were confirmed by running a sample of the purified DNA on a 1 % agarose EthBr gel.

As can be seen from the EthBr gel (shown in figure 3.15), the DNA digests of *α-syn* plasmid produced two bands, one at approximately 3 Kbp (consistent with the pRK172 vector) and a band at approximately 500 bp (consistent with the size of the *α-syn* gene of ~ 400 bp) (figure 3.15A).

The *A53T α-syn* and *β-syn* genes were successfully removed and purified from their respective plasmids, with the appearance of a 500 and 700 bp band respectively, on a 1 % EthBr gel used to check the gene were removed (figure 3.15 B). However, the

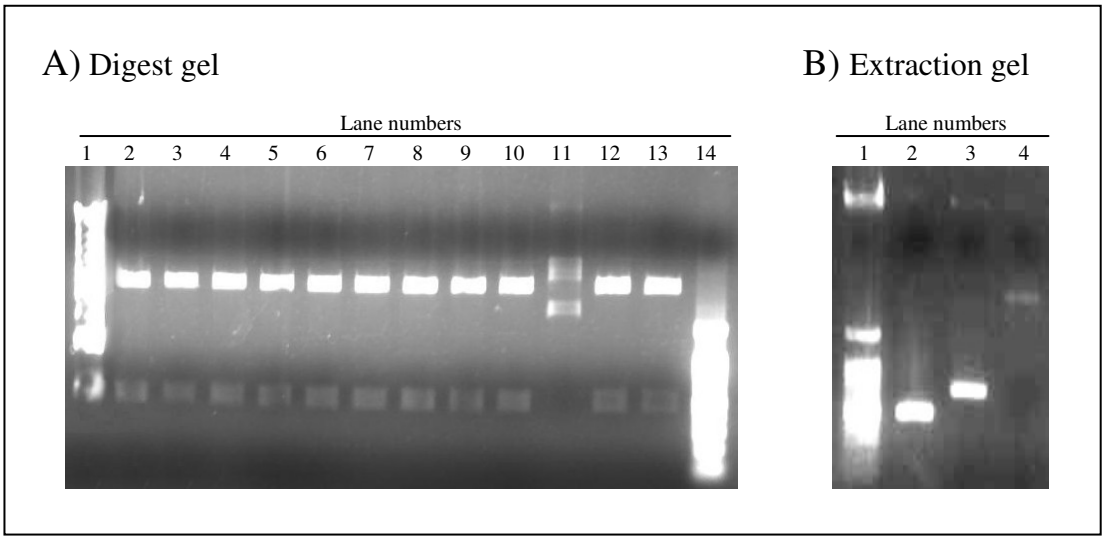

Figure 3.15: Restriction digest and isolation of *α-syn* from pRK172 plasmids.

The EthBr gels show the presence of *α-syn* gene and isolation of the *syn* gene from the plasmid. **A) Digest gel:** shows 1 % agarose EthBr gel of the restriction digests of *α-syn* plasmid samples using Nde I and Hind III restriction enzyme, where lane 1) 1000 bp marker, 2) *α-syn* 1.1, 3) *α-syn* 1.2, 4) *α-syn* 1.3, 5) *α-syn* 1.4, 6) *α-syn* 2.1, 7) *α-syn* 2.2, 8) *α-syn* 2.3, 9) *α-syn* 2.4, 10) *α-syn* 2.5, 11) *α-syn* 2.6, 12) *α-syn* 2.7, 13) *α-syn* 2.8, 14) 100 bp marker. The sample in lane 11 does not to contain *α-syn* plasmid. The remaining samples all contained *α-syn* plasmid with the digest producing 2 bands at either ~ 3000 bp correct size for pRK172 minus *α-syn*, and a band at ~ 500 bp correct for *α-syn* gene. **B) Extraction gel:** shows the isolated *syn* gene after being extracted and purified from LMP agarose. Lane order; 1) 100 bp marker, 2) *A53T α-syn*, 3) *β-syn*, 4) *α-syn. A35T* and *β-syn* shows correct size band after isolation and purification, the *α-syn* extraction sample produced a ~ 1000 bp band that is not consistent with the *α-syn* gene (~ 500 bp).

α- syn gene sample did not show a band at 500 bp, representative for the *α-syn* gene, but did have a band at ~ 1000 bp. This would imply the DNA of the *α-syn* genes were ligating during the purification process, rendering the extracted DNA unusable (figure 3.15 B).

3.5.2 Changing the culture growth protocol did not increase α-syn plasmid.

From the previous study (section 3.5.1), only a low level of *α-syn* plasmid was present within DH5α cells compared to the amount of pRK172 vector without the *α-syn* gene. The low level of *α-syn*-containing plasmid resulted in a reduction in the effectiveness of isolating the *α-syn* gene from pRK172 vector. We speculated that by altering the growth conditions used, we should be able to increase the amount of *α-syn* plasmid expressed within the cells and therefore increase the efficiency of the DNA digests used to remove the *α-syn* gene from the pRK172 vector.

Glycerol stocks of DH5α cells and BL21 cells, transformed previously with the original *α-syn* plasmid, were plated on agar plates containing either amp or both amp and chlora. Colonies were randomly selected and cultured in LB broth with the relevant antibiotics at which point the cultures were grown to an OD_{600} of ~ 0.1 before being pelleted, re-suspended in fresh LB broth (containing either amp or both amp and chlora) and grown for a further 3 h, whereas in previous experiments the cultures would have been grown overnight. Cells were then harvested and *α-syn* plasmid DNA was isolated as described in section 2.2.4. The isolated *α-syn* plasmids were digested using Nde I and Hind III restriction enzymes and run on a 1 % agarose EthBr gel (sections 2.2.5 and 2.2.6).

As can be seen from the EthBr gel (figure 3.16), only one band at ~ 3000 bp is present from the digestion of the *α-syn* plasmid DNA isolated from DH5α cells. This would indicate that the plasmid does not contain the *α-syn* gene. Whereas DNA digests of the *α-syn* plasmid isolated from BL21 cells produced three bands; one band of very low intensity at 500 bp, which is coincides with the *α-syn* gene, a strong band at ~ 3000 bp consistent with pRk172 vector and a stronger band at ~ 4000 bp consistent with linearised plasmid (figure 3.16). This would suggest the efficiency of the DNA digest is very low and the *α-syn* gene is not effectively being removed from the pRK172 vector.

Altering the growth conditions in an attempt to increase the quantity of *α-syn* plasmid did not successfully increase the plasmid concentration. However, the quantity of pRK172 vector without insert did increase. Interestingly, BL21 cells transformed with *α-syn* plasmid were not affected by the alteration in growth conditions. The experiment highlighted the low efficiency of DNA digest at removing the *α-syn* gene from the pRK172 vector.

3.5.3 MWG primers successfully isolated *α-syn* from pRK172 plasmid.

From the previous studies (sections 3.5.1 and 3.5.2) the *α-syn* plasmid was shown to be rejected from *E.coli* cells used. To prevent the loss of the *α-syn* gene, we attempted to isolate the *α-syn* gene and reconstruct the *α-syn* plasmid using a commercial expression vector. However, initial attempts at removing *α-syn* gene by DNA digest identified too insufficient an amount of the *α-syn* plasmid was present within the cells to successfully remove *α-syn* gene by this method (sections 3.5.1

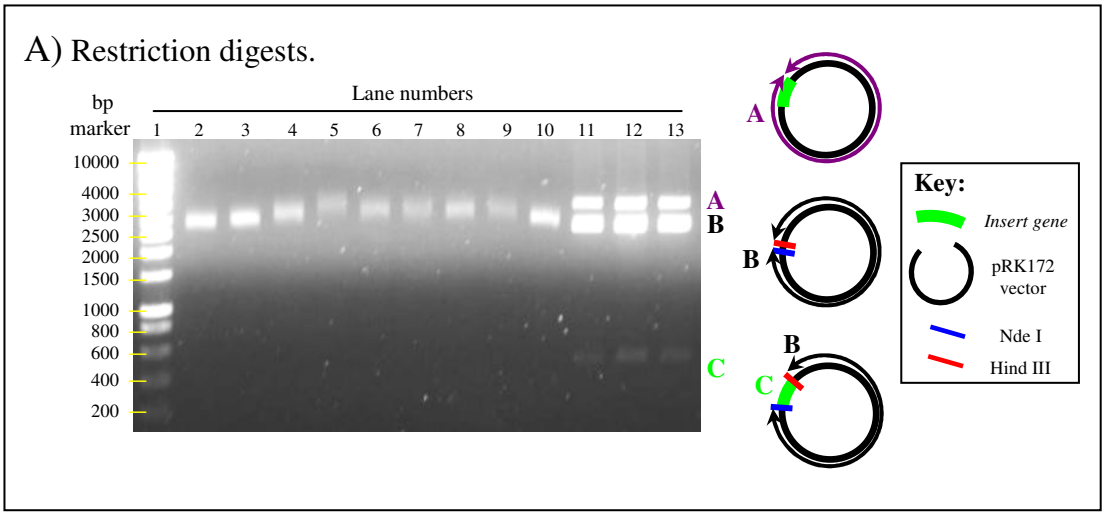

Figure 3.16: Restriction digest of *α-syn*pRK172 plasmids isolated from DH5α and BL21 (DE3) cells.

Agarose EthBr gel showed DNA bands from the *α-syn* plasmid digests. A schematic diagram illustrating the band orientation and cutting sites (red line Hind III and blue lines Nde I cutting sites) is also shown. Lane order; 1) HyperLadder I marker, lanes 2 – 10) digests of *α-syn* plasmid isolated from DH5α cells, 11 – 13) digests of *α-syn* plasmid isolated from BL21. None of *α-syn* plasmid isolated from DH5α cells contained a band consistent with *α-syn* gene (~ 500 bp). *α-Syn* plasmid isolated from BL21 cells show 3 bands, very low intensity band at ~ 500 bp consistent with *α-syn* gene, a band at ~ 3000 bp consistent with pRK172 minus *α-syn* gene and a band at ~ 4000 bp consistent with uncut *α-syn* plasmid.

and 3.5.2). This study attempted to amplify and remove the *α-syn* gene from the pRK172 vector using specifically designed primers. The PCR primers were used to add specific restriction cutting sites immediately in front of the start codon and immediately after the stop codon of the *α-syn* gene (section 2.2.9).

α-Syn plasmid was transformed into DH5α cells and cultured on agar plates containing amp (section 2.2.2). Colonies were randomly selected and cultured overnight in LB broth with amp. *α-Syn* plasmid was isolated from the cells as described in section 2.2.4. The isolated *α-syn* plasmid was then utilised within a PCR reaction using specifically designed primers (MWG) as described in section 2.2.9. A sample of the PCR products was analysed by 1 % agarose EthBr gel (figure 3.17).

As can be seen from the EthBr gel, a band of ~ 400 bp (consistent with the *α-syn* gene size) was identified in half of the *α-syn* PCR products (figure 3.17). This indicates the PCR successful amplified the *α-syn* gene.

3.5.4 Isolated α-*syn* gene did not successfully ligated into pET-22b(+) expression plasmid.

The earlier study showed the successful amplification and removal of the *α-syn* gene from the pRK172 vector by PCR (section 3.5.3). To construct the new *α-syn* plasmid the isolated *α-syn* gene was ligated into the pET-22b(+) commercial vector. Using colony growth of JM109 cells transformed with the newly constructed α-syn plasmid would indicate whether the new *α-syn* plasmid was successfully constructed and transformed. The colonies produced were cultured overnight and the *α-syn* plasmid

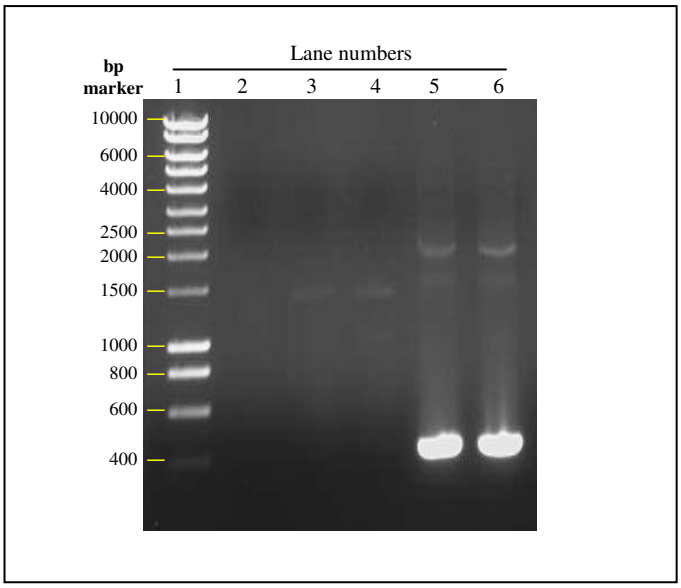

Figure 3.17: Amplification of *α-syn* by PCR.

The EthBr gel showed the PCR products of *α-syn* plasmid isolated from DH5α cells. Lane order; 1) HyperLadder I marker, 2) water control, 3) *α-syn* 1, 4) *α-syn* 2, 5) *α-syn* 3, 6) *α-syn* 4. Two out of the four *α-syn* plasmid samples show a band at ~ 500 bp consistent with *α-syn* gene.

isolated and assessed by restriction digests and PCR.

The isolated *α-syn* gene from section 3.5.3 along with the commercial pET-22b(+) vector was digested using Nde I and Hind III restriction enzymes and extracted from the 1 % LMP agarose EthBr gel (sections 2.2.5.1 and 2.2.7; figure 3.18). This digest produces sticky ends on the *α-syn* gene and opens the pET-22b(+) plasmid ready to for the ligation. The *α-syn* gene and pET-22b(+) vector were ligated overnight and transformed into JM109 *E.coli* cells (sections 2.2.2 and 2.2.10). The transformed JM109 cells were grown on amp containing agar plates.

Although the positive control transformation were successful, no colonies were seen on plates spread with the *α-syn* plasmid-transformed JM109 cells, suggesting that the ligation of the *α-syn* gene into the pET-22b(+) vector was not successful.

3.5.5.1 Comparison of DNA purification protocols after digestion of either the *α-syn* gene or pET-22b(+) vector.

From the previous studies we successfully isolated the *α-syn* gene from the pRK172 vector by PCR, however the isolated *α-syn* gene was not successfully inserted into the pET-22b(+) vector (sections and 3.5.3 and 3.5.4). This could be due to insufficient amounts of *α-syn* gene with sticky ends and open pET-22b(+) vector produced by restriction digest preventing the ligation reaction (section 3.5.2), or the PCR reaction failing to replicate the restriction cutting sites onto the *α-syn* gene (section 3.5.4).

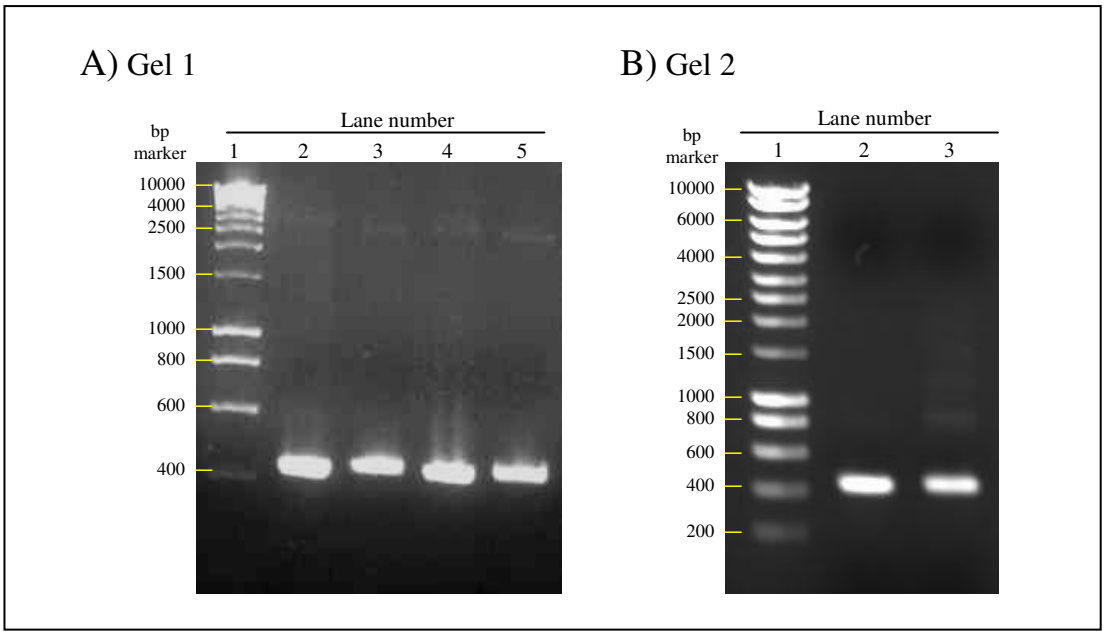

Figure 3.18: Restriction digest and purification of *α-syn* PCR products.

Agarose EthBr gel showed ~ 400bp bands for all *α-syn* samples. **A) Gel 1** Restriction Digest shows comparison of uncut and cut *α-syn* PCR products. Loading order; 1) HyperLadder I marker, 2) *α-syn* 1 cut, 3) *α-syn* 1 uncut, 4) *α-syn* 2 cut, 5) *α-syn* 2 uncut. **B) Gel 2** Purification of restriction digest samples. Loading order; 1) HyperLadder I marker, 2) *α-syn* 1, 3) *α-syn* 2 the gels show that there are no alterations to the *α-syn* PCR products by restriction digests or purification.

To investigate why the *α-syn* gene did not successfully insert into the pET-22b(+) vector we altered the protocol for the restriction digest from a combined restriction digest to two independent digestions. By performing the restriction digest independently, we speculated that each restriction enzyme cutting efficiency would be increased. To assess these two purification protocols, gel extraction and ethanol precipitation, were compared.

The *α-syn* gene isolated by PCR in section 3.5.3 was utilised for the experiment and labelled *α-syn* 1 and *α-syn* 2, along with two samples of the pET-22b(+) vector which were labelled vector 1 and vector 2. Each sample of *α-syn* and vector were digested with Nde I restriction enzymes. The *α-syn* and pET-22b(+) digests were purified either by gel extraction, *α-syn* 1 and vector 1 (section 2.2.7), or ethanol precipitation, *α-syn* 2 and vector 2 (section 2.2.8). The *α-syn* and pET-22b(+) samples were then digested with Hind III and were purified as previously. The digested *α-syn* and vector samples were analysed by 1 % agarose (figure 3.19 A and B).

From the EthBr gels the *α-syn* sample purified by gel extraction showed a reduction in the quantity *α-syn* after Nde I digestion and no DNA appeared to be left after the final purification by gel extraction (figure 3.19 A). In comparison, purification by ethanol precipitation did not appear to reduce levels of *α-syn* between stages (figure 3.19 A). This was mirrored by the digestion and purification of pET-22(+) which also showed a loss of DNA by gel extraction but not by ethanol precipitation (figure 3.19 B).

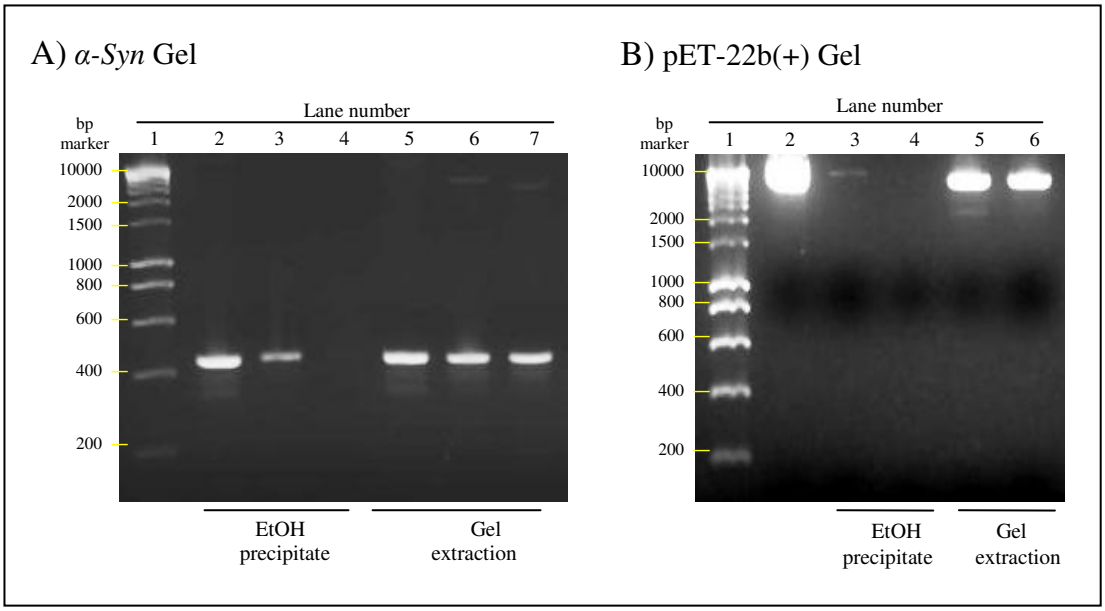

Figure 3.19: Comparison of gel and ethanol purification of *α-syn* PCR products and pET-22b(+).

Agarose EthBr gels show a comparison of purification of *α-syn* and pET-22b(+) by gel extraction or ethanol precipitation. **A) *α-Syn* Gel:** shows purification by gel extraction in lanes 2- 4 and ethanol (EtOH) precipitation in lanes 5 -7. Loading order; 1) HyperLadder I marker, 2) *α-syn* 1 PCR, 3) *α-syn* 1 Nde I, 4) *α-syn* 1 Nde I and Hind III, 5) *α-syn* 2 PCR, 6) *α-syn* 2 Nde I, 7) *α-syn* 2 Nde I and Hind III,. **B) pET-22b(+) Gel:** shows purification by gel extraction in lanes 3- 4 and ethanol precipitation in lanes 5-6. Loading order; 1) HyperLadder I marker, 2) pET-22b(+) 1 uncut, 3) pET-22b(+) 1 Nde I, 4) pET-22b(+) 1 Nde I and Hind III 5) pET-22b(+) 2 Nde I, 6) pET-22b(+) 2 Nde I and Hind III. Both A) and B) show that ethanol precipitation does not reduce DNA levels as much as DNA purification by gel extraction.

3.5.5.2 Separate restriction digests did not increase success of ligation.

From the previous study, using separate restriction digest reactions and ethanol precipitated purification, digested *α-syn* gene and digested pET-22b(+) vector concentrations were not diminished by the purification protocol. To verify whether the alternative protocol improved the ligation reaction, the ethanol precipitated samples were ligated and transformed in to *E.coli cells*. As previously colonies growths was used to indicate successful ligation with PCR confirmation.

The newly constructed *α-syn* plasmid was transformed into JM109 cells and grown on amp containing agar plates. Plates streaked with JM109 cells transformed with the new *α-syn* plasmid showed good colony coverage. From these plates, 87 colonies containing the new *α-syn* plasmid were selected and used directly in PCR reactions (section 2.29.1). The PCR products were run on 1 % agarose EthBr gel (figure 3.20).

None of the colonies used contained the *α-syn* gene (figure 3.20). The absence of any bands for any of the PCR reactions showed that the *α-syn* gene was not inserted into the pET-22b(+) vector. This would imply the isolation of the *α-syn* gene by PCR did not correctly add the restriction cutting sites onto the ends of the *α-syn* gene preventing correct restriction digest and insertion into pET-22b(+) vector.

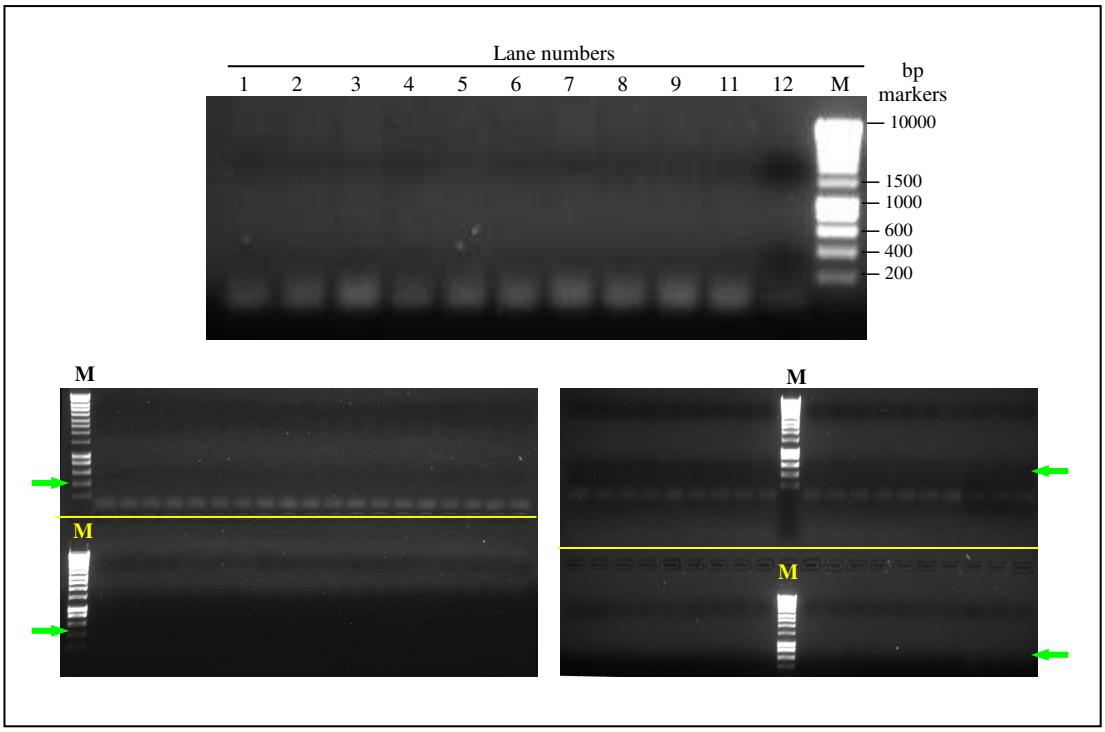

Figure 3.20: EthBr gel identifying the presence of the *α-syn* gene within JM109 cells transformed with *α-syn*pET-22b(+) plasmid.

The EthBr gels show all 87 JM109 cell colonies used in PCR reactions to identify the presence of plasmids containing the *α-syn* gene. The green arrow indicates where the *α-syn* band should be located. M marks the HyperLadder I marker lanes. No bands were seen within any of the colonies tested.

3.5.6 Invitrogen primers successfully isolated *α-syn* from pRK172 vector.

In earlier studies, construction of a new *α-syn* plasmid failed due to errors with PCR replication of the *α-syn* gene from the original *α-syn*pRK172 plasmid (section 3.5.5). Our results imply that the primers did not successfully add the additional restriction cutting sites to the start and terminus of the *α-syn* gene. This prevented the insertion of the *α-syn* gene into the pET-22b(+) expression vector. To investigate whether the lack of insertion was due to the PCR primers used, this study used primers (with the same sequence) from an alternative source.

The original *α-syn*pRK172 plasmid was transformed into DH5α cells and cultured on agar plates containing amp (section 2.2.2). Colonies were randomly selected and cultured overnight in LB broth with amp. The *α-syn* plasmid was isolated from the cells as described in section 2.2.4 and utilised within a PCR reaction using our designed primer produced by Invitrogen (section 2.2.9). The PCR reactions were analysed by 1 % agarose EthBr gel (figure 3.21).

As can be seen from the EthBr gel, a band at ~ 400bp was seen in all the lanes containing *α-syn* PCR samples, consistent with the size *α-syn* gene (figure 3.21). Invitrogen primers are therefore capable of amplifying and removing *α-syn* gene from pRK172 vector.

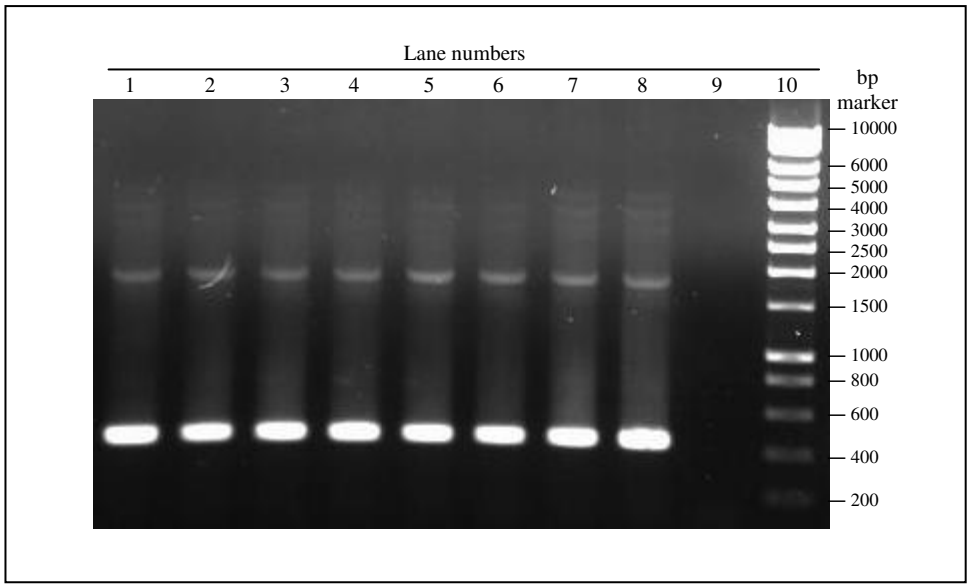

Figure 3.21: Amplification of *α-syn* by PCR.

The EthBr gel shows the amplification of the *α-syn* gene from the *α-syn* plasmids by PCR. Lane order; 1) *α-syn* 1.1, 2) *α-syn* 1.2 3) *α-syn* 2.1, 4) *α-syn* 2.2, 5) *α-syn* 3.1, 6) *α-syn* 3.2, 7) *α-syn* 4.1, 8) *α-syn* 4.2, 9) water control, 10) HyperLadder I marker. A band at ~ 400 bp was seen in all *α-syn* plasmid samples, which is consistent with the size of the *α-syn* gene.

3.5.6.1 Evaluation of *α-syn* inserts produced by Invitrogen primers.

Our previous studies showed that the *α-syn* gene could be isolated and amplified by PCR using primers produced by Invitrogen (section 3.5.6). The *α-syn* gene and pET-22b(+) vector were digested by the restriction enzymes Nde I and Hind III in individual reactions and purified by ethanol precipitation as previously described in sections 2.2.5.2, 2.2.8 and 3.5.5.1. The *α-syn* gene was then inserted into the pET-22b(+) vector and transformed in to JM109 cells. As described previously, the number of colonies on the plate was used as an indication of the number of *α-syn* plasmid containing cells. Confirmation was provided by PCR (section 3.5.5.2).

A huge number of colonies were apparent in plates of JM109 cells after transformation with *α-syn*pET-22b(+) plasmid. From these plates, 43 colonies were selected and used directly in PCR assays (section 2.2.9.1). Analysis after PCR was by running the PCR products on 1 % agarose EthBr gel (figure 3.22).

From the EthBr gels 35 colonies used in the PCR reactions showed a band at ~ 400 bp (figure 3.22). This would implies that the *α-syn* gene, generated with Invitrogen primers, was successfully inserted into the pET-22b(+) vector and that the new *α-syn* plasmid was transformed into the JM109 cells.

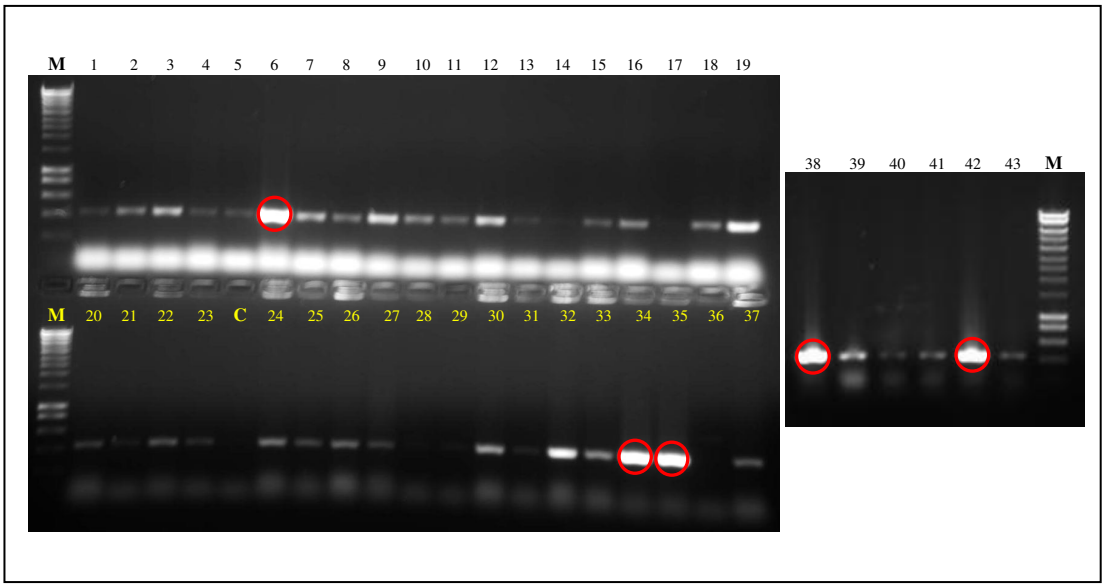

Figure 3.22: Identification of *α-syn* within *α-syn*pET-22b(+)-transformed JM109 cells by PCR.

EthBr gels identifies JM109 colonies transformed with new *α-syn* plasmid containing the *α-syn* gene. Out of the 43 colonies used in the PCR, 36 colonies showed a band ~ 400 bp, consistent with the *α-syn* gene size. Colony numbers are located at the top of each gel row. M = HyperLadder I marker and C = water control. The red circles identify the colonies that exhibited the highest intensity of ~ 400 bp band.

3.5.6.2 Assessment of the orientation of the *α-syn* gene within the *α-syn* pET-22b(+) plasmid.

Within the previous study we identified colonies that contained our newly constructed *α-syn* plasmid. Although we showed successful ligation, the orientation and the sequence of the *α-syn* gene is unknown. By using our reverse *α-syn* primer and a T7 PCR primer in a PCR, the orientation of the *α-syn* gene can be established by examining the band size produced. In *α-syn* plasmids, which show the correct orientation, the *α-syn* DNA would be confirmed by DNA sequencing using our designed primers.

To investigate the orientation and sequence of the *α-syn* gene, colonies showing the highest amplification of *α-syn* gene were selected from the previous study (section 3.5.6.1), and grown overnight in LB both containing amp. The new *α-syn* plasmid was isolated from the cells (section 2.2.4). The isolated *α-syn* plasmid was used in the PCR, using T7 primer and *α-syn* reverse primer (section 2.2.9.1). The PCR products were analysed using 1 % agarose EthBr gel (figure 3.23).

From the EthBr gel, four of the *α-syn* plasmids showed a band at ~ 400 bp (figure 3.23) and are therefore in the correct orientation. The *α-syn* plasmids which were identified to have the correct orientation where sent for DNA sequencing using reverse T7 primer and our designed reverse *α-syn* primer to MWG. The DNA sequence for all the *α-syn* pET-22b(+) plasmids were shown to contain the correct DNA sequence for *α-syn* gene.

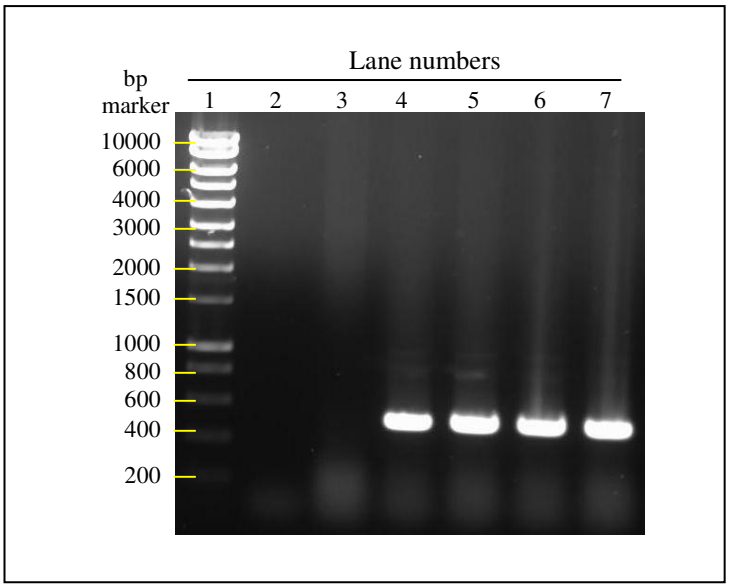

Figure 3.23: *α-Syn* orientation within pET-22b(+).

The EthBr gel showed the PCR products produced by the PCR reactions of selected 5 *α-syn* pET-22b(+) plasmids isolated from JM109 cells using T7 reverse primer and reverse *α-syn* primer. Lane order; 1) HyperLadder I marker, 2) water control, 3) *α-syn* 5, 4) *α-syn* 34, 5) *α-syn* 35, 6) *α-syn* 38, 7) *α-syn* 42. A band at ~ 400 bp was seen for four of the five *α-syn* pET-22b(+) plasmids, this consistent with the size of the *α-syn* gene. No bands with observed for the *α-syn* pET-22b(+) plasmid within lane 3.

3.6 Failure of validation of the newly constructed *α-syn*pET-22b(+) expression plasmid in JM109 cells.

From the previous study, we successfully constructed a new expression vector by removing the *α-syn* gene from the original pRK172 plasmid and successfully inserting the *α-syn* gene into the commercial pET-22b(+) expression vector (section 3.5). To validate both the correct orientation of plasmid and ability of this system to produce α-syn protein a small scale expression experiment was preformed.

From the previous experiment colony 35 (which contained the new *α-syn* plasmid with the correct *α-syn* gene; sections 3.5.6.1 and 3.5.6.2), was streaked onto an amp agar plate. Colonies from the plate were randomly selected and grown overnight in LB broth with amp. The overnight cultures were used to inoculate two 100 ml volumes of LB broth with amp and grown to an OD_{600} of 0.5 – 0.6, protein expression induced by the addition of IPTG. For one culture, cell samples were collected at 0 h, 30 min, 1 h, 2 h, 4 h, 6 h and overnight after induction. The cells from each time point were centrifuged and resuspended in 1:1 ratio of water and SDS loading buffer. For the second expression culture, a cell sample was taken at 0 h and all the cells were harvested 4 h after induction, lysed and heat treated as described in section 2.3.8. All the time-point samples and heat-treated samples were analysed by NuPAGE gel.

The NuPAGE gel showed no expression for either of the cultures (figure 3.24). This indicates that this system is not suitable for α-syn protein production. In hindsight the JM109 *E.coli* cells were a poor choice of cell line as they are not designed to

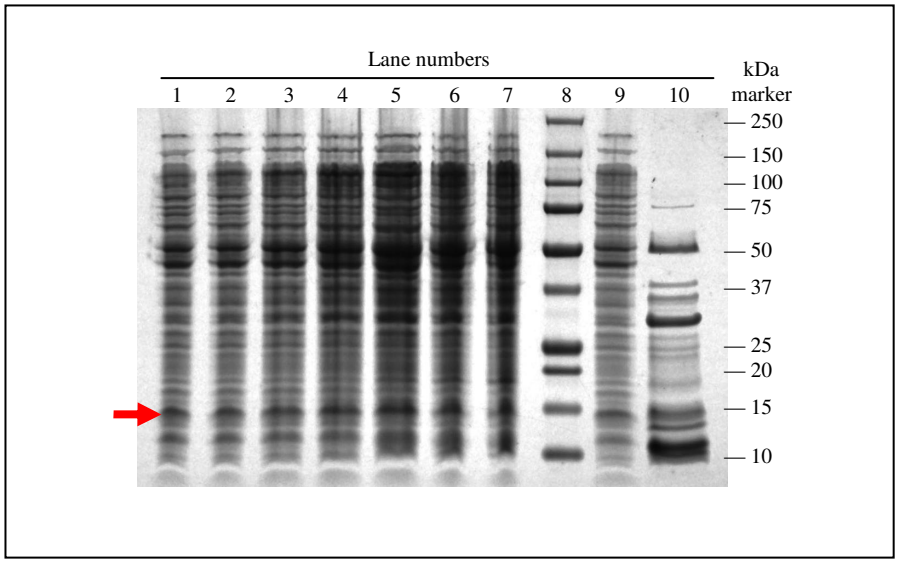

Figure 3.24: Analysis of α-syn expression from *α-syn*pET-22b(+) transformed in JM109.

The gels show two α-syn expressions analysed by NuPAGE gel. The red arrow indicates the correct size for the α-syn protein band (~ 14 kDa). Lane order; 1) 0 h after induction, 2) 30 min after induction, 3) 1 h after induction, 4) 2 h, after induction 5) 4 h after induction, 6) 6 h after induction, 7) incubation overnight after induction, 8) Precision plus Protein unstained standards. 9) 0 h after induction for heat treated sample, 10) heat-treated sample 4 h after induction. No obvious band at ~ 14 kDa was observed for either expression culture.

accommodate the pET-22b(+) vector. JM109 cells do not contain T7 phage RNA polymerase which is required for the expression of the target gene in the pET-22b(+) vector. However, the BL21(DE3)pLysS *E.coli* cells contain λDE3 lysogen which carries T7 phage RNA polymerase under the control of the lacUV5 promoter (which requires IPTG for activation), for the expression of the target gene.

3.6.1 Successful α-syn production with alternative expression system.

The unsuccessful system in the previous study used JM109 cells (section 3.6). As these cells are primarily used for plasmid storage rather than expression, this study investigated whether using BL21 (DE3)pLySs *E.coli* cells (specifically designed for protein expression) would enable α-syn expression.

Colony 38, (validated in sections 3.5.6.1 and 3.5.6.2), was streaked onto an amp agar plate. Colonies from the plate were randomly selected and grown overnight in LB broth with amp and the *α-syn* plasmid was isolated from the cells as described in section 2.2.4. The isolated *α-syn* plasmid was transformed into BL21 (DE3)pLySs cells as described in section 2.2.3. Colonies were randomly selected and grown overnight in LB broth with amp and chlora. The overnight cultures were used to inoculate 100 ml volumes of LB broth with amp and chlora. BL21 (DE3)pLySs expression cultures were grown to an OD_{600} of 0.2 before inducing with IPTG and cell samples were collected at 0 h, 0.5 h, 2.5 h, 4.5 h and overnight after induction. All the cell samples were lysed, heat-treated and run on a NuPAGE gel.

Samples taken from the BL21 (DE3)pLySs cells show a band at ~ 14 kDa on the NuPAGE gel increases in intensity with time but is diminished with overnight incubation (figure 3.25). This shows that *α-syn* plasmid can be successfully used to express α-syn once transformed into expression specific BL21 (DE3)pLySs cells.

3.6.2 Optimisation of expression protocol.

Initial studies using the original *α-syn*pRK172 plasmid (section 3.2), suggested that high expression levels of or prolonged exposure to α-syn, induced toxicity. The pET-22b(+) vector, which has been used to construct the new plasmid, contains the *Lac z* gene that reduces the expression of α-syn prior to induction with IPTG. The BL21(DE3)pLySs cells produce T7 lysozymes which further reduce the basal levels of α-syn expression. Reducing the production of α-syn before induction should decrease any toxicity due to prolonged exposure. In the previous study (section 3.6.1) however, high basal levels of protein expression was observed within the time zero sample. This study investigated whether prevention of 'pre-induction' protein expression could increase yields. By altering the inoculation protocol to use only one colony, direct from the culture plate, we speculated this would lower the basal level of α-syn.

Glycerol stocks of BL21 (DE3)pLySs cells transformed with *α-syn* plasmid (produced in section 3.6.1) were grown on agar plates containing amp and chlora. Colonies were randomly selected and used to directly inoculate 100 ml volumes of LB broth with amp and chlora. The cultures were grown to an OD_{600} between 0.4 – 0.6 before inducing with IPTG. For one culture, cell samples were taken at 0 h, 1 h,

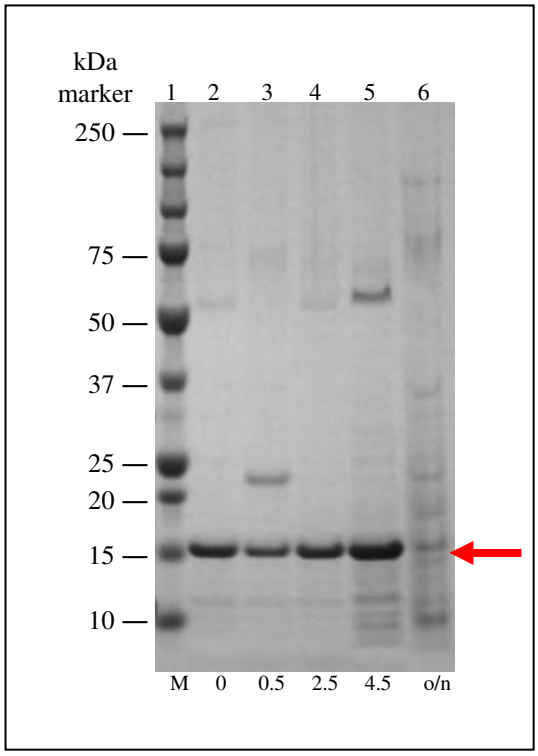

Figure 3.25: Analysis of α-syn expression from *α-syn*pET-22b(+) transformed into BL21 (DE3)pLysS cells.

The gel shows α-syn expression overtime in BL21 (DE3)pLysS cells on a NUPAGE gel. The red arrow indicates α-syn protein at 14 – 15 KDa. Loading order; 1) Precision plus Protein unstained standards, 2) 0 h before induction of expression, 3) 0.5 h after induction of expression, 4) 2.5 h, 5) 4.5 h, 6) overnight. Expression of α-syn can be seen in all samples.

2h, 4 h, 5 h and overnight after induction. From the second culture, a cell sample was taken at 0 h and the remaining cells harvested 4 h after induction. For both cultures, the cell samples and the harvested cells, were lysed, heat-treated and run on a NuPAGE gel.

A reduction in the basal levels of α-syn expression was seen at time zero (see figures 3.25 and 3.26) and expression of α-syn was seen in both cultures (figure 3.26). The α-syn expression increased over time, but still decreased with overnight incubation (figure 3.26). Reduced level of basal protein expression, does not appear to affect the level of protein expression.

3.6.3 Generation of purified α-syn.

The current study evaluated the FPLC method (section 3.3.3) of protein purification for α-syn generated by the new protocol. Now the *α-syn*pET-22b(+) plasmid has been optimised and shown to successfully express α-syn in BL21 (DE3)pLySs cells, we needed to establish if similar quantities of α-syn protein can be collected and purified by FPLC as seen with the previous *α-syn*pRK172 plasmid (section 3.3.3).

BL21 (DE3)pLySs cells containing *α-syn*pET-22b(+) (see section 3.6.1) were plated onto agar plates containing amp and chlora and incubated overnight. A colony was randomly selected and used to inoculate 2 L of expression media directly. The culture was grown to an OD_{600} 0.4 – 0.6 and induced with IPTG. The culture was incubated for 4 h and the whole culture harvested, the cells lysed, heat treated and

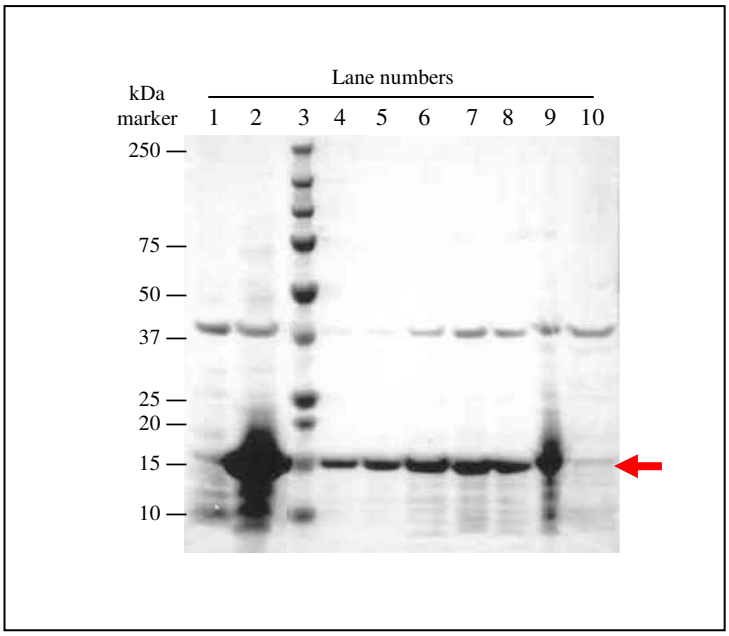

Figure 3.26: Increasing α-syn expression with increasing incubation periods within BL21 (DE3)pLysS cells.

The NUPAGE gel shows the expression of α-syn in BL21 (DE3) pLySs cells. The red arrow indicates the location of α-syn protein (14 – 15 KDa). Lane order; 1) 0 h after induction α-syn expression 2) 4 h after induction of expression culture which was harvested, 3) Precision plus Protein unstained standards, 4) 0 h after induction, 5) 1 h after induction, 6) 2 h after induction, 7) 4 h after induction, 8) 4 h after induction, 9) 5 h after induction, 10) incubation overnight after induction. The α-syn was observed within all the samples, with α-syn expression increasing over time, however α-syn expression was reduced when incubated overnight.

centrifuged to remove debris. The supernatant was dialysed overnight into 0.02 M Tris pH 8.2.

As described previously (section 3.3) a HiTrap Q HP anion exchange column was used, although for these studies the columns were scaled-up to 5ml. The column was equilibrated with 0.02 M Tris pH 8.2. Dialysed α-syn was analysed by BCA assay to establish the total protein concentration of ~ 2.9 mg/ml (data not shown). 9 ml of the α-syn sample was centrifuged and loaded directly onto the column. The same protocol was used previously (section 3.4), taking into account the larger column volume by increasing the flow rate to 5 ml/min (figure 3.27A). Elution of the proteins was monitored by UV at 280 nm reading during the run (data not shown). Samples were taken from each fraction and run on a NuPAGE gel for analysis (figure 3.27B).

Analysis of the fractions from the column run showed that α-syn was eluted into more fractions than previous, with the majority of α-syn in fractions 14 to 18 (figure 3.27B). Fractions 14 to 18 were pooled together and dialysed overnight into water. The concentration of protein in the dialysed sample was 1.4 mg/ml (quantified using the BCA assay), approximately ~ 48 % of the total protein loaded. α-Syn was divided into 1 mg aliquotes (714 µl), snap-frozen using liquid nitrogen and lyophilised overnight (courtesy of Edinburgh University Chemistry department).

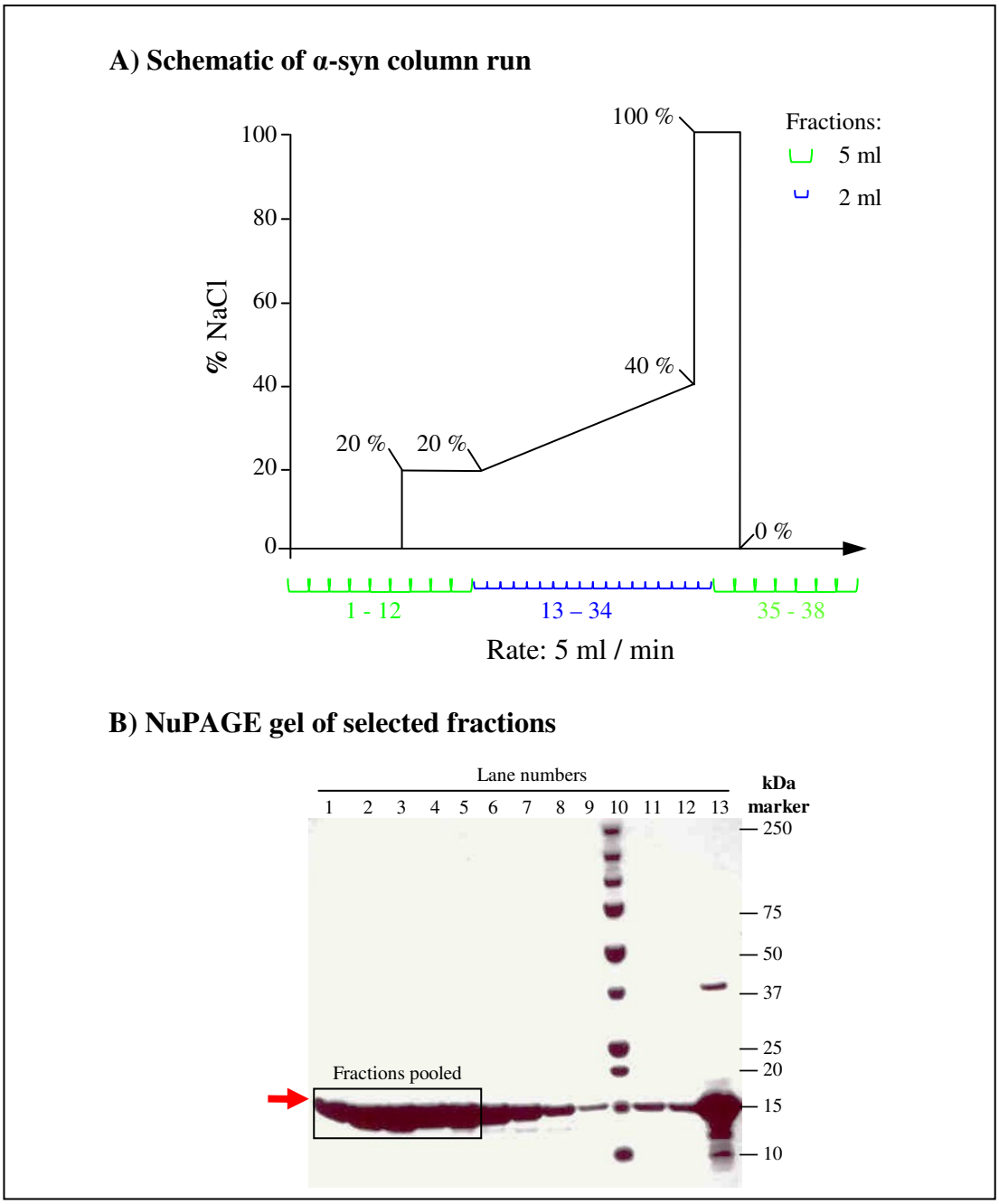

Figure 3.27: FPLC run and NuPAGE of selected fractions containing α-syn.

A) Schematic of α-syn column run: using a 5 ml HiTrap Q HP column. The percentage NaCl elution gradient is shown with the fraction numbers and volumes listed below. **B) NuPAGE gel of selected fractions**. The gel shows fractions containing α-syn purified from the FPLC run. The red arrow indicates the location of the band for α-syn protein at 14 – 15 KDa. Loading order (fraction numbers); 1) 14, 2) 15, 3) 16, 4) 17, 5) 18, 6) 19, 7) 20, 8) 21 9) 22, 10) Precision plus Protein unstained standards, 11) 27, 12) 28, 13) pre-column sample. Fractions 14 to 18 were pooled together for use in further experiments.

3.7 Scale up of α-syn expression using 10 L fermentation.

This study investigated whether increasing culture volumes and scaling up the purification protocol could produce larger amounts of α-syn protein.

Through our collaboration with Dr. White (EPIC) and using a Brunswick BioFlo4500s fermentor, expression cultures were scaled up from 2L to 10 L. The *α-syn*pET-22b(+) plasmid was transformed directly into *E.coli* expression cells for every fermentation run (section 2.3.1.4). Using the same growth condition as for the 2 L cultures, the 10 L growth cultures were grown to an OD_{600} of 0.4 – 0.6 before inducing with IPTG. A sample was taken prior to induction to check expression. The fermentation was then allowed to incubate for 4 – 5 h at which point the cells were harvested, pelleted and stored at -20 ^{o}C.

A large increase in α-syn expression can be seen after a 4 h incubation (figure 3.28), compared with time zero. Once expression was confirmed, cell pellets were de-frosted and the cells lysed and heat-treated as previously. The supernatant was dialysed into 0.02 M Tris pH 8.2 overnight. The concentration of total protein was ~5.5 mg/ml dialysed (determined by BCA assay). The sample (~ 20 – 30 ml) was then centrifuged to remove any debris and loaded directly onto an in house prepared column containing 35 ml of Q Sepharose High Performance matrix.

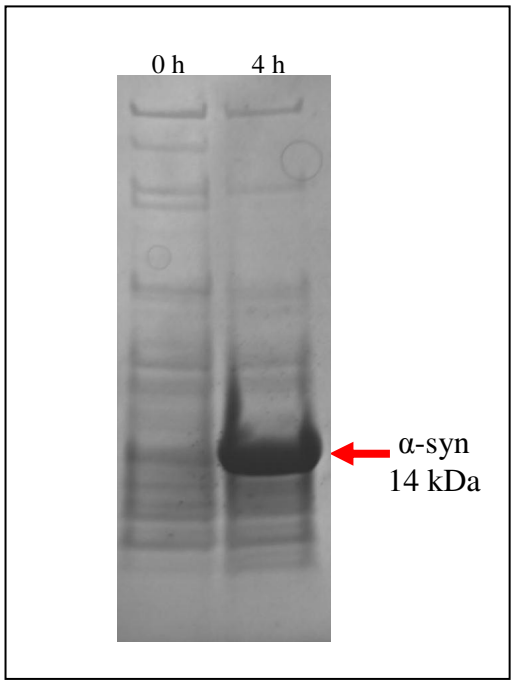

Figure 3.28: α-Syn expression produced from a 10 L fermentation.

The gel shows α-syn expression 4 h after induction of expression with IPTG with compared to expression at time of induction. Red arrow marks the α-syn 14 kDa protein band.

The protocol from section 3.3 and section 3.6.3 was adapted for the increase in column and sample size. Although the flow rate was maintained at 5 ml/min the fraction volumes were increase to 3 ml. The elution of the proteins was monitored by UV at 280 nm throughout the column run (data not shown). Samples were taken from each fraction and run on a NuPAGE gel (figure 3.29).

The majority of α-syn was eluted in fractions 23, 24 and 25 with no apparent contamination from other proteins (figure 3.29). As the bands produced by these fractions were large, samples of the bands were cut from the gel and analysed by mass spectrometry (Dr. D Short, A.C.E.) as shown in figure 3.30. The results from the mass spectrometry determined the gel samples contained α-syn and no contaminating proteins. Figure 3.30 shows an example of the mass spectrometry reading for the expression gel in figure 3.29. This was repeated on a number of other expression runs and the same results were obtained.

Fractions 23, 24 and 25 were pooled together and dialysed overnight into water. The concentration of protein in the dialysed sample was quantified using the BCA assay showing the pooled fractions of α-syn to contain ~ 11.5 mg/ml, a total of 99 mg of purified α-syn from one 10 L expression culture. Scaling the culture up has increased the quantity of α-syn by ~ 10 fold compared to 2 L cultures, without reducing the purity.

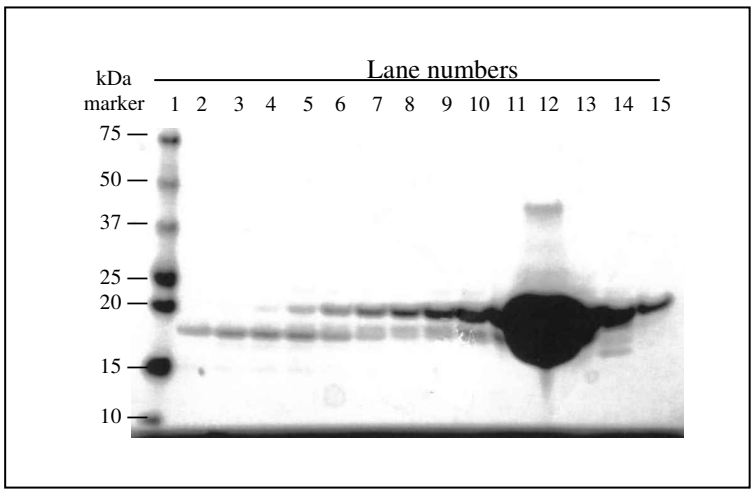

Figure 3.29: FPLC fractions of α-syn produced from 10 L fermentation.

NuPAGE gel showing a representation of the fractions produced from an FPLC run of a 10 L fermentation run of α-syn. Lane order; 1) Precision plus Protein unstained standards, 2) fraction 14, 3) 15, 4) 16, 5) 17, 6) 18, 7) 19, 8) 20, 9) 21 10) 22, 11) 23, 12) 24, 13) 25 14) 29 15) 31. The majority of the α-syn is eluted in fractions 23, 24 and 25.

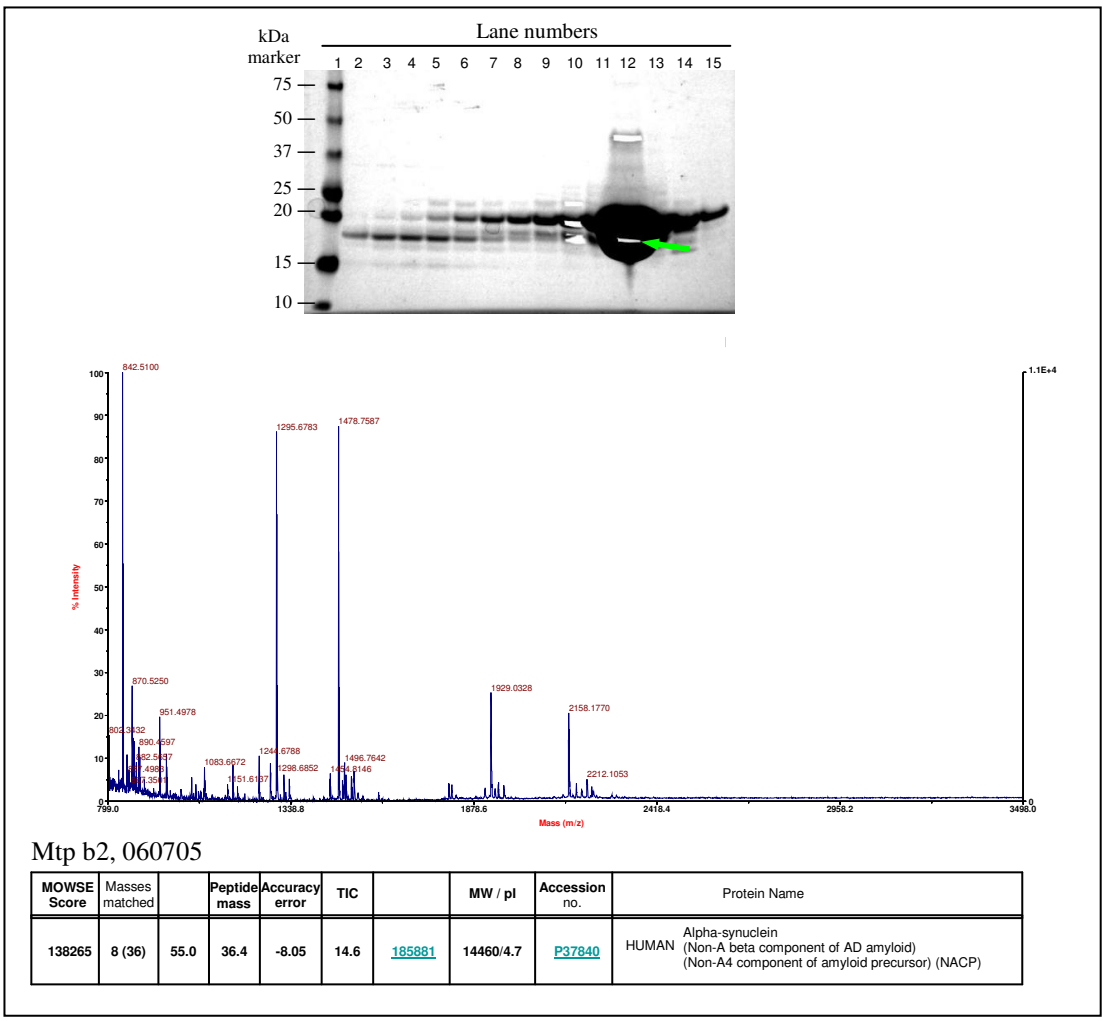

Mtp b2, 060705

MOWSE Score	Masses matched		Peptide mass	Accuracy error	TIC		MW / pI	Accession no.	Protein Name
138265	8 (36)	55.0	36.4	-8.05	14.6	185881	14460/4.7	P37840	HUMAN Alpha-synuclein (Non-A beta component of AD amyloid) (Non-A4 component of amyloid precursor) (NACP)

Figure 3.30: Mass spectrometry analysis confirming the presence of α-syn.

The protein bands selected and removed from the NuPAGE gel for mass spectrometry are shown in the above panel, where the green arrow indicates the band confirmed to be α-syn. The lower panel shows the mass spectrometry results which confirm the α-syn protein band.

3.8 Chapter 3 Summary.

Within this chapter a successful method of generating purified recombinant α-syn protein was identified and optimised. Initially the expression of α-syn, A53T α-syn and β-syn was achieved using BL21 (DE3) cells and the pRK172 vector. However, protein expression was reduced due to selective rejection of the plasmid from the *E.coli* cell line. This was successfully addressed by constructing a new plasmid using a commercial pET-22b(+) vector and transferring the *α-syn* gene from the original pRK172 vector by PCR. The re-constructed *α-syn* plasmid best expressed α-syn protein in BL21 (DE3)pLysS, designed to reduce pre-induction or 'leaky' expression. Subsequently it was found that the yield of α-syn was significantly increased compared to the original pRK172 vector. Through our collaboration with Dr J. White we were successfully able to scale up expression from 2 L to 10 L fermentation cultures. The increased culture volume our optimised purification protocol, using anion exchange chromatography, gave an increased yield of purified α-syn of approximately 100 mg per fermentation run. Purified α-syn was identified by using western blotting and mass spectrometry.

Though *A53T α-syn* and *β-syn* genes were not transferred to the new pET-22b(+) vector their expression within the original pRK172 vector was not diminished. The successful large scale expression and optimised purification protocol have allowed the reproducible production of large quantities of purified α-syn that will facilitate future experiments into the role of α-syn within PD *in vitro* model.

Chapter 4: Effects of α-syn in normal and disease conditions.

4.1 Cytotoxic effects of α-syn.

4.1.1 In-house wild-type α-syn did not induce cell death.

As mentioned previously in section 1.1.3, there are may hypothesises about the effect of α-syn in cells. It has been speculated that soluble and aggregated forms of α-syn induce toxicity and subsequent cell death. As we have been able to produce soluble recombinant α-syn, we treated cells with either soluble or pre-aggregated recombinant (see section 2.4.4) protein at varying concentrations and incubated the cells for 24 h. The MTS assay contains a novel tetrazolium compound which is reduced by NAD(P)H released from metabolically active cells. A decrease in MTS reduction is an indication of cytotoxicity and cell death.

SHSY-5Y cells were treated with vehicle (serum-free – medium containing 0.1 % water) (which was used as a measure of 100 % MTS reduction with treatments shown as percentage of vehicle), in-house produced soluble α-syn (0.1 – 10.0 μM) or in-house α-syn aggregated (0.1 – 10.0 μM) and incubated for 24 h. Cells treated with soluble α-syn (0.1 1.0 and 10.0 μM) for 24 h did not alter MTS reduction levels (99.1 ± 10.1, 100.5 ± 11.3 and 89.8 ± 7.4 % respectively) compared to vehicle (figure 4.1A). Similarly SHSY-5Y cells treated with aggregated α-syn (0.1, 1.0 and 10.0 μM) showed no significant alteration of MTS reduction (84.1 ± 6.2, 81.8 ± 13.8 % and 70.3 ± 12.9 % respectively) (figure 4.1B).

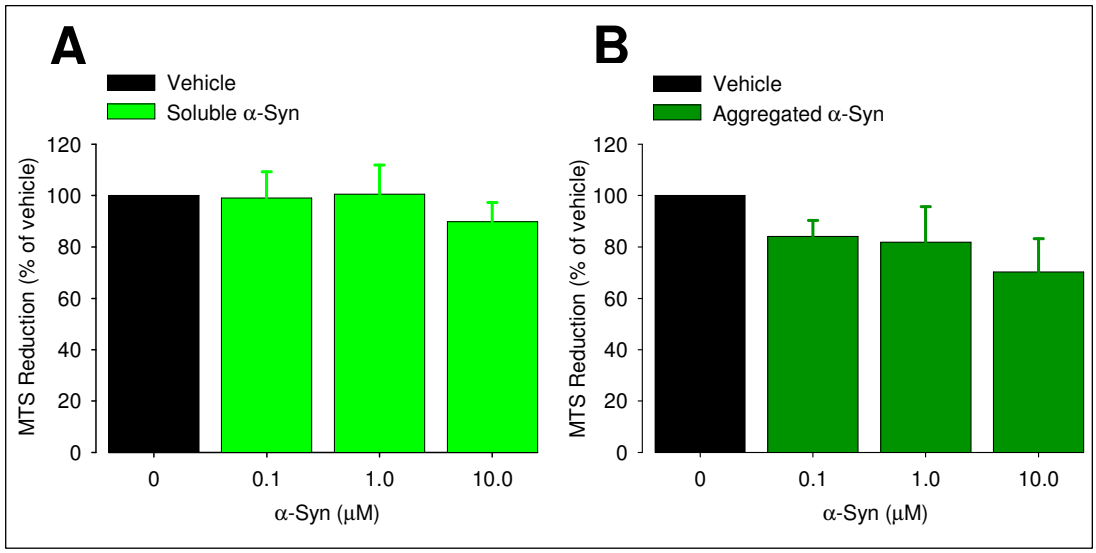

Figure 4.1: In-house produced α-syn did not induce cell death.

SHSY-5Y cells were incubated for 24 h with vehicle (serum-free media with 0.1 % water), in-house soluble α-syn (0.1 – 10.0 μM) or in-house aggregated α-syn (0.1 – 10.0 μM) with MTS reduction shown as a percentage of vehicle. **(A) Soluble α-syn:** Soluble α-syn did not lower or increase MTS reduction significantly. **(B) Aggregated α-syn:** Aggregated α-syn did not significantly lower MTS reduction, although there may be a trend towards a decrease in the percentage of MTS reduction with the highest concnetrations of α-syn. For all treatments N = 3.

This study showed that α-syn did not alter MTS reduction irrespective of aggregation state. However the highest concentration of aggregated α-syn may suggest a decrease in MTS reduction and possibly expanding the concentration range to include higher concentrations α-syn may induce a cytotoxic effect.

4.1.2 Validation of in-house wild-type α-syn with commercial α-syn.

A commercial source (rPeptide, USA) of wild-type α-syn was used to validate the results observed with previous in-house toxcity assay whether the same toxicity stands (section 4.1.1).

SHSY-5Y cells were treated as previously with vehicle (serum-free media with 0.1 % water), commercially soluble α-syn (0.1 – 10.0 μM) or aggregated commercial α-syn (0.1 – 10.0 μM) for 24 h. Soluble α-syn (0.1, 1.0 and 10.0 μM) did not significantly affect MTS reduction (99.2 ± 6.8, 96.6 ± 5.8 and 87.1 ± 10.1 % respectively) (figure 4.2A). Similarly with aggregated α-syn (0.1, 1.0 and 10.0 μM) did not significant change MTS reduction compared to vehicle (93.0 ± 6.1, 86.5 ± 8.6 and 76.8 ± 7.7 % respectively) (figure 4.2B).

This study provides validation for our previous study, showing that commercially produced wild-type α-syn (soluble or aggregated), failed to induce toxicity in SHSY-5Y cells. The results for commercial wild-type α-syn are very similar to the results for the in-house produced α-syn (figure 4.1B and 4.2B).

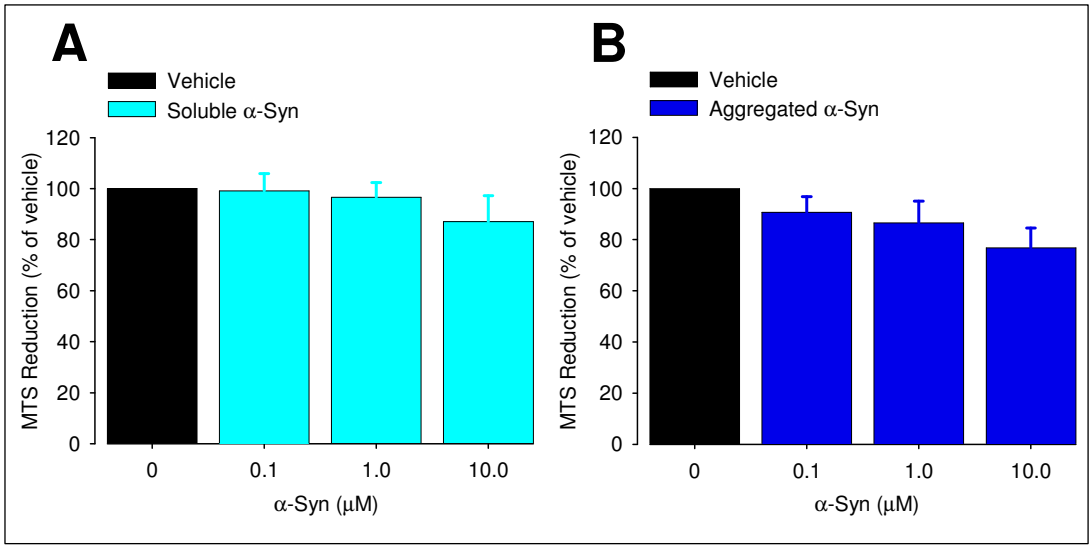

Figure 4.2: Commercially produced α-syn did not induce cell death.

SHSY-5Y cells were incubated for 24 h with vehicle (serum-free media with 0.1 % water), soluble commercial α-syn (0.1 – 10.0 μM) or aggregated commercial α-syn (0.1 – 10.0 μM). MTS reduction was shown as percentage of vehicle. **(A) Soluble α-syn:** Soluble α-syn did not significantly effect MTS reduction. **(B) Aggregated α-syn:** Aggregated α-syn did not significantly lower MTS reduction. For all treatments N = 3.

4.1.3 In-house A53T mutant α-syn does not induce cell death.

Further to investigating the toxicity of wild-type α-syn, we similarly examined the putatively more toxic A53T mutant form of α-syn.

SHSY-5Y cells were incubated for 24 h with vehicle (serum-free media with 0.1% water), in-house soluble A53T α-syn (0.1 – 10.0 μM) or aggregated in-house A53T α-syn (0.1 – 10.0 μM). Soluble A53T α-syn (0.1, 1.0 and 10.0 μM) showed no statistical significant change in MTS levels compared to vehicle (94.9 ± 3.9, 94.6 ± 10.0, and 82.7 ± 15.0 % respectively) (figure 4.3A). Aggregated A53T α-syn at 0.1 μM significantly decreased MTS reduction to 78.4 ± 4.4 % compared to vehicle. However, 1.0 μM aggregated A53T α-syn did not alter MTS reduction compared to vehicle (96.1 ± 9.1 %) and surprisingly, 10.0 μM aggregated A53T α-syn increased MTS reduction further to 122.4 ± 16.8 %, though no significance was determined compared to the vehicle (figure 4.3B). However it is important to note that the increase in MTS reduction observed for 10.0 μM aggregated A53T α-syn is due to one out lying point of 168 % of vehicle, which if removed lowers MTS reduction mean to 107.5 ± 11.1 %.

In this study, soluble A53T α-syn did not alter MTS reduction whereas aggregated A53T α-syn at 0.1 μM decreased MTS reduction, suggesting a cytotoxic effect within the cells. However, the cytotoxic effect of 0.1 μM aggregated A53T α-syn was reversed by increasing the concentration of aggregated A53T α-syn (1.0 and 10.0 μM) (figure 4.1B and 4.3B).

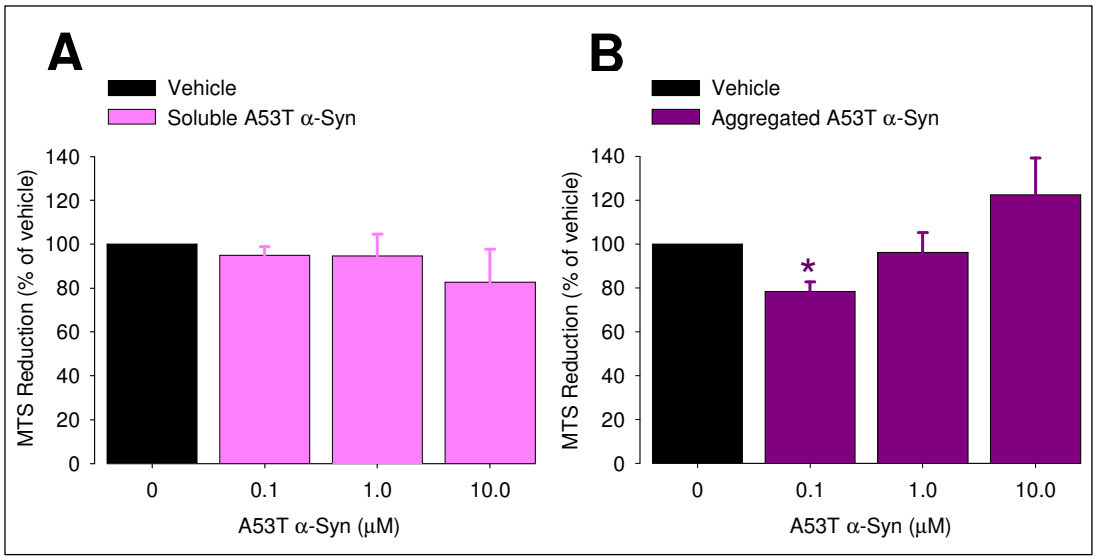

Figure 4.3: In-house A53T α-syn induced state- and concentration-dependent cell death.

Cells were incubated for 24 h with vehicle (serum-free media with 0.1 % water), in-house soluble A53T α-syn (0.1 – 10.0 μM) or in-house aggregated A53T α-syn (0.1 – 10.0 μM). Levels of MTS reduction are shown as percentage of vehicle. **(A) Soluble A53T α-syn:** Soluble A53T α-syn did not significantly alter MTS reduction. **(B) Aggregated A53T α-syn:** Aggregated 0.1 μM A53T α-syn significantly lowered MTS reduction compared to vehicle. A53T α-syn (1.0 and 10.0 μM) did not significantly alter MTS reduction. For all treatments N = 4 and significance was determined by one-way ANOVA with Student-Newman-Keuls post-hoc test where * $P < 0.05$ verses vehicle.

4.1.4 Validation of in-house A53T α-syn with to commercial A53T α-syn.

As with wild-type α-syn, a commercial source (rPeptide, USA) of A53T α-syn was used to validate the previous results with an alternative source of A53T α-syn within SHSY-5Y cells in a manner similar to the previous study.

As described earlier, SHSY-5Y cells were incubated for 24 h with vehicle (serum-free media with 0.1 % water), commercially produced soluble A53T α-syn (0.1 – 10.0 μM) or pre-aggregated A53T α-syn (0.1 – 10.0 μM). Soluble A53T α-syn at 0.1 and 1.0 μM did not effect MTS reduction (101.1 ± 3.4 % and 102.9 ± 2.5 % respectively). 10.0 μM soluble A53T α-syn significantly decreased MTS reduction to 81.4 ± 12.6 % compared to vehicle (figure 4.4A). Aggregated commercial A53T α-syn (0.1, 1.0 and 10.0 μM) also did not alter MTS reduction compared to vehicle (95.7 ± 2.8 %, 102.8 ± 3.7 and 94.4 ± 4.0 % respectively) (Figure 4.4B).

In constrast to in-house soluble A53T α-syn, the commerical protein induced slight cytotoxicity at the highest concentration (figure 4.3B and 4.4B). Aggregated α-syn from a commerical source showed no toxic effects, in a slight discrepancy with in-house produced α-syn that induced 22.6 % toxicity at 0.1 μM (figure 4.3A and 4.4A).

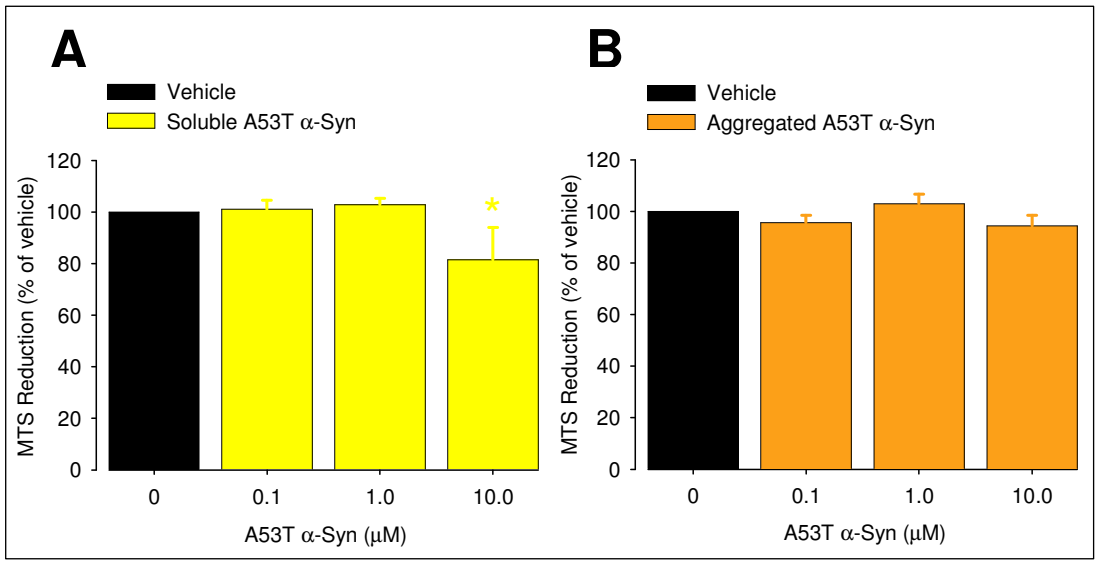

Figure 4.4: Commercially produced A53T α-syn induced state- and concentration-dependent cell death.

Cells were incubated for 24 h with vehicle (serum-free media with 0.1 % water), soluble commercial A53T α-syn (0.1 – 10.0 μM) or aggregated commercial A53T α-syn (0.1 – 10.0 μM) with MTS reduction are shown as percentage of vehicle. **(A) Soluble A53T α-syn:** Soluble α-syn (0.1 or 1.0 μM) had no effect on MTS reduction compared to vehicle whereas 10.0 μM soluble A53T α-syn significantly lowered MTS reduction compared to vehicle. **(B) Aggregated A53T α-syn:** Aggregated A53T α-syn had no effect on MTS reduction compared to vehicle. Soluble A53T α-syn decreased MTS reduction in concentration-dependent manner, whereas aggregation of A53T α-syn had no effect MTS reduction. Significance was determined by one-way ANOVA with Student-Newman-Keuls post-hoc test where * $P < 0.05$ verses vehicle. For all treatments $N = 4$.

4.1.5 Validation of MTS assay by Staurosporine.

To ensure that the results of previous section were not due to the inablity of the assay to detect cell death in these cells the effectiveness of the MTS assay at measuring toxicity was validated with staurosporine (STS). Staurosporine is a protein kinase C inhibitor which induces concentration-dependent apoptosis, making it ideal for validating the MTS assay (Koh *et al.,* 1995; Boix *et al.,* 1997; Posmantur *et al.,* 1997; Gescher 1998; Ha *et al.,* 2004)

Two validation studies were performed; examining the concentration-dependent and time-dependent toxicity of STS. In the first cells were treated with either vehicle (serum-free media with 0.1 % DMSO) or STS (0.003 – 10.0 μM) and incubated for 5 h. STS (0.1 - 10.0 μM) induced a significant decrease in MTS reduction in a concentration-dependent manner. Within this range, STS lowered MTS reduction to 50 % of vehicle between 0.3 and 1.0 μM (57.6 ± 23.9 and 33.3 ± 6.8 % respectively). Increasing the STS concentration to 10.0 μM significantly decreased MTS reduction to less than 20 % MTS reduction indicating almost total cells death (15.7 ± 1.4 %) (figure 4.5). At the lower concentrations of STS (0.003 – 0.03 μM) did not affect MTS reduction levels. STS induced concentration-dependent decrease in cell viability, with a lethal dose of 50 % (LD_{50}) between 0.3 and 1.0 μM at 5 h (figure 4.5).

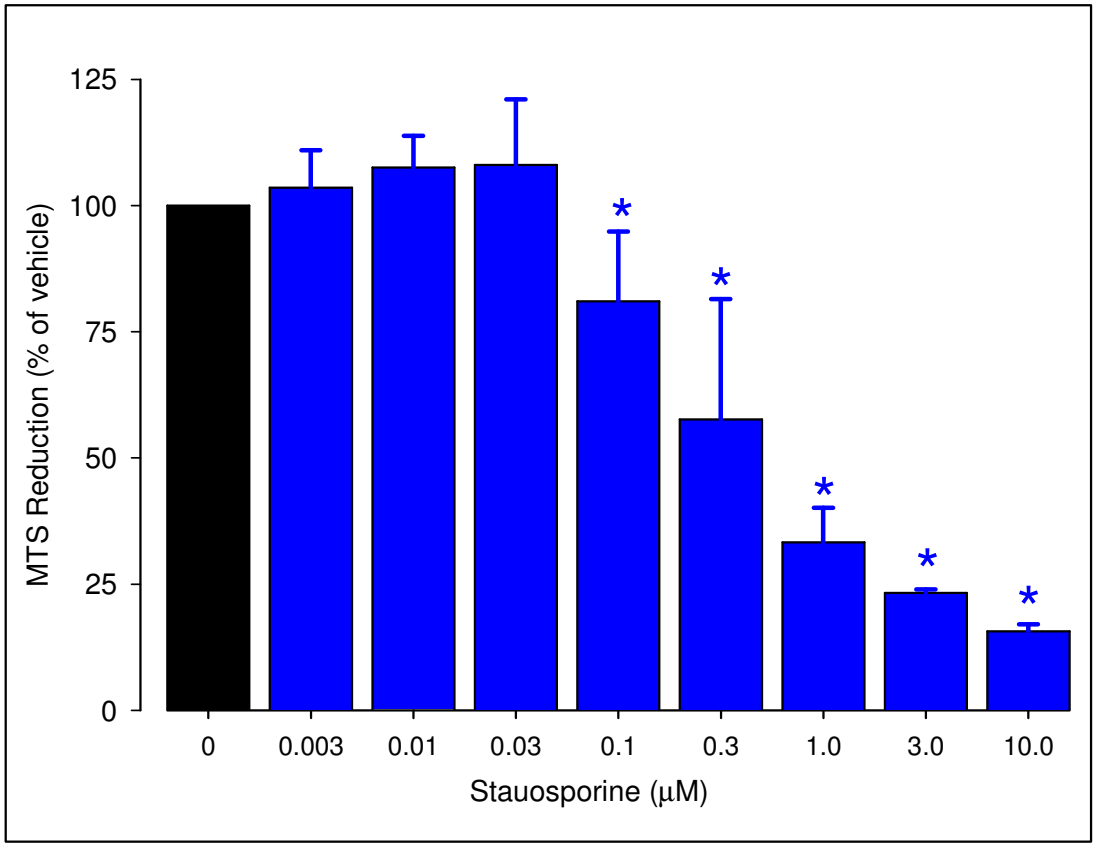

Figure 4.5: Staurosporine induced cell death in a concentration-dependent manner.

SHSY-5Y cells were incubated for 5 h with vehicle (serum-free media with 0.1 % DMSO) or Staurosporine (0.003 – 10.0 µM) with MTS reduction shown as percentage of vehicle. STS (0.003 – 0.03 µM) did not alter MTS reduction. However higher concentration of STS (0.1 – 10.0 µM) significantly decreased MTS reduction in a concentration-dependent manner. Significance was determined by one-way ANOVA with Student-Newman-Keuls post-hoc test where * $P < 0.05$ verses Vehicle. For all treatment N = 3.

For the temporal study SHSY-5Y cells were treated with either vehicle (serum-free media with 0.1 % DMSO) or STS (1.0 μM) and incubated for 1 – 7 h. The level of MTS reduction was presented as percentage of vehicle at 1 h. The vehicle did not significantly alter MTS reduction over the 7 h incubation (91.2 – 126.8 % MTS reduction). In contrast STS (1.0 μM) induced a time-dependent decrease in MTS reduction with significance (compared to vehicle) after 3 h (69.4 ± 7.9 %). At 4 h, STS induced ~ 50 % MTS reduction cell death (48.3 ± 6.4 %) before plateaoing between 5 – 7 h (figure 4.6).

This study shows STS-induced cell death can be monitored overtime by the MTS assay (figure 4.6). As well as validating the MTS assay the two STS studies show consistentcy, where 1.0 μM STS decreased MTS reduction to 33.3 ± 6.8 % in the concentration-dependent study and to 27.7 ± 3.8 % at 5 h in the time course study (figure 4.5 and 4.6).

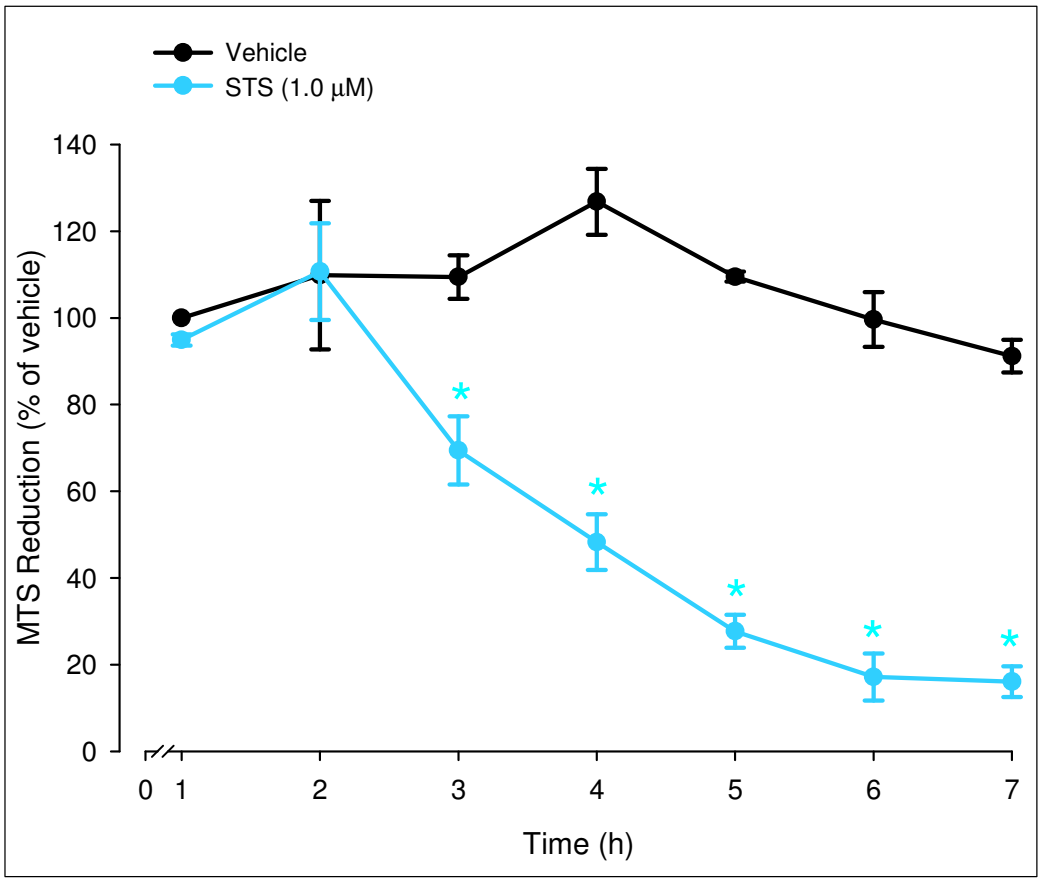

Figure 4.6: Staurosporine induced decrease in cell viability in a time-dependent manner.

Cells were incubated with either vehicle (serum-free media with 0.1 % DMSO) or STS (1.0 µM) for 1 - 7 h. MTS reduction is shown as percentage of vehicle at 1 h. Vehicle alone did not significantly alter MTS reduction over the 7 h. STS induced time-dependent decrease in MTS reduction with STS inducing a significant decrease MTS reduction at 3 h, compared to vehicle at 3 h. STS induced decrease in MTS reduction plateaued at 6 h and 7 h with less than 20 % MTS reduction observed compared to relevant vehicle. Significance was determined by one-way ANOVA with Student-Newman-Keuls post-hoc test where * $P < 0.05$ verses vehicle (at relevant time point). For all treatments $N = 3$.

4.1.6 α-Syn concentration-dependent decrease in MTS reduction.

Soluble α-syn did not induce significant cell death after 24 h incubation at the concentration previously used (figure 4.1A and 4.2A). However, the results implicated a potential trend towards cytotoxicity with increasing concentrations. Increasing concentration range used for α-syn might therefore induce cytotoxicity of the cells. Increasing α-syn incubation time similarly increase any toxic effects.

α-Syn (0.001 – 30.0 μM) was incubated for 48 h with SHSY-5Y cells. α-Syn induced a concentration-dependent decrease in MTS reduction. This was not significant at lower concentrations (0.001 – 3.0 μM), but α-syn at 10 and 30 μM did significantly decrease MTS reduction compared to vehicle (56.6 ± 8.5 % and 47.2 ± 9.3 % respectively) (figure 4.7).

The study has shown that increasing incubation time to 48 h and the concentration range of α-syn, has identified that α-syn induces concentration-dependent decrease in MTS reduction, indicative of a cytotoxicity effect.

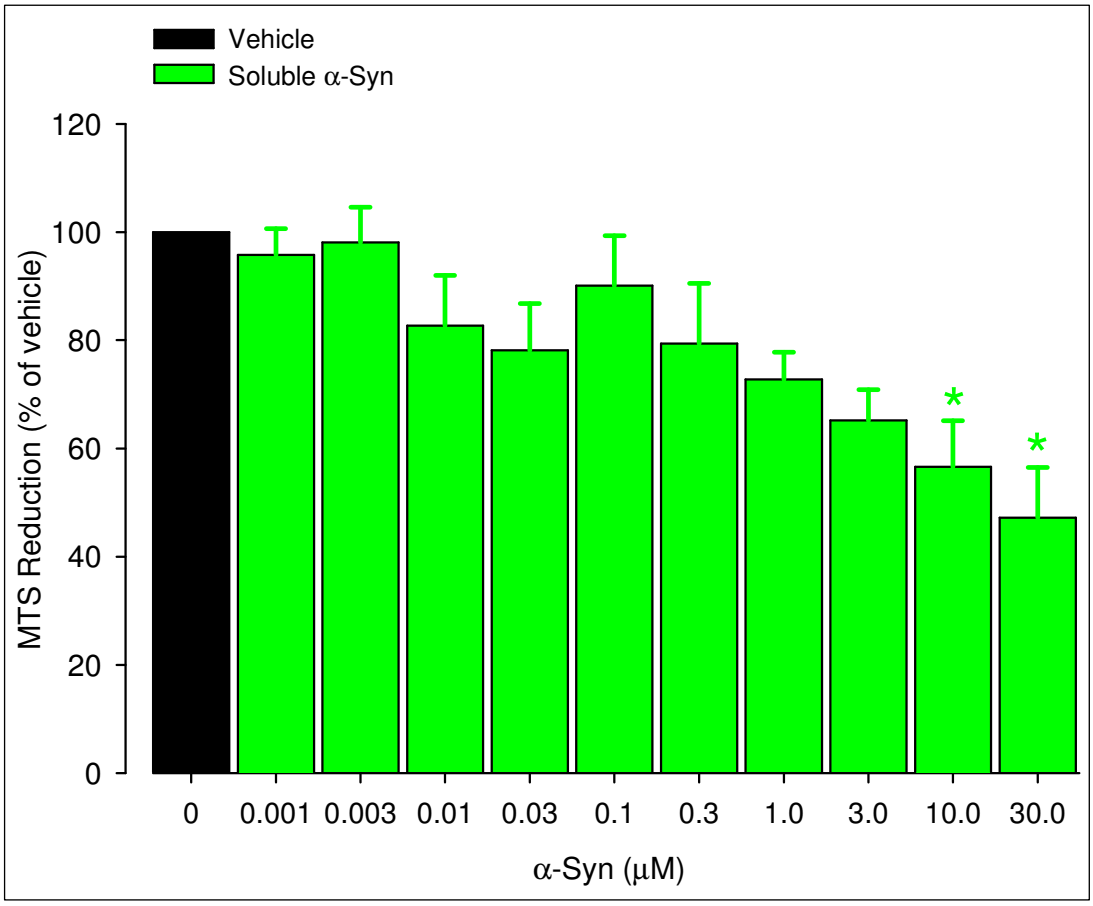

Figure 4.7: α-Syn concentration-dependent decrease in MTS reduction.

Cells were treated with either vehicle (serum-free media with 0.1 % water) or in-house soluble α-syn (0.001 – 30.0 μM) and incubated for 48 h MTS reduction is shown as percentage of vehicle. α-Syn decreased MTS reduction ina concentration-dependent manner with significancy compared to vehicle at higher concnetrations (10.0 and 30.0 μM). For all treatments N = 3 and significance was determined by one-way ANOVA with Student-Newman-Keuls post-hoc test where * $P < 0.05$ verses vehicle.

4.1.7 α-Syn does not induce cell death.

α-Syn (10.0 and 30.0 μM) induced a significant decrease in MTS reduction at 48 h, suggesting that α-syn was cytotoxic. To confirm these results an alternative cell death assay was employed. This secondary assay analysies the release of lactate dehydrogenase (LDH), a stable cytosolic enzyme that is only released from lysed cells.

As described previously, SHSY-5Y cells were treated with α-syn (0.1 – 30.0 μM) and incubated for 24 h or 48 h. Cell death was presented as a percentage to vehicle (serum-free media). At 24 h α-syn (0.1 – 30.0 μM) did not induce any cell death compared to vehicle. The maximum cell death observed was 0.975 ± 0.975% with 30 μM α-syn (figure 4.8A). With increasing incubation time (48 h), α-syn still did not induce any cell death, with a maximum cell death observed of 4.0 ± 3.2 % using 0.1 μM α-syn (figure 4.8B).

This shows α-syn does not induce cell death within SHSY-5Y and is therefore not inherently toxic to cells (figures 4.8A and 4.8B). This would imply that the previous MTS experiments are detecting a decrease in cellular metabolism (as the MTS asssay measures NAD(P)H levels), that is independent of cell death (figures 4.7, 4.8A and 4.8B).

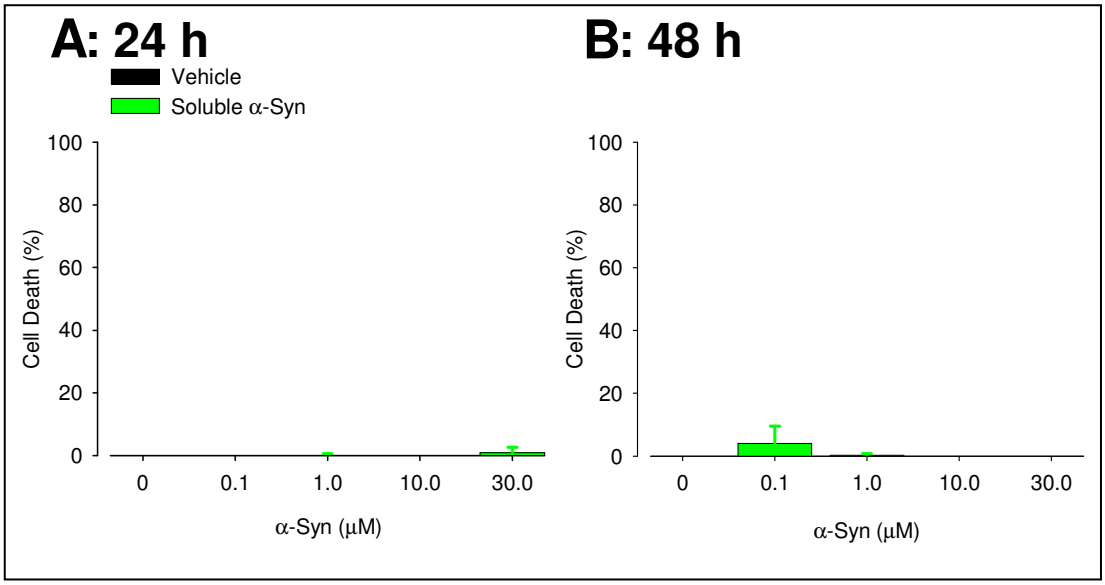

Figure 4.8: α-Syn did not induce cell death.

α-Syn (0.1 – 3.0 μM) was used to treat SHSY-5Y cells for 24 and 48 h and used on the LDH asaay with cell death determined as a percentage to vehicle (serum-free media) **(A) 24 h:** α-Syn (0.1 – 30.0 μM) did not induce cell death compared to vehicle. **(B) 48 h:** α-syn did not cell death with increased incubation. For all treatments N = 3

4.1.8 Summary of Section 4.1

In summary, α-syn induces a reduction in SHSY-5Y cell metabolic output in a concentration- and time-dependent manner but does not, however, induce cell death. The reduction in MTS would appear to be dependent on the addition of soluble α-syn rather than aggregated α-syn, as aggregated α-syn had no significant effect on cell metabolic output after 24 h incubation. This would suggest that either the soluble, or protofibril, form of α-syn is affecting the cells rather than the aggregated form. Of these two forms the most likely candidate is the protofibril for a number of reasons. Firstly, soluble α-syn can be taken up into the cells within 60 seconds after addition to the media (Sung *et al*., 2001). It could be speculated that such a fast uptake of soluble protein would result in a more rapid affect on the cells than is actually observed. Secondly, the reduction of total metabolic output is concentration- and time-dependent, two factors known to be important in the aggrgation of the protein. While this may suggest that aggregated form of α-syn is responsible for the metabolic effect, our studies show that the fully aggregated α-syn does not mediate a similar response. Therefore, the protofibril, the intermediate between soluble and aggregated, α-syn is a more likely candidate.

4.2 Metabolic effects of α-syn.

4.2.1 Effects on the translocation of cytochrome c into the cytosol by α-syn.

We showed previously (section 4.1) that α-syn induced a concentration-dependent decrease in total metabolic content, which was not due to cell death (figures 4.7 and 4.8). To investigate whether this decrease was due to mitochondrial dysfunction, we monitored the translocation of cytochrome c (cyt c) to the cytosol by ELISA. Mitochondrial dysfunction causes the translocation of cyt c from the mitochondrial to the cytosol through the mitochondrial permeable transition pore (mitochondrial pore) which can be inhibited with cyclosporine A (CsA).

SHSY-5Y cells were treated with vehicle (serum-free media with 0.1 % DMSO), α-syn (30.0 μM), CsA (10.0 μM) or CsA (10.0 μM) with α-syn (30.0 μM) and incubated for 6 h. N = 3 for all treatments and cells cytosol analysed by cyt c ELISA. Cytosolic concentrations of cyt c in control cells were 23.7 ± 2.0 ng/ml. With the addition of α-syn (30.0 μM) cytosolic cyt c levels rose to 38.2 ± 5.7 ng/ml, which although caused a 62 % increase, was not significantly different from vehicle. Cells treated with CsA (10.0 μM), the mitochondrial pore inhibitor, showed no alteration in cytosolic cyt c levels compared to vehicle (21.2 ± 3.5 ng/ml). However, the addition of CsA (10.0 μM) and α-syn (30.0 μM) significantly reduced the concentration of cytosolic cyt c to 12.2 ± 1.1 ng/ml compared to vehicle (figure 4.9).

This study shows that α-syn (30.0 μM) or CsA (10.0 μM) do not significantly alter cytosolic levels of cyt c. However, cells treated with both CsA (10.0 μM) and α-syn

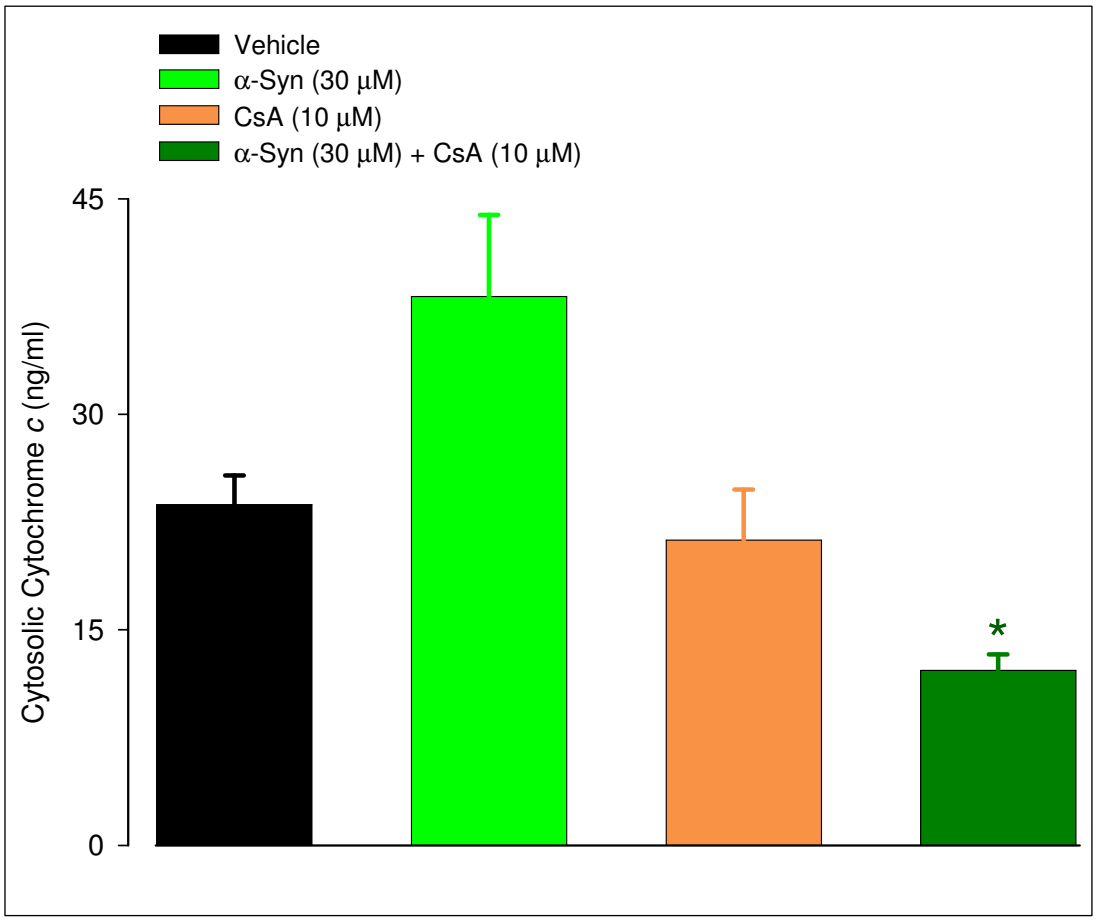

Figure 4.9: Effect of the mitochondrial transition pore inhibitor, cyclosporine A, and α-syn on the translocation of cyt c to the cytosol.

SHSY-5Y cells treated with vehicle (serum-free media with 0.1 % DMSO) saw a concentration of cytosolic cyt c at 23.7 ± 3.5 ng/ml. Treating cells with α-syn (30.0 μM) cytosolic cyt c concentrations rose to 38.2 ± 5.7 ng/ml, a 62 % increase, though not significant. Cytosolic cyt c levels of cells treated with CsA (10.0 μM) alone were unaltered compared to vehicle. However, the addition of both CsA (10.0 μM) and α-syn (30.0 μM) significantly reduced cytosolic levels of cyt c compared to vehicle. All treatments were incubated with cells for 6 h (N = 3). Significance was determined by one-way ANOVA with Student-Newman-Keuls post-hoc test where * $P < 0.05$ verses α-syn

(30.0 μM) in combination, significantly reduces cytosolic levels of cyt c after 6h incubation.

4.2.2 No translocation of cytochrome c to the cytosol after increased exposure to α-syn.

The previous study suggests that incubation with α-syn for 6 h increased cytosolic cyt c levels, though not significantly. We speculated that increasing the incubation time would further increase α-syn induced translocation of cyt c to the cytosol. In this study therefore, incubation duration was increased to 48 h as α-syn significantly decreased SHSY-5Y cells total metabolic output at this time point in our previous studies (figure 4.7).

SHSY-5Y cells were treated with vehicle (serum-free media with 0.1 % DMSO) or α-syn (30.0 μM) and incubated for a total of 48 h. After 36 h CsA (10.0 μM) was added to both α-syn and vehicle cells. The cytosol was analysed by cyt c ELISA. Control levels of cytosolic cyt c in the presence of vehicle were 21.3 ± 3.2 ng/ml after 48 h incubation (figure 4.10). Cells treated with α-syn did not alter the translocation of cyt c to the cytosol compared to vehicle (19.9 ± 1.2 ng/ml). CsA (10 μM) showed a significant loss of cyt c from the cytosol (decreased to 5.7 ± 0.7 ng/ml compared to vehicle). Similarly with the addition of CsA (10 μM) to α-syn treated cells cytosolic cyt c levels significantly dropped to 4.1 ± 1.4 ng/ml compared to vehicle and α-syn alone (figure 4.10).

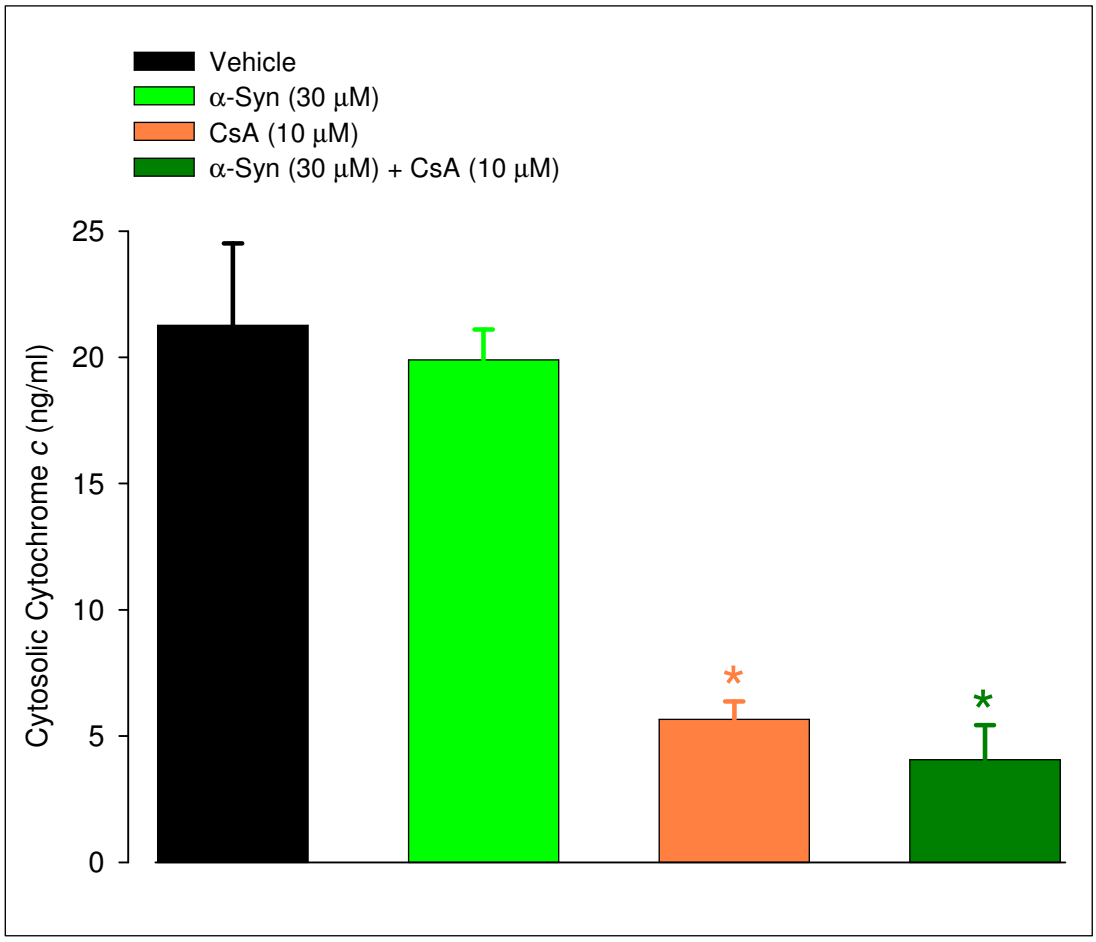

Figure 4.10: Cytosolic cyt c was not increased with increase incubation with α-syn.

SHSY-5Y cells were treated with vehicle (serum-free media with 0.1 % DMSO) or α-syn (30.0 µM) and incubated for 48 h. CsA (10.0 µM) was added to cells at 36 h. N = 3 for all treatments. Vehicle treated cells showed 21.3 ± 3.2 ng/ml cytosolic cyt c. α-Syn treated cells did not increase cytosolic cyt c compared to vehicle. CsA (10.0 µM) significant lowered cytosolic cyt c levels compared to vehicle. CsA (10.0 µM) co-treated with α-syn significantly lowered cytosolic cyt c levels compared to vehicle and α-syn alone. Significance was determined by one-way ANOVA with Student-Newman-Keuls post-hoc test where * $P < 0.05$ verses vehicle

Our results presented here suggest that the addition of α-syn alone (30.0 μM for 48 h) had no overall effect on the translocation of cyt c to the cytosol (figure 4.10). However, the addition of 10.0 μM CsA alone produced a significant reduction in the concentration of cytosolic cyt c, a result mirrored when CsA was also added to the α-syn treated cells. However, this result may be misleading as the presence of CsA in these experiments should not alter the concentration of cytosolic cyt c in normal cells. The fact that a significant reduction is seen in cyt c concentration may be an indication that the addition of CsA at this concentration is inducing cell death. As previous experiments (sections 4.2.1 and 4.2.2) showed no significant reduction in cytosolic cyt c after 6 h incubation, this effect may be time dependent.

4.2.3 Temporal profile of CsA induced cell death by the LDH assay.

The previous data (sections 4.2.1 and 4.2.2) implied that CsA may be inducing a time-dependent decrease in cytosolic cyt c concentration that is independent of α-syn (figure 4.9 and 4.10). However, it may be the case that the reduction in cytosolic cyt c concentrations may be a result of cell death. To investigate this further we investigated CsA-induced cell death using the LDH assay.

Cells were treated with either vehicle (serum-free media with 0.1 % DMSO) or CsA (0.1 - 10.0 μM) and incubated for 6, 12, 24 or 48 h. CsA at 0.1 and 1.0 μM did not show induced cell death between 6 – 24 h. However, after 48 h incubation, CsA (0.1 and 1.0 μM) significantly increased cell death compared to the earlier time points (15.2 ± 7.7 % and 41.3 ± 12.8 % respectively) (figure 4.11). In contrast, CsA at 10.0 μM significantly increased cell death at all time points (i.e. 6, 12 and 24 h saw an

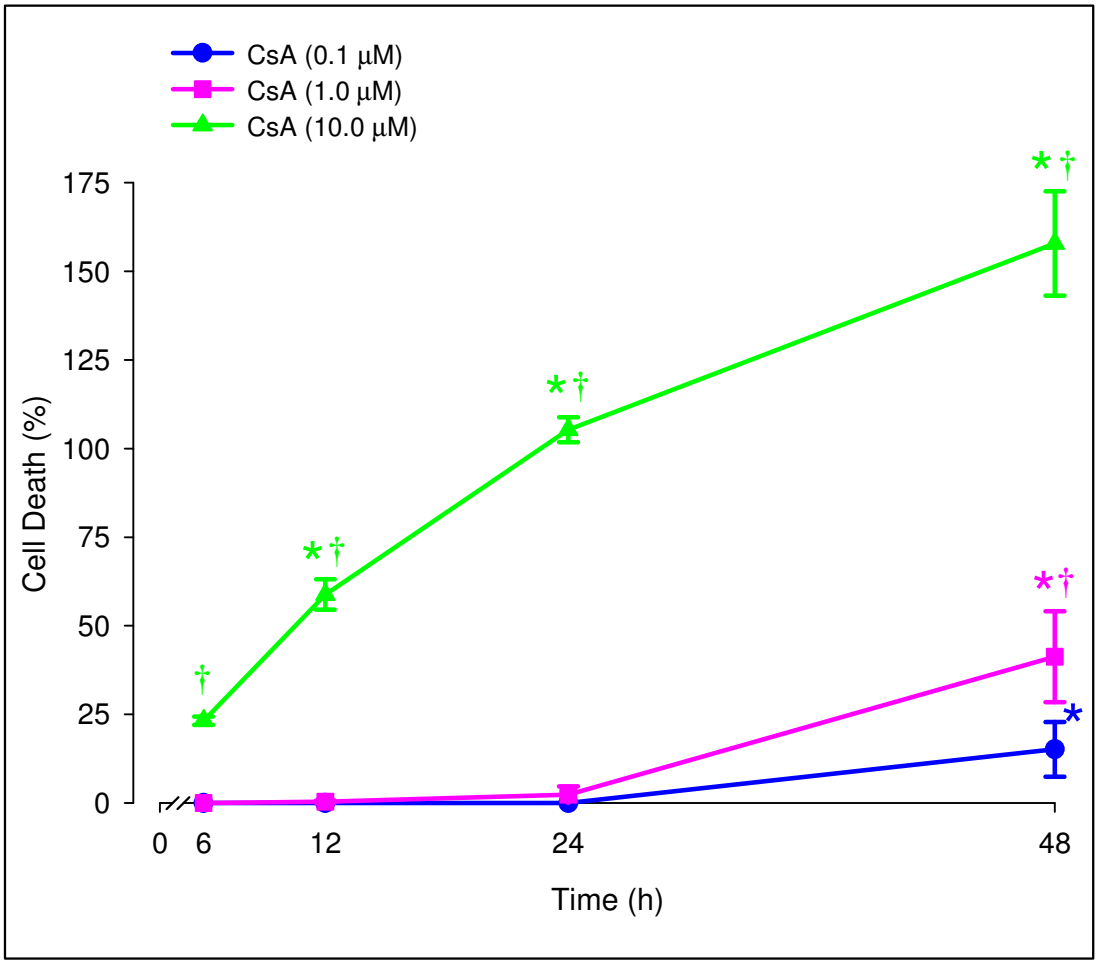

Figure 4.11: Temporal profile of CsA concentrations.

Cells were treated with either vehicle (serum-free media with 0.1 % DMSO) or CsA (0.1-10.0 µM) and incubated for 6, 12, 24 or 48 h with cell death presented as a percentage to the vehicle (n = 3). CsA at 0.1 and 1.0 µM did not increase cell death at 6, 12 or 24 h, but significantly increased cell death at 48 h, where 1.0 µM CsA induced significantly higher cell death than 0.1 µM CsA. Increasing CsA to 10.0 µM significantly increased cell death at all time points when compared to lower concentrations. CsA (10.0 µM) induced a time-dependent increase in cell death with each time point significantly higher than the previous one. Significance was determined on ranks as normality test failed by two-way ANOVA with Student-Newman-Keuls post-hoc test where * $P < 0.05$ verses earlier time point (within specified concentration) and † $P < 0.05$ verses lower concentrations (within specified time point).

increase to 23.2 ± 1.1 %, 58.8 ± 4.3 % and 105.3 ± 3.6 % compared to the lower concentrations respectively). It is worthy to note that 10 μM CsA (and MPP^+ in subsequent experiments using LDH assay) appears to be more efficient at inducing cell death than the commercial lysis buffer used here to induced 'total' cell death (figure 4.11).

This study shows that CsA induces cell death in a time- and concentration-dependent manner (figures 4.11). Therefore, the reduction in the concentration of cyt c in the cytosol induced by CsA seen previously (figure 4.10), was due to CsA inducing cell death.

4.2.4 The effect of α-syn on CsA induced cell death.

Previously, we have shown that CsA significantly increases cell death in a concentration and time-dependent manner (section 4.2.3, figure 4.11). This would imply that the decrease in the cytosolic concentrations of cyt c seen previously (section 4.2.2, figure 4.10) was due to CsA induced cell death. The previous experiments also included the use of α-syn in combination with CsA that also saw a reduction in cyt c concentrations. It may be assumed that the reduction of cyt c in this case was solely due to the CsA induced cell death irrespective of α-syn. It may also be the case that the concentration of CsA used in the cytosolic cyt c ELISA was excessive, causing inappropriate cell death rather than just inhibiting the mitochondrial pore. To confirm that α-syn did not contribute to CsA-induced cell death we used the LDH assay as described previously (section 4.2.3).

Cells were treated with vehicle (serum-free media with 0.1 % DMSO), CsA alone or CsA with α-syn at varying concentrations for 6, 12, 24 or 48 h. Here, we show that a low CsA concentration (0.1 μM) resulted in an increase in cell death only when either 10.0 or 30.0 μM α-syn is added (figure 4.12A). However, at a higher concentration of CsA (1.0 μM) only 10.0 μM α-syn appears to have a significant effect on cell death (figure 4.12B). However, neither 0.1 nor 1.0 μM CsA concentrations showed an increase in cell death as high as observed with 10.0 μM CsA alone. Furthermore, the level of cell death caused by 10.0 μM CsA is not affected by any of the α-syn concentrations used (figure 4.12C).

This would imply that the use of 10.0 μM CsA in the cytosolic cyt c ELISA experiments (section 4.2.2) was indeed too high and induced inappropriate cell death, but that a lower concentration (0.1 – 1.0 μM) could be used in future experiments. It is also important to note that the combination of CsA (0.1 – 1.0 μM) and α-syn (10.0 and 30.0 μM) induced a ~20 % toxicity that was not apparent whrn given alone.

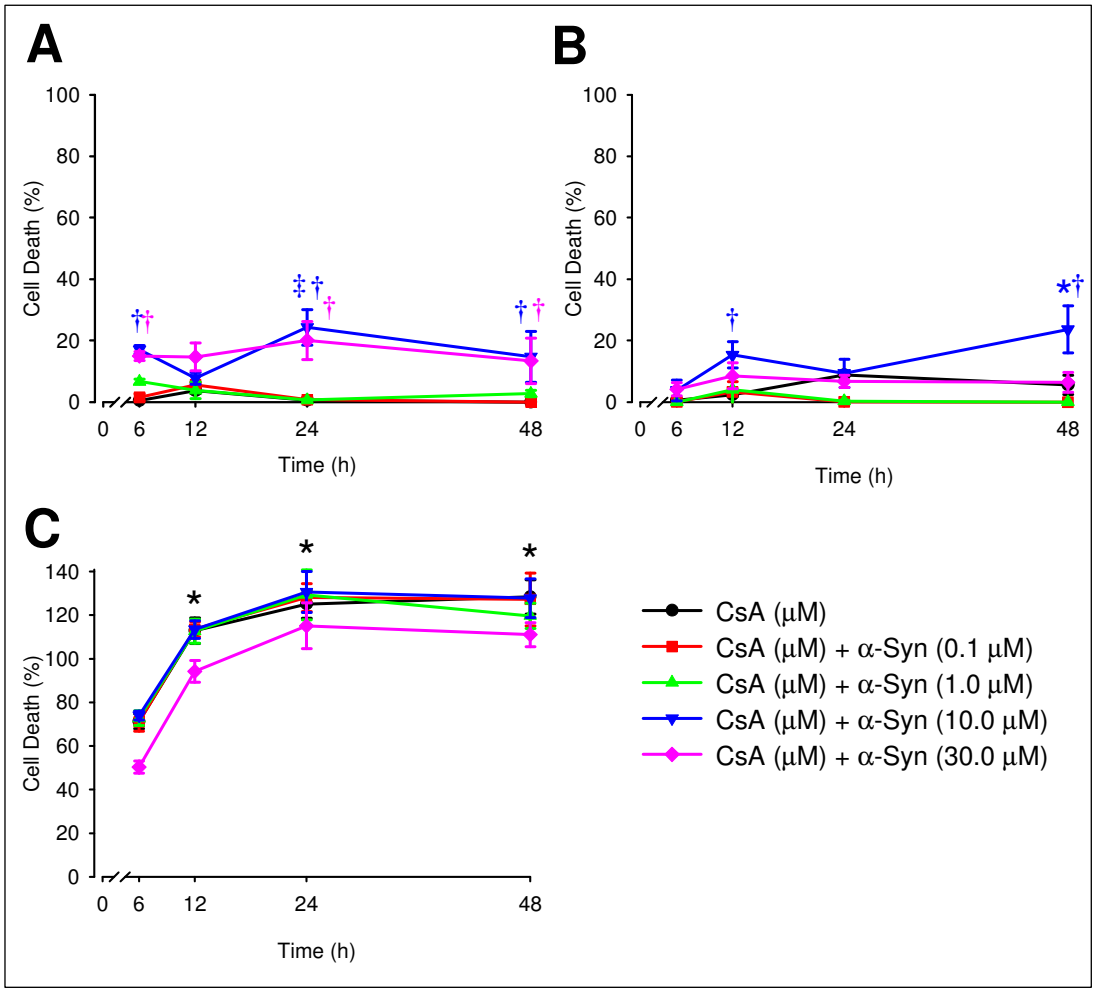

Figure 4.12: Concentration–dependent toxicity of CsA in the presence of α-syn.

Cells were incubated for 6, 12, 24 or 48 h with vehicle (serum-free media with 0.1 % DMSO), CsA (0.1 – 10.0 μM) or CsA (0.1 – 10.0 μM) with α-syn (0.1 - 30.0 μM). N = 3 for all treatments with cell death presented as percentage to vehicle. **(A) 0.1 μM CsA:** CsA alone does not cause cell death. CsA co-treated with α-syn (10.0 or 30.0 μM) significantly increase cells death compared to CsA alone. CsA and α-syn (10.0 and 30.0 μM) induced cell death did not increase with time. **(B) 1.0 μM CsA:** again, CsA alone does not increase cell death. Significant cell death is only seen in the presence of α-Syn at 10.0 μM at 12 and 48 h time points when compared to 1.0 μM CsA alone. **(C) 10.0 μM CsA:** CsA alone increased cell death independently of α-Syn. No concentration of α-syn studied (0.1 – 30.0 μM) effected the level of cell death observed. For graphs A and B significance was performed on the data ranking because data failed normality and equal variance tests. All significance was determined by two-way ANOVA with Student-Newman-Keuls post-hoc test where * $P < 0.05$ verses 6 h (specified concentration, and black stars specifying all concentrations), ‡ $P < 0.05$ 24 h verses 12 h (within specified concentration), † $P < 0.05$ verses CsA μM (within specified time point).

4.2.5 Induced changes in cytosolic Ca^{2+} levels.

Calcium can be released through the opening of the mitochondrial pore similar to the release of cyt c, but also through the changes in the mitochondrial membrane potential. Furthermore, mitochondrial dysfunction can also be identified through an increase in cytosolic calcium (Ca^{2+}) levels. In contrast to the cyt c ELISA, the FLIPR Plus Ca^{2+} assay is able to measure the Ca^{2+} concentrations within live cells using a cytoplasmic fluorescent dye and so therefore is not as invasive as the cytosolic cyt c ELISA (which requires the lysing of the cells). The lack of cell disruption involved in the FLIPR Plus Ca^{2+} assay leads to more accurate and consistent results being obtained. With this in mind, we employed the FLIPR Plus Ca^{2+} assay to elucidate α-syn-induced intracellular effects within live cells.

Cells were incubated for 6, 12, 24 or 48 h with either vehicle (serum-free media) or α-syn at varying concentrations (0.1 – 30.0 μM). In each case the fluorescence was measured at 527 nm. Lower concentrations of α-syn (0.1 and 1.0 μM) did not alter cytosolic Ca^{2+} concentrations compared to vehicle controls (figure 4.13 A and B). However, α-syn at 10.0 and 30.0 μM induced an increase in the concentration of Ca^{2+} (figure 4.13 C and D). α-Syn at 10.0 μM induced a significant increase in Ca^{2+} concentration at 6 and 12 h ($2.4 \pm 0.25 \times 10^4$ A.U. and $3.0 \pm 0.12 \times 10^4$ A.U. respectively), which fell to concentrations comparable with the vehicle at 24 and 48 h (figure 4.13 C). Similarly, 30.0 μM α-syn induced a significant increase in Ca^{2+} concentration at 12 and 24 h (with an increase of $3.4 \pm 0.20 \times 10^4$ A.U. and $3.6 \pm 0.18 \times 10^4$ A.U. respectively). Again, the increase in Ca^{2+} concentration returned to vehicle levels by 48 h (figure 4.13 D).

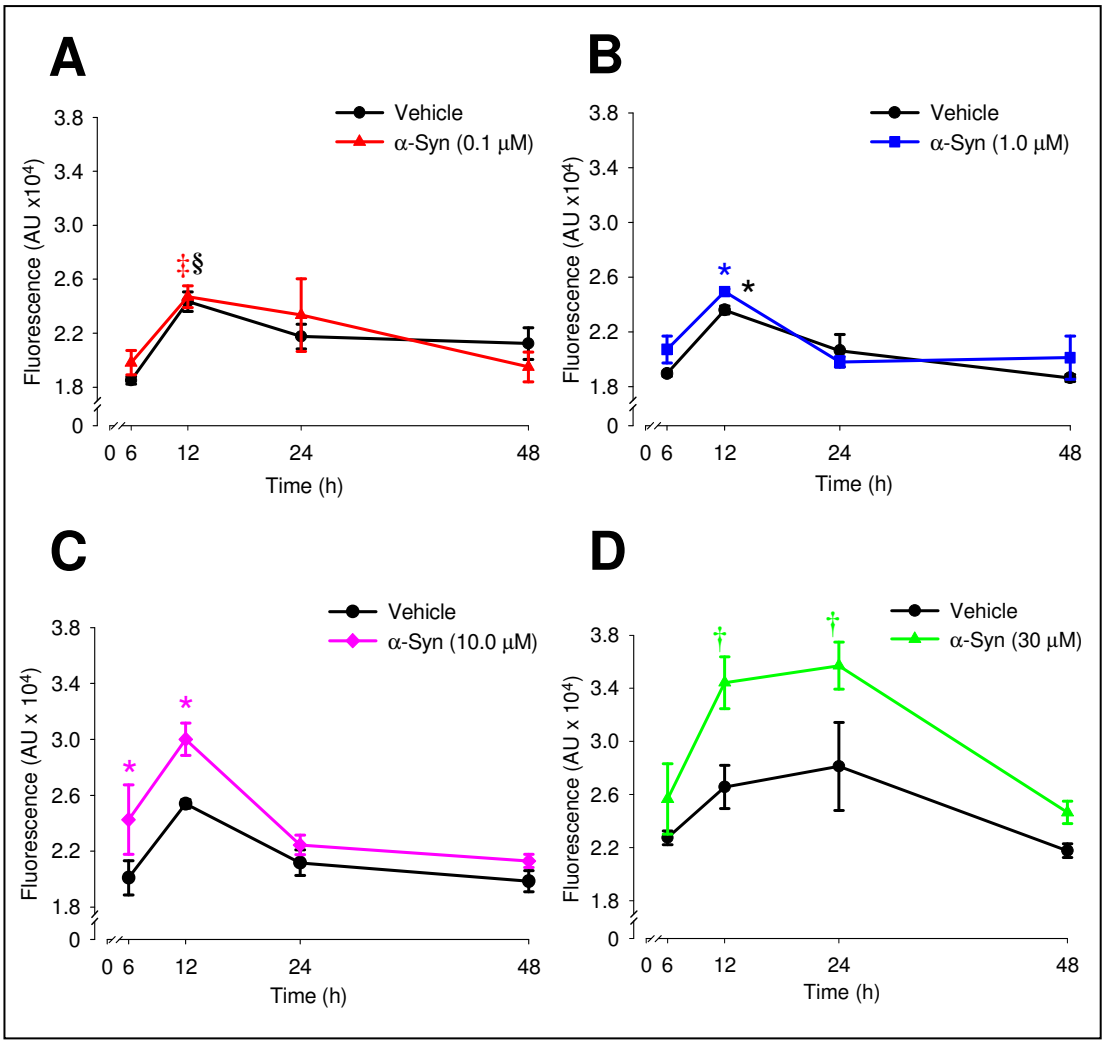

Figure 4.13: Temporal profile of varying concentrations of α-syn on cytosolic Ca^{2+}.

α-Syn induced a concentration- and time-dependent increase in cytosolic Ca^{2+} measured by increase in fluorescence at 527 nm. Cells were treated with either vehicle (serum-free media) or α-syn (0.1 – 30.0 μM) and fluorescence measured after 6, 12, 24 or 48 h incubation. **(A) 0.1 μM α-syn and (B) 1.0 μM α-syn:** α-Syn (0.1 or 1.0 μM) did not alter the cytosolic Ca^{2+} concentrations compared to their respective vehicle control at any time point. **(C) 10.0 μM α-syn:** α-Syn significantly increased fluorescence compared to vehicle at both 6 and 12 h, where a significantly higher fluorescence was observed for the 12 h time point (when compared to the other time points). **(D) α-Syn 30.0 μM:** α-Syn significantly increased fluorescence at 12h and 24 h when compared to vehicle and the other time points. Significance performed on ranks for the data presented in graph B (data failed normality test). Significance was determined by two-way ANOVA with Student-Newman-Keuls post-hoc test where * $P < 0.05$ verses 24 and 48 h (within specified concentration), ‡ $P < 0.05$ verses 6 and 48 h (within specified concentration), § $P < 0.05$ verses 6 h, and † $P < 0.05$ verses vehicle (within specified time point).

These data shows that α-syn causes a concentration- and time-dependent increase in the concentration of cytosolic Ca^{2+}. At present, it is not clear whether this change in Ca^{2+} concentration is due to α-syn inducing the opening of the mitochondrial pore or causing disruption of the mitochondrial membrane potential. Interestingly, the pattern of Ca^{2+} concentration increase shown by 30.0 μM α-syn is similar to that suggested by the increase of cytosolic cyt c translocation by 30.0 μM α-syn (sections 4.2.1 and 4.2.2). In both cases an increase was indicated for the 6 h time point that had dissipated by 48 h. It may be the case that both Ca^{2+} and cyt c release into the cytosol is via the same mechanism.

4.2.6 CsA does not prevent α-syn induced cytosolic Ca^{2+} increase.

As we have shown previously (section 4.2.5) α-syn increases the concentration of cytosolic Ca^{2+} in a concentration- and time-dependent manner. However, the mechanism by which this is mediated is not currently known. It may be the case that α-syn is inducing mitochondrial dysfunction by opening the mitochondrial pore or by disrupting the mitochondrial membrane potential. To examine this further, we utilised the CsA-induced inhibition of the mitochondrial pore to ascertain whether this prevented α-syn-induced increase in cytosolic Ca^{2+} concentration.

Cells were treated with vehicle (serum-free media with 0.1 % DMSO), 30.0 μM α-syn alone, CsA (0.1-10.0 μM) alone or 30.0 μM α-syn with CsA (0.1-10.0 μM). Cells were incubated for 6, 12, 24 or 48 h and the fluorescence was measured at 527 nm, where an increase in fluorescence represented an increase in cytosolic Ca^{2+} concentration. CsA at 0.1 μM and 1.0 μM did not alter the fluorescence compared to

vehicle at any time point (figure 4.14A and B). However, cells treated with both CsA (0.1 μM) and α-syn (30.0 μM) significantly increased fluorescence at 48 h compared to vehicle. This increase in fluorescence was mirrored by cells treated with α-syn (30.0 μM) alone, which also significantly increased fluorescence after 48 h incubation compared vehicle (figure 4.14 A). The addition of CsA at 10.0 μM did not alter fluorescence compared to α-syn (30.0 μM) alone at 6, 12 or 24 h. However, CsA (10.0 μM) with α-syn (30 μM) did significantly decrease fluorescence at 48 h ($2.5 \pm 0.12 \times 10^4$ A.U.) compared to vehicle and α-syn (30 μM) alone (figure 4.15 C).

Our data presented here shows that CsA at either 0.1 or 1.0 μM does not reduce the α-syn- (30.0 μM) mediated increase in cytosolic Ca^{2+} (figure 4.14 A and B). It is also implied that increasing CsA to 10.0 μM inhibited the α-syn-induced increase in cytosolic Ca^{2+}. However, it is important to recall that CsA (10.0 μM, alone or in combination with α-syn), previously induced total cell death at 24 h and 48 h (figure 4.11 and 4.12). It may therefore be assumed that the lower fluorescence observed at 24 h and 48 h induced by CsA at 10.0 μM alone and with α-syn (30.0 μM) is due to cell death and not inhibition of the mitochondrial pore. Similarly, results from preliminary experiments suggest cells treated with bongkrekic acid, an inhibitor of adenine nucleotide translocase and a component of the mitochondrial pore, did not reduce α-syn increase in cytosolic Ca^{2+} (data not shown).

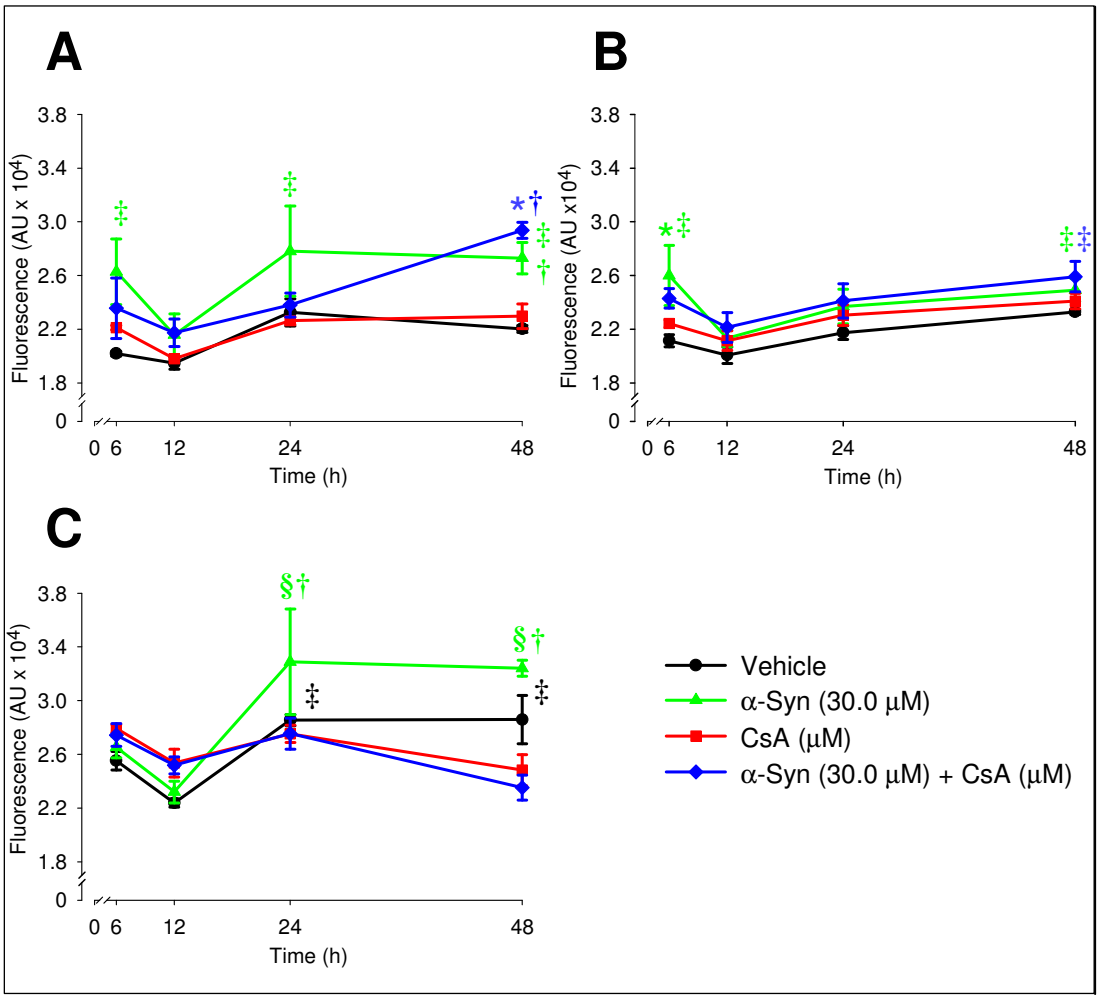

Figure 4.14: Inhibitory effect of CsA on α-syn induced increase in cytosolic Ca^{2+}.

Ca^{2+} levels were measured by fluorescence at 527 nm. Cells were treated with vehicle (serum-free media with 0.1% DMSO), α-syn (30 µM) or CsA (0.1 - 10.0 µM) with and without α-syn (30.0 µM) and the fluorescence measured at 6, 12, 24 or 48 h. **(A) 0.1 µM CsA:** α-Syn (30.0 µM) significantly increased fluorescence at 6 and 48 h compared to vehicle. CsA at 0.1 µM has no significant effect on the fluorescence levels compared to vehicle. When CsA (0.1 µM) is treated with α-syn (30 µM) the fluorescence significantly increases at 48 h compared to vehicle and CsA (0.1 µM) alone, but does not significantly increase compared to α-syn (30.0 µM) alone. **(B) 1.0 µM CsA:** The addition of α-syn (30.0 µM) alone significantly increased fluorescence at 6 h compared to vehicle. Similarly, an increase at 48 h is also seen. Furthermore, the addition of 1.0 µM CsA did not alter the effect of α-syn induced cytosolic Ca^{2+} concentration. **(C) 10.0 µM CsA**: α-syn fluorescence significantly increases at 24 h and 48 h compared to vehicle. The addition of CsA alone and in combination with α-syn (30.0 µM) does not significantly change fluorescence compared to vehicle at 6, 12 or 24 h, however the fluorescence is significantly lower than vehicle or α-syn alone at 48 h. Significance performed on ranks for the data presented in graphs A and C as the data failed normality test. All significance was determined by two-way ANOVA with Student-Newman-Keuls post-hoc test where * $P < 0.05$ verses 6, 12 and 24 h (within specified concentration), ‡ $P < 0.05$ verses 12 h (within specified concentration), § $P < 0.05$ verses 6 and 12 h, and † $P < 0.05$ verses vehicle and CsA (within specified time point).

4.2.7 Loss of mitochondrial potential induced by α-syn.

As α-syn causes an increase in cytosolic Ca^{2+}, which can not be blocked using mitochondrial pore inhibitors. To determine whether the α-syn-induced mitochondrila dysfunction suggested above translates into a loss of mitochondrial membrane potential the MitoPT assay was used. MitoPT accumulates in the mitochondria in an aggregated form that fluoresces red. Loss of mitochondrial membrane potential causes the MitoPT to dissipate through the cell in a monomeric form, which itself fluoresces green. Therefore, a reduction in the level of red fluorescence is indicative of a loss of membrane potential.

Cells were treated with either vehicle (serum-free media) or α-syn (30.0 μM) and incubated for 6, 12, 24 or 48 h, at which point MitoPT was added. Fluorescence was measured at 527 nm for green fluorescence (cytosolic) and 595 nm for red fluorescence (mitochondrial). α-Syn (30.0 μM) induced an increase in mitochondrial, red fluorescence at 6 h and 12 h (126.4 ± 27.2 % and 139.1 ± 23.8 % respectively), which decreased with longer incubation times. α-Syn lowered the mitochondrial fluorescence to 92.3 ± 11.5 % at 24 h and significantly decreased fluorescence to 60.8 ± 6.1 % at 48 h when compared to 6 h and 12 h time points. This data shows that α-syn induces a time-dependent loss of mitochondrial membrane potential. Furthermore, cytosolic fluorescence was unaltered by treatment with 30.0 μM α-syn, showing that α-syn did not increase apoptosis (figure 4.15).

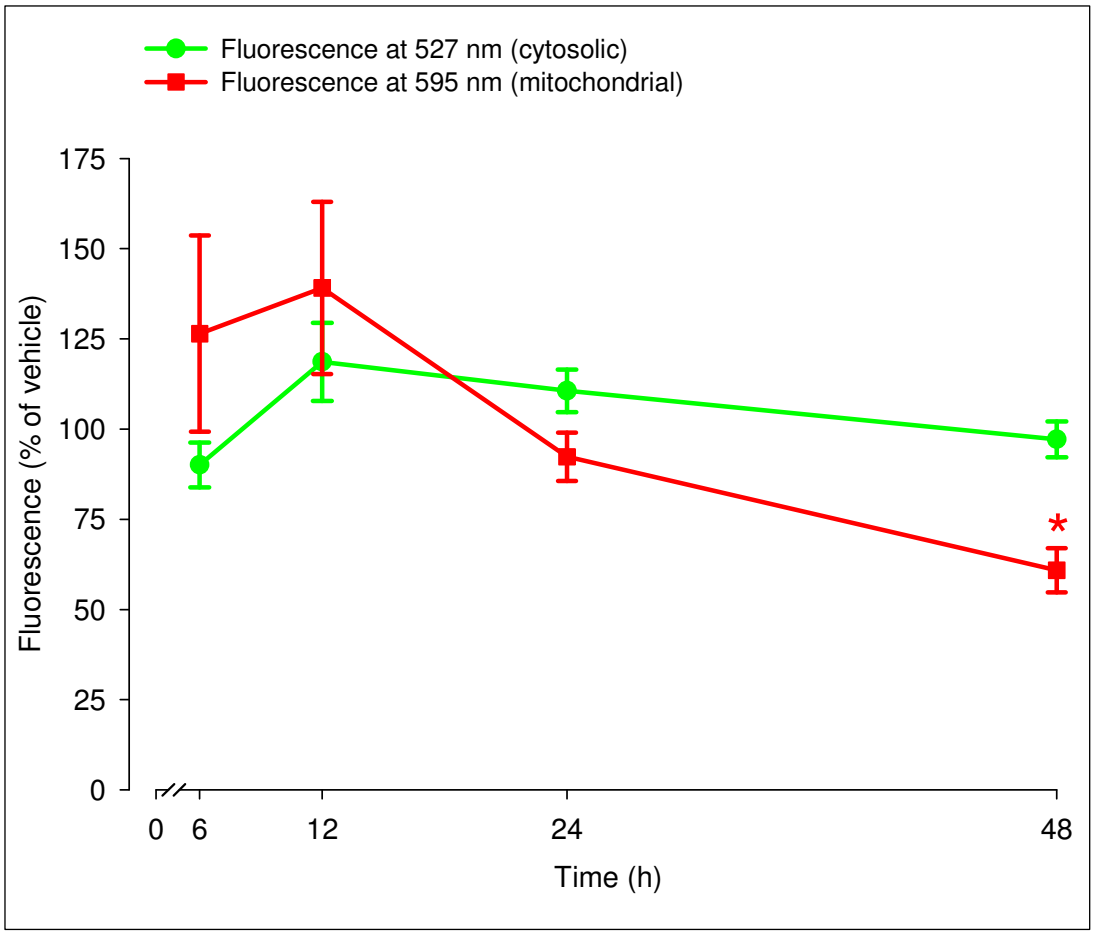

Figure 4.15: α-Syn induced time-dependent loss of mitochondrial membrane potential.

α-Syn induces a time-dependent loss of mitochondrial membrane potential without increasing apoptosis. Cells were treated with either vehicle (serum-free media) or α-syn (30.0 µM) and incubated for 6, 12, 24 or 48 h. Fluorescence was measured at 527 nm for green fluorescence (cytosolic) and 595 nm for red fluorescence (mitochondrial). The data is presented as a percentage of vehicle (where vehicle = 100 % for both fluorescences). α-Syn (30.0 µM) initially increased mitochondrial (red fluorescence) at 6 h and 12 h. However, the mitochondrial fluorescence at 24 h appeared to be lower and by 48 h the mitochondrial fluorescence was significantly lower compared to the 6 h and 12 h time points. Cytosolic (green) fluorescence was unaltered by treatment with α-syn (30.0 µM), showing that α-syn was not increasing apoptosis. Significance was determined by one-way ANOVA with Student-Newman-Keuls post-hoc test where * $P < 0.05$ verses 6 and 12 h.

4.2.8 Summary of Section 4.2

From our studies we have shown that α-syn causes an increase in cytosolic Ca^{2+} in SHSY-5Y cells after 12 h incubation. This observed increase is not blocked by the addition of the mitochondrial pore inhibitor, CsA, which would suggest the observed increase in Ca^{2+} is either via α-syn affecting the mitochondria by a different mechanism other than the mitochondrial pore or α-syn is causing the release of Ca^{2+} from an alternative intracellular store. From the data it may be suggested that the cytosolic cyt c release mirrors Ca^{2+} release, however, this study is inconclusive. In the absence of data at 12 and 24 h incubation it may be that cytosolic cyt c levels are not affected (section 4.2.1 and 4.2.2). To investigate the method by which cytosolic Ca^{2+} concentrations were increasing we investigated the mitochondrial membrane potential. Our study found that upon addition of α-syn to cell media, mitochondrial membrane potential was lost after 48 h incubation. This could mean that the increase in cytosolic Ca^{2+} is due to mitochondrial membrane disruption resulting in mitochondrial dysfunction. Mitochondrial dysfunction would, of course, help explain the reduction in cellular metabolic output see in section 4.1.6. The reduction in cytosolic Ca^{2+} seen after 48 h incubation may be due to the sequestering of the cytosolic Ca^{2+} by other Ca^{2+} stores, e.g. the endoplasmic reticulum, perhaps leaking out of the cells altogether (see section 4.1).

The study above suggests α-syn is forming independent pores in the membrane of the mitochondria, a mechanism which would not be possible if the α-syn protein involved was in its soluble form, but has been associated to the protofibril form (Volles *et al.,* 2001; Lashuel *et al.,* 2002; Volles and Lansbury, 2002; Furukawa *et*

al., 2006; Tsigelny *et al.,* 2007). Furthermore, the fact that Ca^{2+} release was not prevented in the presence of the mitochondrial pore inhibitor CsA would suggest α-syn is working independently of the mitochondrial pore.

4.3: α-Syn within an *in vitro* model of Parkinson's disease.

Within our previous studies (sections 4.1 and 4.2), α-syn was shown to induce a concentration- and time-dependent reduction in total metabolic output without increasing cell death. This reduction in metabolic output (section 4.1.6) was speculated to be through α-syn inducing mitochondrial dysfunction via loss of mitochondrial membrane potential, resulting in an increase in cytosolic Ca^{2+} and possibly cyt c (sections 4.2.5 and 4.2.7).

4.3.1 MPP^+-induced cytotoxicity.

α-Syn has been suggested to have both detrimental and protective effects within PD models. From our work described previously (sections 4.1 and 4.2), these data suggest increasing concentrations of α-syn, though not toxic independently, could cause an increase level of cellular sress. To investigate whether this stress is detrimental to cells under pathological conditions, the response to α-syn was investigated in the MPP^+ model of PD. Intiall experiments aimed to establish the toxic concentration range of MPP^+ within SHSY-5Y cells, using the LDH assay (Section 4.1.7)

SHSY-5Y cells were incubated for 48 h with either vehicle (serum-free media with 0.1 % water) or MPP^+ (1.0 – 3000 μM). MPP^+ (1.0 – 1000 μM) did not induce any

significant cell death compared to vehicle. MPP^+ at 3000 μM, however, significantly increased cell death to 84.4 ± 6.9 % compared to vehicle (figure 4.16).

From this study MPP^+ did not significantly alter cell death at concentrations lower than 1000 μM after 48 h incubation. However, MPP^+-induced a significant increase in cell death between 1000 and 3000 μM, which would imply that suitable concentrations of MPP^+ for future experiments would lie between these two concentrations.

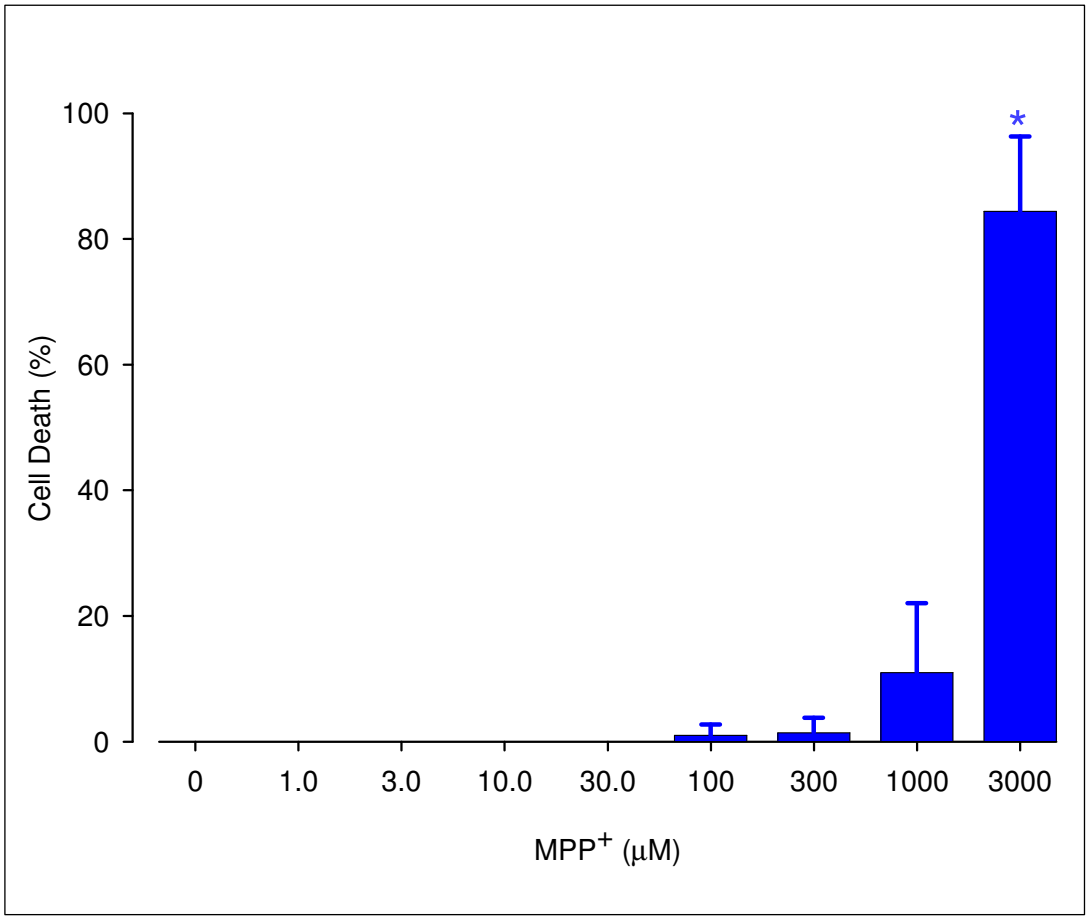

Figure 4.16: MPP^+-induced a concentration-dependent increase in cell death.

Cells were treated with vehicle (serum-free media with 0.1 % water) or MPP^+ (1.0 – 3000 µM) and incubated for 48 h. Cell death is shown as a percentage to vehicle (N = 3). MPP^+ (1.0 – 1000 µM) did not significantly increase cell death compared to vehicle, with cell death ranging from 0 – 11.0 ± 6.4 % respectively. MPP^+ at 3000 µM significantly increased cell death to 84.4 ± 6.9 % compared to vehicle. Significance was determined by one-way ANOVA with Student-Newman-Keuls post-hoc test where * $P < 0.05$ verses 0 µM MPP^+

4.3.2 Study investigating the temporal profile of MPP^+ toxicity.

In order to investigate whether α-syn is detrimental or protective against cell death in a MPP^+ model, the model would require optimisation. To this end we investigated the effect of varying concentrations of MPP^+ on cell death over time. This allows us to build a MPP^+ temporal profile and to establish the LD_{50} of MPP^+, a concentration optimal for monitoring any changes induced by the addition of α-syn between 12 and 48 h.

The temporal profile was established by treating cells with either vehicle (serum-free media with 0.1 % water) or MPP^+ (1.0 – 10.0 mM) and incubated for 0, 4, 6, 12, 24 or 48 h. MPP^+ at the highest concentration (10.0 mM) induced a rapid increase in cell death (from 7.3 ± 6.5 % at 6 h to 97.3 ± 10.6 % at 12 h) compared to lower concentrations (figure 4.17). Halving the concentration of MPP^+ (5.0 mM) showed a similar pattern of cell death, although total cell death was not reached until 24 h and a slower initial increase in cell death was observed. MPP^+ at 3.0 mM induced a steady increase in cell death from 12 h (11.2 ± 1.2 %) and total cell death was only just achieved at the final time point of 48 h. The two lowest concentrations of MPP^+ used in this study (1.0 mM and 2.0 mM) both showed slow, progressive cell death after 12 h but neither reach total cell death by 48 h (38.5 ± 3.6 % and 78.7 ± 13.1 % cell death respectively).

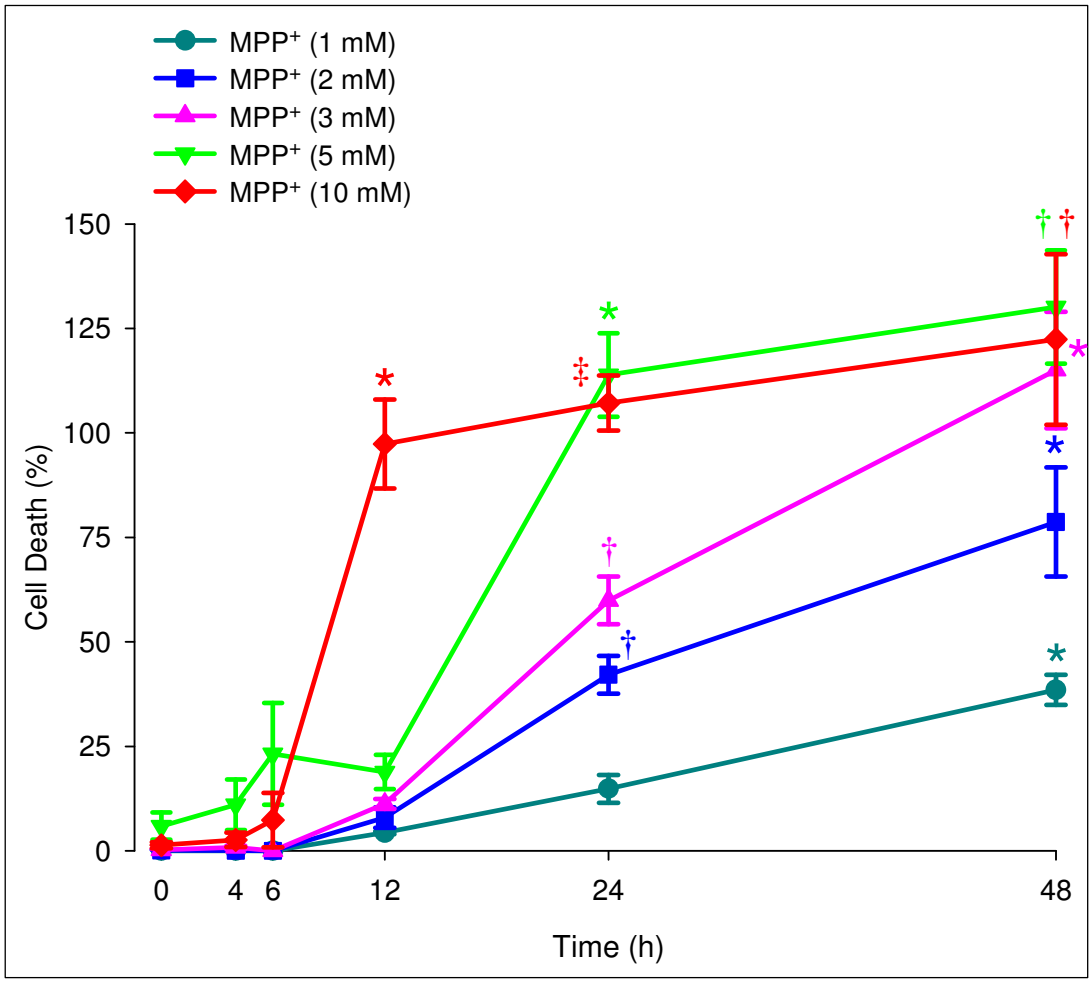

Figure 4.17: Temporal profile of MPP^+.

SHSY-5Y cells were treated with either vehicle (serum-free media with 0.1 % water) or MPP^+ (1.0 – 10.0 mM) and incubated for 0, 4, 6, 12, 24 or 48 h. N = 3 for all treatments and cell death was shown as a percentage to vehicle. MPP^+ (10.0 mM) induced low level cell death at 6 h, significantly increasing at 12 h compared to earlier time points. MPP^+ at 5.0 mM slowly increased cell death up to 12 h and then significantly increased cell death at 24 h compared to earlier time points. MPP^+ at 3.0 mM did not significantly increase cell death before 24 h, where at 24 h and 48 h cell death significantly increased compared to all earlier time points. MPP^+ (2.0 mM) significantly increased cell death at 24 and 48 h compared to all earlier time points, 2.0 mM MPP^+ unlike 3.0, 5.0 and 10.0 mM MPP^+ did not induce total cell death by 48 h. 1.0 mM MPP^+ induced low level cell death with only a significant increase in cell death at 48 h. Significance was determined by two-way ANOVA with Student-Newman-Keuls post-hoc test where * $P < 0.05$ verse earlier time points, † $P < 0.05$ verse 0, 4, 6 and 12 h, ‡ $P < 0.05$ verse 0, 4 and 6 h.

From this temporal profile of MPP^+-induced cell death it may be concluded that a concentration of 2.0 mM MPP^+ would provide an LD_{50} at 24 h, which would be the optimal concentration of MPP^+ to use to monitor any changes in cell death caused by α-syn.

4.3.3 MPP^+-induced toxicity is exacerbated by α-syn.

In our previous studies (section 4.1 and 4.2), α-syn was implicated in inducing mitochondrial dysfunction by causing loss of the mitochondrial membrane potential in SHSY-5Y cells, but without inducing cell death. MPP^+ has been shown to induce cell death in a concentration- and time-dependent manner (section 4.3.2). In order to investigate potentially detrimental effects on cell survival by α-syn, we used the MPP^+ *in vitro* PD model and the LDH assay with varying concentrations of α-syn.

Cells were treated with vehicle (serum-free media with 0.1%), MPP^+ (0.1 – 3.0 mM) or MPP^+ (0.1 – 3.0 mM) with α-syn (0.1 – 30.0 μM) and incubated for 24 h. Where either 0.1 or 1.0 mM MPP^+ was treated with α-syn at $\leq$ 1.0 μM no significant cell death was observed when compared to the MPP^+ alone (figure 4.18 A and B). However, the addition of α-syn at 10.0 and 30.0 μM to 0.1 mM MPP^+ saw a significant increase in cell death (23.2 ± 3.3 % and 16.7 ± 1.8 % respectively) (figure 4.18 A). This trend was matched with the 1.0 mM MPP^+ experiment but here the 30.0 μM α-syn data was found to not be significantly higher than the MPP^+ control, where 10.0 and 30.0 μM α-syn lead to an increase in cell death of 67.0 ± 12.5 % and 42.6 ± 8.1 % respectively (figure 4.18 B). At 2.0 mM MPP^+ only the addition of 30.0 μM α-syn induced a significant increase in cell death to 65.2 ± 2.6 % (figure 4.18 C).

MPP^+ (3.0 mM) alone induced 96.6 ± 4.5 % cell death, producing a ceiling effect on the data. Therefore, it is unsurprising that the co-treatment of α-syn (0.1 – 30.0 μM) with 3.0 mM MPP^+ resulted in 100 % cell death for all α-syn concentrations (figure 4.18 D).

This study shows that MPP^+-induced cell death, independent of MPP^+ concentration, is exacerbated by the addition of α-syn in a concentration-dependent manner.

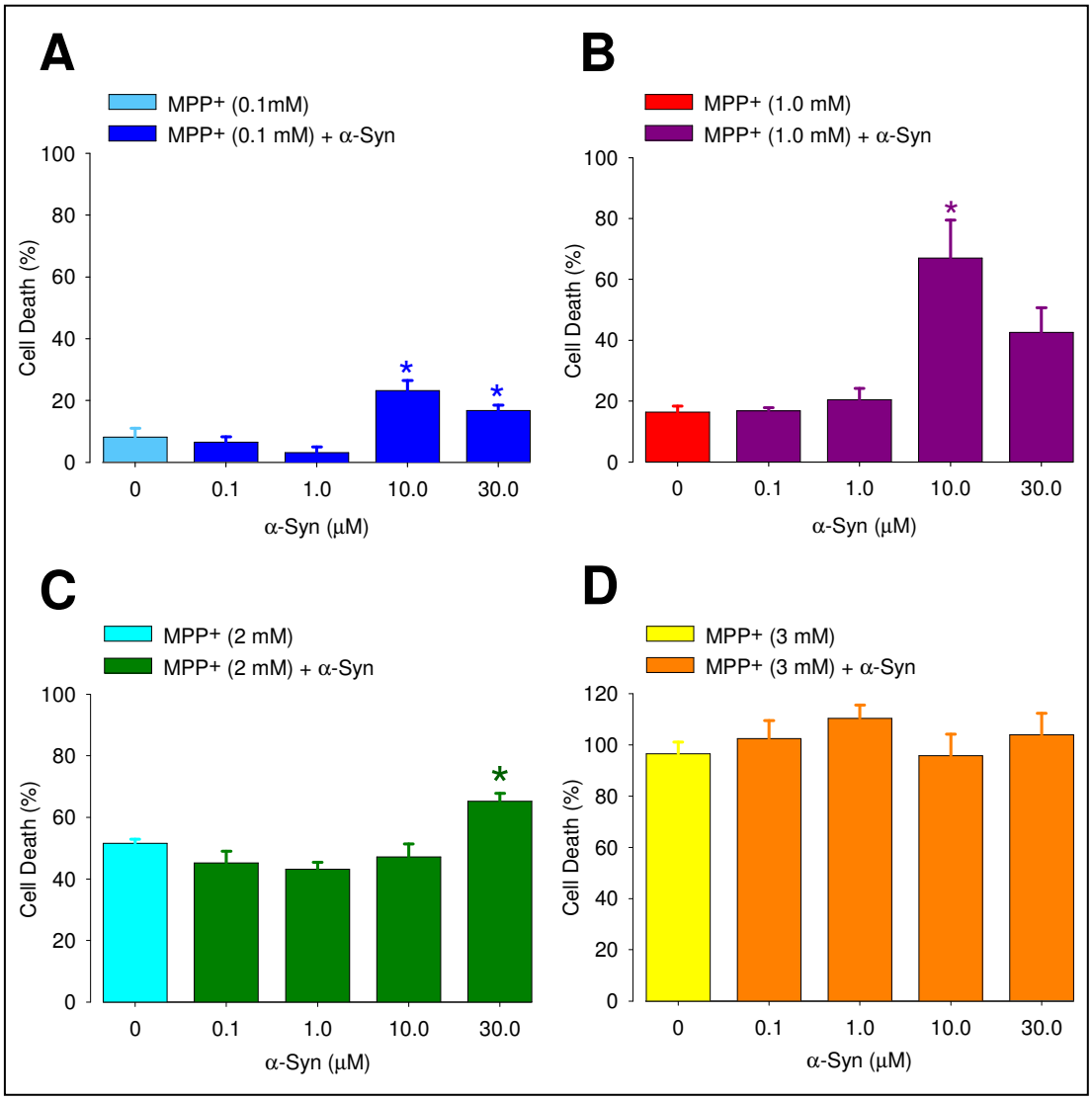

Figure 4.18: MPP$^+$-induced toxicity is exacerbated by α-syn in a concentration-dependent manner.

Cells were treated with vehicle (serum-free media with 0.1%), MPP$^+$ (0.1 – 3.0 mM) or MPP$^+$ (0.1 – 3 mM) with α-syn (0.1 – 30.0 μM) and were incubated for 24 h. Cell death is shown as a percentage to the vehicle control (N = 4). **(A) 0.1 mM MPP$^+$:** the MPP$^+$ control induced 8.2 ± 2.8 % cell death at 24 h. MPP$^+$ co-treated with α-syn at either 0.1 or 1.0 μM did not change the of level cell death. Treating the cells with MPP$^+$ and either 10.0 or 30.0 μM α-syn significantly increased MPP$^+$-induced cell death compared to the MPP$^+$ control. **(B) 1.0 mM MPP$^+$:** the MPP$^+$ control here increased cell death to 16.3 ± 2.0 % cell death. Again, co-treatment of MPP$^+$ and α-syn (0.1 or 1.0 μM) did not affect the level of MPP$^+$-induced cell death. Whereas, MPP$^+$ with 10.0 μM α-syn significantly increased cell death compared to MPP$^+$ alone. MPP$^+$ with 30.0 μM α-syn increased cell death, but not significantly (P = 0.093). **(C) 2 mM MPP$^+$:** the MPP$^+$ control induced 51.6 ± 1.3 % cell death. MPP$^+$ co-treated with 30.0 μM α-syn significantly increased cell death compared to the MPP$^+$ control. **(D) 3 mM MPP$^+$:** the MPP$^+$ control induced almost complete cell death after 24 h; co-treatment with α-syn (0.1 – 30.0 μM) did not decrease MPP$^+$-induced toxicity. Significance was determined by one-way ANOVA with Student-Newman-Keuls post-hoc test where * P < 0.05 verses MPP$^+$ (mM).

4.3.4 α-Syn and MPP^+-induced toxicity over time.

Our previous study (section 4.3.3) showed that α-syn exacerbated MPP^+-induced cell death in a concentration-dependent manner in SHSY-5Y cells with 24 h incubation. This time point coincides with earlier data (section 4.2.5) that identified an α-syn-induced increase in cytosolic Ca^{2+}. To further investigate the enhancement of MPP^+-induced cell death by α-syn, the incubation time was increased to 48 h as α-syn was shown to reduce SHSY-5Y cells total metabolic output at 48 h (section 4.1.6).

Cells were treated as in the previously study, with vehicle (serum-free media with 0.1%), MPP^+ (0.1 – 2.0 mM) alone or MPP^+ (0.1 – 2.0 mM) with α-syn (0.1 – 30.0 μM) for 48 h incubation. Cells treated with α-syn (0.1 – 30.0 μM) in combination with MPP^+ at 0.1 mM did not significantly change the level of cell death compared to MPP^+ alone (figure 4.19A). Whereas treatment with 1.0 mM MPP^+ in combination with either 10.0 or 30.0 μM α-syn significantly increased cell death compared MPP^+ alone, increasing cell death to 53.7 ± 7.3 % and 45.0 ± 9.8 % respectively (figure 4.19B). Surprisingly, 2.0 mM MPP^+ treated with α-syn (1.0 – 30.0 μM) did not significantly increase cell death compared to MPP^+ alone (figure 4.19C). However, 10.0 and 30.0 mM α-syn, in combination with 2 mM MPP^+, do increase cell death to show complete cell death (110.1 ± 22.3 and 103.8 ± 19.7 % respectively) though not significant when compared to MPP^+ alone (figure 4.19C).

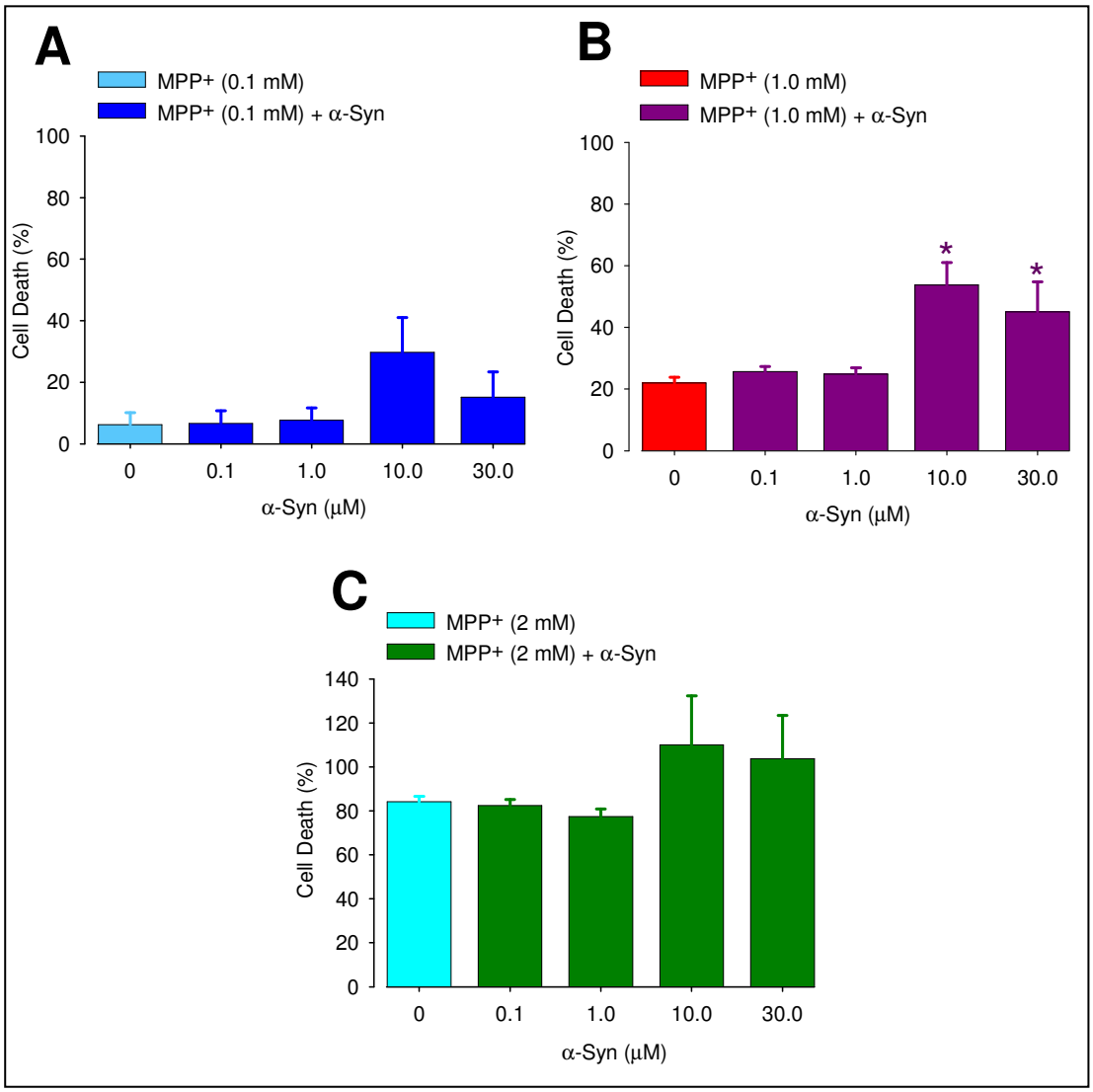

Figure 4.19: α-Syn exacerbates MPP^+-induced toxicity.

Cells were incubated for 48 h with vehicle (serum-free media with 0.1%), MPP^+ (0.1 – 2.0 mM) or MPP^+ (0.1 – 2.0 mM) with α-syn (0.1 – 30.0 μM). Cell death was presented as a percentage to the vehicle control (N = 3). **(A) 0.1 mM MPP^+:** the MPP^+ control induced 6.2 ± 3.9 % cell death at 48 h. MPP^+ co-treated with α-syn (0.1 – 30.0 μM) did not level of cell death. **(B) 1.0 mM MPP^+:** the MPP^+ control induced 22.0 ± 1.8 % cell death at 48 h. MPP^+ treated in combination with α-syn at either 0.1 or 1.0 μM did not induce a change in cell death. Whereas α-syn at either 10.0 or 30.0 μM with MPP^+ significantly increased cell death compared to MPP^+ alone. **(C) 2.0 mM MPP^+:** the MPP^+ control induced 84.2 ± 2.4 % cell death at 48 h, which was not changed with co-treatment of α-syn (0.1 – 30.0 μM) though an increase is implied with both 10.0 or 30.0 μM α-syn, though not significant. Significance was determined by one-way ANOVA with Student-Newman-Keuls post-hoc test where * $P < 0.05$ verses MPP^+ (mM)

In agreement with the previous studies (section 4.3.3) these data previously indicate that α-syn exacerbates MPP^+-induced toxicity in a concentration-dependent manner. However, this exacerbation did not appear to be augmented by an increase in incubation time (figure 4.18 and 4.19).

4.3.5 Potentiation of MPP^+-induced cell death by CsA.

As described previously (chapter 1.3), MPP^+ is a mitochondrial complex I inhibitor which induces mitochondrial dysfunction. Through our previous studies, 2.0 mM MPP^+ has been shown to induce ~ 50 % cell death of SHSY-5Y cells after 24 h (section 4.3.2 and 4.3.3). To examine whether inhibition of the mitochondrial pore reduces the toxicity of MPP^+ (an inhibitor of the electron transport chain), the effects of CsA on MPP^+-induced toxicity was characterised.

As previously, cells were treated with vehicle (serum-free media with 0.1 % DMSO and 0.1 % water), MPP^+ (2.0 mM) alone or with MPP^+ (2.0 mM) in combination with CsA (0.1 – 10.0 μM) and incubated for 6, 12, 24 or 48 h. At short incubation times (6 and 12 h) CsA at 0.1 and 1.0 μM in combination with 2 mM MPP^+ did not alter cell death compared to MPP^+ alone. On increasing the incubation time to 24 and 48 h, CsA, at all concentrations (0.1 – 10.0 μM), significantly increased 2.0 mM MPP^+-induced cell death (figure 4.20). CsA at 0.1 μM with MPP^+ (2.0 mM) increased cell death to 26.0 ± 1.7 % at 24 h which was further increased to induce complete cell death at 48 h incubation (101.8 ± 8.3 %) (figure 4.20). This increase in cell death was amplified by CsA at 1.0 μM with MPP^+ (2.0 mM) at 24 and 48 h (58.0 ± 4.9 and 143.1 ± 11.8 % respectively). CsA at 10.0 μM in combination with 2 mM

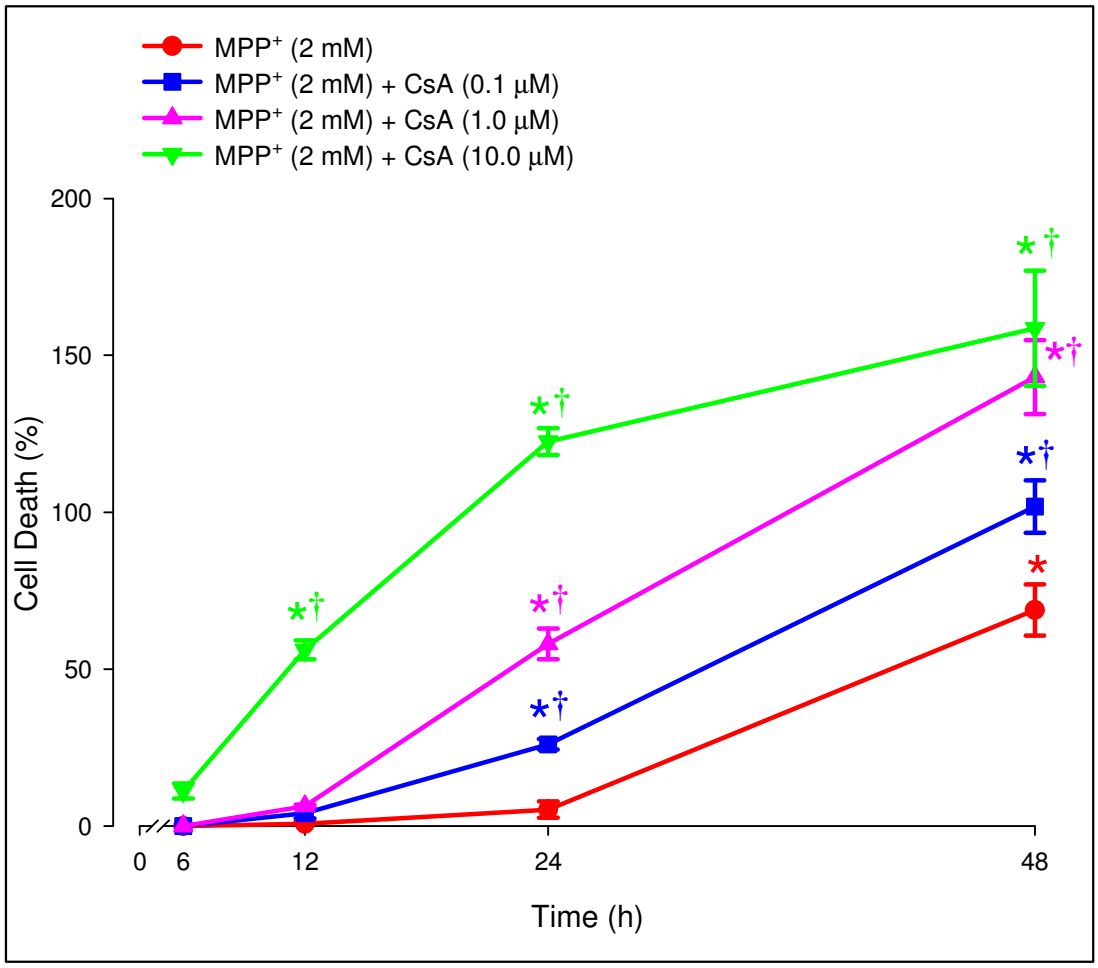

Figure 4.20: Temporal profile of CsA effect on MPP^+-induced toxicity.

SHSY-5Y were treated with vehicle (serum-free media with 0.1 % DMSO and 0.1 % water), MPP^+ (2.0 mM) alone or with MPP^+ (2.0 mM) with CsA (0.1-10.0 µM) and incubated for 6, 12, 24 or 48 h. Cell death was show as a percentage to vehicle control (N = 3). MPP^+ (2.0 mM) significantly increased cell death at 48 h compared to all earlier incubation times. Co-treatment with CsA (0.1 µM) did not increase cell death at 6 and 12 h, but significantly increased cell death at 24 and 48 h compared to MPP^+ alone at relevant time points. The trend in cell death was followed with MPP^+ (2.0 mM) treated with 1.0 µM CsA, where significant increased cell death was seen at 24 and 48 h compared MPP^+ alone and MPP^+ (2.0 mM) with CsA (0.1 µM) at relevant time points. CsA (10.0 µM) significantly increased cell death at 12 compared to all other treatment and induced total cell death at 24 h. Significance was determined by two-way ANOVA with Student-Newman-Keuls post-hoc test where * $P < 0.05$ verse earlier time points, † $P < 0.05$ verse MPP^+ (2.0 mM).

MPP^+ significantly increased cell death after 12 h, inducing total cell death by 24 h (figure 4.20). However, CsA at 10.0 μM increased cell death as expected (previously shown in section 4.2.3).

CsA (0.1 – 10.0 μM) treated in combination with MPP^+ (2.0 mM) significantly increased cell death in a concentration- and time-dependent manner. These results show the addition of mitochondrial pore inhibitor is not protective against MPP^+-induced mitochondrial dysfunction, augmenting cell death.

4.3.6 α-Syn effect on CsA enhanced MPP^+-induced toxicity.

In the previous study CsA was shown to potentiate MPP^+-induced cell death (figure 4.20). CsA enhancement of MPP^+-induced cell death could possibly be via increasing oxidative stress and ROS levels within the mitochondria resulting in an increased rate of mitochondrial dysfunction and cell death (Fall and Bennett., 1998). α-Syn- (30.0 μM) induced increase in cytosolic Ca^{2+} was shown not to be blocked by CsA (figure 4.14). With this in mind our data would suggest that α-syn affects mitochondria via another mechanism other than the mitochondrial pore (section 4.2), potentially by the formation of an α-syn protofibril pore, in the mitochondra membrane. This is supported by our data that shows α-syn caused a reduction in mitochondrial membrane potential (section 4.2.7). Therefore we speculate that the CsA effect of increasing MPP^+-induced cell death may be reduced by the addition of α-syn, possibly through α-syn ablity to form an altenerative pore to the mitochondrial pore which is blocked by the CsA.

To examine this hypothesis cells were treated with vehicle (serum-free with 0.1 % DMSO and 0.1 % water), MPP^+ (2.0 mM) alone, MPP^+ (2.0 mM) with α-syn (30.0 μM), MPP^+ (2.0 mM) with CsA (0.1 – 10.0 μM), or MPP^+ (2.0 mM) with α-syn (30.0 μM) and CsA (0.1 – 10.0 μM) and incubated for 24 h. Cells treated with CsA (0.1 μM) and MPP^+ (2.0 mM) did not alter cell death compared to MPP^+ (2.0 mM alone) (figure 4.21 A). Whereas co-treating with α-syn (30.0 μM), MPP^+ (2.0 mM) and CsA at 0.1 μM significantly increased cell death compared to MPP^+ alone increasing cell death to 81.7 ± 6.5 % (figure 4.21 A). Increasing CsA to 1.0 μM in combination with either MPP^+ (2.0 mM) alone or MPP^+ (2.0 mM) with α-syn (30.0 μM) significantly increased cell death to 90.0 ± 7.9 and 104.6 ± 9.3 % respectively compared MPP^+ alone (figure 4.21 B). Interestingly, CsA at 1.0 μM in combination with α-syn and MPP^+ also resulted in an increase in cell death compared to α-syn and MPP^+, although not significantly ($P = 0.077$) (figure 4.21 B). As previously shown (section 4.3.5) increasing CsA to 10.0 μM induced total cell death when (with MPP^+ increased cell death to 101.2 ± 7.8 % and in combination with MPP^+ and α-syn increased cell death to 96.5 ± 4.1 % respectively) (figure 4.21 C). CsA (10.0 μM) was previously shown to be inherently toxic (figure 4.11).

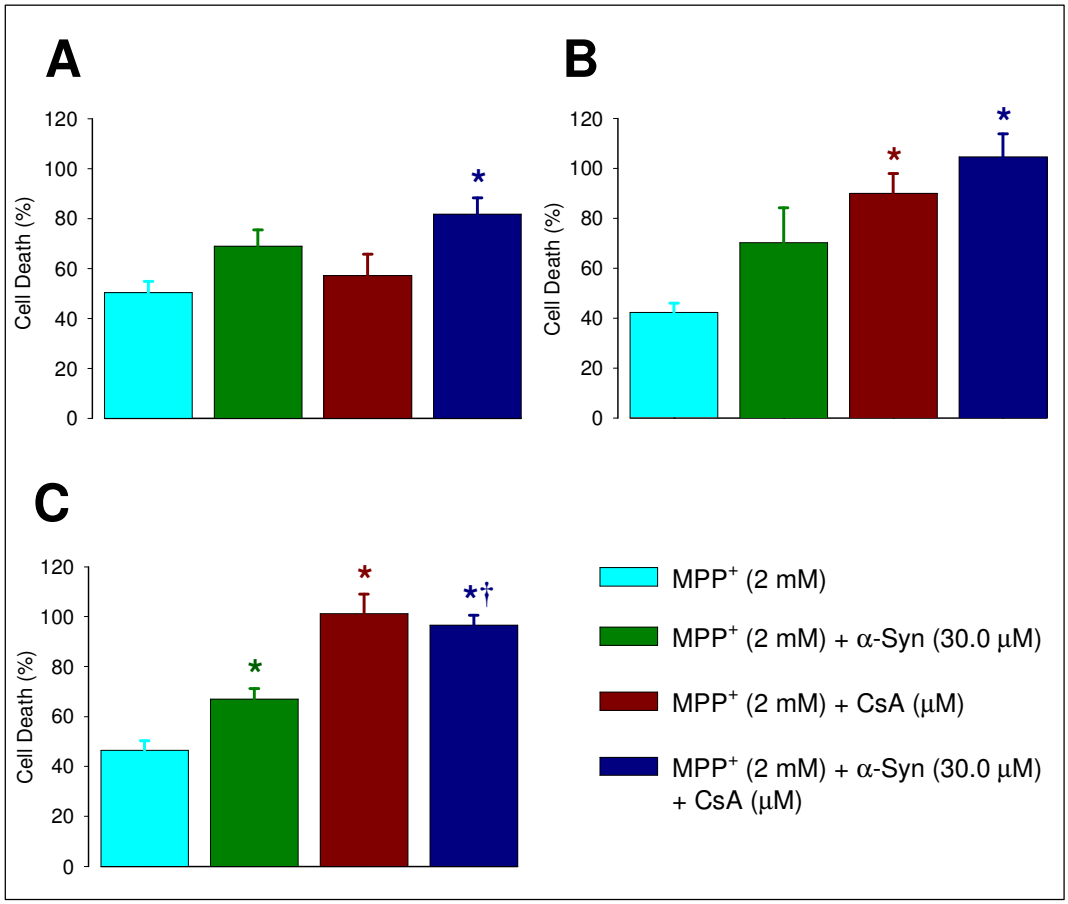

Figure 4.21: CsA enhances MPP^+ and MPP^+-α-syn induced toxicity in a concentration-dependent manner.

Cells were incubated for 24 h with vehicle (serum-free with 0.1 % DMSO and 0.1 % water), MPP^+ (2 mM), MPP^+ (2 mM) with α-syn (30 µM), MPP^+ (2 mM) with CsA (0.1 - 10.0 µM), or MPP^+ (2 mM) with α-syn (30 µM) and CsA (0.1 or 1.0 µM). Cell death is present as a percentage to the vehicle (N = 3). **(A) 0.1 µM CsA:** MPP^+ induced ~ 50 % cell death. Co-treatment with α-syn (30 µM) increased cell death to ~ 68 % without significance. MPP^+ (2 mM) induced cell death did not increase when co-treated with CsA (0.1 µM). MPP^+ with α-syn and CsA significantly increased cell death compared to MPP^+ alone. **(B) 1.0 µM CsA:** MPP^+ induced 42 % cell death. Co-treating MPP^+ (2 mM) with α-syn (30 µM) increased cell death induced by MPP^+ (2 mM) to ~70 %, though no significance determined. MPP^+ (2 mM) and CsA (1.0 µM) significantly increased MPP^+-induced cell death compared to MPP^+ alone. MPP^+ (2 mM) with α-syn (30 µM) and CsA (1.0 µM) increased cell death compared to MPP^+ (2 mM) and α-syn (30 µM) though not significant ($P = 0.077$) and significantly compared to MPP^+ (2 mM). **(C) 10.0 µM CsA:** MPP^+ induced 46 % cell death consistent with graphs A and B. MPP^+ (2 mM) with α-syn (30 µM) significantly increased cell death compared to MPP^+ (2 mM). CsA (10.0 µM) treated with either MPP^+ or MPP^+ with α-syn (30 µM) significantly increased cell death compared to MPP^+ (2 mM) and MPP^+ (2 mM) with α-syn (30 µM) inducing complete cell death. CsA at 1.0 and 10.0 µM significantly increases MPP^+ and MPP^+-α-syn induced toxicity. Significance was determined by one-way ANOVA with Student-Newman-Keuls post-hoc test where * $P < 0.05$ verse MPP^+ (2 mM) and † $P < 0.05$ verse MPP^+ (2 mM) with α-syn (30 µM).

From these data the addition of α-syn (30.0 μM) increases CsA and MPP^+-induced cell death compared to MPP^+ alone. This shows that α-syn induced effects are not protective within in a PD *in vitro* model, but detrimental increasing cell death after 24 h incubation.

4.3.7 Increased incubation with α-syn effects CsA enhanced MPP^+-induced toxicity.

Our previous study (section 4.3.6) identified that the addition of α-syn (30 μM) in combination with CsA and MPP^+ and incubated for 24 h, increased cell death. However, our previous data (described in sections and 4.1 4.2) identified that α-syn's primary effects were more pronounced after 48 h incubation. This study examined the effect with the incubation time extended to 48 h.

Cells were treated as in the previous study with the exception of using 10 μM CsA, as 10 μM CsA has been previously identified to induce total cell death after 48 h incubation (section 4.2.3) and the incubation time was extended to 48 h.

MPP^+ (2 mM) incubated for 48 h increased cell death to between 85 - 89 % compared to MPP^+ cell death at 24 h (42 – 50 %). MPP^+-induced cell death is comparable to MPP^+ (2 mM) induced cell death at 48 h, as shown previously in figure 4.18 and 4.20 C. Previously, it was determined that the co-treatment of α-syn (30 μM) potientated MPP^+ (2 mM) induced cell death increasing cell death to 101.0 ± 10.4% and 93.7 ± 6.4 % (figure 4.22 A and B). Cells which were co-treated with MPP^+ and CsA (0.1 μM) saw no change in the level of MPP^+-induced cell death of

91.2 ± 4.0 % (figure 4.22 A). As with the 24 h incubation, CsA (0.1 µM) with MPP^+ (2 mM) and α-syn (30 µM) at 48 h increased cell death compared to 2 mM MPP^+ (108.2 ± 9.1 %) though not significantly (figure 4.22 A). Increasing the CsA concentration to 1.0 µM increased MPP^+ (2 mM) cell death to 106.1 ± 8.7 %, though this was not significant compared to 2 mM MPP^+ (figure 4.22 B). CsA (1.0 µM) with MPP^+ (2 mM) and α-syn (30 µM) induced total cell death increasing cell death to 108.2 ± 5.7 % compared to 2 mM MPP^+, though no significance (figure 4.22 B). CsA (1.0 µM) potentiation of MPP^+ cell death is consistent with figure 4.21, where CsA (1.0 µM) was shown to significantly increase MPP^+ cell death at 24 and 48 h. Furthermore, in figure 4.21B CsA (1.0 µM) was shown to significantly increase MPP^+ and α-syn (30 µM) after 24 incubation. CsA shows no protection against MPP^+ or MPP^+ (2 mM) and α-syn (30 µM) induced toxicity.

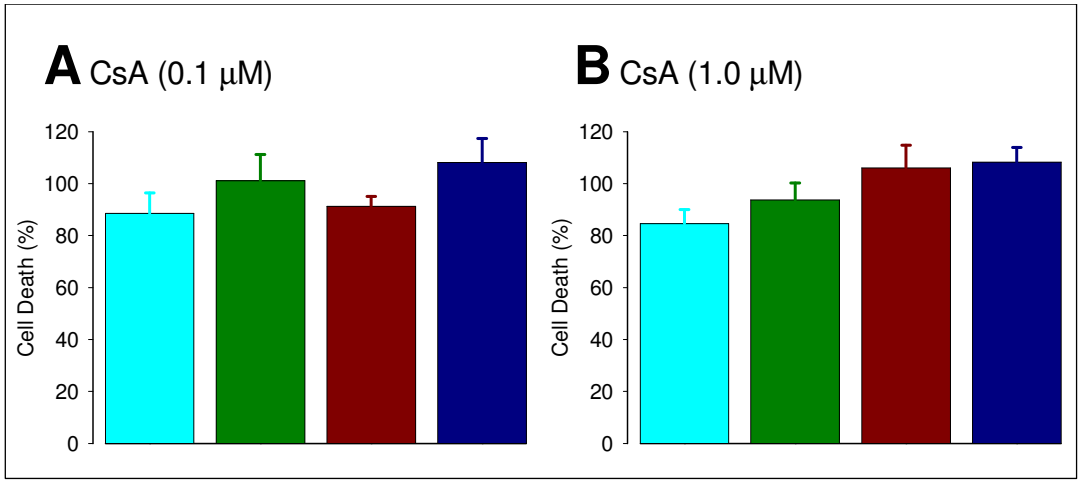

Figure 4.22: CsA increases MPP^+-induced toxicity in a concentration-dependent manner.

Cells were treated with vehicle (serum-free with 0.1 % DMSO and 0.1 % water), 2 mM MPP^+ (light blue bars), 2 mM MPP^+ with 30 µM α-syn (dark green bars), 2 mM MPP^+ with 0.1 or 1.0 µM CsA (dark red bars), or 2 mM MPP^+ with 30 µM α-syn or 0.1, 1.0 µM CsA (dark blue bars) for 48 h. N = 3 for all treatment and cell death is presented as a percentage of the vehicle. **(A) 0.1 µM CsA:** MPP^+-induced ~ 89 % cell death. MPP^+ with CsA (0.1 µM) did not increase or decrease cell death. MPP^+ (2 mM) co-treated with α-syn (30 µM) or α-syn (30 µM) with CsA (0.1 µM) increase cell death inducing total cell death, though not significant. **(B) 1.0 µM CsA:** MPP^+ induced ~ 85 % cell death. Co-treatment with α-syn indicates an increased cell death, without significance. MPP^+ with CsA (1.0 µM) increased cell death compared to MPP^+ and compared to MPP^+ with α-syn though no significance. MPP^+ (2 mM) with α-syn (30 µM) and CsA (1.0 µM) increased % of cell death higher compared other treatments, inducing complete cell death. Though no significance was determined, the results imply CsA increases MPP^+ and MPP^+ with α-syn induced toxicity in a concentration dependent manner.

4.3.8 α-Syn induced increase in cytosolic Ca^{2+} is independent of MPP^+.

From our previous studies, we have shown that α-syn decreases SHSY-5Y cells total metabolic out, possibly by disrupting the mitochondrial membrane potential resulting in an increase in cytosolic Ca^{2+} (section 4.2). Though α-syn does not induce cell death (figure 4.8), when applied to our MPP^+ *in vitro* PD model, α-syn augments MPP^+-induced cell death. At this point it is important to remember that MPP^+, a mitochondrial complex I inhibitor, induces cell death by causing mitochondrial dysfunction by inhibiting the production of ATP and increasing oxidative stress and ROS within cells. The previous studies have identified that α-syn induced mitochondrial dysfunction is independent of the mitochondrial pore (section 4.2) and speculate that α-syn induced mitochondrial dysfunction is also via a different mechanism than that induced by MPP^+. To examine this hypothesis, the FLIPR Plus Ca^{2+} assay (section 4.2.5) was utilised to monitor the effect of MPP^+ with and without α-syn on cytosolic Ca^{2+} levels. An increase of cytosolic Ca^{2+} levels by MPP^+ alone would be an indication that MPP^+ and α-syn may induce mitochondrial dysfunction by similar mechanisms.

For this experiment, cells were treated with vehicle (serum-free with 0.1 % DMSO and 0.1 % water), MPP^+ (2.0 mM), MPP^+ (2.0 mM) with α-syn (30.0 μM), MPP^+ (2.0 mM) with CsA (0.1 μM), or MPP^+ (2.0 mM) with α-syn (30.0 μM) and CsA (0.1 μM). Fluorescence was measured at 527 nm after 24 h incubation of treatments with an increase in fluorescence indicating an increase in cytosolic Ca^{2+}. Cells treated with either MPP^+ (2.0 mM) alone or MPP^+ (2.0 mM) with CsA (0.1 μM) had no significant on fluorescence ($1.8 \pm 0.04 \times 10^4$ and $1.9 \pm 0.05 \times 10^4$ A.U.

respectively) compared to the vehicle control (figure 4.23). Whereas cells treated with either α-syn (30.0 μM) with MPP^+ (2.0 mM) or CsA (0.1 μM) with MPP^+ (2.0 mM) and α-syn (30.0 μM) fluorescence was significantly increased ($2.1 \pm 0.08 \times 10^4$ and $2.0 \pm 0.06 \times 10^4$ A.U.) compared to MPP^+ (2.0 mM) alone (figure 4.23).

From these data, MPP^+ alone or in combination with CsA had no significant effect on cytosolic Ca^{2+} levels, whereas, the addition of α-syn significantly increased cytosolic Ca^{2+} which were not reduced by CsA, mitochondrial pore inhibitor. This shows α-syn and MPP^+-induced mitochondrial dysfunction are through different mechanisms, which are both independent of the mitochondrial pore, with α-syn induced effects further exacerbating MPP^+-induced toxicity.

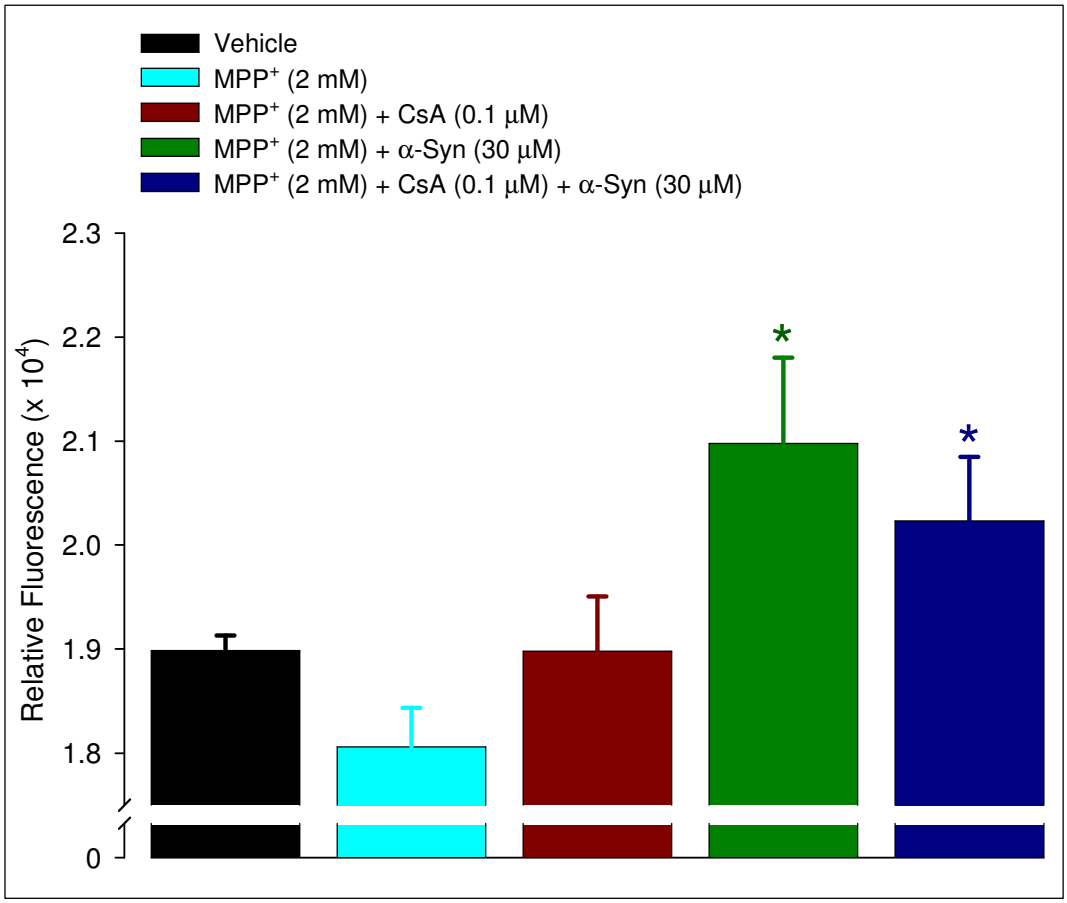

Figure 4.23: α-Syn increased cytosolic Ca^{2+} is independent of MPP^+.

Cells were treated for 24 h with vehicle (serum-free with 0.1 % DMSO and 0.1 % water), MPP^+ (2 mM), MPP^+ (2 mM) with α-syn (30 µM), MPP^+ (2 mM) with CsA (0.1 µM), or MPP^+ (2 mM) with α-syn (30 µM) and CsA (0.1 µM). For all treatments, fluorescence at 527 nm was taken at 24 h (N = 6). Increase in fluorescence shows an increase in cytosolic Ca^{2+}. Vehicle fluorescence averaged 1.9 ± 0.01 x 10^4 A.U. MPP^+ (2 mM) decreased fluorescence to 1.8 ± 0.04 x 10^4 A.U. compared to vehicle but not significantly. MPP^+ with CsA (0.1 µM) increased MPP^+ fluorescence to similar level to vehicle, though not significantly. α-Syn (30 µM) treated with MPP^+ (2 mM) significantly increased fluorescence compared to MPP^+ (2 mM), though significance was not tested MPP^+ (2 mM) with α-syn (30 µM) increased fluorescence compared vehicle with P = 0.041. MPP^+ (2 mM) with CsA (0.1 µM) and α-syn (30 µM) increased fluorescence compared to vehicle and MPP^+ (2 mM) with CsA (0.1 µM), significantly increasing fluorescence compared to MPP^+ (2 mM). MPP^+ (2 mM) does not increase cytosolic Ca^{2+} levels, co-treating with α-syn (30 µM) significantly increased cytosolic Ca^{2+} which was not blocked by CsA (0.1 µM). Significance was determined by one-way ANOVA with Student-Newman-Keuls post-hoc test where * P < 0.05 verses MPP^+ (2 mM).

4.3.9 Summary of Section 4.3

The study reported in this chapter has described our success at establishing an *in vitro* PD model utilising the mitochondrial complex I inhibitor MPP^+. This MPP^+ *in vitro* PD model allowed us to investigate the effects of α-syn on mitochondrial dysfunction in human neuroblastoma cells (SHSY-5Y) and to elucidate the potential role of α-syn in PD disease progression.

Using our MPP^+ PD model we show that the addition of α-syn alone does not cause cell death through mitochondrial dysfunction (also seen previously in section 4.1) but when added with MPP^+, enhanced the MPP^+-induced toxicity in a concentration-dependent manner. The addition of MPP^+ alone causes the mitochondrial pores to open. To investigate whether the closing of the mitochondrial pores in the presence of MPP^+ would offer protection from mitochondrial dysfunction we added the mitochondrial pore inhibitor CsA along with MPP^+. Surprisingly, the inhibition of the mitochondrial pores by CsA did not reduce the level of MPP^+-induced cell death, but in fact increased it in a concentration-dependent manner. Our previous experiments have shown that it may be possible that α-syn forms protofibril pores in the mitochondrial membrane independent of the mitochondrial pores (section 4.2). Therefore, it may be assumed that the addition of α-syn could replace the pores inhibited by CsA and therefore reduce the level of cell death to similar levels seen in the presence of MPP^+ alone. However, the addition of α-syn in the presence of both CsA and MPP^+ led to a further increase in cell death. This result would suggest that MPP^+, CsA and α-syn all induce mitochondrial dysfunction by separate pathways.

To confirm that the mechanism of mitochondrial dysfunction by α-syn is independent of MPP^+ we investigated the concentration of cytosolic Ca^{2+} with the addition of CsA, both in the presence and absence of α-syn, in our MPP^+ model. Our results show that MPP^+ alone did not affect the concentration of cytosolic Ca^{2+}. The addition of α-syn, however, saw a significant increase in cytosolic Ca^{2+}, an effect not inhibited by the addition of CsA. This result seems to confirm our belief that the mechanism of mitochondrial dysfunction by α-syn is different to that of MPP^+. Furthermore, we have identified that α-syn does not have any protective effects against mitochondrial dysfunction, counter to the suggestions of other reports (Hashimoto *et al.,* 2002; Manning-Bog *et al.,* 2003; Lee *et al.,* 2006; Quilty *et al.,* 2006).

Chapter 5: Discussion and conclusion.

The identification of α-syn as a major component of LBs, LNs and the identification of PD-associated mutations within the *α-syn* gene (discussed in section 1.2.1.1 and 1.2.4), has led to the implication of the involvement of α-syn in the progression of PD and other neurodegenerative disorders. There are two differing theories on the role of α-syn in PD that α-syn may be directly involved in the cellular degradation process, or may merely be epiphenomenal with no role in disease progression (Manning-Boğ *et al.,* 2003; Klivenyi *et al.,* 2005; Quilty *et al.,* 2006; Zhou *et al.,* 2006).

PD is a progressive neurological disorder affecting 1 in 500 people (www.parkinsons.org.uk). While the majority of patients present with idiopathic PD, 5 – 10 % of PD patients have a family history of a neurodegenerative disorder (Cordato and Chan, 2004; Gandhi and Wood, 2005). Regardless of idopathic or familial, there is a progressive loss of dopaminergic neurones, accumulation of LBs and LNs in the brain (especially in the SN, LC and hypothalamus), with symptoms developing after approximately 50 % of the dopaminergic neurones are lost (especially within the SN, hypothalamus, LC, cerebral cortex and olfactory bulb) (section 1.2.1and 1.2.1.1) (Lowe *et al.,* 1988; Cornford *et al.,* 1995; Spillantini *et al.,* 1997; Mezey *et al.,* 1998; Zhang *et al.,* 2000; Wood-Kaczmar *et al.,* 2006).

α-Syn protein is found primarily in the aggregated state in LB leading to the hypothesis that it is the aggregated form of α-syn that is involved in causing PD-associated toxicity (El-Agnaf *et al.,* 1998). However, a number of alternative theories

have since been suggested. The fibril formation of α-syn could potentially be protective by sequestering a potentially toxic intermediate (protofibril) form of α-syn (Conway *et al.,* 2000a). Integral to this theory is the concept that the protofibril form of α-syn is the pathogenic entity. Evidence for a toxic intermediate is suggested by studies correlating the aggregation rates of the mutant forms of α-syn with their toxicity. The A30P mutation form protofibrils quicker than WT α-syn (Narhi *et al.,* 1999; Greenbaum *et al.,* 2005), although full aggregation appears to be at the same rate (i.e. A30P promotes the formation of protofibrils). In contrast, A53T α-syn has been shown to result in a more rapid formation of full fibrils. Rapid aggregation removes α-syn from the cellular system, one concequence of which is to increase α-syn expression, inducing further aggregation and potentally the presence of protofibrils (Conway *et al.,* 1998). Triplication of the *α-syn* gene increases α-syn protein expression (Miller *et al.,* 2004) and has been linked to early-onset PD (Farrer *et al.,* 2004; Singleton *et al.,* 2004) as increased concentration of α-syn promotes aggregation, this further links the process of α-syn aggregation to PD progression (section 1.1.2.1 and 1.2.4) (Singleton *et al.,* 2003; Farrer *et al.,* 2004; Singleton *et al.,* 2004). α-Syn has the potential to self-aggregate, with the rate of aggregation rate potentiated by a number of environmental factors, such as heavy metals (Paik *et al.,* 1999), neurotoxins (the MPTP metabolite MPP^+) (Kalivendi *et al.,* 2004), as well as cellular components such as cyt c (Hashimoto *et al.,*1999) and DA (Cappai *et al.,* 2005). This has led to the hypothesis that the aggregated or protofibril forms of α-syn are the toxic forms of α-syn suggesting that the aggregation process of α-syn is an important component in the progression of PD, rather than the soluble form of α-syn (Ding *et al.,* 2002; Lashuel *et al.,* 2002; Volles *et al.,* 2002; Tsigelny *et al.,* 2007). In

contrast, soluble α-syn has also been implicated as being toxic and inducing cell death through the use of inducable over-expression of α-syn in cell cultures (Iwata *et al.,* 2001; Oluwatosin-Chigbu *et al.,* 2003). Although toxicity of soluble α-syn has been suggested other reports show it to be protective. One potential protective mechanism may be the reduction of oxidative stress and inactivation of apoptotic agents (JNK) by interaction with JIP-1b/IB1 (Hashimoto *et al.,* 2002). α-Syn has been shown to be up-regulated in response to increased oxidative stress, increasing cell survival (da Costa *et al.,* 2000; Quilty *et al* 2006). From this evidence it could be suggested that α-syn plays a protective role under normal conditions, but under pathological conditions (excessive oxidative stress or breakdown of cellular process such as UPS) α-syn becomes toxic. By investigating the physiological effects of α-syn in normal and PD-like conditions, we sought to elucidate α-syn role further.

5.1 Chapter 3 discussion.

The physiological effects of α-syn in a human neuroblastoma cell line were examined using exogenously applied α-syn. Exogenous application of α-syn has a number of advantages over an over-expressing system. For example, the duration of exposure of cells to α-syn protein is known and can be easily adapted. The aggregation state of α-syn protein can also be determined prior to application and concnentration also titrated. To establish such an approch a protocol to generate recombinant synuclein proteins had to be established. Within chapter three, initial experiments designed, established and validated a recombinant protein expression system for the generation of α-syn. The production of the recombinant α-syn protein was initially tested using the pRK172 vector. However within this system the

expression of the synuclein proteins (α-syn, A53T α-syn and β-syn) showed varying levels of expression, with both α-syn and A53T α-syn failing to generate suitable levels of recombinant protein (section 3.1). We showed that the *synuclein* genes were present within the plasmids and examined whether altering the media would induce expression. The growth media was changed from LB broth to peptone media to reduce the glucose source and increase the lag-phase of the growth cycle of BL21 (DE3) cells, promoting protein expression. This did not, however, induce expression for α-syn, but did cause a reduction in the total level of proteins within the expression cultures. However for A53T α-syn expression cultures, low level expression was observed and confirmed by western blot. These results suggest that the varying expression between the *synuclein* plasmids (specifically *α-syn* plasmid) was more likely to be due to a problem within the pRK172 vector that effecting the induction of the target gene prior to protein expression.

In an attempt to induce α-syn expression we transformed the original sample of *α-syn* plasmid (gifted from Prof. Buchman) directly into BL21 (DE3) expression cells. Upon induction of expression, α-syn protien generation was observed. This suggested that the amplification of the *α-syn* plasmid, by DH5α cells, inducing an alteration in the *α-syn* plasmid preventing the induction of α-syn expression.

However, analysis showed that continuous use of the BL21 cells transformed with the original *α-syn* plasmid, decreased expression over time (section 3.4, table 3.1). We showed that the decline in expression was due to the BL21 (DE3) cells rejecting the plasmids containing the *α-syn* gene, as there was a decrease in the intensity of the

amount of *α-syn* gene without a similar reduction in the band intensity for pRK172 vector (section 3.4.2). This result shows that the BL21 (DE3) cells were selecting the smaller empty plasmid over the *α-syn* containing plasmid.

An attempt to increase the *α-syn* plasmid in propagating cells resulted in increasing the pRK172 vector without *α-syn* gene (section 3.5.2). Therefore, we decided to remove the *α-syn* gene from the pRK172 vector and re-insert it into a commercial vector (pET-22b(+) from Novagen). The commercial vector was selected over re-using the pRK172 vector as the pRK172 is a relatively unknown expression vector (originally derived from the pAR3038 expression vector (Mcleod *et al.,* 1987)). While the pRK172 vector is commonly used in synuclein expression systems (Goedert and Jakes, 1990; Jakes *et al.,* 1994; Giasson *et al.,* 1999), our problems imply that the pRK172 expression vector we are using may not be the same as the original pRK172 vector as the full sequence of pRK172 has not been published, we can not confirm the degree of alteration.

The pET-22b(+) commercial vector was selected to replace the pRK172 vector for a number of reasons (table 3.2), but principally because the vector is designed to reduce pre-induction expression leakage, and allows the option of tagging the target protein. As for many commercial vectors a full DNA and restriction site map is available (figure 3.14). The pET-22b(+) vector is designed to reduce toxicity induced by toxic proteins by reducing leaky expression (Novagen pET Ststem Manual (TB055, 11th Edition)). This was important as we suspected the inherent protein expression (not related to deliberate experimental induction of expression) caused

toxicity within *E.coli* cells. We subsequently showed this to be the case as the newly constructed *α-syn* plasmid showed a reduction in α-syn yield in overnight cultures inoculations compared to single colony inoculation (section 3.6.2).

Confirmation of the corruption of the pRK172 plasmid (possibly from the insertion and removal of gene inserts over time) was shown by our ligation studies. The restriction sites used to remove the *α-syn* gene from the plasmid did not cut effectively, though a number of methods were used to optimise the restriction digests (section 3.5), and prevented the ligation of the *α-syn* gene into the pET-22b(+) vector. This was resolved by using PCR with specifically designed primers that integrated new restriction sites into the terminals of the *α-syn* genes and amplified the *α-syn* gene removing the old restriction sites and any additional nucleotides around the *α-syn* gene when in the pRK172 vector. The *α-syn* gene was then successfully ligated into the pET-22b(+) vector. The new *α-syn* pET-22b(+) plasmid showed increased expression and α-syn protein yield compared the original *α-syn* pRK172 plasmid that was maintained with subsequent expression cultures.

There are a number of purification protocols in the literature that produce varying quantities of pure recombinant α-syn ranging from 1 mg/L (Choi *et al.,* 2002) to 80 mg/L (Huang *et al.,* 2005). Our purification protocols for β-syn, α-syn and A53T α-syn were established by adapting previously published methods (Goedert and Jakes, 1990; Jakes *et al.,* 1994; Giasson *et al.,* 1999). The expression cultures were induced for 4 – 5 h before harvesting the cells. The purification of the synuclein protein was divided into two main steps, extraction and anion exchange chromatography.

Synuclein protein was extracted by lysing the harvested cells (using a high salt lysis buffer) before heat treating. Synuclein proteins are heat resistant and are not denatured by the heat treatment and remain in the supernatant (Weinreb *et al.,* 1996; Kim *et al.,* 2000). The heat treatment was shown to significantly reduce the contaminants from the synuclein samples compared to whole cell lysate (section 3.2.2, figure 3.6). The supernatant containing synuclein was dialysed into equilibration buffer (0.02M Tris pH 8.2) and the synuclein protein was isolated via anion exchange chromatography. The subsequently isolated α-syn was shown to be of a purity that could be used within future *in vitro* experiments by way of SDS-PAGE (or NuPAGE) gel and mass spectrometry (through our collaboration with Dr D Short) analysis (figure 3.30).

This protocol was shown to be consistent and could be utilised for purification of all the synuclein proteins. The protocol was also scaled up to deal with increased protein yield produced by scaling up α-syn expression from 2 L cultures to 10 L cultures grown by fermentation (through our collaboration with Dr J. White within the Edinburgh Protein Interaction Centre).

Initially, purification protocols were established using recombinant β-syn protein. This was because the purification protocols were established at the same time as the issues with α-syn expression were being resolved. Initially a mono-Q anion exchange column was used for the fine purification. Although β-syn protein was primarily eluted into 2 fractions, a lot of β-syn was lost in contaminated fractions either side of those collected. By changing to a HiTrap Q HP column, a stronger anion exchange

column compared to mono-Q, and adding of a 20 % NaCl step prior to the gradient increase, we were able to elute the β-syn protein into fewer fractions with no contaminating bands (section 3.3.1 and 3.3.2). The HiTrap Q HP column and adapted protocol were used for the purification of α-syn and was scaled up (increasing column size and flow rate) at all stages to ensure maximum yield and purification of α-syn when α-syn expressions culture size was increased. With the plasmid reconstruction (using the pET-22b(+) expression vector) and the increase in culture volume we successfully increased our yield of purified recombinant α-syn from 2 mg/L to 10 mg/L.

The purification could have been done, as mentioned previously, by a number of different methods such as using a GST-tag to increase the efficiency of the purification procedure of the recombinant α-syn protein. However, the GST-tag reduces the α-syn expression level in comparison to other methods including our own, without significantly increasing the purity of the target protein (Choi *et al.,* 2002). Alternatively, we could have used the purification protocol described by Huang *et al.* (2005), which increased the yield of purified α-syn to 80 mg/L (Huang *et al.,* 2005). The difference between our purification protocols and that of Huang *et al.* (2005) was they used osmotic shock to extract the α-syn protein expressed within the cells, rather than high salt lysis buffer and heat treatment utilised within our own study. After the extraction of the target protein from the cells, α-syn protein was purified by chromatography using a Sepharose Q column and NaCl gradient, which is very similar to our own protocol. Extraction of the protein by osmotic shock uses low temperatures and a high sucrose concentration to release the target protein from

the cells. However, although the protocol of Huang *et al.* (2005) increased the yield of protein per culture run, this may simply be due to the use of an alternative expression vector (pET-3a expression vector), rather than their use of osmotic shock. It is unlikely that the increased expression levels seen in Huang *et al.* are due to the protocol as the only difference between the protocols is the lysis of the cells (as described above) therefore, it is more likely the increase in yeild is through their use of an alternative expression vector (pET-3a). We found that to reduce the toxicity induced by the *α-syn* gene and expression of the protein, using the pET-22b(+) vector minimised α-syn effects and led to a constant expression between cultures, ensuring a stable plasmid that could be used in a number of cell lines. Though our expression levels are lower compared to Huang, the expression and protein yield is comparable with the more conventional protocols used which generally produced 5 to 10 mg/L (Goedert and Jakes, 1990; Jakes *et al.,* 1994; Giasson *et al.,* 1999; Kloepper *et al.,* 2006). Through our collaboration with Dr J. White (within the EPIC) we successfully increased our initial yield from 2 mg/L to approximately 10 mg/L upon scaling up the process to 10 L fermentation.

5.2 Chapter 4 dissucsion.

5.2.1 Section 4.1.

Our studies reported in chapter four of this thesis details our investigation into the effects of α-syn on cellular mechanisms in an *in vitro* system. We utilised the MTS assay (measures the total metabolic output of cells) as a method of measuring cell viability validated by control experiments using STS, a bacterial toxin. These studies showed the expected concentration- and time-dependent cell death in SHSY-5Y cells

(see section 4.1.5) Previous resports have shown similar toxicity *in vitro* (Koh *et al.*, 1995; Boix *et al.*, 1997; Posmantur *et al.*, 1997; Ha *et al.*, 2004). We showed STS induced 50 % cell death at 1.0 μM after 5 h incubation and using this concentration, cell death was shown to increase with incubation time (section 4.1.5, figure 4.5 and 4.6) This was also consistent with the results obtained by other members of our research group and through the literature (Boix *et al.,* 1997; Ha *et al.,* 2004; Koh *et al.,* 1995; Posmantur *et al.,* 1997). This showed that consistent results can be generated using the MTS assay and SHSY-5Y cells.

Using the MTS assay, we showed that α-syn and A53T α-syn (0.1 – 10.0 μM), in soluble or aggregated form, had no significant effect on the total metabolic output of SHSY-5Y cells after 24 h incubation with either in-house or commercially produced recombinant α-syn protein. A small (non-significant) decrease in the MTS assay with 24 h incubation of either soluble or aggregated α-syn suggested that subjecting the cells to an increase insult could induce a more significant loss in total metabolic output.

Increasing the incubation duration to 48 h and widening the concentration range of soluble α-syn (0.01 – 30.0 μM), α-syn (10 and 30 μM) was shown to induce a significant decrease in the total metabolic output of SHSY-5Y cells. This showed that α-syn induced a concentration- and time-dependent effect in SHSY-5Y cells.

Increased aggregation has been shown to occur with increased concentration and length of incubation. A study by Chen *et al.,* (2007) has shown that aggregation of α-

syn occurs within 12 h of incubation of high concentrations of α-syn (69.2 μM upwards) at 37 ^{o}C with continuous agitation (Chen *et al.,* 2007). Full α-syn fibril formation occurs within 7 days of incubation at 37 ^{o}C (with or without agitation) as has been demonstrated in a number of studies (El-Agnaf *et al.,* 1998; Miake *et al.,* 2002; Zhang *et al.,* 2005). With this in mind, the observed reduction in metabolic output induced by α-syn (10.0 and 30.0 μM) after 48 h incubation could be suggested to be due to the generation of α-syn either fibrils or protofibrils within the cells. Our data argues that protofibrils are more likely responsible as soluble α-syn (10.0 μM) after 48 h incubation induced a decrease in metabolic output that was not reflected by aggregated α-syn (10.0 μM) after 24 h incubation. Although different incubations times were used, if the aggregated form was toxic, it would be anticipated that aggregated α-syn (10.0 μM) would induce a decrease in metabolic output with a shorter incubation (as the aggregation of soluble α-syn occurs relatively slowly, see above). However the lack of effect with aggregated α-syn could be due to a slower uptake into cells of aggregated α-syn (fibrils) compared to soluble α-syn. This not only has been shown not to be the case, but aggregated α-syn is taken up at a greater rate than soluble α-syn (Sung *et al.,* 2001; Fortin *et al*., 2005). By observing this metabolic effect only with soluble α-syn only after prolonged incubation and not with aggregated α-syn, our data would suggest that the intermediary form, the protofibrils, maybe the cause.

The observed decrease in metabolic output induced by α-syn should imply an increase in cell death. However, α-syn (0.1 – 30.0 μM) did not induce cell death at either 24 h or 48 h as determined by the LDH assay. This demonstrates that neither

soluble nor aggregated α-syn are inherently toxic. It also suggests that the decrease in total metabolic output, from the previous studies, are not due to cell death, but a reduction in metabolism (production of NAD(P)H) within cells and could be indicative of mitochondrial dysfunction.

There are a number of further reasons as to why the protofibril form of α-syn, rather than the soluble form, maybe responsible for the decrease in metabolism. The addition of an oligomer form of α-syn (protofibril) at a low concentration (0.125 and 0.25 μM) caused a reduction in the level of MTT activity (another marker of metabolism) after 3 h incubation (Chen *et al*., 2007). This effect is considerably more rapid than observed with soluble α-syn. Importantly the lower toxic concnetration suggests that the conversion of only a small amount of the soluble α-syn in our studies (10 – 30 μM) would be enough to observe a response. Secondly, the reduction of total metabolic output is concentration- and time-dependent, where increasing the concentration of α-syn results in a greater reduction in total metabolic output (see section 4.1). An effect linking the increased rate of aggregation with increased α-syn concentration. This hypothesis supported by the identification doubling α-syn expression (in family with a triplication of the *α-syn* gene) leads to an autosomal dominant form of PD (Singleton *et al*., 2003; Farrer *et al*., 2004; Miller *et al*., 2004). Miller *et al*. (2004) suggested that the doubling of expression promoted aggregation of all forms (including both fibrils and protofibrils) leading to a concentration dependent phenomenon, agreeing with the data reported in this thesis.

Our data is consistent with a number of studies which also show α-syn is not inherently toxic (da Costa *et al.,* 2000; Rathke-Hartlieb *et al.,* 2001; Quilty *et al* 2006). Many of the studies imply that toxicity of α-syn is dependent on the aggregation state of the protein through the use of 'aged' or aggregated α-syn on dopamaniergic cells line (e.g. SHSY-5Y or MES cells) and using the MTT and immunostaining to assess α-syn effects (El-Agnaf *et al*., 1998; Chen *et al.,* 2007). This is indicative with our own data with the varying effects between the soluble and aggregated α-syn. This was also observed in studies using α-syn over-expression, where there was no effect on cell viability, but was an increae in mitochondrial dysfunction that correlated with expression levels (as ascertaind using the MTT assay) (Kanda *et al*., 2000; Iwata *et al*., 2001) (see section 4.1). In conclusion, α-syn did reduce total metabolic output of SHSY-5Y cells (see section 4.1), without causing cells death in, and this physiological effect was most likely atiributable to the protofibril form.

5.2.2 Section 4.2.

From the results presented in chapter 4 of this thesis, we have suggested that α-syn effects mitochondrial function by causing the release of cyt c and Ca^{2+} from mitochondria leading to mitochondrial dysfunction in SHSY-5Y cells, which cannot be blocked by using a mitochondrial pore inhibitor (CsA). This would suggest that either α-syn affects the mitochondria by a mechanism other than the mitochondrial pore, or induces the release of Ca^{2+} from an alternative intracellular store. We showed that α-syn induced a loss in mitochondrial membrane potential, impling that the increase in cytosolic cyt c and Ca^{2+} is through α-syn-induced mitochondrial

membrane disruption. This disruption to the mitochondria could explain the reduction in metabolic output of the cells discussed in the previous section. Diruption of the mitochondrial membrane would lead to the dyfunction of the E.T.C and therfore a decrease in the NAD(P)H, which was shown through the reduction in total metabolic output of SHSY-5Y cells and is indication of mitochondrial dysfunction (section 4.1.6).

We showed that α-syn (30 μM) caused an increase in cytosolic cyt c after 6 h incubation which decreased after 48 h incubation. The α-syn induced cyt c increase was significantly reduced by co-treatment with the mitochondrial pore inhibitor CsA (10 μM). This implies that α-syn increase in cytosolic cyt c is linked to the mitochondrial pore. However, CsA significantly reduced cytosolic cyt c compared to the vehicle control independent of α-syn. The apparent mediated effect may simply be due to the presence of CsA.

Investigation into the effects of CsA on cell viability using the LDH assay showed a concentration- and time-dependent induction of cell death. This cells death was independent of the presence of α-syn (with CsA at 10 μM). Lower concentration of CsA (0.1 – 1.0 μM) did not increase cells death and could still be justifiably used as a mitochondrial pore inhibitor at these concentrations. The experiment confirmed that the effect of α-syn in the presence of CsA above was almost certainly due to the toxicity of the pore inhibition.

To futher investigate α-syn induced mitochondial disruption we switched from using the cyt c ELISA to use the FLIPR Plus Ca^{2+} assay. Like cyt c, Ca^{2+} can be regulated by the mitochondria either via mitochondrial pores or disruption mitochondrial membrane (Albert *et al.,* 1994; Gunter *et al.,* 2000; Smaili *et al.,* 2000; Smaili *et al.,* 2003). Although cytosolic Ca^{2+} is regulated by a large number of mechanisms (e.g. intracellular stores, NMDA receptors (Albert *et al.,* 1994; Rizzuto, 2001)), changes in levels could also be indicative of mitochondrial disruption. This means that cytosolic Ca^{2+} could be used to identify mitochondrial dysfunction. As the cyt c ELISA used cell lysate, it could not identify subtle changes within the concentration of cytosolic cyt c. The Ca^{2+} assay used a cytoplasmic dye (Molecular Devices Limited) used in live cells, allowing a more sensitive measure that could take readings overtime. By using the Ca^{2+} assay we showed that α-syn caused concentration- and time-dependent increase in cytosolic Ca^{2+}. α-Syn (30 μM) increase cytosolic Ca^{2+} after 6 h incubation. α-Syn (30 μM) significantly increased cytosolic Ca^{2+} at 12 and 24 h before decreasing after 48 h incubation. The decrease in cytosolic Ca^{2+} could be due to alternative Ca^{2+} stores sequestering the mitochondrial released Ca^{2+} or the Ca^{2+} could be being release from the cells. The decrease is similar to the decrease in cytosolic cyt c observed by ELISA after 48 h incubation with α-syn (30 μM). This would suggest that α-syn induces a similar release of cyt c and Ca^{2+} into the cytosol, and implies that they are released by the same mechanism.

As cyt c ELISA data was inconclusive on whether α-syn release of cyt c was through a mechanism which involved the mitochondrial pores, CsA was used in combination

with α-syn and the Ca^{2+} assay. As CsA had no effect on α-syn induced increase in cytosolic Ca^{2+}, the α-syn effect on cytosolic Ca^{2+} is independent of CsA-sensitive mitochondrial pores. This means that α-syn increase in cytosolic Ca^{2+} is either by an alternative mechanism involving the mitochondria or from an alternative Ca^{2+} store.

α-Syn has been shown in a number of studies to form protofibril pores and has been implicated as the possible toxic form of α-syn. The protofibrils have been suggested to have the ability to permeablise cellular membranes in a similar manner to some bacterial toxins or detergents, by forming large pores within the membranes and disrupting membrane potential (Tanaka *et al*., 2001; Ding *et al*., 2002; Orth *et al*., 2003; Furukawa *et al.,* 2006). The pores are thought to be non-selective and allow the passage of cations (Furukawa *et al.,* 2006; Tsigelny *et al.,* 2007). It is also interesting to note that a study has shown that cyt c attenuates α-syn aggregation and promotes α-syn protofibril formation (Hashimoto *et al.,*1999). This suggests a mechanism by which α-syn could increase cytosolic cyt c and Ca^{2+} as seen in this thesis and that the release of cyt c could further promote protofibril formation and perpetuate the α-syn effect.

To investigate if α-syn-induced release of cyt c and Ca^{2+} was due to mitochondria membrane dysfunction we established an assay to monitor the mitochondria membrane potential. Using this approach we showed that α-syn (30 μM) caused the loss of mitochondrial membrane potential over-time, with a significant decrease observed after 48 h incubation with α-syn. This correlates with the decrease in total metabolic output of SHSY-5Y cells seen previously (section 4.1.6).

From our observations we showed that soluble α-syn once taken up into the cells induces mitochondrial dysfunction causing a loss of membrane poteintal and an in flux of Ca^{2+} and cyt c in to the cytosol. We have also suggested that it is the formation of protofibrils, forming independent pores in the membrane of the mitochondria that is most likely responsible.

5.2.3 Section 4.3.

A number of *in vitro* PD studies have utilised the mitochondrial complex 1 inhibitor MPP^+ (see section 1.3) in human neuroblastoma (SHSY-5Y) cells as a model of PD. However, a lower concentration range of MPP^+ (μM concentrations rather an mM) was generally used in combination with over extend incubation times, such as 5 days (Gómez-Santos *et al*., 2002; Storch *et al*., 2000; Kalivendi *et al*., 2004), compared to our model which used a mM concentration with maximum incubation time of 48 h.

In our model the addition of α-syn, together with MPP^+, significantly enhanced MPP^+-induced cell death in a concentration dependent manner (section 4.3.3), were α-syn alone did no induce toxicity. When mitochondrial pores were inhibited by the addition of CsA we found no reduction to the level of MPP^+-induced cell death (section 4.3.5). In fact, the addition of CsA resulted in an increase in MPP^+-induced cell death in a concentration dependent manner (section 4.3.5). This result is somewhat surprising given that two previous studies have described the addition of the same concentration of CsA as being protective against MPP^+-induced apoptosis (Seaton *et al*., 1998; Chalmers-Redman *et al*., 1999). Fall and Bennett (1998) showed that 24 h incubation with 1 μM CsA and 5 mM MPP^+ (also in SHSY-5Y cells)

doubled the MPP^+ toxicity of the cells. This result may be misleading in that our study has shown the addition of 5 mM MPP^+ alone is enough to induce total cell death after 24 h irrespective of the presence of CsA (see section 4.3.1, figure 4.16).

We showed that CsA at low concentrations has no protective effect against MPP^+ toxicity. This would imply that MPP^+ toxicity is independent of mitochondrial pores, though the subsequent effects of MPP^+-induced toxicity may lead to an opening of the mitochondrial pores and loss of membrane potential (Wong *et al.*, 1999; Smeyne and Jackson-Lewis, 2005). It may be the case that the previous studies by Seaton *et al*. (1998) and Chalmers-Redman *et al*. (1999) observed a protective role for CsA because of the lower MPP^+ concentrations used. This would lead to a prolonged exposure to MPP^+ increasing the length of time needed to induce cell death. The higher concentrations of MPP^+ used in our study allowed us to see the ultimate effect in a shorter time-span.

To further investigate the role of α-syn in the progression of PD we included α-syn in our MPP^+ *in vitro* PD model. As we showed previously, the inhibition of the mitochondrial pores with CsA increased MPP^+-induced cell death. After addition of CsA which blocks the mitochondrial pore, we speculate the addition of α-syn would form an alternative pore to the inhibited mitochondrial pore. However, this was shown to not be the case (see section 4.3.6) in fact it appears to further increase the level of cell death observed, something which has never been reported before. Our results described above would suggest that MPP^+, CsA and α-syn all induce mitochondrial dysfunction by separate pathways (section 4.3.5 and 4.3.8).

To confirm that the effect of α-syn on mitochondrial dysfunction is by a mechanism difference to that of both MPP^+ (ETC complex I inhibition) and CsA (mitochondrial pore inhibition), we investigated the level of cytosolic Ca^{2+} in our MPP^+ *in vitro* PD model. We identified that MPP^+ alone did not affect the concentration of cytosolic Ca^{2+}, whereas the addition of α-syn with MPP^+ significantly increased the concentration of cytosolic Ca^{2+} (see section 4.3.8). This increase was not reduced by the addition of CsA. This result and α-syn effect on cytosolic Ca^{2+} alone (section 4.2.5) seems to confirm our belief that the mechanism of mitochondrial dysfunction by α-syn is different to that of MPP^+ (ETC complex I inhibition) and is independent of the mitochondrial pore. Furthermore, this implies that α-syn does not have any protective effects but instead increases mitochondrial dysfunction, a concequence that becomes toxic in pathologically compromised cells.

5.3 Conclusion.

In conclusion, we showed α-syn does not induce cell death, but has a detrimental effect on cells that would appear to be dependent on the formation of protofibrils. From our studies we show that α-syn causes an increase in cytosolic cyt c, Ca^{2+}, disruption of the mitochondrial membrane and a reduction in total metabolic output in SHSY-5Y cells. This suggests that α-syn causes time- and concentration-dependent mitochondrial dysfunction. We showed that α-syn-induced mitochondrial dysfunction was independent of mitochondrial pores, and have speculated that it could be via the formation of α-syn protofibrils. As we have shown α-syn does not induce cells death this would suggest the SHSY-5Y cells are able to compensate for the detrimental effects of α-syn or that these effects are part of the physiological role

of endogenous α-syn. However, when α-syn was exogenously added to our MPP^+ PD model, it increased cell death. This shows that the MPP^+ stressed cells can not compensate for mitochondrial dysfuction caused by α-syn. Therefore we have shown a possible mechanism by which the potentially physiological role of α-syn may be involved in the pathology of PD.

This would suggest that that accumulation of soluble α-syn in cells plays an important role in the progression of neurodegenerative disorders like PD, though is not the initial factor. As we have shown under normal cellular conditions α-syn does induce abnormal effects at low concentrations (less 10 μM) (section 4.1). However the accumulation of α-syn induces mitochondrial dysfunction (possibly through the formation of protofibril pore) which is exacerbated by cellular stresses leading to cell death (section 4.2 and 4.3). In neurodegenerative disorders (such as PD) dopaminergic neurones, especially in the SN, are exposed to increased oxidative stress and ROS generation due to the synthesis of DA (Wersinger and Sidhu, 2003b). This may make the neurones more susceptible to the effects of accumulation of α-syn. α-Syn could accumulate due to; build of protein overtime, disruption in the UPS and degradation pathways or increased expression and up-regulation due to increase oxidative stress (da Costa *et al.,* 2000; Quilty *et al* 2006). The accumulation of α-syn would promote α-syn-induced mitochondrial dysfunction, possibly through protofibril pore formation, which in combination with the additional cellular stresses in dopaminergic neurones leads cell death and disease progression.

5.4 Future work.

Interestingly, β-syn and γ-syn have been shown to inhibit the formation of α-syn protofibrils (Park and Lansbury Jr., 2003; Uversky *et al.,* 2002; Tsigelny *et al.,* 2007), therefore it would be interesting to establish whether β-syn or γ-syn are able to prevent the effects of α-syn observed in SHSY-5Y cells. This would be best achieved by using our MPP^+ PD model. In doing so we would also be able to investigate whether β-syn and γ-syn would be able to prevent the increase in cytosolic Ca^{2+} or the loss of mitochondrial membrane potential, indicating if either β-syn or γ-syn are natural inhibitors of protofibril formation. It would also be advantageous to establish whether similar effects of α-syn were observed in primary culture and not a neuroblastoma cell line.

In order to elucidate the mechanism of α-syn induced loss of mitochondrial membrane potential, further investigations into α-syn interactions with mitochondrial proteins would be advisable. This may be facilitated through the tagging of the α-syn protein in a manner to allow the visualisation and localisation of the protein within the cell. Further to this the tagged α-syn and bound ligand may be isolated and analysed by way of mass spectrometry. Such experiments may be able to identify potential protein ligands for α-syn and therefore allow us to develop therapeutic strategies for the prevention of α-syn protofibril pore formation thus reducing mitochondrial dysfunction.

References.

Albert B, Bray D, Lewis J, Raff M, Roberts K, Watson JD. (1994) Molecular Biology of the Cell 3rd Edition. *Gardland Publishing Inc. New York.*

Abou-Sleiman PM, Healy DG, Wood NW. (2004) Causes of Parkinson's disease: genetics of DJ-1. *Cell Tiss. Res.* **318:** 185 – 188.

Alim MA, Ma Q-L, Takeda K, Aizawa T, Matsubara M, Nakamura M, Asada A, Saito T, Kaji H, Yoshii M, Hisanaga S, Ueda K. (2004) Demonstration of a role for α-synuclein as a functional microtubule-associated protein. *J. Alzheimers Dis.* **6:** 435 – 442.

Alvarez V, Guisasola LM, Moreira VG, Lahoz CH, Coto E. (2001) Early-onset Parkinson's disease associated with a new parkin mutation in a Spanish family. *Neurosci. Lett.* **313:** 108 – 110.

Arawaka S, Saito Y, Murayama S, Mori H. (1998) Lewy body in neurodegeneration with brain iron accumulation type 1 is immunoreactive for alpha-synuclein. *Neurol.* **51:** 887 – 889.

Baptista MJ, O'Farrel C, Daya S, Ahmad R, Miller DW, Hardy J, Farrer M, Cookson MR. (2003) Co-ordinate by α-synuclein in human neuroblastoma cell lines. *J. Nurochem.* **85:** 957 – 968.

Bisaglia M, Trolio A, Bellanda M, Bergantino E, Bubacco L, Mammi S. (2006) Structure and topology of the non-amyloid-β component fragment of human a-synuclein bound to micelles: implications for the aggregation process. *Protein Sci.* **15:** 1408 – 1416.

Bittar RG. (2006) Neuromodulation for movement disorders. *J. Clini. Neurosci.* **13:** 315 – 318.

Blandini F, Nappi G, Tassorelli C, Martignoni E. (2000) Functional changes of the basal ganglia circuitry in Parkinson's disease. *Prog. Neurobiol.* **62:** 63 – 88.

Boix J, Llecha N, Yuste VJ, Comella JX. (1997) Characterization of the cell death process induced by staurosporine in human neuroblastoma cell lines. *Neuropharmacol*. 36: 811 – 821.

Bozzi Y, Borrelli E. (2006) Dopamine in neurotoxicity and neuroprotection: What do D2 receptors have to do with it? *Trends. Neurosci.* **29:** 167 – 174.

Braak H, de Vos RA, Bohl J, Del Tredici K. (2006) Gastric alpha-synuclein immunoreactive inclusions in Meissner's and Auerbach's plexuses in cases staged for Parkinson's disease-related brain pathology. *Neurosci Lett.* **396:** 67 – 72.

Braak H, Del Tredici K. (2004) Poor and protracted myelination as a contributory factor to neurodegenerative disorders. *Neurobiol. Aging.* **25:**19 – 23.

Braak H, Del Tredici K, Rub U, de Vos RA, Jansen Steur EN, Braak E. (2003) Staging of brain pathology related to sporadic Parkinson's disease. *Neurobiol Aging.* **24:**197 – 211.

Braak H, Ghebremedhin E, Rub U, Bratzke H, Del Tredici K. (2004) Stages in the development of Parkinson's disease-related pathology. *Cell Tis. Res.* **318:** 121 – 134.

Brooks WJ, Jarvis MF, Wagner GC. (1988) Attenuation of MPTP-induced dopaminergic neurotoxicity by a serotonin uptake blocker. *J. Neural. Transm.* **71:** 85 – 90.

Brooks WJ, Jarvis MF, Wagner GC. (1989) Astrocytes as a primary locus for the conversion MPTP into MPP+. *J. Neural. Transm.* **76:** 1 – 12.

Buchman VL, Hunter HJA, Pinõn LGP, Thompson J, Privalova EM, Ninkina NN, Davies AM. (1998) Persyn, a member of the synuclein family, has a distinct pattern of expression in the developing nervous system. *J. Neurosci.* **18:** 9335-9341.

Burns RS, Chiueh CC, Markey SP, Ebert MH, Jacobowitz DM, Kopin IJ. (1983) A primate model of parkinsonism: selective destruction of dopaminergic neurons in the pars compacta of the substantia nigra by N-methyl-4-phenyl-1,2,3,6-tetrahydropyridine. *Proc. Natl. Acad. Sci. U.S.A.* **80:** 4546 – 4550.

Bussell RJr, Eliezer D. (2003) A structural and functional role for 11-mer repeats in α-synuclein and other exchangeable lipid binding proteins. *J. Mol. Biol.* **329:** 763 – 778.

Cappai R, Leck SL, Tew DJ, Williamson NA, Smith DP, Galatis D, Sharples RA, Curtain CC, Ali FE, Cherny RA, Culvenor JG, Bottomley SP, Masters CL, Barnham KJ, Hill AF. (2005) Dopamine promotes α-synuclein aggregation into SDS-resistant soluble oligomers via a distinct folding pathway. *F.A.S.E.B.J.* **19:** 1377 – 1379.

Carlsson T, Bjöklund T, Kirk D. (2007) Restoration of striatal dopamine synthesis for Parkinson's disease: viral vector-mediated enzyme replacement strategy. *Curr. Gene Ther.* **7:** 109 – 120.

Cassarino DS, Fall CP, Smith TS, Bennett JP Jr. (1998) Pramipexole reduces reactive oxygen species production in vivo and in vitro and inhibits the mitochondrial permeability transition produced by the parkinsonian neurotoxin methylpyridinium ion. *J. Neurochem.* **71:** 295 – 301.

Castagnoli N, Jr., Chiba K, Trevor AJ. (1985) Potential bioactivation pathways for the neurotoxin 1-methyl-4-phenyl-1,2,3,6-tetrahydropyridine (MPTP). *Life Sci.* **36:** 225 – 230.

Chalmers-Redman RME, MacLean Fraser AD, Carlie GW, Pong A, Tatton WG. (1999) Glucose protection from MPP^+-induced apoptosis depends on mitochondrial membrane potential and ATP synthase. *Biochem. Biophys. Res. Comm.* **257:** 440 – 447.

Chandra S, Chen X, Rizo J, Jahn R, Südhof TC. (2003) A broken α-helix in folded α-synuclein. *J. Biol. Chem.* **278:** 15313 – 15318.

Chang MY, Lee SH, Kim JH, Lee KH, Kim YS, Lee YS. (2001) Protein kinase C-mediated functional regulation of dopamine transporter is not achieved by direct phosphorylation of the dopamine transporter protein. *J. Neurochem.* **77:** 754 – 761.

Chartier-Harlin MC, Kachergus J, Roumier C, Mouroux V, Douay X, Lincoln S, Levecque C, Larvor L, Andrieux J, Hulihan M, Waucquier N, Defebvre L, Amouyel P, Farrer M, Destee A. (2004) Alpha-synuclein locus duplication as a cause of familial Parkinson's disease. *Lancet.* **364:** 1167 – 1169.

Chen L, Jin J, Davis J, Zhou Y, Wang Y, Liu J, Lockhart PJ, Zhang, J. (2007). Oligomeric α-synuclein inhibits tubulin polymerization. *Biochem. Biophys. Res. Comm.* **356:** 548 – 553.

Chiba K, Peterson LA, Castagnoli KP, Trevor AJ, Castagnoli N Jr. (1985a) Studies on the molecular mechanism of bioactivation of the selective nigrostriatal toxin 1-methyl-4-phenyl-1,2,3,6-tetrahydropyridine. *Drug Metab. Dispos.* **13:** 342 – 347.

Chiba K, Trevor AJ, Castagnoli N Jr. (1985b) Active uptake of MPP+, a metabolite of MPTP, by brain synaptosomes. *Biochem. Biophys. Res. Commun.* **128:** 1228 – 1232.

Choi JY, Sung YM, Park HJ, Hur EH, Lee SJ, Hahn C, Min BR, Kim IK, Kang S, Rhim H. (2002) Rapid purification and analysis of alpha-synuclein proteins: C-terminal truncation promotes the conversion of alpha-synuclein into a protease-sensitive form in Escherichia coli. *Biotechnol. Appl. Biochem.* **36:** 33 – 40.

Choi W, Zibaee S, Jakes R, Serpell LC, Davletov B, Crowther RA, Goedert M. (2004) Mutation E46K increases phospholipid binding and assembly into filaments of human alpha-synuclein. *F.E.B.S. Lett.* **576:** 363 – 368.

Chuang TT, Paolucci L, De Blasi A. (1996) Inhibition of G-protein-coupled receptor kinase subtypes by Ca^{2+}/calmodulin. *J. Biol. Chem.* **271:** 28691 – 28696.

Clarkson ED, Freed CR. (1999) Development of fetal neural transplantation as a treatment for Parkinson's disease. *Life Sci.* **65:** 2427 – 2437.

Colley WC, Sung T-C, Roll R, Jenco J, Hammond SM, Altshuller Y, Bar-Sagi D, Morris AJ, Frohman MA. (1997) Phospholipase D2, a distinct phospholipase D isoform with novel regulatory properties that provokes cytoskeletal reorganisation. *Curr. Biol.* **7:** 191 – 201.

Conway KA, Harper JD, Lansbury PT Jr. (1998) Accelerated in vitro fibril formation by a mutant alpha-synuclein linked to early-onset Parkinson disease. *Nat. Med.* **4:** 1318 – 1320.

Conway KA, Harper JD, Lansbury PT Jr. (2000b) Fibrils formed in vitro from α-synuclein and two mutant forms linked to Parkinson's disease are typical amyloid. *Biochem.* **39:** 2552 – 2563.

Conway KA, Lee S-J, Rochet J-C, Ding TT, Williamson RE, Lansbury PT Jr. (2000a) Acceleration of oligomerization, not fibrillization, is a shared property of both α-synuclein mutations linked to early-onset Parkinson's disease: Implications for pathogenesis and therapy. *Proc. Natl. Acad. Sci. U.S.A.*. **97:** 571 – 576.

Cordato DJ, Chan DK. (2004) Genetics and Parkinson's disease. *J. Clin. Neurosci.* **11:** 119 – 123.

Cornford ME, Chang L, Miller BL. (1995) The neuropathology of Parkinsonsim: An overview. *Brain Cogn.* **28:** 321 – 341.

Crampton JM, Runice CE, Doyle TJ, Lau YS, Wilson JA. (1988) MPTP in mice: treatment, distribution and possible source of contamination. *Life Sci.* **42:** 73 – 78.

da Costa CA, Ancolio K, Checler F. (2000) Wild-type NOT Parkinson's disease-related Ala-53 → Thr mutant α-synuclein protects neuronal cells from apoptotic stimuli *J. Biol. Chem.* **275:** 24065 – 24069.

Davidson WS, Jonas A, Clayton DF, Goerge JM (1998) Stabilization of α-synuclein secondary structure upon binding to synthetic membranes. *J. Biol. Chem.* **273:** 9443 – 9449.

Davis GC, Williams AC, Markey SP, Ebert MH, Caine ED, Reichert CM, Kopin IJ. (1979) Chronic Parkinsonism secondary to intravenous injection of meperidine analogues. *Psychiatry Res.* **1:** 249 – 254.

de Rijk MC, Launer LJ, Berger K, Breteler MM, Dartigues JF, Baldereschi M, Fratiglioni L, Lobo A, Martinez-Lage J, Trenkwalder C, Hofman A (2000) Prevalence of Parkinson's disease in Europe: A collaborative study of population-based cohorts. Neurologic Diseases in the Elderly Research Group. *Neurol.* **54:** S21 – S23.

de Rijk MC, Tzouio C, Breteler MM, Dartiques JF, Amaducci L, Lopez-Pousa S, Manubens-Bertran JM, Alperovitch A, Rocca WA. (1997) Prevalence of parkinsonism and Parkinson's disease in Europe: the EUROPARKINSON Collaborative Study. European Community Concerted Action on the Epidemiology of Parkinson's disease. *J. Neurol. Neurosur. Ps.* **62:** 10 – 15.

Delwaide PJ, Pepin JL, De Pasqua V, de Noordhout AM. (2000) Projections from basal ganglia to tegmentum: a subcortical route for explaining the pathophysiology of Parkinson's disease signs? *J. Neurol.* **247** (Suppl 2)**:** II75 – II81.

Dev KK, van der Putten H, Sommer B, Rovelli G. (2003) Part I: parkin-associated proteins and Parkinson's disease. *Neuropharm.* **45:** 1 – 13.

Dexter DT, Wells FR, Agid F, Agid Y, Lees AJ, Jenner P, Marsden CD. (1987) Increased nigral iron content in postmortem parkinsonian brain. *Lancet.* **2:** 1219 – 1220.

Ding TT, Lee S-J, Rochet J-C, Lansbury PT Jr. (2002) Annular α-synuclein protofibrils are produced when spherical protofibrils are incubated in solution or bound to brain-derived membranes. *Biochem.* **41:** 10209 – 10217.

Dinis-Oliveira RJ, Remião F, Carmo H, Duarte JA, Sánchez Navarro A, Bastos ML, Carvalho F. (2006) Paraquat exposure as an etiological factor of Parkinson's disease. *NeuroToxicol.* **27:** 1110 – 1122.

Drolet RE, Behrouz B, Lookingland KJ, Goudreau JL. (2004) Mice lacking alpha-synuclein have an attenuated loss of striatal dopamine following prolonged chronic MPTP administration. *Neurotoxicol*. **25:** 761 – 769.

Duda JE, Lee VM, Trojanowski JQ. (2000) Neuropathology of synuclein aggregates. *J Neurosci Res.* **61:** 121 – 127.

Duvoisin RC. (1978) Parkinson's disease: A guild for patient and family. *Raven Press Books Ltd. New York*

Eidelberg E, Brooks BA, Morgan WW, Walden JG, Kokemoor RH. (1986) Variability and functional recovery in the N-methyl-4-phenyl-1,2,3,6-tetrahydropyridine model of parkinsonism in monkeys. *Neurosci.* **18:** 817 - 822.

El-Agnaf OM, Jakes R, Curran MD, Middleton D, Ingenito R, Bianchi E, Pessi A, Neill D, Wallace A. (1998) Aggregates from mutant and wild-type α-synuclein proteins and NAC peptide induce apoptotic cell death in human neuroblastoma cells by formation of β-sheet and amyloid-like filaments. *F.E.B.S. Lett.* **440:** 71-75.

Fall CP, Bennett JP Jr. (1998) MPP^+ induced SHSY-5Y apoptosis is potentiated by cyclosporin A and inhibited by aristolochic acid. *Brain Res.* **811:** 143 – 146.

Farrer M, Kachergus J, Forno L, Lincoln S, Wang DS, Hulihan M, Maraganore D, Gwinn-Hardy K, Wszolek Z, Dickson D, Langston JW. (2004) Comparison of kindreds with parkinsonism and alpha-synuclein genomic multiplications. *Ann. Neurol*. **55:** 174 – 179.

Fernagut PO, Chesselet MF. (2004) Alpha-synuclein and transgenic mouse models. *Neurobiol. Dis.* **17:** 123 – 130.

Filion M, Tremblay L, Bedard PJ. (1988) Abnormal influences of passive limb movement on the activity of globus pallidus neurons in parkinsonian monkeys. *Brain Res.* **444:** 165 – 176.

Flint Beal M. (2001) Experimental models of Parkinson's disease. *Nat. Rev. Neurosci.* **2:**325 – 332.

Follmer C, Romão L, Einsiedler CM,Porto TC, Lara FA, Moncores M, Weissmüller G, Lashuel HA, Lansbury P Neto VM, Silva JL, Foguel D. (2007) Dopamine affects the stability, hydration, and packing of protofibrils and fibrils of the wild type and variants of alpha-synuclein. *Biochem.* **46:** 472 – 482.

Foley P, Riederer P. (2000) Influence of neurotoxins and oxidative stress on the onset and progression of Parkinson's disease. *J. Neurol.* **247**(Suppl 2)**:** II82 - II94.

Forloni G, Bertani I, Calella AM, Thaler F, Invernizzi R. (2002) α-Synuclein and Parkinson's disease: selective neurodegenerative effect of alpha-synuclein fragment on dopaminergic neurons in vitro and in vivo. *Ann. Neurol.* **47:** 632 – 640.

Forno LS. (1996) Neuropathology of Parkinson's disease. *J. Neuropath. Exp. Neurol.* **55:** 259 – 272.

Forno LS, Langston JW, DeLanney LE, Irwin I, Ricaurte GA. (1986) Locus ceruleus lesions and eosinophilic inclusions in MPTP-treated monkeys. *Ann. Neurol.* **20:** 449 – 455.

Fortin DL, Nemani VM, Voglmaier SM, Anthony MD, Ryan TA, Edwards RH. (2005) Neural activity controls the synaptic accumulation of α-synuclein. *J. Neurosci.* **25:** 10913 – 10921.

Frei B, Richter C. (1986) N-methyl-4-phenylpyridine (MMP+) together with 6-hydroxydopamine or dopamine stimulates Ca2+ release from mitochondria. *F.E.B.S. Lett.* **198:** 99 – 102.

Fuchs J, Nilsson C, Kachergus J, Munz M, Larsson EM, Schule B, Langston JW, Middleton FA, Ross OA, Hulihan M, Gasser T, Farrer MJ. (2007) Phenotypic variation in a large Swedish pedigree due to SNCA duplication and triplication. *Neurol.* **68:** 916 – 922.

Fukushima T, Yamada K, Isobe A, Shiwaku K, Yamane Y. (1993) Mechanism of cytotoxicity of paraquart. I. NADH oxidation and paraquat radical formation via complex I. *Exp. Toxicol. Pathol.* **45:**345 – 349.

Fuller RW, Steranka LR. (1985) Central and peripheral catecholamine depletion by 1-methyl-4-phenyl-tetrahydropyridine (MPTP) in rodents. *Life Sci.* **36:** 243 – 247.

Furukawa K, Matsuzaki-Kobayashi M, Hasegawa T, Kikuchi A, Sugeno N, Itoyama Y, Wang Y, Yao PJ, Bushlin I, Takeda A. (2006) Plasma membrane ion permeability induced by mutant α-synuclein contributes to the degeneration of neural cells. *J. Neurochem.* **97:** 1071 – 1077.

Gainetdinov RR, Fumagalli F, Wang YM, Jones SR, Levey AI, Miller GW, Caron MG. (1998) Increased MPTP neurotoxicity in vesicular monoamine transporter 2 heterozygote knockout mice. *J. Neurochem.* **70:** 1973 – 1978.

Galvin JE, Lee VM, Trojanowski JQ. (2001) Synucleinopathies: clinical and pathological implications.*Arch. Neurol.* **58:** 186 – 190.

Gandhi S and Wood NW. (2005) Molecular pathogenesis of Parkinson's disease. *Hum. Mol. Genet.* **14:** 2749 – 2755.

George JM, Jin H, Woods WS, Clayton DF. (1995) Characterization of a novel protein regulated during the critical period for song learning in the zebra finch. *Neuron.* **15:** 361–372.

Gescher A. (1998) Analogs of staurosporine: potential anticancer drugs? *Gen. Pharmacol.* 31: 721 – 728.

Geser F, Wenning GK, Poewe W, McKeith I. (2005) How to diagnose dementia with Lewy bodies: state of the art. *Mov. Disord.* **20**(Suppl 12)**:** S11 – S20.

Giasson BI, Covy JP, Bonini NM, Hurtig HI, Farrer MJ, Trojanowski JQ, Van Deerlin VM. (2006) Biochemical and pathological characterization of Lrrk2. *Ann Neurol.* **59:** 315 – 322.

Giasson BI., Uryu K, Trojanowski JQ, Lee VM-Y. (1999) Mutant and wild type human α-synuclein assemble into elongated filaments with distinct morphologies *in vitro*. *J. Biol. Chem.* **274:** 7619 – 7622.

Goedert M, Jakes R. (1990) Expression of separate isoforms of human tau protein: correlation with the tau pattern in brain and effects on tubulin polymerization. *E.M.B.O. J.* **9:** 1225 – 4230.

Goedert M, Spillantini MG, Davies SW. (1998) Filamentous nerve cell inclusion in neurodegenerative diseases. *Curr. Opin. Neurobiol.* **8:** 619 – 632.

Golovko MY, Faergeman NJ, Cole NB, Castagnet PI, Nussbaum RL, Murphy EJ. (2005) α-Synuclein gene deletion decreases brain palmitate uptake and alters the palmitate metabolism in the absence of α-synuclein palmitate binding. *Biochem.* **44:** 8251 – 8259.

Golts N, Snyder H, Frasier M, Theisler C, Choi P, Wolozin B. (2002) Magnesium inhibits spontaneous and iron-induced aggregation of alpha-synuclein. *J. Biol. Chem.* **277:** 16116 – 16123.

Gómez-Santos C, Ferrer I, Reiriz J, Vinals F, Barrachina M, Ambrosio S. (2002) MPP^+ increases α-synuclein expression and ERK/MAP-kinase phosphorylation in human neuroblastoma SH-SY5Y cells. *Brain Res.* **935:** 32 – 39.

Graham DG. (1984) Catecholamine toxicity: a proposal for the molecular pathogenesis of manganese toxicity and Parkinson's disease. *Neurotoxicol.* **5:**83 – 96.

Greenbaum EA, Graves CL, Mishizen-Eberz AJ, Lupoli MA, Lynch DR, Englander SW, Axelsen PH, Giasson BI. (2005) The E46K mutation in α-synuclein increases amyloid fibril formation. *J. Biol. Chem.* **280:** 7800 – 7807.

Gunter TE, Buntinas L, Sparagna G, Eliseev R, Gunter K. (2000) Mitochondrial calcium transport: mechanisms and functions. *Cell. Calcium.* **28:** 285 – 296.

Ha MW, Hou KZ, Liu YP, Yuan Y. (2004) Effect of staurosporine on cycle of human gastric cancer cells. *World J. Gastroenterol.* 10: 161 – 166.

Hallett M, Khoshbin S. (1980) A physiological mechanism of bradykinesia. *Brain.* **103:** 301 – 314.

Hames BD, Hooper NM. (2000) Instant Notes Biochemistry Second Edition. *BIOS Scientific Publishers Ltd.*

Hansen L, Salmon D, Galasko D, Masliah E, Katzman R, DeTeresa R, Thal L, Pay MM, Hofstetter R, Klauber M, Rice V, Butters N, Alford M. (1990) The Lewy body variant of Alzheimer's disease: a clinical and pathologic entity. *Neurol.* **40:** 1 – 8.

Harhangi BS, Farrer MJ, Lincoln S, Bonifati V, Meco G, De Michele G, Brice A, Durr A, Martinez M, Gasser T, Bereznai B, Vaughan JR, Wood NW, Hardy J, Oostra BA, Breteler MM. (1999) The Ile93Met mutation in the ubiquitin carboxy-terminal-hydrolase-L1 gene is not observed in European cases with familial Parkinson's disease. *Neurosci. Lett*. **270:** 1 – 4.

Harik SI, Schmidley JW, Iacofano LA, Blue P, Arora PK, Sayre LM. (1987) On the mechanisms underlying 1-methyl-4-phenyl-1,2,3,6-tetrahydropyridine neurotoxicity: the effect of perinigral infusion of 1-methyl-4-phenyl-1,2,3,6-tetrahydropyridine, its metabolite and their analogs in the rat. *J. Pharmacol. Exp. Ther.* **241:** 669 – 676.

Hashimoto M, Takeda A, Hsu LJ, Takenouchi T, Masliah E. (1999) Role of cytochrome c as a stimulator of alpha-synuclein aggregation in Lewy body disease. *J. Biol. Chem.* **274:** 28849 – 28852.

Hashimoto M, Hsu LJ, Rockenstein E, Takenouchi T, Mallory M, Masliah E. (2002) α-Synuclein protects against oxidative stress via inactivation of the c-Jun N-terminal kinase stress-signalling pathway in neuronal cells. *J. Biol. Chem.* **277:** 11465 – 11472.

Hashimoto M, Yoshimoto M, Sisk A, Hsu LJ, Sundsmo M, Kittel A, Saitoh T, Miller A, Masliah E. (1997) NACP, a synaptic protein involved in Alzheimer's disease, is differentially regulated during megakaryocyte differentiation. *Biochem. Biophys. Res. Com.* **237:** 611 – 616.

Haycock JW. (1990) Phosphorylation of tyrosine hydroxylase in situ at serine 8, 19, 31, and 40. *J. Biol. Chem.* **265:** 11682 – 11691.

Heikkila RE, Cabbat FS, Manzino L, Duvoisin RC. (1984a) Effects of 1-methyl-4-phenyl-1,2,5,6-tetrahydropyridine on neostriatal dopamine in mice. *Neuropharm.* **23:** 711 – 713.

Heikkila RE, Hess A, Duvoisin RC. (1984b) Dopaminergic neurotoxicity of 1-methyl-4-phenyl-1,2,5,6-tetrahydropyridine in mice. *Sci.* **224:** 1451 – 1453.

Herman J-P, Abrous ND. (1994) Dopaminergic neural grafts after fifteen years: Results and perspectives. *Prog. Neurobiol.* **44:** 1 – 35.

Hoyer W, Antony T, Cherny D, Heim G, Jovin TM, Subramaniam V. (2002) Dependence of α-synuclein aggregate morphology on solution conditions. *J. Mol. Biol.* **322:** 383 – 393.

Hoyer W, Cherny D, Subramaniam V, Jovin TM. (2004) Rapid self-assembly of α-synuclein observed by *In Situ* atomic force miscopy. *J. Mol. Biol.* **340:** 127 – 139.

Huang C, Ren G, Zhou H, Wang C-C. (2005) A new method for purification of recombinant human α-synuclein in *Escherichia coli*. *Protein. Exp. Purif.* **42:** 173 – 177.

Hynes M and Rosenthal A. (2000) Embryonic stem cells go dopaminergic. *Neuron.* **28:** 11 – 14.

Ibáñez P, Bonnet AM, Débarges B, Lohmann E, Tison F, Pollak P, Agid Y, Dürr A, Brice A. (2004) Causal relation between alpha-synuclein gene duplication and familial Parkinson's disease. *Lancet.* **364:** 1169 – 1171.

Jensen PH, Nielsen MS, Jakes R, Dotti CG, Goedert M. (1998) Binding of alpha-synuclein to brain vesicles is abolished by familial Parkinson's disease mutation. *J. Biol. Chem.* **273:** 26292 – 26294.

Inzelberg R, Bornstein NM, Reider I, Korczyn AD. (1994) Basal ganglia lacunes and parkinsonism. *Neuroepidemiol.* **13:**108 – 112.

Ischiropoulos H. (2003) Oxidative modifications of alpha-synuclein. *Ann. N.Y. Acad. Sci.* **991:** 93 – 100.

Itagaki C, Isobe T, Taoka M, Natsume T, Normura N, Horigome T, Omata S, Ichinose H, Nagatsu T, Greene LA, Ichimura T. (1999) Stimulus-coupled interaction of tyrosine hydroxylase with 14-3-3 proteins. *Biochem.* **38:** 15673-15680.

Iwai A, Masliah E, Yoshimoto M, Ge N, Flanagan L, de Silva HA, Kittel A, Saitoh T. (1995) The precursor protein of non-A beta component of Alzheimer's disease amyloid is a presynaptic protein of the central nervous system. *Neuron.* **14:** 467 – 475.

Iwata A, Maruyama M, Kanazawa I, Nukina N. (2001) α-synuclein affects the MAPK pathway and accelerates cell death. *J. Biol. Chem.* **276**: 45320 – 45329.

Jaber M, Robinson SW, Missale C, Caron MG. (1996) Dopamine receptors and brain function. *Neuropharm.* **35:** 1503 – 1519.

Jakes R, Spillantini MG, Goedert M. (1994) Identification of two distinct synucleins from human brain. *F.E.B.S. Lett.* **345:** 27 – 32.

Janetzky B, Hauck S, Youdim MB, Riederer P, Jellinger K, Pantucek F, Zochling R, Boissl KW, Reichmann H. (1994) Unaltered aconitase activity, but decreased complex I activity in substantia nigra pars compacta of patients with Parkinson's disease. *Neurosci. Lett.* **169:** 126 – 128.

Javitch JA, D'Amato RJ, Strittmatter SM, Snyder SH. (1985) Parkinsonism-inducing neurotoxin, N-methyl-4-phenyl-1,2,3,6 -tetrahydropyridine: uptake of the metabolite N-methyl-4-phenylpyridine by dopamine neurons explains selective toxicity. *Proc. Natl. Acad. Sci. U.S.A.* **82:** 2173 – 2177.

Jenco JM, Rawlingson A, Daniels B, Morris AJ. (1998) Regulation of phospholipase D2: Selective Inhibition of mammalian Phospholipase D isoenzymes by α- and β-synuclein. *Biochem.* **37:** 4901 – 4909.

Jensen PH, Hager H, Nielson MS, Højrup P, Gliemann J, Jakes R. (1999a) α-Synuclein binds to tau and stimulates the protein kinase A-catalyzed tau phosphorylation of serine residues 262 and 356. *J. Biol. Chem.* **274:** 25481 – 25489.

Jensen PH, Li JY, Dahlstrom A, Dotti CG. (1999b) Axonal transport of synucleins is mediated by all rate components. *Eur. J. Neurosci.* **11:** 3369 – 3376.

Ji H, Liu YE, Jia T, Wang M, Liu J, Xiao G, Joseph BK, Rosen C, Shi YE. (1997) Identification of a breast cancer-specific gene, BCSG 1, by direct differential cDNA sequencing . *Cancer Res.* **57:** 759-764.

Jo E, Fuller N, Rand RP, St George-Hyslop P, Fraser PE. (2002) Defective membrane interactions of familial Parkinson's disease mutant A30P alpha-synuclein. *J. Mol. Biol.* **315:** 799 – 807.

Kahle PJ, Neumann M, Ozmen L, Haass C. (2000) Physiology and pathophysiology of alpha-synuclein. Cell culture and transgenic animal models based on a Parkinson's disease-associated protein. *Ann. N. Y. Acad. Sci.* **920:** 33 – 41.

Kalivendi SV, Cunningham S, Kotamraju S, Joseph J, Hillard CJ, Kalyanaraman B. (2004) α-Synuclein up-regulation and aggregation during MPP^+-induced apoptosis in neuroblastoma cells. *J. Biol. Chem.* **279:** 15240 – 15240.

Kanda S, Bishop JF, Eglitis MA, Yang Y, Mouradian MM. (2000) Enhanced vulnerability to oxidative stress by alpha-synuclein mutations and C-terminal truncation. *Neurosci.* **97:** 279-84.

Kim TD, Ryu HJ, Cho HI, Yang CH, Kim J. (2000) Thermal behaviour of proteins: heat-resistant proteins and their heat-induced secondary structural changes. *Biochem.* 39: 14839 – 14846.

Kingsley RE. (2000) Concise Text of Neuroscience. *Lippincott, Williams & Wilkins, A Wolters Kluwer Company.*

Kinumi T, Kimata J, Taira T, Ariga H, Niki E. (2004) Cysteine-106 of DJ-1 is the most sensitive cysteine residue to hydrogen peroxide-mediated oxidation in vivo in human umbilical vein endothelial cells. *Biochem. Biophys. Res. Commun.* **317:** 722 - 728.

Klawans HJ, Stein RW, Tanner CM, Goetz CG. (1982) A pure Parkinsonian syndrome following acute carbon monoxide intoxication. *Arch. Neurol.* **39:** 302 – 304.

Kleppe R, Toska K, Haavik J. (2001) Interaction of phosphotylated tyrosine hydroxylase with 14-3-3 proteins: Evidence for a phosphoserine 40-dependent association. *J. Neurochem.* **77:** 1097 – 1107.

Klivenyi P, Kekesi KA, Hartai Z, Juhasz G, Vecsei L. (2005) Effects of mitochondrial toxins on the brain amino acid concentrations. *Neurochem. Res.* **30:** 1421 – 1427.

Kloepper KD, Woods WS, Winter KA, George JM, Rienstra CM. (2006) Preparation of α-synuclein fibrils for solid-stae NMR: Expression, purification, and incubation of wild-type and mutant forms. *Protein Expr. Purif.* **48:** 112 – 117.

Koh JY, Wie MB, Gwag BJ, Sensi SL, Canzoniero LM, Demaro J, Csernansky C, Choi DW. (1995) Staurosporine-induced neuronal apoptosis. *Exp. Neurol.* 135: 153 – 159.

Kompoliti K, Chu Y, Shannon KM, Kordower JH. (2007) Neuropathological study 16 years after autologous adrenal medullary transplantation in a Parkinson's disease patient. *Mov. Dis.* **22:** 1630 – 1633.

Kowall NW, Hantraye P, Brouillet E, Beal MF, McKee AC, Ferrante RJ. (2000) MPTP induces alpha-synuclein aggregation in the substantia nigra of baboons. *Neuroreport.* **11:** 211 – 213.

Kruger R, Kuhn W, Muller T, Woitalla D, Graeber M, Kosel S, Przuntek H, Epplen JT, Schols L, Riess O. (1998) Ala30Pro mutation in the gene encoding alpha-synuclein in Parkinson's disease. *Nat Genet.* **18:** 106 – 108.

Kumer SC, Vrana KE. (1996) Intricate regulation of tyrosine hydroxylase activity and gene expression. *J. Neurochem.* **67:** 443 – 462.

Kurtz A, Zimmer A, Schnutgen F, Bruning G, Spener F, Muller T. (1994) The expression pattern of a novel gene encoding brain-fatty acid binding protein correlates with neuronal and glial cell development. *Development.* **20:** 2637 – 2649.

Langston JW, Ballard P, Tetrud JW, Irwin I. (1983) Chronic Parkinsonism in humans due to a product of meperidine-analog synthesis. *Sci.* **219:** 979 – 980.

Langston JW, Forno LS, Rebert CS, Irwin I. (1984) Selective nigral toxicity after systemic administration of 1-methyl-4-phenyl-1,2,5,6-tetrahydropyrine (MPTP) in the squirrel monkey. *Brain Res.* **292:** 390 – 394.

Lashuel HA, Petre BM, Wall J, Simon M, Nowak RJ, Walz T, Lansbury PT Jr. (2002) α-Synuclein, especially the Parkinson's disease-associated mutants, forms pore-like annular and tubular protofibrils. *J. Mol. Biol.* **322:** 1089 – 1102.

Lau YS, Crampton JM, Wilson JA. (1988) Urinary excretion of MPTP and its primary metabolites in mice. *Life Sci.* **43:** 1459 – 1464.

Lavedan C. (1998) The synuclein family. *Gen. Res.* **8:** 871 – 880.

Lavedan C, Leroy E Dehejia A, Buchholtz S Dutra A, Nussbaum RL, Polymeropoulos MH. (1998) Identification, localization and characterization of human γ-synuclein gene. *Hum. Genet.* **103:** 106-112.

Le W and Appel SH. (2004) Mutant genes responsible for Parkinson's disease. *Curr. Opin. Pharm.* **4:** 79 – 84.

Lee D, Lee S-Y, Lee E-N, Chang C-S, Paik SR. (2002) α-Synuclein exhibits competitive interaction between calmodulin and synthetic membrances. *J. Neurochem.* **82:** 1007 – 1017.

Lee FJS, Liu F, Pristupa ZB, Niznik HB. (2001) Direct binding and functional coupling of α-synuclein to the dopamine transporters accelerate dopamine-induced apoptosis. *F.A.S.E.B.J.* **15:** 916-926.

Lee H-G, Zhu X, Takeda A, Perry G, Smith MA. (2006) Emerging evidence for the neuroprotective role of α-synuclein. *Exp. Neurol.* **200:** 1 – 7.

Lee H, Patel S, Lee S. (2005) Intravesicular localization and exocytosis of α-synuclein and its aggregates. *J. Neurosci.* **25:** 6016 – 6024.

Leroy E, Anastasopoulos D, Konitsiotis S, Lavedan C, Polymeropoulos MH. (1998) Deletions in the Parkin gene and genetic heterogeneity in a Greek family with early onset Parkinson's disease. *Hum. Genet.* **103:** 424 - 427

Lestienne P, Nelson J, Riederer P, Jellinger K, Reichmann H. (1990) Normal mitochondrial genome in brain from patients with Parkinson's disease and complex I defect. *J. Neurochem.* **55:** 1810 – 1812.

Lewy FH. (1912) Paralysis agitans. I. Pathologische Anatomie. *Handbuch der Neurologie.* (German) **3:** 920- 933.

Li QX, Campbell BC, McLean CA, Thyagarajan D, Gai WP, Kapsa RM, Beyreuther K, Masters CL, Culvenor JG. (2002) Platelet alpha- and gamma-synucleins in Parkinson's disease and normal control subjects. *J. Alzheimers Dis.* **4:** 309-315.

Lieberman AH, Williams FL. (1993) Parkinson's Disease-The complete guide for patients and caregivers. *The Philip Lief Group Inc.*

Lindvall O and Kokaia Z. (2006) Stem cells for the treatment of neurological disorders. *Nat.* **441:**1094 – 1096.

Liou HH, Chen RC, Tsai YF, Chen WP, Chang YC, Tsai MC. (1996) Effects of paraquat on the *substantia nigra* of the wistar rats: neurochemical , histological, and behavioral studies. *Toxicol. Appl. Pharmacol.* **137:**34 – 41.

Longstaff, A. (2000) Instant Notes Neurosciece. *BIOS Scientific Publishers Ltd.*

Lopiano L, Rizzone M, Bergamasco B, Tavella A, Torre E, Perozzo P, Lanotte M. (2002) Deep brain stimulation of the subthalamic nucleus in PD: an analysis of the exclusion causes. *J. Neurol. Sci.* **195:** 167 – 170.

Lowe J, Blanchard A, Morrell K, Lennox G, Reynolds L, Billett M, Landon M, Mayer RJ. (1988) Ubiquitin is a common factor in intermediate filament inclusion bodies of diverse type in man, including those of Parkinson's disease, Pick's disease, and Alzheimer's disease, as well as Rosenthal fibres in cerebellar astrocytomas, cytoplasmic bodies in muscle, and mallory bodies in alcoholic liver disease. *J. Pathol.* **155:** 9 – 15.

Lowe R, Pountney DL, Jensen PH, Gai WP, Voelcker NH. (2004) Calcium(II) selectively induces α-synuclein annular oligomers via interaction with the C-terminal domain. *Protein Sci.* **13:** 3245 – 3252.

Lozano A. (2001) Deep brain stimulation: challenges to integrating stimulation technology with human neurobiology, neuroplasticity, and neural repair. *J. Rehabil. Res. Dev.* **38:** x-xix.

Lücke C, Gantz DL, Klimtchuk E, Hamilton JA. (2006) Interactions between fatty acids and α-synuclein. *J. Lipid Res.* **47:** 1714 – 1724.

MacDonald ME. (1999) Gadzooks! *Nat. Genet.* **23:** 10 – 11.

Manning-Bog AB, McCormack AL, Purisai MG, Bolin LM, Di Monte DA. (2003) α-Synuclein overexpression protects against paraquatinduced neurodegeneration. *J. Neurosci.* **23:** 3095 – 3099.

Marini AM, Lipsky RH, Schwartz JP, Kopin IJ. (1992) Accumulation of 1-methyl-4-phenyl-1,2,3,6-tetrahydropyridine in cultured cerebellar astrocytes. *J. Neurochem.* **58:** 1250 – 1258.

Markey SP, Johannessen JN, Chiueh CC, Burns RS, Herkenham MA. (1984) Intraneuronal generation of a pyridinium metabolite may cause drug-induced parkinsonism. *Nat.* **311:** 464 – 467.

Maroteaux L, Scheller RH. (1991) The rat brain synucleins; family of proteins transiently associated with neuronal membrane. *Mol. Brain Res.* **11:** 335-343.

Marsden CD, Fahn S. (1995) Blue Books of Practical Neurology: Movement Disorders 1 and 2. *Butterworth-Heinemann Ltd.*

Martin FL, Williamson SJ, Paleologou KE, Hewitt R, El-Agnaf OM, Allsop D. (2003) Fe(II)-induced DNA damage in alpha-synuclein-transfected human dopaminergic BE(2)-M17 neuroblastoma cells: detection by the Comet assay. *J. Neurochem.* **87:** 620 – 630.

Martinez J, Moeller I, Erdjument-Bromage H, Tempst P, Lauring B. (2003) Parkinson's disease-associated α-synuclein is a calmodulin substrate. *J. Biol. Chem.* **278:** 17379 – 17387.

McKeith IG, Galasko D, Kosaka K, Perry EK, Dickson DW, Hansen LA, Salmon DP, Lowe J, Mirra SS, Byrne EJ, Lennox G, Quinn NP, Edwardson JA, Ince PG, Bergeron C, Burns A, Miller BL, Lovestone S, Collerton D, Jansen EN, Ballard C, de Vos RA, Wilcock GK, Jellinger KA, Perry RH. (1996) Consensus guidelines for the clinical and pathologic diagnosis of dementia with Lewy bodies (DLB): report of the consortium on DLB international workshop. *Neurol.* **47:** 1113 – 1124.

McLeod M, Stein M, Beach D. (1987) The product of the mei3+ gene, expressed under control of the mating-type locus, induces meiosis and sporulation in fission yeast. *E.M.B.O. J.* **6:** 729 – 736.

McNaught KS, Olanow CW, Halliwell B, Isacson O, Jenner P. (2001) Failure of the ubiquitin-proteasome system in Parkinson's disease. *Nat. Rev. Neurosci.* **2:** 589 - 594.

Mellick GD, Silburn PA. (2000) The ubiquitin carboxy-terminal hydrolase-L1 gene S18Y polymorphism does not confer protection against idiopathic Parkinson's disease. *Neurosci. Lett.* **293:** 127 – 130.

Meredith GE, Totterdell S, Petroske E, Santa CK, Callison RC, Jr., Lau YS. (2002) Lysosomal malfunction accompanies alpha-synuclein aggregation in a progressive mouse model of Parkinson's disease. *Brain Res.* **956:** 156 – 165.

Mezey E, Dehejia AM, Harta G, Suchy SF, Nussbaum RL, Brownstein MJ, Polymeropoulos MH. (1998) Alpha synuclein is present in Lewy bodies in sporadic Parkinson's disease. *Mol. Psych.* **3:** 493 – 499.

Miake H, Mizusawa H, Iwatsubo T, Hasegawa M. (2002) Biochemical characterization of the core structure of alpha-synuclein filaments. *J. Biol. Chem.* **277:** 19213 – 19219.

Michell AW, Luheshi LM, Barker RA. (2005) Skin and platelet alpha-synuclein as peripheral biomarkers of Parkinson's disease. *Neurosci. Lett.* **3813:** 294 – 298

Miller DW, Hague SM, Clarimon J, Baptista M, Gwinn-Hardy K, Cookson MR, Singleton AB. (2004) Alpha-synuclein in blood and brain from familial Parkinson disease with SNCA locus triplication. *Neurol*. **25:** 1835 – 1838.

Mitchell IJ, Cross AJ, Sambrook MA, Crossman AR. (1985) Sites of the neurotoxic action of 1-methyl-4-phenyl-1,2,3,6-tetrahydropyridine in the macaque monkey include the ventral tegmental area and the locus coeruleus. *Neurosci. Lett.* **61:** 195 – 200.

Mizuno Y, Hattori N, Mori H. (1999) Genetics of Parkinson's disease. *Biomed. Pharmacother.* **53:** 109 – 116.

Mizuno Y, Ohta S, Tanaka M, Takamiya S, Suzuki K, Sato T, Oya H, Ozawa T, Kagawa Y. (1989) Deficiencies in complex I subunits of the respiratory chain in Parkinson's disease. *Biochem. Biophys. Res. Commun.* **163:** 1450 – 1455.

Mizuno Y, Suzuki K, Ohta S. (1990) Postmortem changes in mitochondrial respiratory enzymes in brain and a preliminary observation in Parkinson's disease. *J. Neurol. Sci.* **96:** 49 – 57.

Montgomery EB Jr. (1995) Heavy metals and the etiology of Parkinson's disease and other movement disorders. *Toxicol.* **97:** 3 – 9.

Moussa CE, Wersinger C, Rusnak M, Tomita Y, Sidhu A. (2004) Abnormal migration of human wild-type alpha-synuclein upon gel electrophoresis. *Neurosci. Lett.* **371:** 239 – 243.

Murray IVJ. Lee VMY, Trojanowski JQ. (2001) Synucleinopathies: a pathological and Molecular review. *Clinical Neurosci. Res.* **1:** 445 – 455.

Nakajo S, Omata K, Aiuchi T, Shibayama T, Okahashi I, Ochiai H, Nakai Y, Nakaya K, Nakamura Y. (1990) Purification and characterization of a novel brain-specific 14-kDa protein. *J. Neurochem.* **55:** 2031 – 2038.

Nakajo S, Tsukada K, Omata K, Nakamura Y, Nakaya K. (1993) A new brain-specific 14 kDa protein is a phosphoprotein. Its complete amino acid sequence and evidence for phosphorylation. *Eur. J. Biochem.* **217:** 1057-1063.

Nakano M. (1993) A Possible mechanism of iron meurotoxicity. *Eur. J. Neurol.* **33:**44 – 51.

Narayanan V, Scarlata S. (2001) Membrane binding and self-association of α-synuclein. *Biochem.* **40:** 9927 – 9934.

Narhi L,Wood SJ, Steavenson S, Jiang Y, Wu GM, Anafi D, Kaufman SA, Martin F, Sitney K, Denis P, Louis J-C, Wypych J, Biere AL, Citron M. (1999) Both familial Parkinson's disease mutations accelerate α-synuclein aggregation. *J. Biol. Chem.* **274:** 9843 – 9846.

National collaboration centre for chronic conditions (NCC-CC) (2006) Parkinson's disease: national clinical guidelines for diagnosis and management in primary and secondary care. *London: Royal College of Physicians.*

Nicotra A, Parvez S. (2002) Apoptotic molecules and MPTP-induced cell death. *Neurotoxicol. Teratol.* **24:** 599 – 605.

Ninkina NN, Alimova-Kost MV, Paterson JW, Delaney L, Cohen BB, Imreh S, Gnuchev NV, Davies AM, Buchman VL. (1998) Organization, expression and polymorphism of the human persyn gene. *Hum. Mol. Genet.* **7:** 1417 – 1424.

Ninkina NN, Privalova EM, Pinõn LGP, Davies AM, Buchman VL. (1999) Developmentally regulated expression of persyn, a member of the synuclein family, in skin. *Exp. Cell Res.* **246:** 308-311.

Nirenberg MJ, Chan J, Liu Y, Edwards RH, Pickel VM. (1996) Ultrastructural localization of the vesicular monoamine transporter-2 in midbrain dopaminergic neurons: potential sites for somatodendritic storage and release of dopamine. *J. Neurosci.* **16:** 4135 – 4145.

Nishizuka Y. (1995) Protein kinase C and lipid signaling for sustained cellular responses. *F.A.S.E.B.J.* **9:** 484 – 496.

Offen D, Beart PM, Cheung NS, Pascoe CJ, Hochman A, Gorodin S, Melamed E, Bernard R, Bernard O. (1998) Transgenic mice expressing human Bcl-2 in their neurons are resistant to 6-

hydroxydopamine and 1-methyl-4-phenyl-1,2,3,6- tetrahydropyridine neurotoxicity. *Proc. Natl. Acad. Sci. U.S.A.* **95:** 5789 – 5794.

Olanow CW. (1993) A radical hypothesis for neurodegeneration. *T.I.N.S.* **16:** 439 – 444.

Oluwatosin-Chigbu Y, Robbins A, Scott CW, Arriza JL, Reid JD, Zysk JR. (2003) Parkin suppresses wild-type α-synuclein-induced toxicity in SHSY-5Y cells. *Biochem. Biophy. Res. Com.* **309:** 679 – 684.

Onn S-P, West AR, Grace AA. (2000) Dopamine-mediated regulation of striatal neuronal and network interactions. *Trends. Neurosci.* **23:** S48 - S56.

Orth M, Tabrizi SJ, Schapira AHV, Cooper JM. (2003) α-synuclein expression in HEK293 cells enhances the mitochondrial sensitivity to rotenone. *Neurosci. Lett.* **351:** 29 – 32.

Ostrervoa N, Petrucelli L, Farrer M, Mehta N, Choi P, Hardy J, Wolozin B. (1999) α-Synuclein shares physical and functional homology with 14-3-3 proteins. *J. Neurosci.* **19:** 5782 – 5791.

Paik SR, Shin H-J, Lee J-H, Chang C-S, Kim J. (1999) Copper(II)-induced self-oligomerization of α-synuclein. *Biochem. J.* **340:** 821 – 828.

Paisán-Ruíz C, Jain S, Evans EW, Gilks WP, Simón J, van der Brug M, López de Munain A, Aparicio S, Gil AM, Khan N, Johnson J, Martínez JR, Nicholl D, Carrera IM, Peňa AS, de Silva R, Lees A, Martí-Massó JF, Pérez-Tur J, Wood NW, Singleton AB. (2004) Cloning of the gene containing mutations that cause PARK8-linked Parkinson's disease. *Neuron.* **44:** 595 – 600.

Park JY, Lansbury PT Jr. (2003) β-synuclein inhibits formation of α-synuclein protofibrils: a possible therapeutic strategy against Parkinson's disease. *Biochem.* **42:** 3696 – 3700.

Park SM, Jung HY, Kim HO, Rhim H, Paik SR, Chung KC, Park JH, Kim J. (2002a) Evidence that α-synuclein functions as a negative regulator of Ca^{++}-dependent α-granule release from human platelets. *Blood.* **100:** 2506 – 2514.

Parkinson J. (2002) An essay on the shaking palsy. 1817. *J. Neuropsych. Clin. Neurol.* **14:** 223 – 236.

Payton J, Perrin RJ, Woods WS, George JM. (2004) Structural determinants of PLD2 inhibition by α-synuclein. *J. Mol. Biol.* **337:** 1001 – 1009.

Perez RG, Waymire JC, Lin E, Liu JJ, Guo F, Zigmond MJ. (2002) A role for α-synuclein in the regulation of dopamine biosynthesis. *J. Neurosci.* **22:** 3090 – 3099.

Polymeropoulos MH, Lavedan C, Leroy E, Ide SE, Dehejia A, Dutra A, Pike B, Root H, Rubenstein J, Boyer R, Stenroos ES, Chandrasekharappa S, Athanassiadou A, Papapetropoulos T, Johnson WG,

Lazzarini AM, Duvoisin RC, Di Iorio G, Golbe LI, Nussbaum RL. (1997) Mutation in the α-synuclein gene identified in families with Parkinson's disease. *Sci.* **276:** 2045 – 2047.

Porrino LJ, Burns RS, Crane AM, Palombo E, Kopin IJ, Sokoloff L. (1987) Changes in local cerebral glucose utilization associated with Parkinson's syndrome induced by 1-methyl-4-phenyl-1,2,3,6-tetrahydropyridine (MPTP) in the primate. *Life Sci.* **40:** 1657 – 1664.

Posmantur R, McGinnis K, Nadimpalli R, Gilbertsen RB, Wang KK. (1997) Characterization of CPP32-like protease activity following apoptotic challenge in SH-SY5Y neuroblastoma cells. *J. Neurochem.* 68: 2328 – 2337.

Pronin AN, Morris AJ, Surguchov A, Benovic JL. (2000) Synucleins are a novel class of substrates for G protein-coupled receptor kinases. *J. Biol.Chem.* **275:** 26515 – 26522.

Przedborski S, Jackson-Lewis V, Yokoyama R, Shibata T, Dawson VL, Dawson TM. (1996) Role of neuronal nitric oxide in 1-methyl-4-phenyl-1,2,3,6-tetrahydropyridine (MPTP)-induced dopaminergic neurotoxicity. *Proc. Natl. Acad. Sci. U.S.A.* **93:** 4565 – 4571.

Quilty MC, King AE, Gai W-P, Pountney DL, West AK, Vickers JC, Dickson TC. (2006) Alpha-synuclein is upregulated in neurones in response to chronic oxidative stress and is associated with neuroprotection. *Experi. Neurol.* **199:** 249 – 250.

Radad K, Gille G, Rausch WD. (2005) Short review on dopamine agonists: insight into clinical and research studies relevant to Parkinson's disease. *Pharmacol. Rep.* **57:** 701 – 712.

Ramsay RR, Krueger MJ, Youngster SK, Singer TP. (1991) Evidence that the inhibition sites of the neurotoxic amine 1-methyl-4-phenylpyridinium (MPP+) and of the respiratory chain inhibitor piericidin A are the same. *Biochem. J.* **273:** 481 – 484.

Ramsay RR, Singer TP. (1986) Energy-dependent uptake of N-methyl-4-phenylpyridinium, the neurotoxic metabolite of 1-methyl-4-phenyl-1,2,3,6-tetrahydropyridine, by mitochondria. *J. Biol. Chem.* **261:** 7585 – 7587.

Rang HP, Dale MM, Ritter JM. (1999) Pharmacology 4th Edition. *Churchill Livingstone.*

Rathke-Hartlieb S, Kahle PJ, Neumann M, Ozmen L, Haid S, Okochi M, Haass C, Schulz JB. (2001) Sensitivity to MPTP is not increased in Parkinson's disease-associated mutant α-synuclein transgenic mice. *J. Neurochem.* **77:** 1181 – 1184.

Reichmann H, Janetzky B. (2000) Mitochondrial dysfunction – a pathogenetic factor in Parkinson's disease. *J. Neurol.* **247** (Suppl 2)**:** II/63 – II/68.

Reinhard JF, Jr., Daniels AJ, Viveros OH. (1988) Potentiation by reserpine and tetrabenazine of brain catecholamine depletions by MPTP (1-methyl-4-phenyl-1,2,3,6-tetrahydropyridine) in the mouse; evidence for subcellular sequestration as basis for cellular resistance to the toxicant. *Neurosci. Lett.* **90:** 349 – 353.

Riachi NJ, Dietrich WD, Harik SI. (1990) Effects of internal carotid administration of MPTP on rat brain and blood-brain barrier. *Brain Res.* **533:** 6 – 14.

Riachi NJ, Harik SI, Kalaria RN, Sayre LM. (1988) On the mechanisms underlying 1-methyl-4-phenyl-1,2,3,6-tetrahydropyridine neurotoxicity. II. Susceptibility among mammalian species correlates with the toxin's metabolic patterns in brain microvessels and liver. *J. Pharmacol. Exp. Ther.* **244:** 443 – 448.

Rizzuto R. (2001) Intracellular Ca^{2+} pools in neuronal signalling. *Cur. Opin. Neurobiol.* **11:** 306 – 311.

Rochet JC, Outeiro TF, Conway KA, Ding TT, Volles MJ, Lashuel HA, Bieganski RM, Lindquist SL, Lansbury PT. (2004) Interactions among alpha-synuclein, dopamine, and biomembranes: some clues for understanding neurodegeneration in Parkinson's disease. *J. Mol. Neurosci.* **23:** 23-34.

Roy S, Winton MJ, Black MM, Trojanowski JQ, Lee VM-Y. (2007) Rapid and intermittent cotransport of slow component-b proteins. *J. Neurosci.* **27:** 3131 – 3138.

Sachs C, Jonsson G. (1975) Mechanism of action of 6-hydroxydopamine. *Pharmacol.* **24:**1 – 8.

Samuel W, Galasko D, Masliah E, Hansen LA. (1996) Neocortical lewy body counts correlate with dementia in the Lewy body variant of Alzheimer's disease. *J. Neuropathol. Exp. Neurol.* **55:** 44 – 52.

Saporito MS, Brown EM, Miller MS, Carswell S. (1999) CEP-1347/KT-7515, an inhibitor of c-jun N-terminal kinase activation, attenuates the 1-methyl-4-phenyl tetrahydropyridine-mediated loss of nigrostriatal dopaminergic neurons In vivo. *J. Pharmacol. Exp. Ther.* **288:** 421 – 427.

Satoh JI, Kuroda Y. (2001) α-Synuclein expression is up-regulated in NTera2 cells during neuronal differentiation but unaffected by exposure to cytokines and neurotrophic factors. *Parkinsonism Relat. Disord.* **8:** 7 – 17.

Schapira AH, Cooper JM, Dexter D, Clark JB, Jenner P, Marsden CD. (1990) Mitochondrial complex I deficiency in Parkinson's disease. *J. Neurochem.* **54:** 823 – 827.

Schapira AH, Cooper JM, Dexter D, Jenner P, Clark JB, Marsden CD. (1989) Mitochondrial complex I deficiency in Parkinson's disease. *Lancet.* **1:** 1269.

Schinelli S, Zuddas A, Kopin IJ, Barker JL, di PU. (1988) 1-Methyl-4-phenyl-1,2,3,6-tetrahydropyridine metabolism and 1-methyl-4-phenylpyridinium uptake in dissociated cell cultures from the embryonic mesencephalon. *J. Neurochem.* **50:** 1900 – 1907.

Seaton TA, Cooper JM, Schapira AHV. (1998) Cyclosporin inhibition of apoptosis induced by mitochondrial complex I toxins. *Brain Res.* **809:** 12 – 17.

Sellbach AN, Boyle RS, Silburn PA, Mellick GD. (2006) Parkinson's disease and family history. *Parkinsonism. Relat. Disord.* **12:** 399 – 409.

Sengstock GJ, Olanow CW, Dunn AJ, Arendash GW. (1992) Iron induces degeneration of nigrostriatal neurones. *Brian Res. Bull.* **28:**645 – 649.

Sharon R, Goldberg MS, Bar-Josef I, Betensky RA, Shen J, Selkoe DJ. (2001) α-Synuclein occurs in lipid-rich high molecular weight complexes, binds fatty acids, and shows homology to the fatty acid-binding proteins. *P.N.A.S.* **98:** 9110 – 9115.

Shibasaki Y, Baillie DA, St Clair D, Brookes AJ. (1995) High-resolution mapping of SNCA encoding α-synuclein, the non-Aβ component of Alzheimer's disease amyloid precursor, to human chromosome 4q21.3 → q22 by fluorescence in situ hybridisation. *Cytogenet. Cell. Genet.* **71:** 54-55.

Shibayama-Imazu T, Okahashi I, Omata K, Nakajo S, Ochiai H, Nakai Y, Hama T, Nakamura Y, Nakaya K. (1993) Cell and tissue distribution and developmental change of neuron specific 14 kDa protein (phosphoneuroprotein 14). *Brian Res.* **622:** 17-25.

Shibayama-Imazu T, Ogane K, Hasegawa Y, Nakago S, Shioda S, Ochiai H, Nakai Y, Nakaya K. (1998) Distribution of PNP 14 (β-synuclein) in neuroendocrine tissue: localised in sertoli cells. *Mol. Reprod. Dev.* **50:** 163-169.

Shimohama S, Sawada H, Kitamura Y, Taniguchi T. (2003) Disease model: Parkinson's disease. *Trends Mol. Med.* **9:** 360 – 365.

Shimoji M, Zhang L, Mandir AS, Dawson VL, Dawson TM. (2005) Absence of inclusion body formation in the MPTP mouse model of Parkinson's disease. *Brain Res. Mol. Brain Res.* **134:** 103 – 108.

Sidhu A, Wersinger C, Vernier P. (2004) α-Synuclein regulation of the dopaminergic transporter: a possible role in the pathogenesis of Parkinson's disease. *F.E.B.S. Lett.* **565:**1 – 5.

Singh N, Pillary V, Choonara YE. (2007) Advances in the treatment of Parkinson's disease. *Prog. Neurobiol.* **81:** 29 – 44.

Singleton AB, Farrer M, Johnson J, Singleton A, Hague S, Kachergus J, Hulihan M, Peuralinna T, Dutra A, Nussbaum R, Lincoln S, Crawley A, Hanson M, Maraganore D, Adler C, Cookson MR, Muenter M, Baptista M, Miller D, Blancato J, Hardy J, Gwinn-Hardy K. (2003) α-Synuclein locus triplication causes parkinsons's disease. *Sci.* **302:** 841

Singleton A, Gwinn-Hardy K, Sharabi Y, Li ST, Holmes C, Dendi R, Hardy J, Singleton A, Crawley A, Goldstein DS. (2004) Association between cardiac denervation and parkinsonism caused by alpha-synuclein gene triplication. *Brain.* **127:** 768 – 772.

Smaili SS, Hsu Y-T, Youle RJ, Russell JT. (2000) Mitochondria in Ca^{2+} Signaling and Apoptosis. *J. Bioenerg. Biomembr.* **32:** 35 – 46.

Smaili SS, Hsu Y-T, Carvalho ACP, Rosenstock TR, Sharpe JC, Youle RJ. (2003) Mitochondria, calcium and pro-apoptotic proteins as mediators in cell death signaling. *Braz. J. Med. Biol. Res.* **36:** 183 – 190.

Smeyne RJ, Jackson-Lewis V. (2005) The MPTP model of Parkinson's disease. *Brain Res. Mol. Brain Res.* **134:** 57 – 66.

Smith WW, Pei Z, Jiang H, Moore DJ, Liang Y, West AB, Dawson VL, Dawson TM, Ross CA. (2005) Leucine-rich repeat kinase 2 (LRRK2) interacts with parkin, and mutant LRRK2 induces neuronal degeneration. *Proc. Natl. Acad. Sci. U.S.A.* **102:** 18676 – 18681.

Sofic E, Paulus W, Jellinger K, Riederer P, Youdim MB. (1991) Selective increase of iron in substantia nigra zona compacta of parkinsonian brains. *J. Neurochem.* **56:** 978 – 982.

Sofic E, Riederer P, Heinsen H, Beckmann H, Reynolds GP, Hebenstreit G, Youdim MB. (1988) Increased iron (III) and total iron content in post mortem substantia nigra of parkinsonian brain. *J. Neural. Transm.* **74:** 199 – 205.

Soto-Otero R, Méndez-Álvarez E, Herminda-Ameijeiras Á, Muñoz-Patiño AM, Labandeira-Garcia JL. (2000) Autoxidation and neurotoxicity of 6-Hydroxydopamine in the presence ofsome antioxidants: Potential Implication in relation to the pathogenesis of Parkinson's disease. *J. Neurochem.* **74:** 1605 – 1612.

Speciale SG. (2002) MPTP: insights into parkinsonian neurodegeneration. *Neurotoxicol. Teratol.* **24:** 607 – 620.

Spillantini MG, Crowther RA, Jakes R, Cairns NJ, Lantos PL, Goedert M. (1998a) Filamentous alpha-synuclein inclusions link multiple system atrophy with Parkinson's disease and dementia with Lewy bodies. *Neurosci. Lett.* **251:** 205 – 208.

Spillantini MG, Crowther RA, Jakes R, Hasegawa M, Goedert M. (1998b) alpha-Synuclein in filamentous inclusions of Lewy bodies from Parkinson's disease and dementia with lewy bodies. *Proc. Natl. Acad. Sci. U.S.A.* **95:** 6469 – 6473.

Spillantini MG, Divane A, Goedert M. (1995) Assignment of human α-synuclein (SNCA) and β-synuclein (SNCB) genes to chromosomes 4q21 and 5q35. *Genomics.* **27:** 379-381.

Spillantini MG, Schmidt ML, Lee VM-Y, Trojanowski JQ, Jakes R, Goedert M. (1997) α-Synuclein in Lewy bodies. *Nat.* **388:** 839 – 840.

Srivastava RK, Mi QS, Hardwick JM, Longo DL. (1999) Deletion of the loop region of Bcl-2 completely blocks paclitaxel-induced apoptosis. *Proc. Natl. Acad. Sci. U.S.A.* **96:** 3775 – 3780.

Staal RG, Hogan KA, Liang CL, German DC, Sonsalla PK. (2000) In vitro studies of striatal vesicles containing the vesicular monoamine transporter (VMAT2): rat versus mouse differences in sequestration of 1-methyl-4-phenylpyridinium. *J. Pharmacol. Exp. Ther.* **293:** 329 - 335.

Storch A, Schwarz J. (2002) Neural stem cells and Parkinson's disease. *J. Neurol.* **249:** III/30 - III/32.

Storch A, Kaftan A, Burkhardt K, Schwarz J. (2000) 1-Methyl-6,7-dihydroxyl-1,2,3,4-tetrahydroisoquinoline (salsolinol) is toxic to dopaminergic neuroblastoma SH-SY5Y cells via impairment of cellular energy metabolism. *Brain Res.* **855:** 67 – 75.

Sung J Y, Kim J, Paik S R, Park JH, Ahn YS, Chung KC. (2001) Induction of neuronal cell death by Rab5A-dependent endocytosis of α-synuclein. *J. Biol. Chem.* **276:** 27441 – 27448.

Surguchov A, Surgucheva I, Solessio E, Baehr W. (1999) Synoretin – A new protein belonging to the synuclein family. *Mol. Cell. Neurosci.* **13:** 95-103.

Takahashi H, Wakabayasgi K. (2001) The cellular pathology of Parkinson's disease. *Neuropath.* **21:** 315 – 322.

Takeda A, Hashimoto M, Mallory M, Sundsumo M, Hansen L, Sisk A, Masliah E. (1998) Abnormal distribution of the non-Abeta component of Alzheimer's disease amyloid precursor/alpha-synuclein in Lewy body disease as revealed by proteinase K and formic acid pretreatment. *Lab. Invest.* **78:** 1169 – 1177.

Tanaka Y, Engelender S, Igarashi S, Rao RK, Wanner T, Tanzi RE, Sawa A, Dawson VL, Dawson TM, Ross CA. (2001) Inducible expression of mutant α-synuclein decreases proteasome activity and increases sensitivity to mitochondrial-dependent apoptosis. *Hum. Mol. Genetic.* **10:** 919 – 926.

Tang B, Xiong H, Sun P, Zhang Y, Wang D, Hu Z, Zhu Z, Ma H, Pan Q, Xia JH, Xia K, Zhang Z. (2006) Association of PINK1 and DJ-1 confers digenic inheritance of early-onset Parkinson's disease. *Hum. Mol. Genet.* **15:** 1816 – 1825.

Tsigelny IF, Bar-On P, Sharikov Y, Crews L, Hashimoto M, Miller MA, Keller SH, Platoshyn O, Yuan JX-J, Masliah E. (2007) Dynamics of α-synuclein aggregation and inhibition of pore-like oligomer development by β-synuclein. *F.E.B.J.* **274:** 1862 – 1877.

Uéda K, Fukushima H, Masliah E, Xia Y, Iwai A, Yoshimoto M, Otero DAC, Kondo J, Ihara Y, Saitoh T. (1993) Molecular cloning of cDNA encoding an unrecognized component of amyloid in Alzheimer disease. *Proc. Natl. Acad. Sci. U.S.A.* **90:** 11280-11286.

Uéda K, Saitoh T, Mori H. (1994) Tissue-dependent alternative splicing of mRNA for NACP, the precursor of non-A beta component of Alzheimer's disease amyloid. *Biochem. Biophys. Res. Commun.* **205:** 1366 – 1372.

Ulmer TS, Bax A, Cole NB, Nussbaum RL. (2005) Structure and dynamics of micelle-bound human α-synuclein. *J. Biol. Chem.* **280:** 9595 – 9603.

Ungerstedt U. (1968) 6-Hydroxydopamine induced degeneration of central monoamine neurones. *Eur. J. Pharmacol.* **5:** 107 – 110.

Uversky VN, Li J, Fink AL. (2001) Metal-triggered structural transformations, aggregation, and fibrillation of human α-synuclein. A possible molecular NK between Parkinson's disease and heavy metal exposure. *J. Biol. Chem.* **276:** 44284 – 44296.

Uversky VN, Li J, Souillac P, Millett IS, Doniach S, Jakes R, Goedert M, Fink AL. (2002) Biophysical properties of the synucleins and their propensities to fibrillate: inhibition of α-synuclein assembly by β- and γ-synucleins. *J. Biol. Chem.* **277:** 11970 – 11978.

Valente EM, Abou-Sleiman PM, Caputo V, Muqit MM, Harvey K, Gispert S, Ali Z, Del Turco D, Bentivoglio AR, Healy DG, Albanese A, Nussbaum R, Gonzalez-Maldonado R, Deller T, Salvi S, Cortelli P, Gilks WP, Latchman DS, Harvey RJ, Dallapiccola B, Auburger G, Wood NW. (2004) Hereditary early-onset Parkinson's disease caused by mutations in PINK1. *Sci.* **304:** 1158 – 1160.

Valls-Sole J, Valldeoriola F. (2002) Neurophysiological correlate of clinical signs in Parkinson's disease. *Clinical Neurophysiol.* **113:** 792 – 805.

Veech GA, Dennis J, Keeney PM, Fall CP, Swerdlow RH, Parker WD, Jr., Bennett JP, Jr. (2000) Disrupted mitochondrial electron transport function increases expression of anti-apoptotic bcl-2 and bcl-X(L) proteins in SH-SY5Y neuroblastoma and in Parkinson disease cybrid cells through oxidative stress. *J. Neurosci. Res.* **61:** 693 – 700.

Vila M, Przedborski S. (2003) Targeting programmed cell death in neurodegenerative diseases. *Nat. Rev. Neurosci.* **4:** 365 – 375.

Volles MJ, Lansbury PT Jr. (2002) Vesicle Permeabilization by protofibrillar α-synuclein is sensitive to Parkinson's disease-linked mutations and occurs by a pore-like mechanism. *Biochem.* **41:** 4595 – 4602.

Volles MJ, Lee S-J, Rochet J-C, Shtilerman MD, Ding TT, Kessler JC, Lansbury PT Jr. (2001) Vesicle permeabilization by protofibrillar α-synuclein: Implications for the pathogenesis and treatment of Parkinson's disease. *Biochem.* **40:** 7812 – 7819.

Wakabayashi K, Takahashi H, Ohama E, Takeda S, Ikuta F. (1993) Lewy bodies in the visceral autonomic nervous system in Parkinson's disease. *Adv. Neurol.* **60:** 609 – 612.

Weekly NJ. (1995) Parkinsonism: An overview. *Geriatric nursing.* **16:** 169 – 171.

Weinreb PH, Zhen W, Poon AW, Conway KA, Lansbury PT Jr. (1996) NACP, a protein implicated in Alzheimer's disease and learning, is natively unfolded. *Biochem.* **35:** 13709 – 13715.

Wersinger C, Prou D, Vernier P, Sidhu A. (2003) Modulation of dopamine transporter function by α-synuclein is altered by impairment of cell adhesion and by induction of oxidative stress. *F.A.S.E.B.J.* **17:** 2151 – 2153.

Wersinger C, Sidhu A. (2003a) Attenuation of dopamine transporter activity by α-synuclein. *Neurosci. Lett.* **340:** 189 – 192.

Wersinger C, Sidhu A. (2003b) Differential cytotoxicity of dopamine and H2O2 in a human neuroblastoma divided cell line transfected with alpha-synuclein and its familial Parkinson's disease-linked mutants. *Neurosci. Lett.* **342:** 124 – 128.

Wersinger C, Sidhu A. (2005) Disruption of the interaction of α-synuclein with microtubules enhances cell surface recruitment of the dopamine transporter. *Biochem.* **44:** 13612 – 13624.

Wersinger C, Vernier P, Sidhu A. (2004) Trypsin disrupts the trafficking of the human dopamine transporter by a-synuclein and its A30P mutant. *Biochem.* **43:**1242 – 1253.

Wirths O, Weickert S, Majtenyi K, Havas L, Kahle PJ, Okochi M, Haass C, Multhaup G, Beyreuther K, Bayer TA. (2000) Lewy body variant of Alzheimer's disease: alpha-synuclein in dystrophic neurites of A beta plaques. *Neuroreport.* **11:** 3737 – 3741.

Wong K, Sidransky E, Verma A, Mixon T, Sandberg GD, Wakefield LK, Morrison A, Lwin A, Colegial C, Allman JM, Schiffmann R. (2004) Neuropathology provides clues to the pathophysiology of Gaucher disease. *Mol. Genet. Metab.* **82:** 192 – 207.

Wong SS, Li RH, Stadlin A. (1999) Oxidative stress induced by MPTP and MPP(+): selective vulnerability of cultured mouse astrocytes. *Brain Res.* **836:** 237 – 244.

Wood-Kaczmar A, Gandhi S, Wood NH. (2006) Understanding the molecular causes of Parkinson's disease. *Trends Mol. Med.* **12:** 521 – 528.

Yavich L, Tanila H, Vepsäläinen S, Jäkälä P. (2004) Role of α-synuclein in presynaptic dopamine recruitment. *J. Neurosci.* **24:** 11165 – 11170.

York DH. (1970) Possible dopaminergic pathway from substantia nigra to putamen. *Brain Res.* **20:** 233 – 249.

Yoshiike Y, Chui DH, Akagi T, Tanaka N, Takashima A. (2003) Specific compositions of amyloid-beta peptides as the determinant of toxic beta-aggregation.
J. Biol. Chem. **278:** 23648 – 23655.

Zach S, Bueler H, Hengerer B, Gillardon F (2007) Predominant neuritic pathology induced by viral overexpression of alpha-synuclein in cell culture. *Cell. Mol. Neurobiol.* **27:** 505 – 515.

Zarranz JJ, Alegre J, Gomez-Esteban JC, Lezcano E, Ros R, Ampuero I, Vidal L, Hoenicka J, Rodriguez O, Atares B, Llorens V, Gomez Tortosa E, del Ser T, Munoz DG, de Yebenes JG (2004) The new mutation, E46K, of alpha-synuclein causes Parkinson and Lewy body dementia. *Ann. Neurol.* **55:**164 – 173.

Zhang Y, Dawson VL, Dawson TM, (2000) Oxidative stress and genetics in the pathogenesis of Parkinson's disease. *Neurobiol. Dis.* **7:** 240 – 250.

Zhou Y, Gu G, Goodlett DR, Zhang T, Pan C, Montine TJ, Montine KS, Aebersold RH, Zhang J (2004) Analysis of a-synuclein-associated proteins by quantitative proteomics. *J. Biol. Chem.* **279:** 39155 – 39164.

Zhou ZD, Yap BP, Gung AYT, Leong SM, Ang ST, Lim TM. (2006) Dopamine-related and caspase-independent apoptosis in dopaminergic neurons induced by overexpression of human wild type or muatnt α-synulcein. *Experi. Cell. Res.* **312:** 156 – 170.